TOWARDS THE DEVELOPMENT OF A MODIFIED INDIRECT METHOD OF ESTIMATING THE SHEAR STRENGTH PROPERTIES OF SHALES USING SHALES OF THE PIETERMARITZBURG FORMATION AS A CASE STUDY

By

PRENOLAN NAIDOO

A dissertation submitted in fulfilment of the academic requirements for the degree of Master of Science (MSc) in Environmental and Engineering Geology in the School of Agricultural, Earth and Environmental Sciences, College of Agriculture, Engineering and Engineering Science

University of KwaZulu-Natal
Westville Campus, Durban,
South Africa.

Supervisor: Dr. E.D.C. Hingston

November 2015

As the candidate's supervisor, I have approved his dissertation for submission

Signed: _____ Name: _____

Date: _____

Abstract

Urban sprawl in the Durban metropolitan area has necessitated for the development of areas underlain by shale which were once deemed unsuitable due to instability and the adverse degradable nature of shales when used in construction. Shale is a highly degradable material which weathers easily when exposed to the physical environment. It is thus extremely difficult and costly to obtain representative samples for laboratory testing especially in the determination of their shear strength properties.

Representative samples of both fresh and weathered shale material of the Pietermaritzburg Formation were sampled from four localities within the Durban-Pietermaritzburg area. The fresh and weathered shale samples were subjected to simple index tests such as the jar slake test, the slake durability test and the Point Load Strength as well as the large scale shear box test. Geochemical analyses were also conducted on the fresh and weathered shales to determine the mineralogy of the shale samples.

Results from the geochemical analyses revealed that the common minerals found in the shale samples are quartz and muscovite mica and these samples contain a low percentage of clay minerals whereby illite is the dominant clay mineral. The results from the index tests and the large scale shear box tests were used to develop a modified method of indirectly predicting the shear strength properties of shales. A shale rating system was subsequently modified and developed which uses simple index tests such as the Atterberg limit test, the slake durability test, the jar slake test and the Point Load Strength test to rate shales and indirectly predict the shear strength properties of shales. The rating system divides shales into three main categories based on a range of index properties and shear strength parameters.

This study revealed that by performing simple index tests, the shear strength parameters of shales can be predicted using such a rating system. The shale rating system will be very useful to geotechnical engineers in the construction industry as they are bound by financial limitations and time constraints. Such a rating system will be very useful as it will enable the use of simple index tests to predict the shear strength properties of shales thus reducing costs and the time spent on performing large scale shear tests that are very laborious.

Key words: Degradable materials; Financial limitations; Pietermaritzburg Formation; Shale rating system; Shale; Shear strength parameters

Preface

The experimental work in this dissertation was undertaken in the discipline of Geological Sciences at the University of KwaZulu-Natal, from January 2014 to November 2015 and at the University of Witwatersrand from July 2014 to August 2014 under the supervision of Dr. Egerton D.C. Hingston.

Declaration – Plagiarism

I, PRENOLAN NAIDOO declare that

1. The research reported in this dissertation, except where otherwise indicated, is my original research.
2. This dissertation has not been submitted for any degree or examination at any other university.
3. This dissertation does not contain other persons' data, pictures, graphs or other information, unless specifically acknowledged as being sourced from other persons.
4. This dissertation does not contain other persons' writing, unless specifically acknowledged as being sourced from other researchers. Where other written sources have been quoted, then:
    a. Their words have been re-written but the general information attributed to them has been referenced.
    b. Where their exact words have been used, then their writing has been placed in italics and inside quotation marks, and referenced.
5. This dissertation does not contain text, graphics or tables copied and pasted from the Internet, unless specifically acknowledged, and the source being detailed in the dissertation and in the References section.

_____

Prenolan Naidoo (Student)

Table of contents

List of figures

List of tables

Chapter 1

Introduction

1.1 General background

Population growth has necessitated for the relocation of people to land that was once deemed unsuitable. This rapid movement of people into these areas has forced engineers and town planners to design and construct buildings on unsuitable areas due to a shortage of available land. These unsuitable areas often consists of highly degradable, flawed, discontinuous and inhomogeneous geological materials of low strength, low lying areas which are prone to flooding or even environmentally unfavourable areas (Walkinshaw and Santi, 1996). These highly degradable materials are grouped as argillaceous materials or mudrocks and consist of mudstones, shales, siltstones and problem clays (Merriman *et al.,* 2003).

Shale is a type of argillaceous material which consists of silt and clay sized particles (Tucker, 2001). The common minerals which are found in most shales consists of quartz, feldspars and clay minerals which are mostly kaolinite, illite and montmorillonite (Clarke, 1924: Pettijohn, 1957; Huang, 1962). Shales exhibit varying degrees of fissility and splits into thin millimetre size layers (Merriman *et al*., 2003) which are parallel to bedding (Fityus *et al*., 2015).

Shale is one of the most problematic type of degradable materials (Walkinshaw and Santi, 1996). When exposed to the physical environment, shales degrade rapidly which includes physical and chemical changes (Pidwirny, 2006). Taylor (1948) also stated that shales degrade easily on exposure to air and water. Several problems have occurred from either constructing dwellings on shale bedrock or from using shale as a fill material. These problems include settlement, landslides and borehole instabilities (Strohm *et al.,* 1981; Bell & Maud, 1996, 1997; Hopkins & Beckham, 1998). Embankments which are constructed using shales are susceptible to settlement problems which are often difficult to predict and control (Hopkins and Beckham, 1998). Settlement often causes cracks in buildings and walls, buckling of pavements and in extreme cases, structures can collapse. Shales can also cause damages to light structures, roads and boundary walls (Dafalla and Al-Shamrani, 2014).

Shales are distributed extensively within the KwaZulu-Natal province and shales constitute one half of the volume of sedimentary rocks in the shallow earth's crust (Picard, 1971; Blatt, 1982; Walkinshaw and Santi, 1996; Merriman *et al.,* 2003). Richards (2006) stated that areas within Pietermaritzburg that are underlain by shale of the Pietermaritzburg Formation are susceptible to inundation, pose excavation difficulties for the installation of ground works as a result of the shallow residual soil cover and these areas may contain erodible, active, expansive or swelling soils. The Pietermaritzburg Formation outcrops frequently in the Durban area and because of its association with landslides, it has been regarded as unstable (Bell and Maud, 1996; 1997). As development in the

Durban area continues to move into areas underlain by shale, there is a need to find an indirect method of estimating the shear strength properties of shales.

1.2 Research rationale

Shales are very problematic rocks in terms of sampling and laboratory testing. It is therefore very difficult to obtain representative samples of shales for geotechnical testing as it exhibits varying degrees of fissility and disintegrates into thin layers. The sampling process thus becomes increasingly difficult when shales have been exposed to the physical environment especially being subjected to periods of extensive rainfall. The coring of the shale materials following the unloading process often causes the development of microcracks in shales and affects its quality (Horsud, 2001). Thus, it is difficult to obtain representative samples to undertake laboratory tests in order to determine the geotechnical properties of shales, which are vital for geotechnical engineering. Additionally, it is difficult to define the deformational properties of shales using conventional consolidation testing due to the large particle sizes of the shale materials which are used in shale embankments (Hopkins and Beckham, 1998).

As a result of the ongoing development of areas that contain shales which were previously considered as being unsuitable and due to the problems that are associated with shales, it is necessary to develop a modified and simple indirect method of predicting the shear strength properties of shales. This method of rating and predicting the shear strength properties of shales should use simple index tests to avoid the time spent and cost implications of performing laborious tests such as the large scale shear box test.

The development of such a shale rating system will be very beneficial to the construction industry since time constraints and financial limitations as stated by Nandi *et al.* (2009) in the working environment make it very difficult to perform lengthy laboratory tests to obtain the shear strength properties of such a problematic material.

1.3 Location of the study areas

Four areas within KwaZulu-Natal where shales of the Pietermaritzburg Formation are well exposed were chosen as sampling sites. The first sampling site is situated within the Cornubia housing and industrial development and is found in Verulam. Sampling sites 2, 3 and 4 are situated within the Pietermaritzburg area. The positions of each locality within KwaZulu-Natal are shown in Figure 1.1.

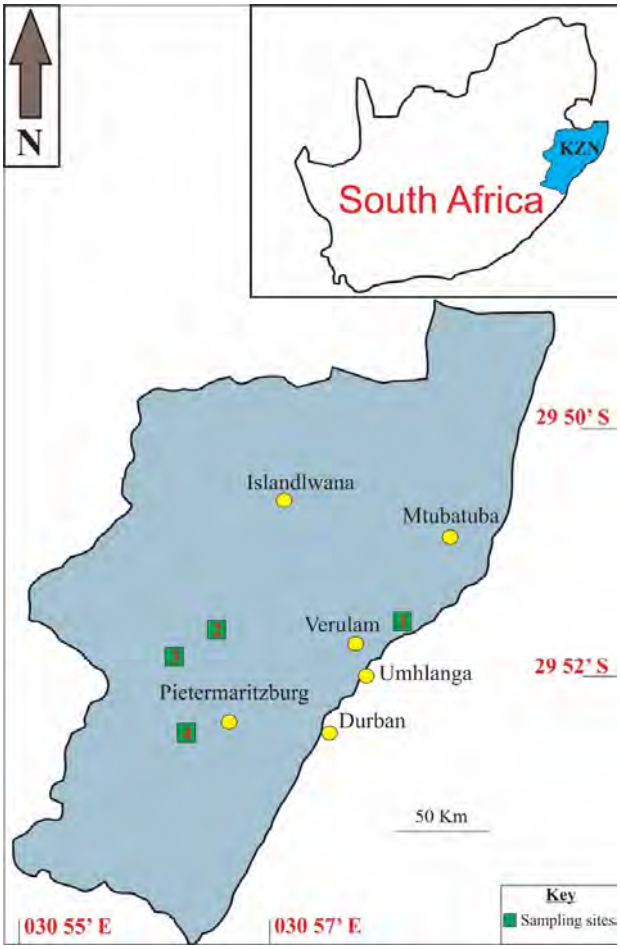

Figure 1.1: Map showing the location of the sampling sites.

1.4 Aim

The aim of this project was to develop a modified method of indirectly estimating the shear strength parameters of shales using shales of the Pietermaritzburg Formation in the Durban-Pietermaritzburg area as a case study.

1.5 Objectives

- To perform geochemical tests on the shales of the Pietermaritzburg Formation in the Durban and Pietermaritzburg areas in order to determine the mineralogy of the shale samples.

- To undertake geotechnical testing of shales of the Pietermaritzburg Formation in the Durban and Pietermaritzburg areas to determine the geotechnical properties of the shale materials from each locality.

- To monitor and determine the rate of natural settlement of platforms constructed in the Cornubia housing and industrial development using shale as fill material in order to predict the amount of settlement when shales are used in construction.

- To develop a modified rating system which can be used to describe and classify shales particularly for individuals within the construction industry using the results from this study and from the available literature. This shale rating system will enable engineers to easily rate and classify shale materials and to indirectly predict the shear strength properties of shales which is based on simple index tests.

1.6 Methodology

The methodology used to complete this dissertation includes:

1.6.1 Primary reconnaissance and literature review

A literature review was conducted to obtain the relevant information regarding shales. This information consists of the chemistry and mineralogy of shales, the geotechnical properties of shales and possible classification systems of shales. A brief overview of shale related instability was also examined. During this stage, topographical, geological and orthophoto maps were used to determine areas of good shale exposures for the sampling process. The areas chosen were based on the ease of obtaining shale materials and also the quality of the shale exposures.

1.6.2 Field work and sampling

After determining areas of good shale outcrops, samples were taken from four different localities. The first sampling site is found in Verulam whilst sampling sites 2, 3 and 4 are situated within the Pietermaritzburg area. GPS co-ordinates were taken to pin-point these locations on the site map and photographs were used to provide a scale for the shale outcrops. These samples comprise block-sized samples, crushed samples and soil samples. Thereafter, all samples were sealed to prevent any loss of moisture and transported to the engineering geology laboratory in the discipline of Geological Sciences at the University of KwaZulu-Natal.

1.6.3 Geochemical and geotechnical testing

Laboratory testing were done to characterize the shale samples from each locality. Geotechnical tests were performed to determine the index properties of the residual materials and assess the durability

and the strength of the rock material. These tests comprise the Particle Size analysis, the Atterberg limits test, the jar slake test, the slake durability test, the Point Load Strength test and the Shear Box test. The jar slake test and the slake durability test were done to assess the durability of the shale materials. Geochemical tests were performed to determine the chemical composition and mineralogy of the shales from each sampling site. Samples were milled to perform geochemical analyses which consist of the X-ray diffraction test (XRD).

1.6.4 Settlement monitoring

The settlement of various platforms containing shale fill material within the Cornubia development were analysed over a period of one year. Settlement monitoring beacons were installed over 4 platforms in the industrial sector whilst 6 settlement beacons were installed in the housing sector of the Cornubia housing and industrial development. Settlement readings (vertical measurements) were recorded each month to assess the amount of settlement which occurred in each of the fill platforms.

1.6.5 Results and discussion

The results from the various geotechnical and geochemical tests were analysed and compared to published literature. A correlation was made between each sampling site and its geochemical and geotechnical properties. The rating system created by Franklin (1981) was modified according to the results from the various laboratory tests and the field monitoring of settlement. A "back-analysis" method was used to assess the validity of this modified rating system using the basic index properties of shales from published literature to predict its shear strength parameters. The modified shale rating system will be very beneficial to geotechnical engineers when dealing with shales in the construction industry.

1.7 Outline of the dissertation

Each chapter in this dissertation focuses on salient aspects which forms a cumulative framework. A brief synopsis is provided below

Chapter 1: General background

This chapter provides a general background to shale, an overview of its chemistry and shale related instability. More importantly, it also focuses on the aims and objectives of this study.

Chapter 2: Regional and local geology

A detailed description of the regional and local geology is provided in this chapter.

Chapter 3: Geology of shales and mudrocks

This chapter provides a detailed description on the chemical and mineralogical composition of degradable materials such as mudrocks, shales and mudstones. Additionally, this chapter presents the mineralogy of shales of the Pietermaritzburg Formation as well as the textural characteristics of shales and mudrocks.

Chapter 4: Geotechnical properties of shales and mudrocks and their geotechnical problems

A detailed account of the geotechnical properties of shales and mudrocks is presented in this chapter. In addition, Chapter 4 highlights the effects of weathering on shales and mudrocks and their geotechnical problems.

Chapter 5: Classification of argillaceous materials and previous studies on rating systems on shales

This chapter presents the field methods and laboratory tests which are used to classify shales and mudrocks. Furthermore, this chapter provides an introduction on the methods used to monitor settlement and highlights the classification systems which have been previously used to describe shales with emphasis on Franklin's (1981) shale rating system.

Chapter 6: Fieldwork and settlement monitoring

Chapter 6 provides a brief description of the geology of each sampling site and the geotechnical problems encountered during the sampling of shales. Also, it provides the methodology used to monitor the field settlement of shale fill over a specified time period.

Chapter 7: Laboratory testing

A detailed description and methodology of the various geochemical and geotechnical tests carried out are presented in this chapter. It focuses on the advantages and disadvantages of performing each laboratory test.

Chapter 8: Laboratory results and discussion

This chapter presents a detailed discussion of the results obtained from the geochemical analyses and the geotechnical tests. A correlation was made between the geochemical analyses and the geotechnical tests to explain the reasons for the slaking of shales. This chapter further discusses the amount of settlement which is likely to occur in the shale filled platforms relative to the amount of rainfall experienced.

Chapter 9: Developing a shale rating system

Based on the results obtained from Chapter 8 and from an extensive literature search, a shale rating system has been modified after Franklin (1981) to predict the shear strength properties of shales. This modified rating system, in addition to Franklin's (1981) shale rating chart, includes the geochemical properties of shales and associated field settlement. This rating system characterises shales which are based on their index properties into three categories which contain a range of shear strengths and potential rates of settlement. The modified rating system can be used by engineers and by individuals in the construction industry, particularly when encountered with shales of the Pietermaritzburg Formation.

Chapter 10: Conclusion

Chapter 10 concludes the findings of this study. It also looks at any limitations and highlights the benefits of further research.

Chapter 2

Regional and Local Geology

2.1 Introduction

This chapter provides a detailed description of the regional geology of KwaZulu-Natal as well as the local geology of the localities sampled which consists of the Durban and Pietermaritzburg area. It also focuses particularly on shales of the Pietermaritzburg Formation of the Ecca Group.

2.2 Regional geology of KwaZulu-Natal

The Kaapvaal Craton forms the basement geology of KwaZulu-Natal which represents a primordial crust (Johnson *et al.*, 2006). The Archaean basement forms part of the basement geology which developed between 3650-2650 Ma comprising large granitic gneisses that have infolded greenstone belts (Johnson *et al.,* 2006). According to the composition of these gneisses, they are called tonalitic, trondhjematic or granodioritic and they have formed from primitive forms of the Archaean plate tectonics in an oceanic-environmental setting. This activity resulted from the subduction and the partial melting of the oceanic basaltic components of the greenstone belts (Johnson *et al.,* 2006).

The Namaqua-Natal Province formed during 2500 Ma – 542 Ma during the Proterozoic. The Natal sector of the Namaqua-Natal Metamorphic province was accreted north-eastwards onto the southern margin of the Kaapvaal Craton. In KwaZulu-Natal, the Mesoproterozoic events are represented by volcanic arcs which developed 1200 Ma (Johnson *et al.,* 2006). These arcs were deformed by the newly formed continental crusts from the obduction of the oceanic crust onto these continental crusts. Rocks such as quartz arenites, grits and conglomerates are characteristic of the Natal Group (Johnson *et al.,* 2006).

During the Phanerozoic, South Africa was the cornerstone for Gondwana. The sea which formed from the melting of the ice during the Permo-Carboniferous period transported a wide range of sediments. As the Karoo basin gradually filled, a change in the tectonic framework occurred (Johnson *et al.,* 2006). This was followed by the development of several magmatic arcs and Gondwana began to move towards the tropics from the polar regions. The formation of these arcs resulted in the deltaic and the turbidic Ecca Group and Beaufort Group sediments (Bell and Maud, 2000). These sediments were then deposited in a retro-arc foreland basin as clastic wedges (Johnson *et al.,* 2006). As the Karoo sedimentation came to an end, the fragmentation of Gondwana occurred and was followed by the intrusion of several dykes and sills (Johnson *et al.,* 2006). Cenozoic deposits now overlie these stratigraphic successions. A map of the regional geology of KwaZulu-Natal is shown in Figure 2.1.

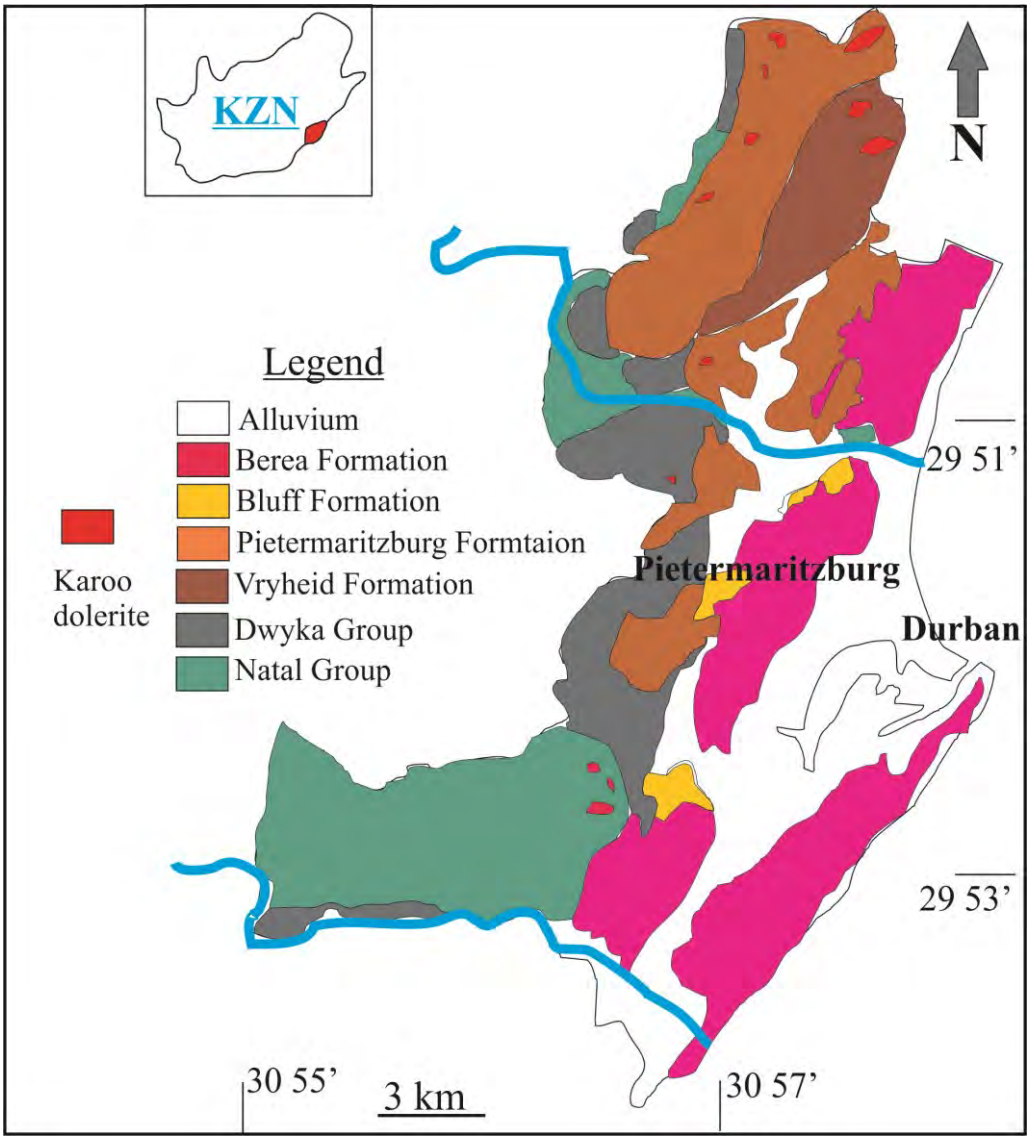

Figure 2.1: Regional geology of KwaZulu-Natal (modified after Bell and Maud, 2000).

2.3 Local geology

The local geology of Verulam consists of the Pietermaritzburg Formation and the Vryheid Formation. In Pietermaritzburg, the Pietermaritzburg Formation extends over a vast area whilst colluvial sediments extend and overlie other areas. The shales in these areas either belong to the Pietermaritzburg Formation and/ or from the Dwyka Group. Both areas show several intrusions of dolerite. The distribution of the Dwyka Group, the Natal Group and the Pietermaritzburg Formation in KwaZulu-Natal is shown in Figure 2.2.

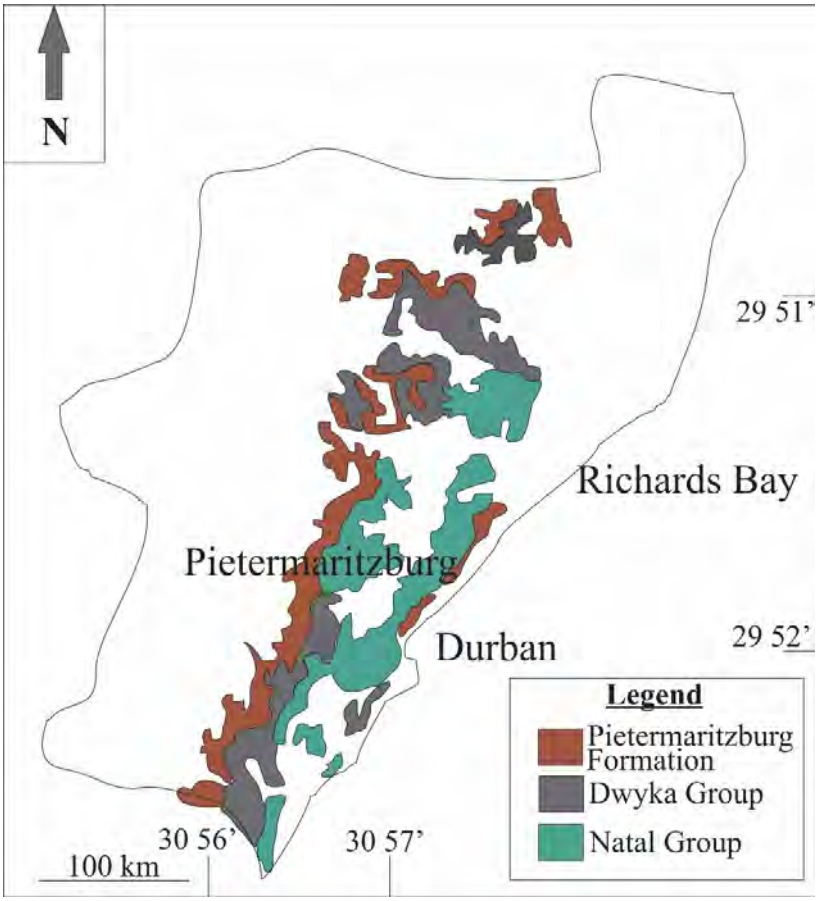

Figure 2.2: Distribution of the Dwyka Group, the Pietermaritzburg Formation and the Natal Group (modified after Johnson *et al.,* 2006).

2.3.1 The Natal Group

According to Marshall (1994), the Natal Group is composed of reddish-grey conglomerates, sandstones, siltstones and mudrocks which underlie the Dwyka Group and overlies the Archaean and Proterozoic basement in KwaZulu-Natal. The reddish brown arenaceous rocks are interbedded with mudrock and conglomerate units. Liu (2002) stated that these lithogical units mostly represent a fluvial sequence which was deposited by braided streams. Hobday and Van Brunn (1979) provided a general overview of the fluvial sedimentology and palaeogeography of the group. According to SACS (1980), rocks of the Natal Group were considered to be a part of the Ordovician-Silurian Table Mountain Series. Marshall (1994) undertook the first basin-wide investigation of the group. The Natal depositional basin extends from Hlabisa in the north to just south of Hibberdene in the south. According to the reviewed scheme by Marshall (1994) and Marshall and Von Brunn (1999), the Natal Group consists of two formations and eight members and has a total thickness between 500-600 m (Table 2.1).

Table 2.1: Stratigraphic subdivision, lithology and member thicknesses of the Natal Group (modified after Johnson *et al.,* 2006).

Group	Formation	Era	Member		Dominant lithology	Maximum thickness (m)	
Natal Group	Mariannhill	Palaeozoic	Westville		Matrix supported conglomerate	30	
			Newspaper		Arkosic sandstone	>368	
			Tulini		Small-pebble conglomerate	28	
	Durban		Dassenhoek	Melmoth	Silicified quartz arenite	42	168
			Situndu		Coarse arkosic sandstone	84	
			Kranskloof		Silicified quartz arenite	51	
			Eshowe		Arkosic sandstone and shales	142	
			Ulundi		Coarse clast-supported monomictic conglomerate	59	

According to Marshall (2006), the thickness of the Natal Group varies spatially whilst the original thickness of 2600 m has been estimated from the ruptured strength of conglomerate clasts from the Ulundi Member. The arenaceous rocks are predominantly coarse to very coarse grained and comprise mainly subarkose and subordinate quartz arenite with the coarser grained rocks being immature and poorly sorted (Johnson *et al.,* 2006). The sandstone beds show horizontal laminations and trough cross beds, scour surfaces and with commonly occurring reactivation surfaces. The mudrocks range from massive to well laminated and often show poorly developed horizontal lamination. Within the Natal Group, only the Durban Formation and the Eshowe Formation have shale as a dominant part of its lithology (Johnson *et al*., 2006).

2.3.2 The Dwyka Group

The Dwyka Group overlies the Natal Group and spans the late Carboniferous (360-300 Ma) to the early Permian (300-250 Ma). In the east, particularly in KwaZulu-Natal, the Dwyka Group uncomformably overlies the Natal Group and the Mitsikaba Formation. A variety of lithofacies have been recorded in the Dwyka Group and these facies are considered to have been deposited in a marine basin (Visser, 1989). This depositional event is believed to have occurred after a period of glaciation as the underlying rocks particularly display well-developed striated glacial pavements in certain areas (Johnson *et al.,* 2006). There is a distinct difference between the facies in the north and south. These facies are dominated by diamictites of different grades and with lesser amount of mudrock, sandstone and conglomerate beds (Johnson *et al.,* 2006). The Carbonaceous mudstone, shale or silty rhythmite has resulted from the suspension settling of mud as well as the fall-out of silt from sediment-laden underflows. Anderson and McLachlan (1976) have discovered biological evidence from the presence of spores, pollen, fish trails and arthropod trackways.

2.3.3 The Ecca Group

The Ecca Group comprises sixteen Formations and can be grouped into three geographical areas. It shows a lateral change in facies and unconformably overlies the Dwyka Group. The northeastern region comprises the Volksrust Formation, the Vryheid Formation and the Pietermaritzburg Formation (Table 2.2).

Table 2.2: The formations comprising the north-eastern part of the Ecca Group.

Period	Group	Formation	Estimates thickness
Permian	Ecca	Volksrust	133 m
		Vryheid	550 m
		Pietermaritzburg	210 m
Carboniferous –Permian	Dwyka	600-750 m	

2.3.3.1 Pietermaritzburg Formation

The Pietermaritzburg Formation generally overlies the Dwyka Group with a sharp contact. It is the lowermost unit of the Karoo Supergroup and is located in the north-eastern part of the basin (Johnson *et al*., 2006). It is composed of greyish to olive-green micaceous shale and dark grey silty mudrock and shales, which coarsen upwards with heavily bioturbated and pene-contemporaneously deformed sandy and silty beds appearing at the top (Johnson *et al.,* 2006). These geological materials have been deposited as deltaic and alluvial sediments in an intercontinental basin during the Permian (Bell and Maud, 2000). Shales within this formation are 100-400 m thick and are found as alternating fissile beds with thinner non-fissile beds (Bell and Maud, 2000). The thickness of these beds usually increases in a southerly direction (Wilson, 1983). The contact between the Vryheid Formation and the Pietermaritzburg Formation is strongly diachronous, with sandstones successively higher up in the succession shaling out towards the south (Johnson *et al*., 2006).

The Pietermaritzburg Formation records a post-glacial transgression. The coarser sediments on the top of the formation represents a shoreline progradation. Johnson *et al*. (2006) stated that widespread carbonate lenses and beds reflects changes in Eh-pH levels which are consistent with relatively shallow water, presumably on an unstable shelf. Mineral fluctuations in shale beds are reflected by their varying degrees of fissility where relatively thick fissile shale beds alternate with much thinner hard non-fissile beds. The non-fissile beds contain a higher proportion of chamosite, chalybite and chlorite whilst the fissile beds are composed of quartz and illite (Wilson, 1983). The degree of fissility of these beds depends on the degree of weathering. The Pietermaritzburg Formation is overlain by the fossiliferous St. Lucia Formation.

The boundaries of the Pietermaritzburg Formation are commonly determined by the numerous faults which are present within the monoclinal structure of the coastal hinterland (Geological Survey, 1988).

The eastern belt lies within the coastal belt at altitudes between 50 to 300 metres. Faulting along the coast has caused shales of the Pietermaritzburg Formation to be bound by sandstones of the Natal Group and Vryheid Formation, sand of the Berea Formation and tillite of the Dwyka Group. A cross sectional view of Durban and Pietermaritzburg is shown in Figure 2.3 and Figure 2.4 respectively.

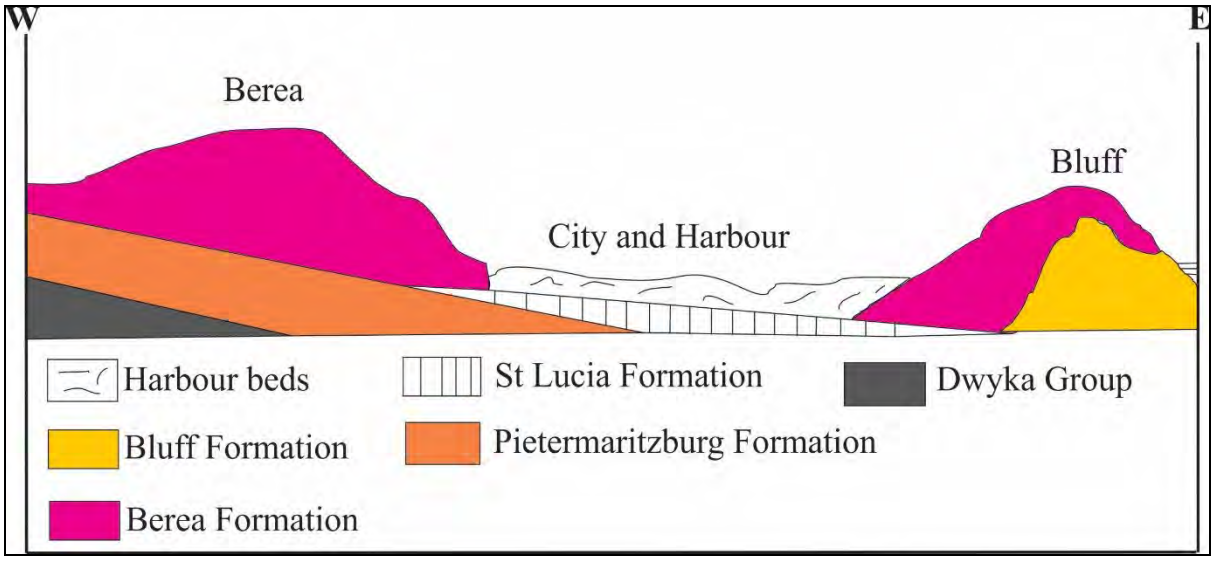

Figure 2.3: West-east cross-section of the Durban city (modified after Brink, 1985).

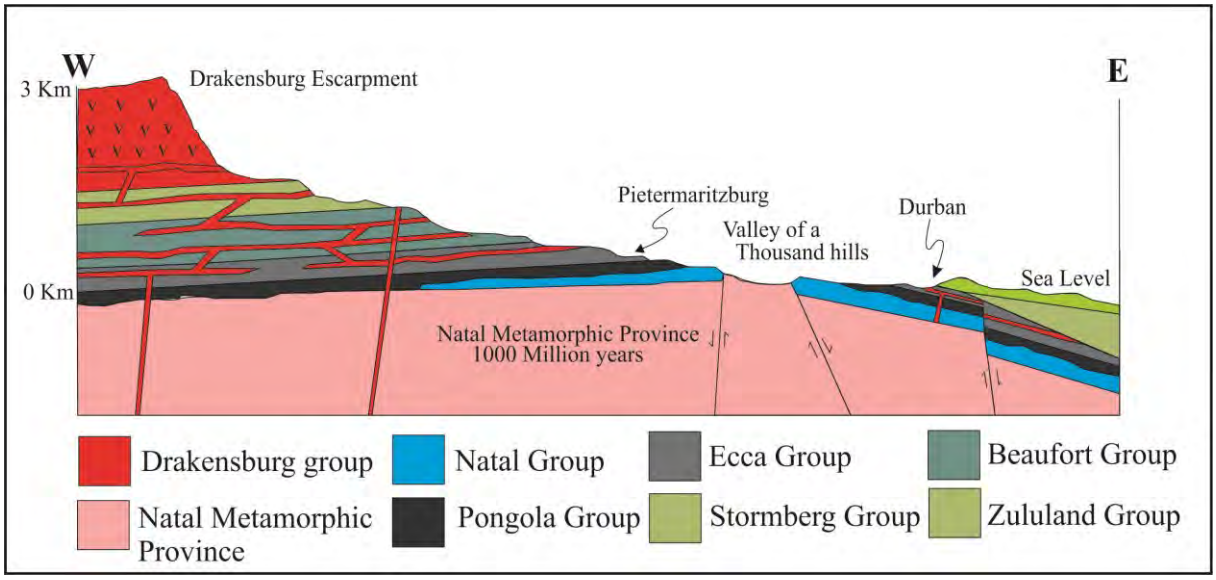

Figure 2.4: West-east cross-section of Pietermaritzburg (modified after Meth *et al.,* 2002).

Some shale changes physically and chemically during the weathering process. During the weathering of shales, it changes in appearance from dark-grey to brown in colour and becomes friable and fissile (Walkinshaw and Santi, 1996). During the weathering process, the vertical expansion of these materials results in the formation of joints, fissures and softening as a consequence of uplift and erosion from the removal of the overburden (Cripps and Taylor, 1981). Shales, particularly of the

Pietermaritzburg Formation, are also well jointed and cause their beds to disintegrate into blocks of variable sizes. The inclinations of these joints generally do not have a preferential azimuth (Wilson, 1983). During the progressive weathering of shales, shales usually weather to a fine grained mass of soil as stated by Hopkins (1988) or to a gravelly clay/ clayey gravel and will result in associated stability and settlement problems (Drennan, Maud and Partners, 2010).

2.3.4 The Karoo Dolerite suite

The Mesozoic Karoo igneous Province is distributed across South Africa and is found extrusively and intrusively (Johnson *et al.,* 2006). Due to the extreme ground conditions, lava was forced to intrude lithological sequences particularly, the sedimentary successions. These intrusions intersected either parallel or at an angle to the bedding planes of these stratigraphic sequences in the form of dykes or sills. The direction of intrusion has a profound effect on its intruding rocks. Brink (1983) stated that mudrocks are transformed to hornfels during this process and unlike sills, dykes affect sediments much stronger in the radial direction than in the vertical direction. It was much easier for the Karoo Igneous Suite to intrude weaker sedimentary units such as the Pietermaritzburg Formation.

In the Pietermaritzburg area, numerous dykes have been found penetrating these weaker successions (Johnson *et al*., 2006*)*. Richards (2006) further stated that dykes and sills intrude all lithostratigraphic units but are predominately associated with the argillaceous rocks of the Ecca Group. A similar scenario has been identified within the Durban area particularly in an area under investigation; the Cornubia housing and industrial development. These intrusions have a significant effect on these sedimentary sequences such as shales and siltstones, which results in the ingress of water into these units. Water then starts to flow into the factures between the contacts of shales and causes weathering of the shales and associated instabilities (Bell and Maud, 1997).

2.4 Summary

This chapter presented the regional and local geology of KwaZulu-Natal. Additionally, this chapter lists the stratigraphic units of the Natal Group and the Dwyka Group with emphasis on the Ecca Group. Furthermore, Chapter 2 provided a detailed description of the Pietermaritzburg Formation and discussed the effects of the Karoo Dolerite Suite on the Pietermaritzburg Formation.

Chapter 3

Geology of shales and mudrocks

3.1 Introduction

This chapter presents an overview of the geology of shales by focusing on the mineralogy, chemical composition and textural properties of shales and mudrocks. Furthermore, it focuses on the geology of shales of the Pietermaritzburg Formation.

3.2 Shales and mudrocks

Fine grained sedimentary rocks account for more than 60 % of sedimentary types (Potter *et al*., 1980). They are composed of particles mainly < 62 μm and are about twice as abundant as sandstones and conglomerates combined (Boggs, 2009). These fine grained rocks are known by a variety of names such as siltstones, mudstones, mudrocks, claystones and shales (Boggs, 2009). Shales constitute approximately 45-55 % of the volume of sedimentary rocks on the earth's crust (Picard, 1971; Blatt 1982; Walkinshaw and Shanti, 1996; Tucker, 2001; Merriman *et al.,* 2003; Boggs, 2009). They are either exposed at the surface or are found under a thin veneer of soil over a third of the land area (Franklin, 1981; Boggs, 2009). Shales are characterised by a fine laminated structure which imparts fissility approximately parallel to bedding and has the tendency to split parallel to bedding (Walkinshaw and Santi, 1996).

Conversely, since mudrocks are easily weathered, they are frequently covered in vegetation and poorly exposed (Tucker, 2001). It is a fine-grained detrital sedimentary rock which is formed from the consolidation of clay, silt and mud (Hopkins and Beckham, 1998). Shale is a laminated and fissile rock whilst mudstones are the indurated blocky equivalent of mud and lacks fissility (Taylor and Spears, 1981; Tucker, 2001). Historically, the term "shale" is used as a member of a class (i.e. as a laminated clayey rock) and as a class name for fine grained siliciclastic sediments (Tourtelot, 1960; Taylor and Spears, 1981; Boggs, 2009). Several authors (e.g. Lundegard and Samuels, 1980; Spears, 1980 and Stow and Piper, 1984) have considered the dual use of the term in this way to be confusing. For example, Lundegard and Samuels (1980) suggested that fissility is a weathering phenomenon and should not be used to classify rocks from below the surface. They propose the practical solution of using stratification or lamination, rather than fissility, to differentiate between shale and stone. Potter *et al.* (2005) have recommended that the term mudstone be used as the general class name for fine-rained rocks. Mudrocks are those fine grained sedimentary rocks which contain more than 50 % clastic grains of less than 60 μm in size. For the purpose of this study, the term shale will be used which describes a fine grained sedimentary unit which displays the property of fissility. The term

mudrocks and mudstones will be used to describe a fine grained sedimentary unit which lacks the property of fissility.

3.3 Geology of shales and mudrocks

3.3.1 Mineralogy and Geochemistry of shales and mudrocks

Previously, little interest was undertaken or known about the depositional environments and likely palaeocurrents of fine grained sediments (Hardwick, 1992). These fine grained sediments were studied in terms of their bulk properties which include its mineralogical and chemical composition. As a result of their fine grained size, the study of mudrocks and shales requires detailed laboratory analyses (Tucker, 2001). These laboratory methods include X-ray diffraction, X-ray fluorescence and scanning electron microscopy (Hardwick, 1992). The mineralogical composition of shales as stated by Merriman *et al*. (2003) are affected by the diagenetic processes which are associated with its burial. This section focuses on the mineralogical and chemical composition of mudrocks and shales.

3.3.1.1 Mineralogy

Tucker (2001) stated that detailed laboratory tests are required to determine the mineralogy of shales and mudrocks. Shales and mudrocks are composed of clay and non-clay minerals. Shale consists of varying amounts of clay minerals, quartz, feldspars and carbonates and contains minor amounts of organic material and accessory minerals such as gypsum and sulphides (Yaalon, 1961; Huang, 1962; Hopkins, 1988; Merriman *et al.,* 2003; Boggs, 2009). The non-clay minerals which are found in shales consists of feldspars and quartz whereby quartz is the most abundant and frequent constituent (Bell and Maud, 1996). The typical clay minerals which are found in shales and mudrocks are chlorite illite, kaolinite and montmorillonite (Boggs, 2009).

During early investigations, Clarke (1924) showed in his average analyses of shales that shales are composed approximately of 22% quartz, 25% clay minerals and 30% feldspars. However, Clark's (1924) higher measurement of feldspars was likely to occur from the potash present within sericite (Yaalon, 1961). Later, Krynine (1948) stated that shales are composed of 50% quartz, 35% clay and 15% of authigenic minerals. Pettijohn (1967) later showed in his average analyses that shales are composed of equant proportions (33%) of clays, quartz and feldspars and contains minor amounts of carbonates, iron minerals and organic material. Based on the investigations mentioned above, it seems that the general composition of shales are limited which contains varying amounts of each mineral. A description of the common minerals found in shales and mudrocks is shown in Table 3.1. Quartz and illite are stable allogenic minerals and transported to their site of deposition whilst chamosite, chlorite and chalybite appear to be of synthetic origin (Wilson, 1983). Chamosite, chlorite and chalybite have formed from the deposition and consolidation of shales. Hopkins (1988) also stated that minerals such as calcite, dolomite and illite can be present which forms during the deposition of primary minerals.

Table 3.1: Description of the common minerals found in mudrocks or shales (modified after Hardwick, 1992; Boggs, 2009).

Mineral	Description
Quartz	Contains biogenic and authigenic silica. Silica may be released during the clay mineral transformations during the early diagenesis in marine sediments. Makes up 20-30 % of the average shale.
Feldspar	Mixture of authigenic and detrital material. Potassium is more resistant and dominates over other potassium - rich feldspars. Less abundant than quartz.
Iron oxides and hydroxides	Present as grain coatings and has a strong influence on the overall colour of the lithified sediment. Haematite is found in older sedimentary rocks whilst hydrous forms such as goethite may dominate in weathered rocks and younger strata.
Sulphides	Pyrite is the most abundant type of sulphide and forms under reducing conditions. Abundant in marine shales.
Sulphates	Gypsum and anhydrite are present but tend to be restricted stratigraphically to evaporite sequences.
Carbonates	Present as discrete clasts or chemically precipitated cements. Calcite (common in marine shales) and dolomite (important cementing agent in some shales) are present whilst siderite forms authigenically in brackish and partly reducing environments.
Gypsum	Present on the bedding planes of weathered shale
Organic material	Accounts for 2-10 % of carbonaceous matter in shale and source of hydrocarbons
Clay minerals	Kaolinite forms under strong leaching conditions; smectite is an expandable clay which alters to illite during burial, muscovite then weathers to illite during burial, chlorite forms particularly during burial diagenesis whilst vermiculite may convert to corrensite and finally to chlorite during burial.

The mineral composition of shales and mudstones are known to vary markedly with grain size. Quartz tends to be more abundant in coarser grained mudstones and shales whereas clay minerals tend to be more abundant in finer-grained mudstones and shales (Boggs, 2009). The mineral composition may vary owing to the tectonic setting or depositional environment. Bhatia (1985) reported that quartz ranges from 17% in passive-margin shales to as much as 46% in shales which are deposited in oceanic-arc shales to more than 75% in passive-margin shales. The common clay minerals which are found in shales and mudrocks are illite, kaolinite, montmorillonite and chlorite. Kaolinite often forms in slightly acidic environments whilst illites and chlorites become more stable in alkaline environments (Hardwick, 1992). Rowsell and De Swardt (1976) found that in the Ecca strata of the Karoo basin, the dominant clay minerals are illite and chlorite in the southern and northern part of the basin whilst the mixed layer montmorillonite-illite occurred more often in the northern part than the southern part of the basin.

Geochemical tests were performed on shales from the Reconcavo basin and the Amazon Basin in Brazil to determine their geochemical composition. The analyses of the shales of the Amazon Basin showed that these shales are composed of montmorillonite, mica and kaolinite whilst shales of the Reconcavo Basin contained quartz and chlorite (Marques *et al.,* 2005). Similarly, the results from X-ray diffraction tests which were performed on the Makarudi shales also showed composition of mixed layer illite/smectite, kaolinite and quartz (Agbede & Smart, 2007). The soils have medium to high percentage of mixed-layer illite/smectite, a high percentage of kaolinite and a small percentage of

illite (Agbede and Smart, 2007). Additionally, the ethylene glycol treatment suggests that the mixed layer clay minerals are expansive. These analyses also showed that the soil consists predominantly of silica, iron oxide, quartz (SiO_2) and aluminia (Al_2O_3) (Agbede and Smart, 2007).

Nandi *et al.* (2009) performed geochemical tests to characterise the Sevier and Rome Shale in East Tennessee. Analyses based on X-ray diffraction tests revealed that the Sevier Shale is composed of quartz, chlorite, gypsum, pyrite, illite, calcite and mixed layer kaolinite whilst the Rome Shale is composed of quartz, feldspar, pyrite and illite. Energy dispersive X-ray results showed that elements such as oxygen, silicon, aluminium, calcium, iron, magnesium, sodium, potassium and sodium were found in Sevier Shale samples (Nandi *et al.,* 2009*)*. The weathered Sevier Shale showed that it had less calcite and more gypsum which is an alteration product of pyrite. The presence of smectite or chlorite could not be justified because their peaks occupied the same position as seen by the X-ray diffraction results (Nandi *et al.,* 2009*)*. The durability of the Rome Shale was explained by the higher amount of quartz and orthoclase. Scanning electron microscope analyses performed on these shales showed calcite infilling in micro-fractures. The infilling of calcite is very susceptible to weathering particularly in acidic environments, with calcite having a significant effect on the physical strength of a rock mass (Nandi *et al.,* 2009*)*.

In addition, the X-ray analyses of mudrocks from near Tow Law and Kirkheaton in Britain revealed that these mudrocks are composed of quartz, feldspars, chlorite, kaolinite and illite (Bell *et al.,* 1996). These analyses also showed that the principal non-clay mineral is quartz whilst the principal clay mineral is kaolinite. Rowe *et al.* (2012) determined the chemistry of shales from the Barnett Formation, the Woodford Formation and the Eagle Formation by performing a series of X-ray fluorescence tests and compared these values to international standards as shown in Table 3.3 and Table 3.2 respectively. Table 3.2 shows that the elements found in these formations are much higher than the international standards except for calcium.

Table 3.2: X-ray fluorescence results of three formations containing shales (adapted from Rowe *et al.,* 2012).

Element (%)	Barnett Formation	Eagle Ford Formation	Woodford Formation	International Standard
Magnesium	2.91	5.26	1.58	0.45
Aluminium	6.71	4.13	4.84	3.53
Silicon	21.25	21.96	19.46	13.18
Phosphorus	0.08	0.25	0.53	0.09
Sulphur	2.68	2.89	1.25	2.07
Potassium	59.23	1.84	1.05	0.88
Calcium	3.21	9.09	16.99	22.03
Titanium	0.30	0.19	0.27	0.22
Manganese	0.03	0.17	0.02	0.02
Iron	4.33	2.77	2.09	2.00

Table 3.3: X-ray diffraction results of the Devonian-Carboniferous marine shales (modified after Ding *et al.,* 2012).

	Quartz, Feldspar and Pyrite	Clay minerals	Carbonates
Barnett Formation and Woodford Formation	< 40 %	< 50 %	> 25 %
Bossier Formation	20-80 %	20- 80 %	< 25 %

3.3.1.2 Chemical composition

The average chemical analyses of the major oxides of shales as determined by Clarke (1924) and Pettijohn (1975) and presented by Hardwick (1992), from laboratory investigations is shown in Table 3.4. Silica is a major component of clay and silicate minerals (Hardwick, 1992). Alumina, magnesium and iron are found in clay and silicate minerals whilst calcium oxide is present in calcite and dolomite. Carbon and Sulphur are derived from organic material whilst carbon dioxide is released from the breakdown of carbonates (Hardwick, 1992).

Since the chemical composition is a direct function of mineralogy, and mineral composition varies with grain size, the major element chemical composition of shales and mudstones is related to its grain size. Coarser grained shales and mudstones contain more quartz than do finer-grained ones thus tend to have higher SiO_2 content. Finer-grained shales and mudstones contain a higher percentage of clay minerals which results in aluminium rich and lower SiO_2 concentrations. Calcium, magnesium and potassium tend to be concentrated in the finer fraction of shales and mudstones. However, the calcium and magnesium content can be strongly influenced by secondary carbonate cement which may be particularly abundant in coarser-grained mudstones and shales. Boggs (2009).

Table 3.4: Average chemistry of shales (modified after Hardwick, 1992).

	Weight (%)	
Oxide	Clarke (1924) 78 shales	Pettijohn (1975) 69 shales
SiO_2	58.1	58.5
Al_2O_3	15.4	17.3
Fe_2O_3	6.4	7.4
MgO	2.4	2.6
CaO	3.1	1.3
Na_2O	1.3	1.2
K_2O	3.2	3.7
TiO_2	0.6	0.8
P_2O_5	0.2	0.1
MnO	Trace	0.1
CO_2	2.6	1.2
S	0.6	0.3
C	0.8	1.2
H_2O	5.0	3.9
Total	99.7	99.6

3.3.2 Textural aspects of shales and mudrocks

Texture is a fundamental attribute of siliciclastic sedimentary rocks and encompasses the three fundamental properties of sedimentary rocks: grain size, grain shape and fabric (Boggs, 2009). In a soil profile, the variation in texture from horizon to horizon can be used to decipher the pedogenic and geological history of a soil (Birkeland, 1974). Fine grained terrigenous clastic sediments do not have a wide range of textures and structures because of the finer grain size, bioturbation and as a result of the cohesive properties of mud (Tucker, 2001). The sedimentary structures which are found in mudrocks and shales consists of lamination, erosional structures which are cut into mud, slump structures, desiccation and syneresis cracks, biogenic structures and rain-spot prints (Tucker, 2001) This section deals with the physical texture and micro-crystalline texture of shales and mudrocks.

3.3.2.1 Physical texture of shales and mudrocks

Wilkins (2013) stated that texture, in terms of grain size, is the most significant property when classifying and describing a single particle in the field. Texturally, clay is defined as all materials finer than 4 μm, silt ranges in size from 4-63 μm and sand ranges from 63 μm - 2 mm. Shales are composed of clay to silt sized particles whereby the size of each particle ranges between 0.06-0.004 mm. A common texture of shales is that of preferred orientation of clay minerals and micas which are parallel to bedding (Tucker, 2001). This texture is a result of the deposition of clay flakes parallel to bedding (Bell, 1993; Tucker, 2001).

Boggs (2009) stated that the shape of the small particles which make up mudstones, unlike the shapes of sand size and larger particles, are little modified by sediment erosion and transport. Kuenen (1959; 1960) demonstrated that very small quartz particles do not become rounded very effectively by any type of aeolian or stream transport. As a result, the shapes of the fine-size and clay-size particles in mudstones reflect mainly the original shapes of the detrital particles, largely unmodified by transport abrasion, or they reflect the shapes of the minerals generated during diagenesis. Thus, most particles in mudstones are very angular (Boggs, 2009). Clay minerals and fine micas have low sphericity (Boggs, 2009). Lamination is a common sedimentary structure which is found in shales and mudrocks (Tucker, 2001). Laminae are defined as strata and have a thickness of less than 10 mm (Boggs, 2009). It results from the variations in grain size and/ or changes in the composition (organic matter or clay content) of a shale or mudstone (Tucker, 2001; Boggs, 2009). Laminae of specific sizes may be deposited in relatively short periods of time from low-density turbidity and suspension currents. Some laminae may develop as a result of fluctuations in sediment supply and/or biological activity over longer periods of time (Tucker, 2001). Mudrocks which contain organic laminae may be produced by seasonal microbial blooms. Parallel laminae are known to form both by deposition from suspension and by traction currents (Boggs, 2009).

An important feature of the Precambrian shales is that they are undisturbed by bioturbation which allows for the development and preservation of depositional structures (Tucker, 2001). Similarly, Schieber (1986) has provided evidence that Carbonaceous shales of the Precambrian are formed beneath benthic microbial mats. Mudrocks also contain nodules of various shapes and are commonly composed of calcite, siderite, calcium phosphate and with some original sediment (Tucker, 2001). These nodules or concretions form whilst sediments are still soft and uncompacted and, within the sediment from the localised precipitation of cement from pore waters during diagenesis (Tucker, 2001). These features are represented by uncrushed fossils within the nodules and from the folding of laminae in the mudrock around the nodule which indicates that compaction took place after the growth of these nodules (Tucker, 2001).

3.3.2.2 Micro-crystalline texture of shale

Shales are composed of very fine material which makes it very difficult to determine its texture by using an ordinary magnifying lens. As a result of its fine grained nature, petrographic analyses of all but the coarser-grained mudstones are difficult (Boggs, 2009). Geochemical tests consisting of scanning and transmission electron microscopy (Tovey *et al.,* 1995) and X-ray diffraction are usually used to determine the microcrystalline texture of shales (Krinsley, *et al.,* 1998; Boggs, 2009). However, these tests are expensive and are seldom performed (Boggs, 2009). An electron microscope photograph of a mudstone which contains quartz and clay minerals is shown in Figure 3.1.

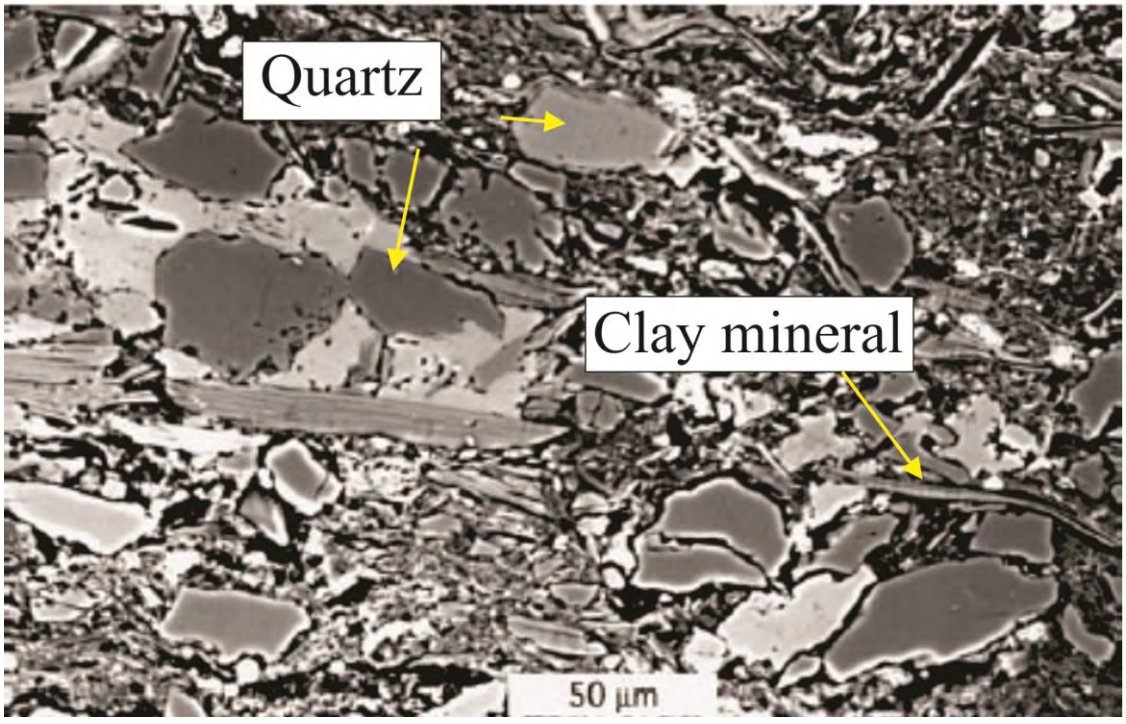

Figure 3.1: Electron microscope photograph of a mudstone which contains various sized quartz (blocky) and clay minerals (flaky) (adapted from Boggs, 2009; courtesy of David Krinsley).

Since shales contain high concentrations of clay minerals that have platy or flaky shapes, they may exhibit microfabrics which result from the preferred orientation of flaky clay minerals (Boggs, 2009). Electron microscopy analyses performed by Sudo *et al.* (1981) revealed that most clay minerals have platy, flaky, or acicular shapes.

Laboratory testing which includes X-ray diffraction, microtomography and scanning and transmission electron microscopy techniques were used to characterise mircostructures and anisotropy of three deeply buried Qusaiba shales from the Rub'al Khali basin. From these analyses, kaolinite, illite-smectite, illite-mica and chlorite show strong preferred orientation (Kanitpanyacharoen *et al.,* 2011). On the other hand, feldspars, quartz and pyrite crystals showed random orientations and random distributions. Similarly, Tucker (2001) stated that the preferred orientation of clay minerals and micas can also be seen in thin-section by areas of common extinction. Kaolinite, illite-mica and chlorite generally show stronger texture whilst nanocrystalline illite-smectite shows weaker preferred orientation. Samples rich in clay generally impart a stronger texture. Images of the Qusaiba shales which were taken using a transmission electron microscope are shown in Figure 3.2.

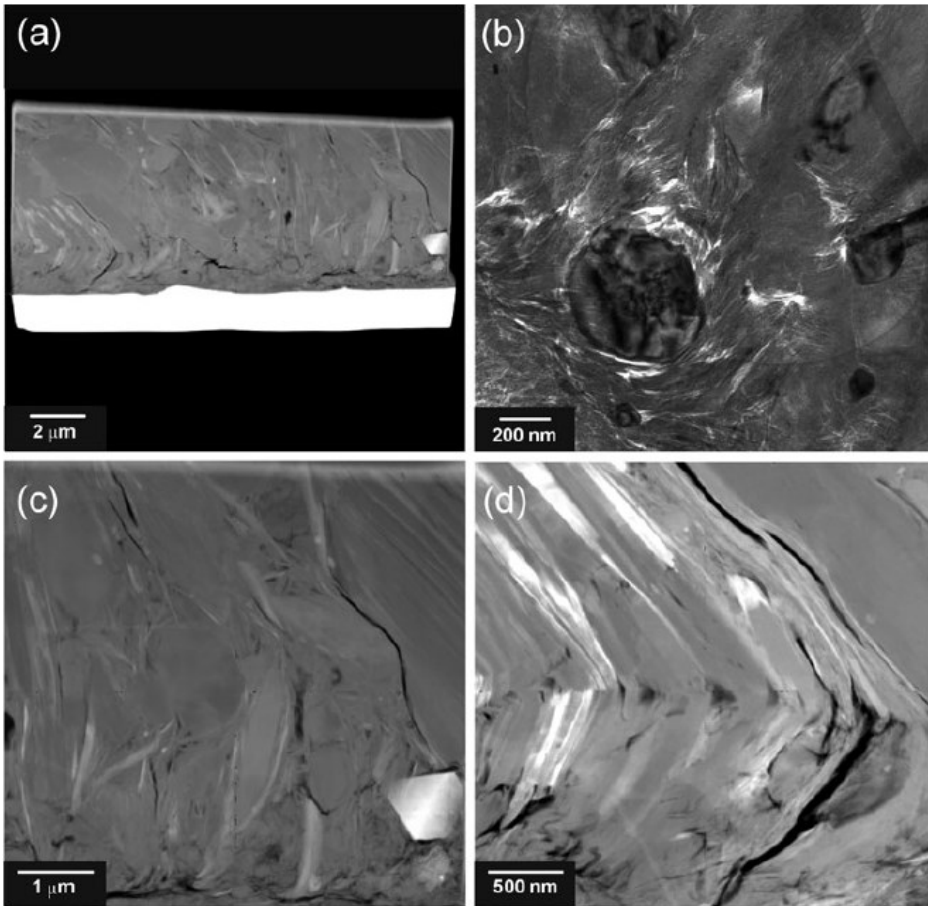

Figure 3.2: Microstructures of Qusaiba Shales where a) a sample cut perpendicular to the bedding plane, b) a quartz grain surrounded by phyllosilicates, c) phyllosilicates and a quartz grain and d) a stack of phyllosilicates which indicates deformation caused during compaction (adapted from Kanitpanyacharoen *et al.,* 2011).

3.3.2.3 The property of fissility

Fissility refers to the tendency of a rock to split along smooth planes which may be parallel to bedding or to a tectonically exposed fabric (Hardwick, 1992). Bates and Jackson (1980) defined fissility as the property possessed by some rocks of splitting easily into thin layers along closely spaced, roughly planar, and approximately parallel surfaces. The term fissility is used to describe a rock which is capable of being easily split along closely spaced planes and by the frequency of splitting, i.e. the thickness of the layers between the fissile planes or plane of parting (Boggs, 2009). Potter *et al.* (1980) used the term fissile to indicate a class of parting, with parting defined as the tendency of rock to split along lamination or bedding which is enhanced by weathering. In summary, fissile fine-grained rocks are those that tend to split relatively easily into thin, approximately parallel layers that range in thickness from about 0.5-1 mm.

The alignment in the orientation of the micaceous clay minerals results from compaction processes and by the presence of laminations (Boggs, 2009). Curtis *et al.* (1980) proposed that the preferred orientation in clay-rich sediments result mainly from compaction strain. They suggested that fissility is not due to clay-mineral orientation, instead it is related to fine-scale lamination. The problem with ascribing clay-mineral orientation to post-depositional compaction is that shales which do not display oriented fabrics can occur stratigraphically below other shale units which display orientated fabrics (Boggs, 2009). Lithification processes cause the additional alignment or parallel orientation of the domains in the muds deposited in anoxic environments, thereby producing fissility (Boggs, 2009). In oxic environments, the domains become more closely packed and do not destroy the random orientation of the domains (Boggs, 2009). Thus, muds which are deposited in oxic environments form non-fissile mudstones.

Fissility is an important environmental indicator which provides information on the formation of mudrocks and shales (Hardwick, 1992). Mud laminae usually has a high preservation potential due to their cohesiveness but will be destroyed by bioturbation (Tucker, 2001). Mudrocks deposited with an inactive fauna is unlikely to become fissile therefore shales are those mudrocks which display the property of fissility (Hardwick, 1992). The degree of fissility as shown by modern mudrocks may be related to weathering of the outcrop (Tucker, 2001).

Spears (1980) conducted a study on shales exposed on the surface compared to those found in boreholes of Carboniferous shales. Spears (1980) showed that the surface samples of shale were more fissile than the shales which were found in boreholes despite containing laminations of comparable thicknesses to fissility. In this case, fissility appears to be a surface (weathered) expression of laminations observed in the fresh samples (Hardwick, 1992). Shales analysed within this study did not appear laminated when samples were taken at a greater depth and were observed to break irregularly into blocky fragments. Bell (1993) further stated that moderate weathering increases the fissility of

shale by partially removing the cementing agents along the planes of laminations or by expansion due to the hydration of the clay particles. Intense weathering produces a soft claylike soil (Bell, 1993).

3.4 Shales of the Pietermaritzburg Formation

Shales of the Pietermaritzburg Formation are distributed throughout the Durban and Pietermaritzburg area. In the Durban area, shales of the Pietermaritzburg Formation exhibit rapid variations in the mineralogy through the succession of beds (Bell and Maud, 1996). The changes in the mineralogy of these shale beds are seen by a change in the degree of fissility. The variation of these minerals throughout this formation is limited and consists of five main minerals namely quartz, illite, chamosite, chlorite and chalybite (commonly known as siderite) (Wilson, 1983; Bell and Maud, 1996; 1997). Small percentages of carbon and pyrite are found in this formation. Carbon is a minor constituent mineral, ranging between 1-4 % and reflects a reducing nature of their depositional environment. Pyrite is sometimes found between the joints and bedding planes in the fresh shale (Wilson, 1983).

Most shale formations, especially from the Ecca Group or Dwyka Group contain a significant clay fraction (≥ 15%). These clay minerals result from the decomposition of the constituent minerals which are found in shale (Nicols, 2009). Fissile beds are found to alternate with thinner hard non-fissile beds of shales of the Pietermaritzburg Formation. In this formation, small quantities of degraded illite are interlayered within the main illite component of shales (Bell and Maud, 1996). The degree of fissility is attributable to the high proportion of quartz and illite (Bell and Maud, 1996). Futhermore, Drennan (1963) stated that Ecca shales which are fissile usually have a low amount of Fe in it. Conversely, the non-fissile beds contain a lower proportion of quartz and illite. Chamosite, chlorite and chalybite are particularly found in the non-fissile beds and tend to act as cementing minerals (Bell and Maud, 1996). Montmorillonite has a high absorption for water as compared to kaolinite and illite (Ollier, 1984). The lower affinity for water by illite, which is a dominant clay mineral in shales of the Pietermaritzburg Formation could reduce the potential problems/degradation that are caused by illite.

Toniolo (2012) found that shales from the Pietermaritzburg Formation contains a high percentage of quartz (>40%) which is similar to results obtained by Krynine (1948), Bhatia (1985) and Bell *et al.* (1996). Laboratory investigations performed by Drennan (1963), Wilson (1983) and Toniolo (2012) on shales of the Pietermaritzburg Formation revealed that the common clay minerals are kaolinite and illite, to shales that are found in other countries. For example, kaolinite is the common clay mineral that is found in shales from the Amazon Basin in Brazil (Marques *et al.,* 2005) and in the Makarudi Shales (Agbede and Samrt, 2007). The minor minerals that are present in shales from the Pietermaritzburg Formation to Sevier Shales and Rome Shales in Tennesse are pyrite and chlorite

3.5 Summary

A detailed description of the mineralogy, chemical composition and the textural properties of shales and mudrocks has been provided in this chapter. It also presented the studies performed on shales of the Pietermaritzburg Formation. The next chapter presents the geotechnical properties of shales and mudrocks and their associated geotechnical problems.

Chapter 4

Geotechnical properties of shales and mudrocks and their geotechnical problems

4.1 Introduction

Most geological materials in their *in-situ* form exhibit rock-like behaviour. When disturbed, some are able to preserve the engineering capability whilst other materials degrade to soil (Walkinshaw and Santi, 1996). In geological terms, Marr (2000) stated that the soil and rock materials on the earth's surface are disturbed and degradable and that these materials will modify over a geological time frame. However, on the human time scale, only comparatively rapid disintegration of a strong or hard rock material into a weaker soil-like material is of major concern (Walkinshaw and Santi, 1996). This characteristic behaviour of highly degradable materials is important during the evaluation of the engineering performance of structures and in ground engineering (Taylor and Spears, 1981; Walkinshaw and Santi, 1996; Santi and Higgins, 1998; Hajdarwish and Shakoor, 2006).

Shales are highly degradable materials that degrade easily when exposed to the physical environment (water and air) (Taylor, 1948; Santi and Higgins, 1998). Their geotechnical properties have a significant influence in the engineering and construction industry. Due to the limited research conducted on shales of the Pietermaritzburg Formation, this chapter presents the geotechnical properties of shales and mudrocks. Additionally it presents the geotechnical problems associated during the sampling and use of shales when used as aggregates

4.2 Factors affecting the strength, durability and hardness of shales

The mineralogy and the geometric arrangement of particles affect the slaking and strength of weak rocks (Koncagul and Santi, 1999). The difficulty that is associated with predicting the strength of shales is that their microfabric includes features of fragmented rocks (composed of grains e.g. sandstones) and argillaceous rocks such as shales and claystones. Therefore, it is difficult to determine the geomechanical characteristics of shales in comparison to other rocks such as sandstone. The factors that affect the strength and durability of shales are presented below.

4.2.1 Grain size

Fine-grained sediments are more susceptible to breakdown and at higher rates than coarse grained sedimentary materials (D' Appolonia Consulting Engineers, 1980). However, finer grained samples are able to withstand higher compressive loads (Brace, 1961). This is due to a higher number of grain to grain contacts between the grains (minerals) of fine grained rocks as compared to coarse grained rocks (Koncagul and Santi, 1999).

4.2.2 Grain shape

Rocks that are characterised by rounded grains have proven to be more durable than rocks characterised by less rounded grains. This is because rocks that contain sharp edges are exposed to a greater degree of abrasion during the slake durability test (D' Appolonia Consulting Engineers, 1980). Depending on the degree of bonding along the edges of the angular grains, the angular shape of these grains may provide a great deal of interlocking therefore increasing its strength (Konagul and Santi, 1999). If it is assumed that the degree of bonding and the mineralogy of the grains and cement are the same, then a rock which contains angular grains should be stronger and harder but less durable than a rock containing rounded grains (Koncagul and Santi, 1999).

4.2.3 Mineralogy of grains

It is believed that rocks which contain a higher abundance of quartz often display a higher degree of strength and durability. Several authors (Handlin and Hager, 1957; Bell, 1978; Barbour *et al.,* 1979; Koncagul and Santi, 1999) have not found a definite correlation between the quartz content and strength but have suggested that the structural interlocking of the quartz grains influences the uniaxial compressive strength. Since clay minerals comprise the dominant portion of shales, the rock-slaking behaviour will differ based on the amount and type of clay minerals that are found in a shale (Koncagul and Santi, 1999).

4.2.3 Porosity

Vallejo *et al.* (1994) have stated that shales with larger pores are more resistant to slaking than shales with small pores. They observed that behaviour is seen by shales which are composed of kaolinite, which slake as a result of pore air compression that break up the hydrogen bonds that connect the individual bonds together. However, Price (1960) and Dube and Singh (1972) stated that the strength properties of all sedimentary rocks decrease with an increase in porosity. Large pores results in a lower compressive strength as stated by Deere and Miller (1966) and a lower hardness and crushing strength of the shale samples during the Point Load Strength test (Vallejo *et al.,* 1994). Studies performed by Lashkaripour and Dusseault (1993) showed that the strength of shales increases with a decrease in porosity.

4.3 Basic index properties of shales and mudrocks

The Atterberg limit is one of the basic index properties of a soil material. The Atterberg limits of shales and mudrocks have been investigated by several authors (e.g. Cripps and Taylor, 1981; Bell and Maud, 1996; Hopkins and Beckham, 1998 and Aghamehlu *et al*., 2010). A summary of the results of their findings is presented in Table 4.1. Since most of the engineering properties of weathered

mudrocks do not show much variation throughout a geological column, values are given in the weathered and unweathered states (Cripps and Taylor, 1981).

Table 4.1: The Atterberg limits of the residual soil material from various shales and mudrocks.

Kentucky Shales (modified after Hopkins and Beckham, 1998)								
	Weathered shales				Unweathered (fresh) shales			
	Upper drakes	Kope	Tradewater	New providence	Lisman	Nancy	Crab orchard	Newman
Liquid limit	24	36	28	40	29	31	22	24
Plastic limit	15	15	7	15	7	11	8	7
Plasticity index	9	21	21	25	22	20	14	17

British Mudrocks (modified after Cripps and Taylor, 1981)						
	Unweathered material			Weathered material		
	Coal measures shale	Coal measures mudstone	Weald clay	Coal measures shale	Coal measures mudstone	Weald clay
Liquid limit	42-45	39-49	42-82	44-51	42	45
Plasticity index	12-19	9-19	28-32	37-87	24-53	28-32

British mudrocks (Bell *et al.,*1996)		
	Lower coal Measures (Tow Law)	Middle Coal Measures (Kirkheaton)
Liquid limit	Range: 27-34	Range: 31-41
Plastic limit	Range: 12-16	Range: 15-25
Plasticity index	Range: 16-18	Range: 15-16

Pietermaritzburg Formation Shales (Bell and Maud, 1996) (Mixture of fresh and weathered shales)	
Liquid limit	Range: 35-70
Plastic limit	Range: 18-35
Plasticity index (%)	Range: 15-35
Linear shrinkage	< 15

Indicator test data for residual mudrock of the Pietermaritzburg Shale Formation (NBRI, 1976)	
Liquid limit (%)	24-70
Plasticity index(%)	5-36
Linear shrinkage (%)	3.7-16

Abakaliki shales (modified after Aghamehlu *et al.,* 2010) (Mixture of fresh and weathered shales)			
	Ntezi Abba	Iyiokwu River	Juju Hill
Liquid limit	54	53	49
Plastic limit	18	15	15
Plasticity index	36	38	34

Table 4.1 presents the range of values obtained from tests performed to determine the Atterberg limit of various shales and mudrocks. The liquid and plastic limit of the shales presented in Table 4.1 show that shales, in general, have a high liquid limit and plastic limit.

Based on the classification of Ola (1980), the residual soil samples which have been tested of the Abakaliki shales are classified as having high to very high plastic limits. Soil samples of the Abakaliki shales have much higher plasticity indices than the soil samples from the Kentucky Shales. In addition, the liquid limits of the British mudrocks are much higher than the liquid limit of the Abakaliki and Kentucky shales. Sowers and Sowers (1970) noted that a plasticity index greater than 31 should be considered high. Thus, the geotechnical assessment by Aghamelu *et al.* (2010) showed that the Abakaliki shales is of high plasticity, most probably, due to its content of expansive clay minerals. Aghamelu *et al.* (2010) stated that materials with high plasticity (e.g. the Abakaliki Shale) includes swelling on moisture influx.

4.4 Strength and durability of shales and mudrocks

4.4.1 Durability of shales and mudrocks

One of the greatest variations that is found in the engineering properties of mudstones can be attributed to the effects of weathering (Bell *et al.,* 1996). Shales are affected by many factors such as the clay content, the degree of weathering, shrink-swell behaviour and by the intensity of fractures. Thus, shales exhibit properties that range from low strength, low durability fissile rocks to hard and compact units (Dick *et al.*, 1994; Yasar and Erdogan, 2004; Santi, 2006 and Shalabi *et al.*, 2007). Hence, durability is one of the most important engineering properties of mudstones when used in the construction industry. Since slaking is one of the principle causes of the breakdown of shales and mudrocks, this section presents the results of slake durability tests that were performed on shales and mudrocks from various localities (e.g. Kentucky shales in the U.S.A and British mudrocks in Britain).

Slake durability tests were performed on mudrocks of the Lower coal Measures near Kirkheaton, England. The results showed that the majority of samples tested from Tow Law have high or extremely high slake durability indices (SDI) ranging from 80 - 96 % and suggest that these mudrocks do not disintegrate easily (Bell *et al.,* 1996). Similarly, slake durability tests were done on shales of various formations in Kentucky in U.S.A. Based on the results obtained, the Kope shales and Crab Orchard shales have very low SDI as compared to the other formations which implies a highly degradable nature. The Kope shales have a wide range of slake durability indices which indicates a highly variable nature of the shale samples. Therefore, these shales are expected to disintegrate and break down easily. The New Albany Formation, the Drake Formation and the Nancy Formation as shown in Table 4.2 display high slake durability indices and imply that these shale materials do not degrade as easily as compared to the Kope shales and the Crab Orchard shales (Hopkins and Beckham, 1998). Similarly, the results obtained by Koncagul and Santi (1999) showed that the Red shales and Gray shales from Pennsylvania have high to very high SDI's. However, the Grey shales display a larger range in their SDI which implies a variable nature than the Red shales.

Table 4.2: Slake durability index (SDI) of shales and mudrocks from different localities.

Kentucky shales (Hopkins and Beckham, 1998)								
	New Albany	Drakes	Kope	Henley	Crab Orchard	Nancy	New Providence	Osgood
SDI (%)	99	65 - 85	10 - 63	33 - 72	11 - 16	62 - 92	34 - 74	61 - 82
Breathitt shales (Koncagul and Santi, 1999)								
	Grey shales				Red shales			
SDI (%)	Range: (61 - 96)				Range: (96 - 98)			
British mudrocks (Bell *et al.,* 1996)								
	Lower Coal Measures (Tow Law)				Lower Coal Measures (Kirkheaton)			
SDI (%)	Range: 80-96				Range : 17-98			
Sevier and Rome shales (Nandi *et al.,* 2009)								
	Sevier shales				Rome shales			
SDI (%) I_D 2	90 – 98				93-99			
SDI (%) I_D 2	94 – 95				86 – 90			

Furthermore, the effects of short-term and prolonged weathering on the Sevier and Rome shales in East Tennessee were investigated by conducting slake durability tests (Nandi *et al.,* 2009). Based on the second cycle of slaking, the slake durability indices of the Sevier shale ranged from 90 - 98 % whilst the slake durability index for the Rome shale ranged from 93 - 99%. These results show that the Rome shales and Sevier shales are durable against short-term wetting and drying cycles. The 5th cycle of slaking represents the durability of a longer term of wetting and drying. The 5th cycle analyses showed that the Rome shales were generally more durable than the Sevier shales which are indicative of the presence of swelling minerals that have a significant influence on the degree of weathering as stated by Nandi *et al* (2009). Also, these results show the importance of conducting five cycles of slaking as compared to the proposed method by Santi (1998) of using the first cycle of slaking to predict further slaking cycles.

4.4.2 Point Load Strength

It is often very difficult to obtain suitable cores of shales for Point Load Strength and uniaxial compressive strength tests. Koncagul and Santi (1999) stated that this is due to the fissility of shales as they break easily during the coring process. Thus, coring becomes extremely difficult when the shale materials become saturated because water is required for the coring process. This is one of the reasons why shales are not tested in detail. Furthermore, Koncagul and Santi (1999) stated that it is easier to obtain core samples from fresh shales than weathered shales as weathered materials disintegrate easily.

The Point Load Strength test causes a material to fail in tension (Broch, 1983). Commonly, the Point Load Strength of a material is usually lower when samples are tested diametrically as compared to being tested axially (Bieniawski, 1975). The observed diametrical strength is lower than the axial

strength since the force applied by the individual platens are parallel to the lamination planes (anisotropy) as stated by Broch (1983) which reduces the force that is required to break shales. Failure usually occurs along these planes of weakness during loading (Koncagul and Santi, 1999).

The results of mudrocks from the Lower coal Measures near Kirkheaton and the Middle coal measures mudrocks in England showed that the Point Load Strength of the mudrocks were much lower when tested diametrically (Bell *et al.,* 1996). The axial strength of these mudrocks showed medium to high strength and the results are shown in Table 4.3. Similarly the Point Load Strength results obtained by Toniolo (2012) on shales of the Pietermaritzburg Formation show that the shale samples tested are characterised as medium to high strength. Page and Solesbury (1983) conducted Point Load Strength tests on shales of the Pietermaritzburg Formation for a proposed railway tunnel in KwaZulu-Natal. During their investigations, they found that the axial strength during Point Load Strength tests were higher than samples which were tested diametrically. Broch and Franklin (1972) found that the Point Load Strength decreases as the diameter of the cores increases.

Table 4.3: Point load strength results of some British mudrocks and shales of the Pietermaritzburg Formation.

Point Load Strength (MPa)				
Point Load Strength test	Lower coal measures (Bell *et al*., 1996)		Pietermaritzburg Formation shales (Toniolo, 2012)	Broch and Franklin (1972) classification
	Tow Law	Kirkheaton		
Axial	[0.74-13.23] {20}	[1.22-2.67] [10]	[1.86-7.33] {15}	Medium to high
Diametrical	[0.11-2.17] {20}	[0.09-0.37] [10]	[0.70-5.13] {15}	Medium to high

(): Range, []: No of samples tested

4.4.3 Shear strength of shales and mudrocks

In a broad perspective, the engineering properties of mudrocks and shales are influenced by their lithology, degree of weathering, exhumation and type and method of testing (Cripps and Taylor, 1981). The shear strength of a material refers to the ability of a material to resist a shear force without that material failing in shear (Craig, 2004; Wylie and Mah, 2004). The shear strength of a material is described in terms of the cohesion (c) and angle of internal friction (φ). Hajdawish and Shakoor (2006) stated that the shear strength is one of the most important properties for the design of engineering structures built on mudrocks or shales.

This section presents the shear strength of shales and mudrocks in terms of its undrained shear strength (c_u & φ_u), the effective shear strength (c' & φ') and the residual shear strength (c_r & φ_r). This section will focus on the shear strength of shales, mudrocks and clays since shales are formed in sedimentary basins by diagenetic processes which turn young clay sediments into compacted and

lithified shales (Gutierrez *et al.,* 2008) and, because they weather to a fine grained mass or soil as stated by Hopkins (1988) or a clayey gravel (Drennan, Maud and Partners, 2010) or to a normally-consolidated clay (Cripps and Taylor, 1981).

I) Undrained shear strength

The undrained shear strength parameters are conventionally used in bearing capacity calculations relating to clay soils (Taylor and Spears, 1981). This is on the basis that the most critical period will immediately follow construction, prior to the dissipation of the excess pore water pressures. The shear box test or the triaxial test can be used to determine the undrained strength of a material (Craig, 2004). The undrained shear strength of mudrocks are influenced by the major component minerals, the percentage of clay minerals, sample disturbance and anisotropy, exhumation, the degree of weathering, the lithology and thickness of the overburden, depth and by the type of cementing agents (Cripps and Taylor, 1981). A competent mudstone at the surface may well behave like a clay in a deep mining situation (Taylor and Spears, 1981). Burnett and Fookes (1974) found that in the London Basin, the undrained shear strength decreases in an easterly direction with an increase in the clay fraction in that direction. Conversely, Russel and Parker (1979) found negative correlations between the strength and the proportion of mixed layer clay. However, during their investigations, they found positive correlations between the undrained shear strength of mudrocks and the diagenetic cementing agents; calcite and pyrite.

Studies that have been performed by Ward *et al.* (1965) on the London Clay and on the Gault Clay by Samuels (1975) show the effects of sample disturbance on the undrained shear strength of these materials. Block samples that were obtained from the London clay had suffered fewer disturbances than open-drive samples. Also, block samples of the Gault Clay were 167 % stronger than open drive samples and 28 % stronger than those which were obtained from rotary coring (Figure 4.1).

Similarly, Samuels (1975) and Ward *et al.* (1965) stated that the undrained shear strength is affected by the orientation of the specimens during testing. Samuels (1975) found that the strength of the block samples which were tested horizontally were 25% stronger than those which were tested vertically. Additionally, Ward *et al.* (1965) showed that the undrained shear strength anisotropy was 46 % higher in horizontal samples than vertical samples and that the strength was 91 % higher than samples which were tested at an orientation of 45°.

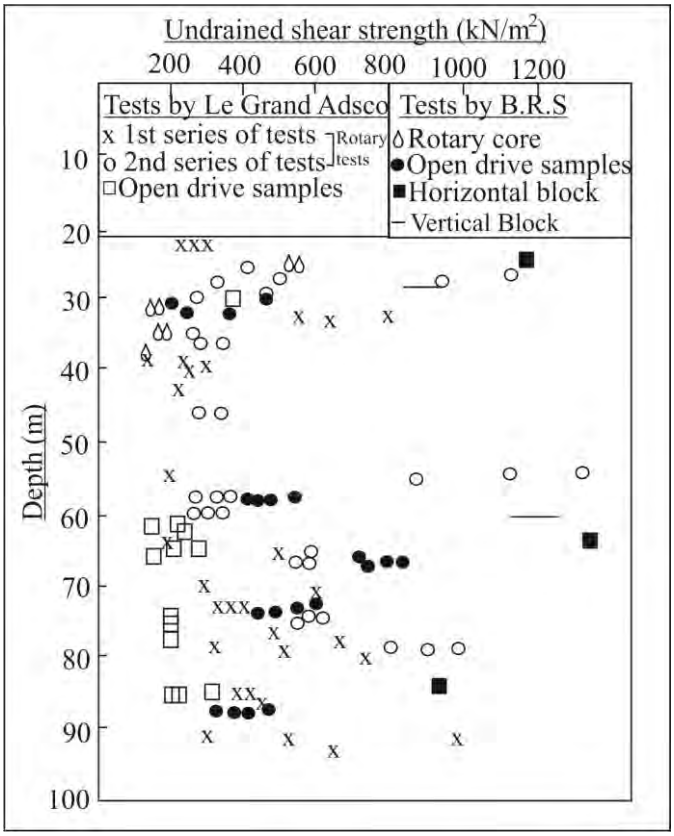

Figure 4.1: Undrained shear strength of 38 mm diameter triaxial samples of Gault Clay (modified after Samuels, 1975).

The results presented in Figure 4.2 demonstrate the significance of weathering and how weathering reduces mudrocks to materials with much of the same properties. For the unweathered material, the undrained shear strength ranges from firm clays to stiff rocks (Anon, 1977). The undrained strength generally increases with depth in any one horizon. The profiles which show the extent of this variation, was observed by the Oxford Clay, the Lias Clay, the Gault Clay and the London Clay. In the case of the London Clay, the undrained shear strength increased from 225 kN/ m^2 to 575 kN/ m^2 from a depth of 23 m to 46 m. Ward *et al.* (1965) earlier showed that the undrained shear strength of the London Clay increases with an increase in depth. Chandler (1972) showed that the undrained shear strength of the Upper Lias Clay was reduced from 200 kN/ m^2 to 63 kN/ m^2 during progressive weathering.

Chandler (1969) has also shown the weathering related modifications to the stress-strain curve during triaxial testing on the Keuper Marl. The expected lower undrained strength of the Kimmeridge Clay is in light of its complex loading history in which reloading with recent deposits has allowed for the removal of the original overburden (Cripps and Taylor, 1981). The comparatively high water content of the Lias Clay is believed to result in its low undrained strength. In Tertiary sediments, smectite is more abundant than mixed layer clays whilst the reverse is true for Mesozoic rocks. Smectites are absent in rocks older than the Carboniferous, while mixed layer clays do not appear to have been

found in rocks which are older than the Silurian. Illite, kaolinite and chlorite are ubiquitous and clearly are the stable species (Bùhmann, 1992). A summary of the undrained shear strength parameters of mudrocks from the United States and British Mudrocks and shales from Poland respectively are presented in Table 4.4. The effects of geological age and depth on the undrained strength of U.K. mudrocks is shown in Figure 4.3.

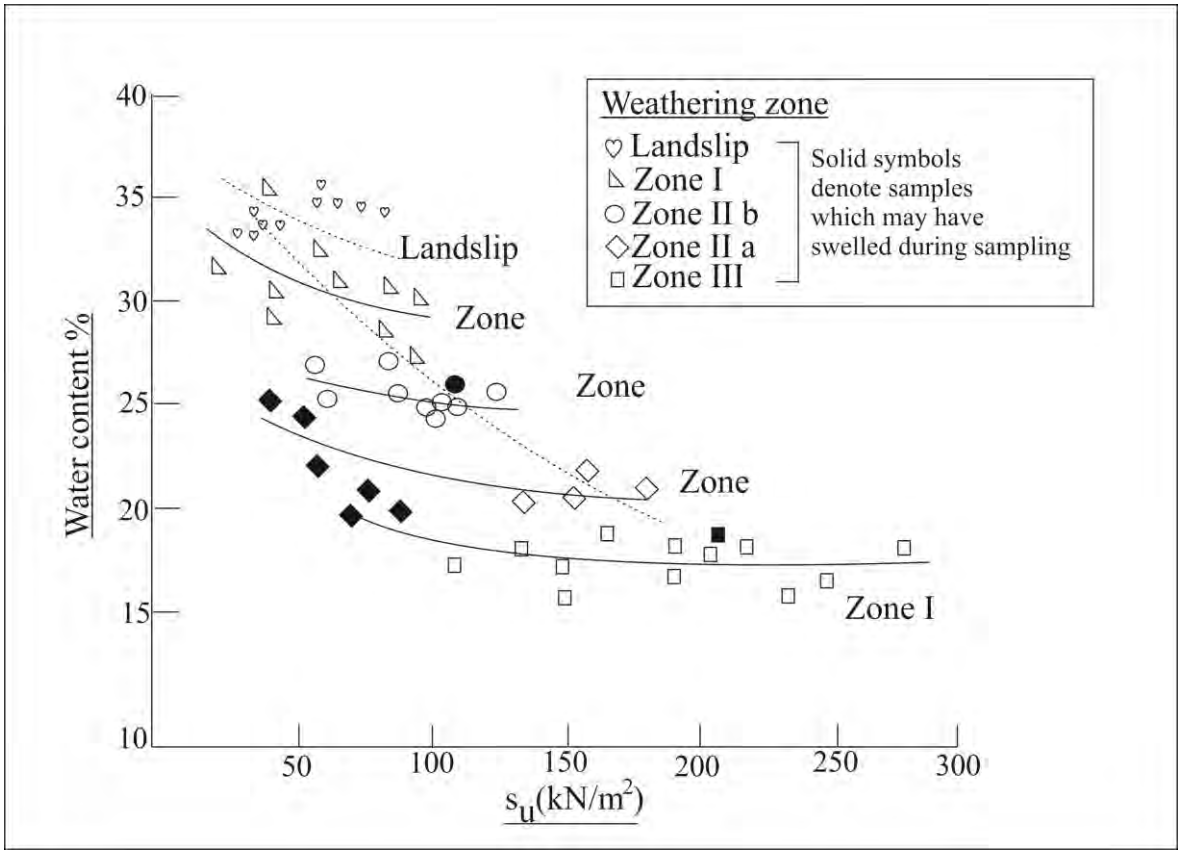

Figure 4.2: Effect of weathering on the undrained shear strength on the Upper Lias Clay (adapted from Chandler, 1972).

Table 4.4: Undrained shear strength of shales from Poland, Abakaliki shales in Nigeria and mudrocks from the United States and Britain.

		Undrained shear strength parameters		
Shear strength	Bell *et al.* (1996)	Hajdarwish and Shakoor (2006)	Aghamelu *et al.* (2010)	Zydron and Zawisza (2011)
Cohesion (c_u)	0 – 50	244 - 7846	48-55	3.0 - 47
Friction angle (φ_u)	38 – 47°	13.8 - 34°	23-31°	6.6 – 42°

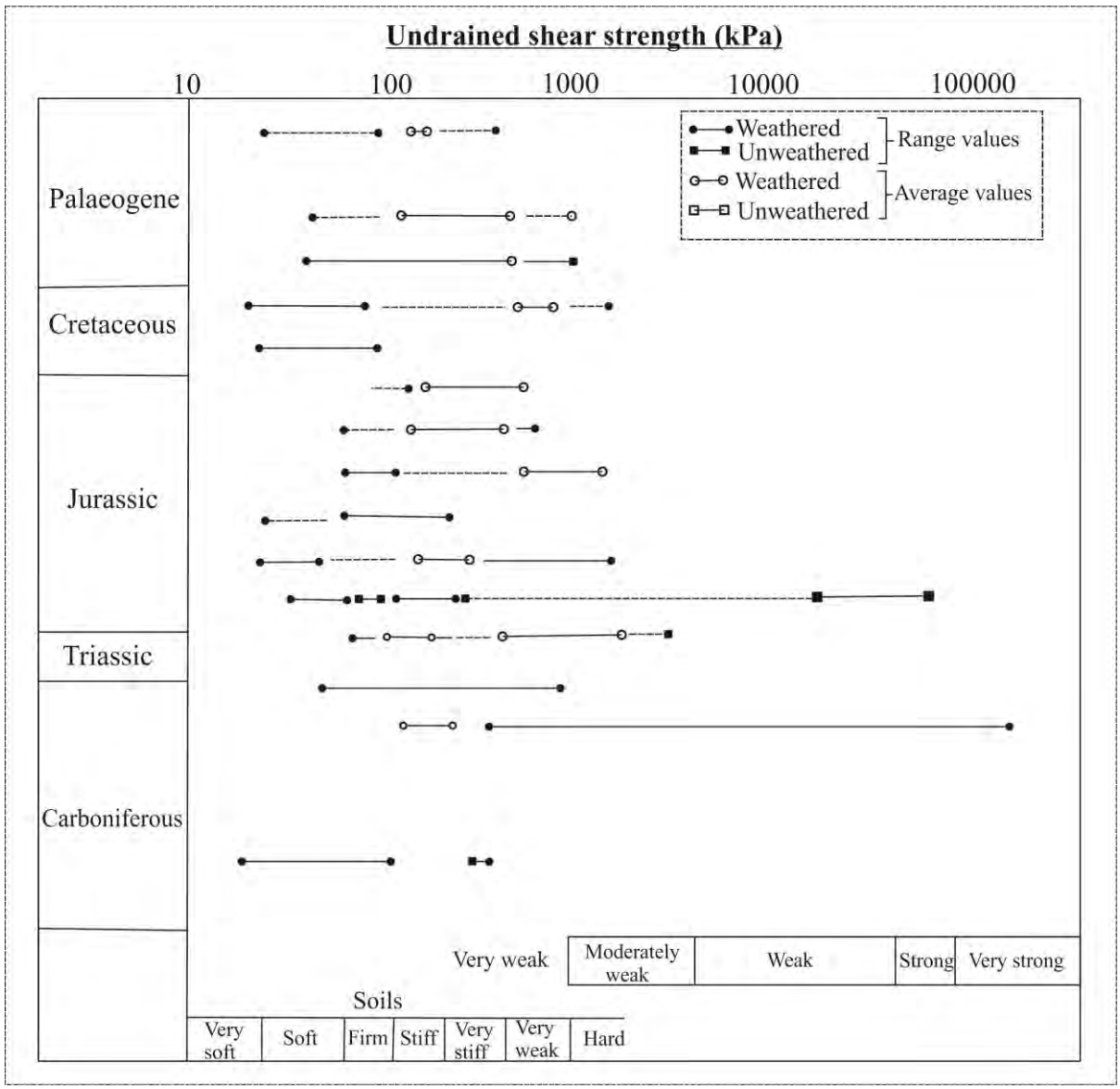

Figure 4.3: The effects of geological age and depth on the undrained strength of U.K. mudrocks (modified after Cripps and Taylor, 1981).

II) Effective shear strength of shales

The effective shear strength parameters (c′ & φ′) are influenced by exhumation, the degree of weathering and by the type and method of testing. For example, during the weakening of the inter-particle bonds, stress relief can cause a large reduction in the effective cohesion with a small reduction in the effective friction angle (Cripps and Taylor, 1981). The effective shear strength properties of a material can be determined using the shear box test or the triaxial test.

The degree of fissuring and jointing significantly influences the effective shear strength parameters and the effective apparent shear strength parameters during triaxial testing (Cripps and Taylor, 1981) (Figure 4.4). Carter and Mills (1976) showed that the apparent shear strength parameters of Coal

Measures mudrocks from the Kielder aqueduct range from 5-7 MN/m^2 for c_a and 25-29 ° for φ_a. Hobbs (1966; 1970) earlier showed that the apparent shear strength parameter of mudrocks from various underground collieries range from 2-13 MN/m^2 for c_a and 28-39° for φ_a. In contrast, Spears and Taylor (1972) showed that the fissured, but largely unweathered, Coal Measures shales and mudstones have effective shear strength parameters that range from 0-131 kN/m^2 for c' and 32-45.5 ° for φ' during triaxial testing. The shear strength parameters of the fissured shales and mudstones are much lower than the shear strength parameters of the intact materials.

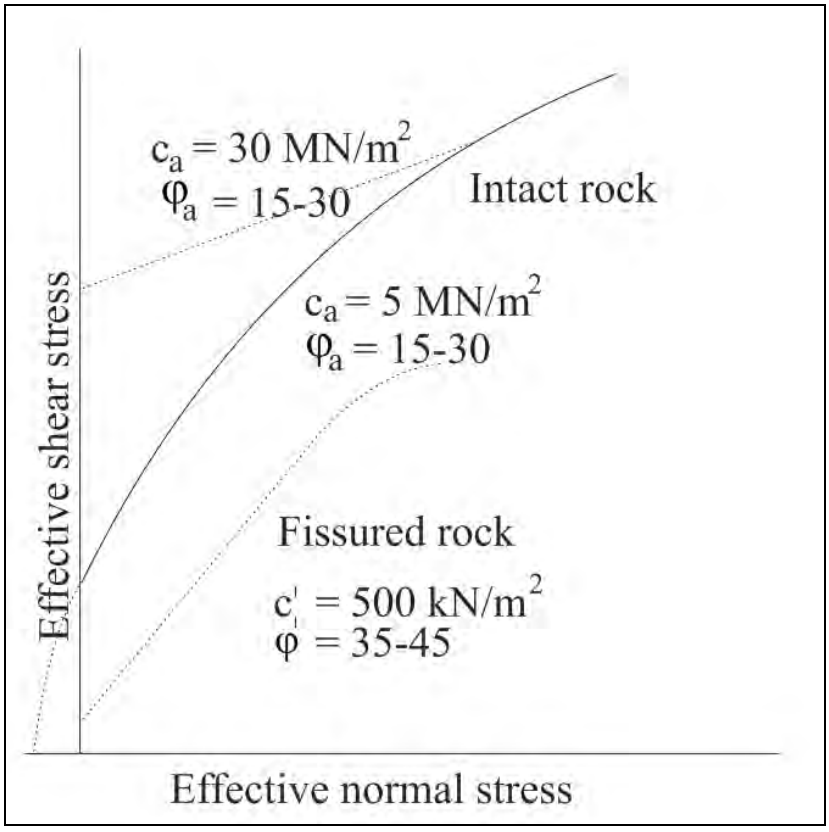

Figure 4.4: Effective shear strength parameters and apparent effective shear strength parameters of fissured and intact rock (adapted from Cripps and Taylor, 1981).

Similarly, studies that have been conducted by Jackson and Fookes (1974) and Parry (1972) on the Oxford Clay have shown the effects of fissuring after the removal of the overburden. These authors found that the φ′ was reduced by approximately 10 - 12° during shear box testing in which the laminations where parallel to the plane of shear as compared to tests which were conducted on specimens orientated with laminations at right angles to the plane of shear.

Weathering is also responsible for the changes in more indurated mudrocks such as those from the Carboniferous period (Cripps and Taylor, 1981). Spears and Taylor (1972) showed a 93 % reduction in c′ and a drop in φ′ to 26°. Furthermore, progressive weathering results in the reduction of the shear strength of mudrocks followed by an increase in the degree of fissuring. During this process, the interparticle bonds are weakened and the stress relief causes a large reduction in c' with a smaller

reduction in φ'. The reduction of these effective shear strength parameters are shown between the fissured rocks and overconsolidated clays (Group II), and the overconsolidated clays and weathered rocks (Group III) in Figure 4.5. It is not surprising or unlikely for some partially weathered mudrocks, for example, the weathered Coal Measure mudstones and the Keuper Marl, to display behaviour intermediate between Groups (II) and (III) (Cripps and Taylor, 1981). Chandler (1969) has also shown that the weathering related modifications to the stress-strain curve as shown in Figure 4.2 during triaxial testing on the Keuper Marl and the results are presented in Table 4.5.

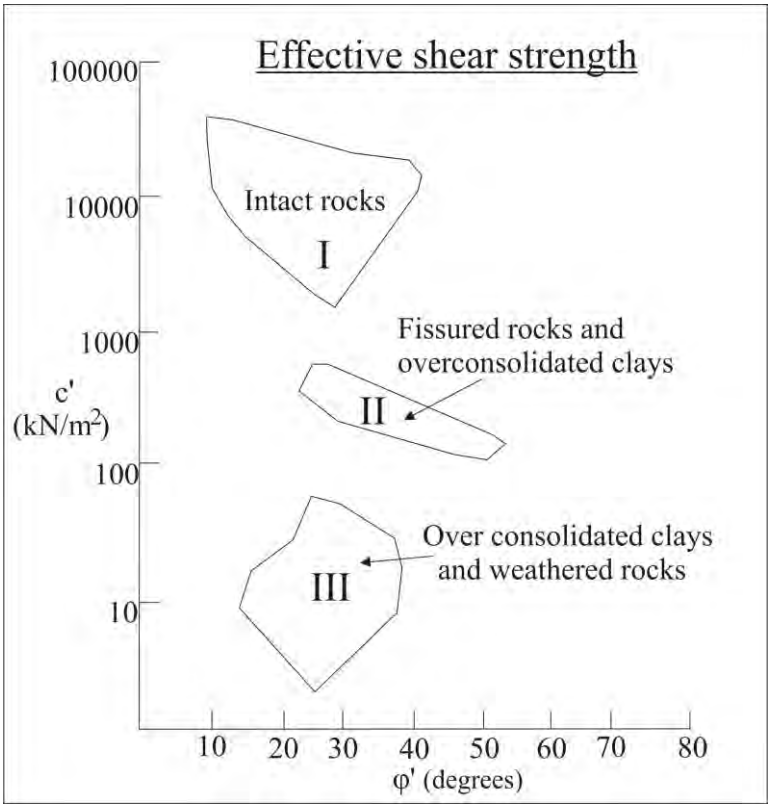

Figure 4.5: The effect of weathering on the effective shear strength of U.K. mudrocks (Cripps and Taylor, 1981).

Table 4.5: Changes in the effective shear strength parameters (modified after Chandler, 1969).

Zone	Effective cohesion (c′) (kN/ m^2)	Effective angle of friction (φ′)
I: Indicating brittle failure, Slightly weathered	28	40°
III: Moderately weathered	17	42-32°
IV: Indicating plastic failure, Highly weathered	17	32-25°

Strength tests were performed on shales from each formation within Kentucky in U.S.A to determine c' & φ' of each formation. Based on the results, a large spread in c' & φ' was observed for each formation as shown in Table 4.6. The New Albany shales and Drake shales showed high values of φ' but low c'. In addition, Kope shales and Nancy shales have lower φ' but high c' than Drakes shales and

New Albany shales (Hopkins and Beckham, 1998). Hopkins and Beckham Further stated that c′ as compared to φ′ is increased dramatically as the compactive energy during the compaction process is increased.

Table 4.6: Effective shear strength parameters of Kentucky shales from U.S.A, Pietermaritzburg Formation shales from Durban and British mudrocks from England.

Kentucky shales (modified after Hopkins and Beckham, 1998)								
Formation	New Albany	Drakes	Kope	Newman	Crab Orchard	Nancy	New Providence	Osgood
φ'	37-44°	27-34°	27-30°	23-27°	23-25°	26-30°	26-30°	27-29°
c' (kN/m^2)	0-109	10-53	1-37	30-54	27-58	10-46	0-49	19-57
British mudrocks (Cripps and Taylor, 1981)								
	Unweathered				Weathered			
Formation	Barton clay	London clay	Bracklesham beds	Lower oxford clay	Barton clay	London clay	Bracklesham beds	Lower oxford clay
φ'	27-39°	20-29°	25°	23-40°	18-24°	17-23°	18-32°	21.5-28°
c' (kN/m^2)	8-24	31-252	34	10-216	7-11	12-18	0-55	0-20
	Drennan, Maud and Partners (2010)							
φ'	13 – 28°							
c' (kN/m^2)	10 – 23							
Underwood (1967)								
Favourable					Unfavourable			
φ'	20 – 65°				10 - 20°			
c' (kN/m^2)	700-10500				37 - 700			

III) Residual shear strength of shales and mudrocks

Cripps and Taylor (1981) stated that the measure of the residual shear strength (c'_r & φ'_r) of a material depends primarily on the clay content, test method and on the value of the effective pressure which is used. Also, Gartung (1986) had stated that the residual strength of a shale is dependent on the degree of weathering. The residual shear strength parameters can be determined by performing laboratory tests such as the ring shear test, reversing the shear box test or by co-planar triaxial tests as shown in Table 4.7.

Jackson and Fookes (1974) stated that fissures should not affect the residual strength of a mudrock. Anisotropic behaviour of the residual strength of a mudrock can be affected by slickensided surfaces or as a result of lithological laminations. Chandler *et al.* (1973) showed the effects of varying the type of tests and the effective normal stress on the Upper Lias Clay from Northamptonshire (Figure 4.6). These results show that the residual strength is reduced as the effective normal stress is increased. Research that was conducted by Bishop *et al* (1971) has produced similar results for the London Clay (Table 4.7). Table 4.8 presents the residual shear strength parameters of clay shales from Texas, shales of the Pietermaritzburg Formation and shales from Poland.

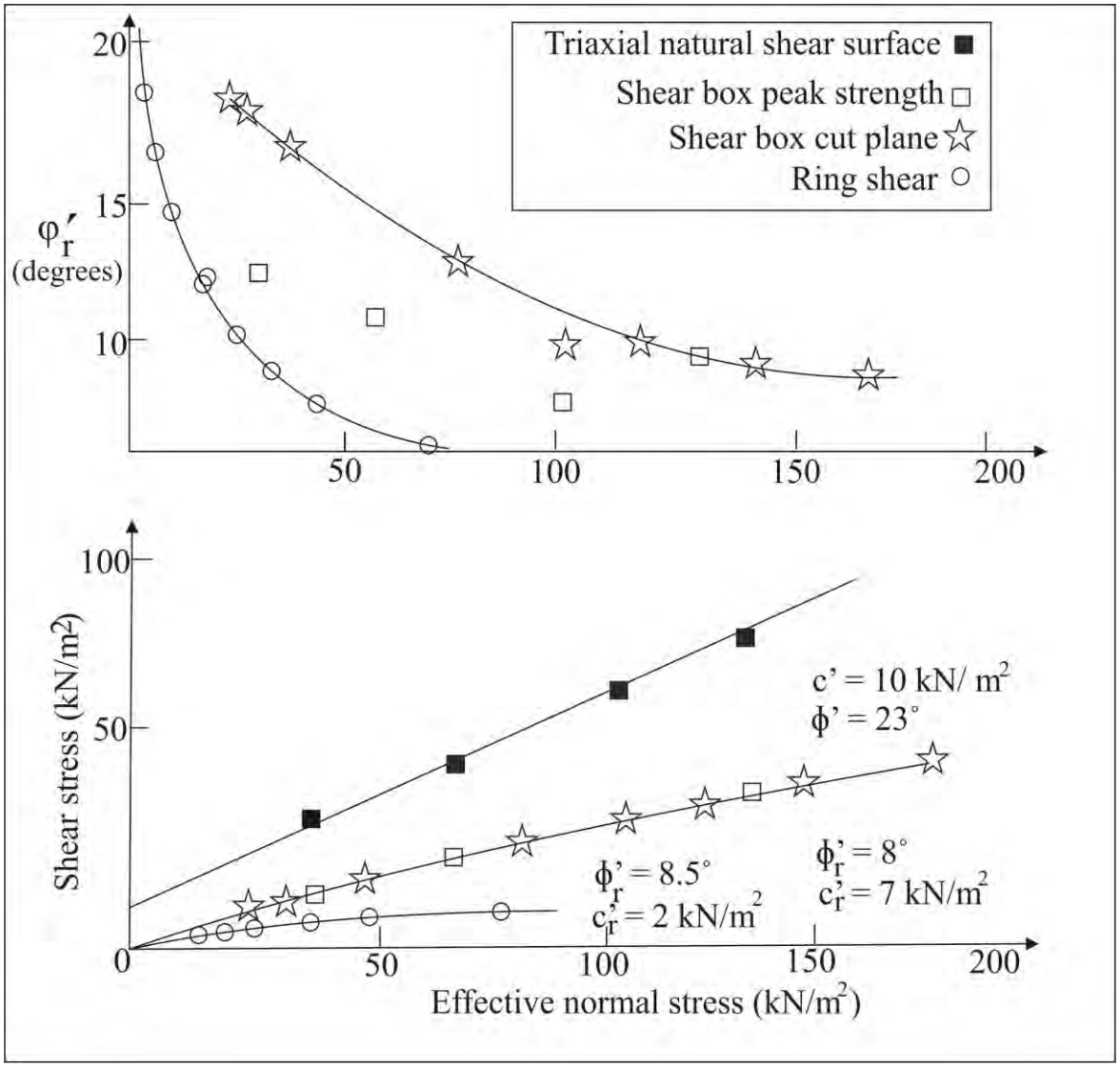

Figure 4.6: Effect of the type of test and method on the residual strength of the Upper Lias Clay from Northamptonshire (modified after Chandler *et al.,* 1973).

Table 4.7: Residual strength of London clay (modified after Bishop *et al.,* 1971).

Method	Residual shear strength	Effective normal stress
Ring shear	8.0-13.8	250-7 kN/ m^2
Reversing shear box	12.9-15.6	240-60 kN/ m^2
Co-planar triaxial	13.2-14.1	257-126 kN/ m^2

Table 4.8: Residual shear strength properties of shales.

Residual shear strength parameters			
Parameter	Strohman *et al.* (1984)	Bell and Maud (1996)	Zydron and Zawisza (2011)
(c'_r) (kN/m^2)	0-4	0	0.2 – 12.5
(φ'_r)	8-34°	9.5 - 12.5°	6.6 – 42.7°

Skempton (1964) established an empirical relationship between the clay fraction to the residual strength (φ'_r) (Figure 4.7). Skempton (1964) showed that on these superimposed envelopes, the minimum residual strength value is assumed to correspond to the maximum clay fraction. This proposes that the line for a particular formation represents a range of points which could theoretically lie anywhere within the rectangle of which the line is diagonal (Cripps and Taylor, 1981). However, in the case of the Etruria Marl and the Weald and Atherfield Clay, the residual shear strength is lower than expected. X-ray diffraction tests can be used to determine the influence of the clay fraction on the residual strength (Cripps and Taylor, 1981).

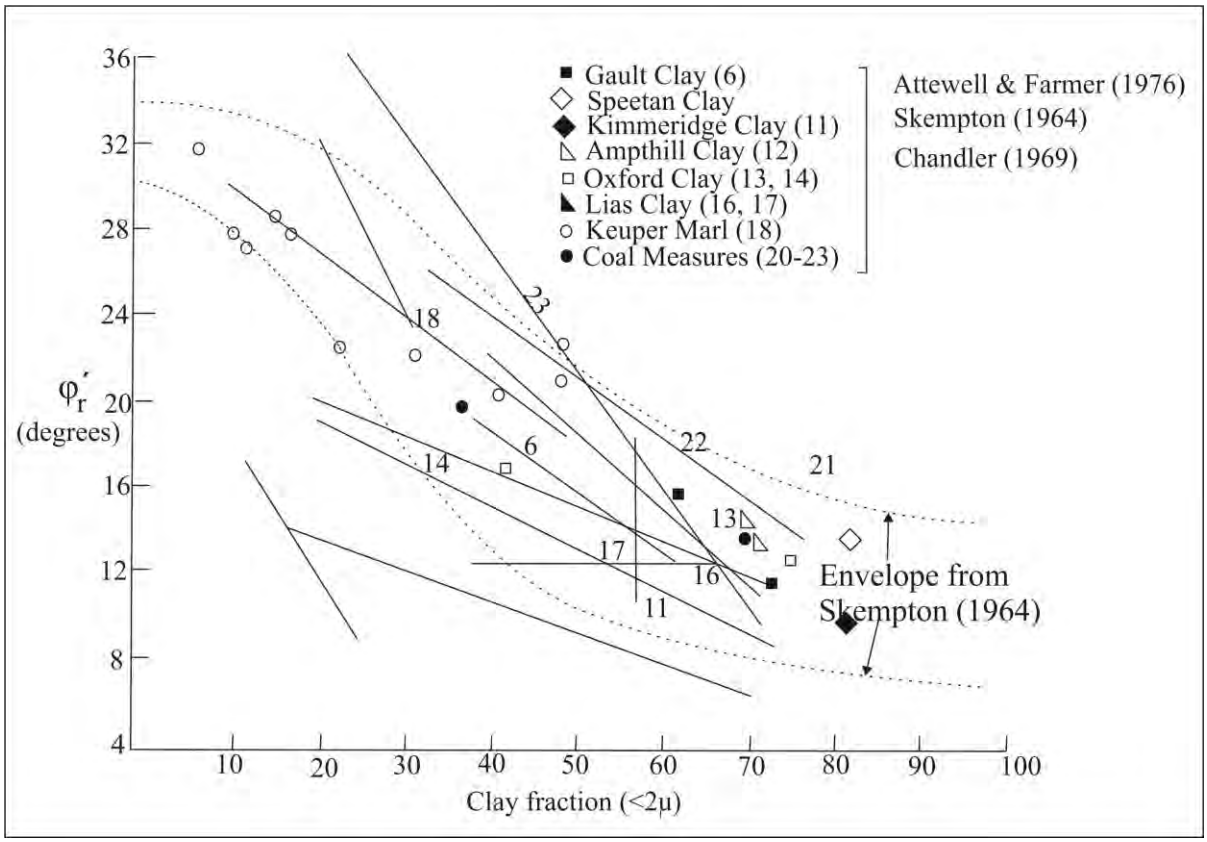

Figure 4.7: Residual shear strength and clay size fraction of U.K. mudrocks (adapted from Skempton 1964; Chandler 1969; Attewell and Farmer 1976).

Many mudrocks from the United Kingdom can suffer a drop of its residual strength by 21.5° as this ratio increases from 1.5-7.8. Also, as a result of all these tests being conducted by the same equipment, the degree of weathering significantly affects the residual strength of these mudrocks. Generally, the more weathered Carboniferous mudrocks have residual strength values which fall in a higher range than over-consolidated clays. Figure 4.8 shows that the residual strength of a material is lower as the ratio of the clay minerals to massive minerals increases (Cripps and Taylor, 1981).

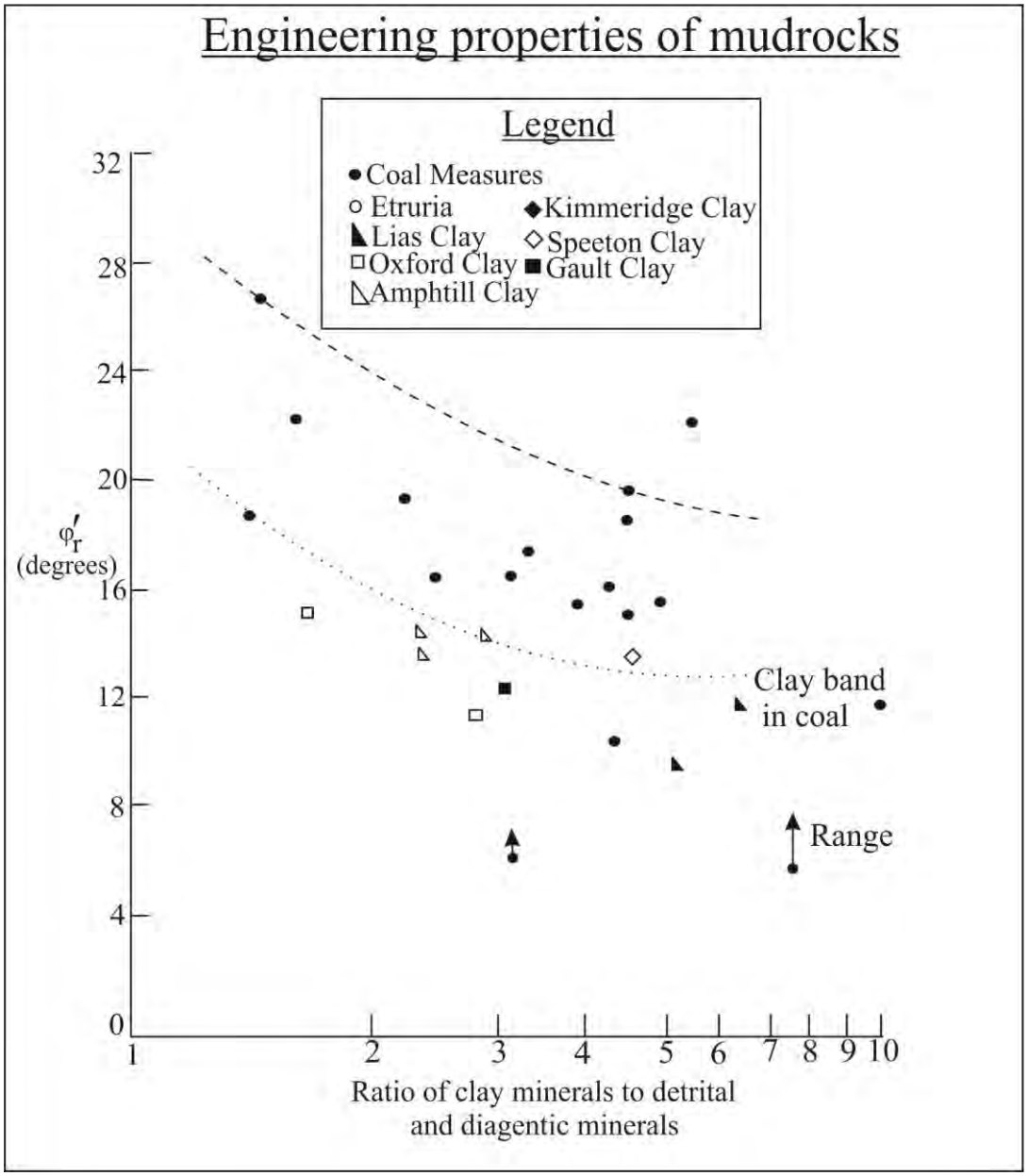

Figure 4.8: Influence of clay minerals on the residual strength on U.K. mudrocks (modified after Cripps and Taylor, 1981).

4.5 Weathering

Weathering is the reverse process of diagenesis which leads to a deterioration in the quality and loss of integrity of a soil or rock (Hardwick, 1992). Diagenesis and weathering result when a material is in equilibrium under a particular pressure and of a certain temperature regime. The degree of weathering is, therefore, directly related to the extent to which a material is brought out of equilibrium with its surrounding environment (Hardwick, 1992). Rock types that are formed under a particular set of temperature and pressure conditions beneath the earth's surface are more susceptible to weathering than soils which have undergone extensive periods of weathering (Hardwick 1992). During unloading, which is the reverse process of diagenesis, the removal of the overburden leads to the

release of strain energy and thus the propagation of high horizontal stress close to the surface (Hardwick, 1992). Cripps and Taylor (1981) stated that because vertical expansion is less restricted than horizontal expansion, the degree of vertical load shedding is greater than that in the horizontal direction. Thus, the horizontal effective stresses would be larger in the in the strongly bonded types as the weakly bonded types tends to inhibit expansion. Bjerrum (1967) stated that this is believed to be an important factor in exacerbating weathering.

Weathering is often intense at the surface and decreases down the profile, but persists along cracks to a much greater depth. Thus the rock is broken into blocks which are fresh inside, but weathered on their faces. The dip of the strata affects the degree of weathering that a material is prone to. In horizontally bedded shale, it is difficult for water to penetrate a geological unit. However if these strata are steeply inclined, then many bedding planes are exposed and this allows for water to easily penetrate these layers. After an extensive weathering regime, Ollier (1984) stated that there is a greater tendency for the weathered product of shales to be removed.

Shales often weather to a clayey gravel or a gravelly clay (Drennan, Maud and Partners, 2010) or to a loose soil mass (Hopkins, 1988). During weathering, illites and chlorites become more stable and smectites are converted to illites or chlorites. Kaolinites are transformed into kandites whereas dickite and nacrite break down completely at temperatures in excess of 200-250 °. If the pore water chemistry changes from acidic to alkaline, then kaolinite may transform to illite, smectite or chlorite and this alteration depends on the type of ionic species present (Hardwick, 1992).

4.5.1 The effects of weathering on shales and mudrocks

The greatest variation in the engineering properties of mudrocks can be attributed to the effects of weathering (Cripps and Taylor, 1981). This process destroys the inter-particle bonds of the material to a normally consolidated condition. The progressive softening and degrading is accompanied by reductions in strength and deformation moduli with a general increase in plasticity and water content (Cripps and Taylor, 1981). Weathering is responsible for the dramatic changes in more indurated mudrocks such as those from the Carboniferous period (Cripps and Taylor, 1981). Spears and Taylor (1972) showed how the shear strength rapidly decreases with accompanying changes in the stress-strain behaviour.

During the weathering process, vertical expansion results in the formation of joints, fissures and softening as a consequence of uplift and erosion from the removal of the overburden (Cripps and Taylor, 1981). During the removal of the overburden (unloading) by natural or man-made processes, strain energy is released and high horizontal stresses (stresses are limited in the horizontal direction) are propagated subparallel to the surface. Fissures decrease the strength of a rock mass particularly when there is a significant amount of clay particles (Cripps and Taylor, 1981).

Physical disintegration is the primary control in the breakdown of non-marine mudrocks and shales and indirectly controls the rate of chemical weathering. The rate of chemical weathering is dependent on the available surface area. Marine shales, especially those which are brittle and fissile, are more susceptible to chemical weathering than non-marine shales because they contain pyrite; pyrite is a mineral that readily oxidises (Hardwick, 1992). Taylor (1988) stated that geologically older marine mudrocks of the Cambrian and Ordovician age tend to be more susceptible to chemical breakdown.

4.6 Geotechnical problems associated with shales and mudrocks

The problems that are associated with mudrocks are often controlled by their lithology, susceptibility to water, the degree of compaction, their anisotropic character and the high frequency of discontinuities (Taylor and Spears, 1981). The degradation of highly degradable materials such as mudrocks and shales commence with the removal of the overburden which leads to associated fissuring and an increase in water content and softening (Cripps and Taylor, 1981). During the removal of the overburden, the shale expands at practically constant horizontal dimensions (Terzaghi and peck, 1967). During expansion the inter-particle bonds are then broken and joints form at regular spacing (Taylor and Spears, 1981). The effect of fissuring is particularly important in the older indurated mudrocks where the "rock-like" shear strength characteristics of the non-fissured and jointed rock are replaced by the "soil-like" characteristics of the fissured material (Cripps and Taylor, 1981).

Shales and other types of degradable materials are vulnerable to many types of failures. These instabilities include the collapse of boreholes, the collapse of engineering structures and shale related landslides. Shales are particularly subjected to loading failure and abrasion failure (Santi, 1998). In addition, shales such as the Saudi Tayma shales have caused serious damage to light structures, roads and boundary walls (Dafalla and Al-Shamrani, 2014).

4.6.1 Geotechnical problems encountered during the sampling of shales

The nature of shales and mudrocks makes it very difficult to obtain good quality, undisturbed samples for testing because they are weak and sensitive to changes in moisture, drilling pressure and time (Fam *et al.*, 2003). Upon exposure and weathering at the surface, the thin laminallae often separates and produces a fissile material which breaks down easily. Subsequently, water can then enter these rocks easily and future successive cycles of wetting and drying leads to its fragmentation (Bell, 2007).

In Durban, weathering has occurred along these bedding planes in shales of the Pietermaritzburg Formation (Bell and Lindsay, 1998). Bell and Maud (1996) further stated that this gives rise to the development of thin layers of clay of 3 - 5 metres in thickness. This process leads to the reduction in the shear strength of the clays whereby these clays act as preferential potential planes where sliding

can occur (Bell, 2007). Richards (2006) stated that Ecca shales generally fail along bedding and the bedrock/soil interface.

4.6.1.1 Slope instability and associated landslides

Changes in the ratio between the shear strength and stress brought about by the change in moisture content or by weathering, in potential slip zones, might also result in natural slope movement (Figure 4.9). During weathering, shales and mudrocks disintegrate into clay size materials. During periods of high rainfall, expansive clays begin to absorb water and expand (Bell and Maud, 1996). The expansion of the shale bedrock or mudstones start to disintegrate into distinct blocks. Subsequently, in an event of very high rainfall, water penetrates into these distinct blocks of shale and the weathered clay material becomes liquefied thus resulting in sliding. Bell and Maud (1996) further stated that failures occur due to high pore-water pressure as water penetrates the slope.

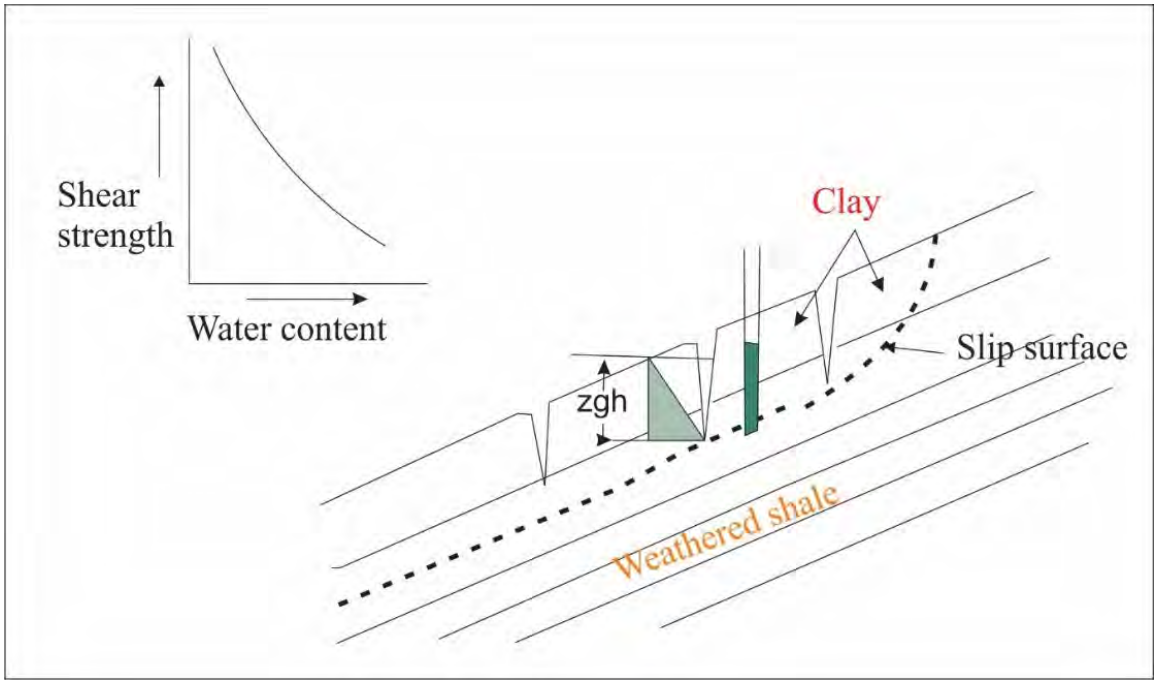

Figure 4.9: Failure caused by pore pressure build up and hydrostatic pressure in the tension cracks (modified after Wilson, 1983).

Shales are particularly susceptible to landslides when interbedded with rocks such as sandstones or limestones (Rib and Liang, 1978). The Ecca shales have a tendency to fail along bedding and the bedrock/ soil interface (Richards, 2006). In Durban, KwaZulu-Natal, many landslides over the past decade have been associated with shales of the Pietermaritzburg Formation (Bell and Maud, 2000) or sandstones of the Natal Group. These failures, particularly landslides, have been associated with high rainfall. Despite the high records of failure from the Natal Group sandstones, the Natal Group sandstone is more stable than shales of the Pietermaritzburg Formation. During 1970-1991, fifty-one

landslides occurred within the Durban area (Oliver *et al.,* 1994). In the Pietermaritzburg area, many slopes dip in excess of 12- 18° of the bedrock dip and these are areas of potential slip zones.

In 1969-1970, a landslide occurred at Mayat Place and Elf Place in Durban, KwaZulu-Natal which destroyed several houses and necessitated for the demolition of others (Bell and Maud, 1996). The initial slope movement began below Mayat Place and was a result of the ingress of water at an excess rate, into the zone of soft clay above the dense shales of the Pietermaritzburg Formation. Slope movement as seen by inspection shafts, occurred in the weathered shale material of the Pietermaritzburg Formation (Bell and Maud, 1996).

4.6.1.2 Embankment failures

The durability of shales is one of the most important considerations that needs to be evaluated when used as fill material for the construction of embankments (Oakland and Lovell, 1982). Widespread pavement, foundation and embankment failures have occurred whilst using Abakaliki shales in Southeastern Nigeria. Geotechnical assessments showed that these failures were as a result of high plasticity soils that contained expansive minerals, low permeability and low shear strength indices (Aghamelu *et al.,* 2010). The Cipularang Toll Road failure, which is situated in Indonesia, occurred as a result of the low shear strength of the weathered clay shales (Irsyam *et al.,* 2008). Back calculated shear strength parameters showed that the shear strength parameters at failure were c = 5 kPa and φ = 13° (Irsyam, *et al.,* 2008).

In June 1978, settlement occurred on the rail track along the North Coast Line at Duffs Road, Umgeni, which is north of Durban. Hard, well laminated and jointed shales underlie the area which had undergone settlement over many years. Rehabilitation of this slope required reballasting of the track and the constant addition of fill material (Bell and Maud, 1997). The most important effects that this downslope movement experienced was that it had caused severe cracking of the walls of the local clinic. Bell and Maud (1997) stated that this structure is presumably located on the toe-bulge of ground movement that had appeared to be marginally restrained by the passive pressure exerted by materials downslope. This resulted in the upward bulging of the toe area and consequent severe cracking of the clinic. (Bell and Maud, 1997)

In 1998, a landslide occurred on the embankment for a railway near the Canelands station, north of Durban (Bell and Maud, 1997). The landslide resulted from the high amount of rainfall and groundwater which resulted in the infilling of joints and contact between shales of the Pietermaritzburg Formation and dolerite. The landslide resulted in the formation of a 130 m tension crack. Consequently, the general ground level below the crack subsided by up to 2 m towards the centre of the landslide. Following these events, settlement gradually occurred on either side of the tension crack for 6 weeks (Bell and Maud, 1997).

The most historical geohazard problem as stated by Richards (2006) in the Pietermaritzburg area is the zone of slope instability around the Rickivy and Athlone areas which is situated below the Worlds View Escarpment. Mass movement began with the failure of the Rickivy fill material during construction in 1957 in an embankment fill that carries the N3 freeway on the slopes of Town Hill north-west of Pietermaritzburg, which continued in 1969 and in 1970, this movement began to accelerate.

Prior to 1996, slopes of 2 (horizontal) to 1 (vertical) were commonly used in the design of all embankments to an angle of 26.6 ° regardless of the height of the embankment as stated by Hopkins and Beckham (1998). These designs caused several instabilities and failures especially in the Kentucky area which contained nondurable, clayey shales. The large variation in particle sizes of shales when used in the construction of embankments makes it very difficult to define deformational properties of shales by using conventional consolidation testing (Hopkins and Beckham, 1998). Despite conducting proper compaction procedures of shales to prevent instabilities of embankments, a large number of slides have occurred at side hill locations when clays or weathered shales were over-stressed, particularly when the overburden contained over-consolidated clays (Hopkins and Beckham, 1998).

4.6.1.3 Settlement related instabilities

Shales create major problems when used as construction materials because in many cases they tend to disintegrate from a hard mass to a fine grained mass of soil (Hopkins and Beckham, 1998). As these materials degrade and disintegrate, associated settlement occurs. Unfortunately with time, and in the presence of wet conditions, compacted shales become less durable. This reduction in durability results in instability such as ground subsidence and the loss of bearing capacity (Bryson *et al.,* 2011).

Compacted shales exhibit small compression in a relatively dry state (Hopkins, 1988; Hopkins and Beckham, 1998). However, compacted shales exhibit large and excessive settlement when soaked (Drnevich *et al*., 1976; Strohm *et al.,* 1981). Shear strain often causes secondary compression and settlement to occur in well compacted shales (Hopkins and Beckham, 1998). For example, in well compacted fills, settlement may amount to approximately 0.3 - 0.6 % of the fill height over a period of 15-20 years (NAVFAC, 1982).

4.7 Summary

This chapter provided a detailed account of the geotechnical properties such as the slake durability index, the Point Load Strength and the shear strength of shales and mudrocks. Furthermore, the chapter discussed the geotechnical problems which are associated with shales and mudrocks.

Chapter 5

Classification of argillaceous materials and previous studies on rating systems on shales

5.1 Introduction

This chapter focuses on the classification of argillaceous materials using field methods and laboratory tests. Furthermore, it presents the studies which were performed for the rating of shales and highlights the deficiency of these rating systems.

5.2 Classification of argillaceous materials based on field identification and laboratory testing

Until the discovery of analytical techniques such as the Scanning Electron Microscopy, X-ray diffraction (XRD) and X-ray fluorescence (XRF), very little was known about the chemistry and mineralogy of shales and other degradable rocks (Hardwick, 1992). Since the 1960's, there have been numerous attempts at developing tests to assist design engineers in the difficult task of classifying argillaceous materials such as shales and to predict their performance in embankment or cut slopes (Walkinshaw and Santi, 1996). The very fine grains constituting these rocks only allowed for a limited study in hand specimens or with an optical microscope. Pettijohn (1975) and Spears (1980) stated that the poor attempts at classifying these argillaceous materials are often a result of their poor exposure in the field as compared to their more weathering resistant counterparts, sandstones. Also, the properties such as the texture and roundness of sandstones can be observed with the naked eye.

The aim of classification schemes is to group objects of concern into classes of similarly defining properties which are meaningful and significant, and that which facilitates giving those divided classes a name (Wilson, 2013). Similarly, the tests aim to reliably differentiate between durable shales which may be treated as a rock in comparison to those with limited durability that are degradable on a human time scale (Walkinshaw and Santi, 1996). Additionally, Blatt *et al*. (1980) stated that classification systems allows for the naming and grouping together of phenomena which have similar properties or attributes.

5.3 Methods of classifying shales

Boggs (2009) stated that the classification of sandstones and conglomerates are based primarily on the mineralogy or particle composition of these rocks, although texture is used as a secondary classification parameter in some classifications. Conversely, the classification of shales and mudstones on the basis of mineralogy has generally been regarded as impractical because of the difficulty in obtaining quantitative data on the composition of shale owing to their fine grain size.

Thus, the proposed classifications are based mainly on the texture and structure (lamination). This section focuses on the field and laboratory methods of classifying shales and mudstones.

5.3.1 Field classification of shales

Tucker (2001) stated that attributes such as the colour, degree of fissility, sedimentary structures, minerals and organic, and fossil content are used to describe mudrocks and shales in the field. Similarly, Griffiths (1967) stated that sedimentary rocks can be classified according to texture, degree of induration, stratification, fissility, chemical and mineral composition and clay mineralogy. Texture in terms of particle size, is one of the most significant properties when describing rocks in the field (Wilson, 2013).

Twenhofel (1937) created a classification system which is based on the composition, the degree of induration and the level of metamorphism (Table 5.2). In this study, Twenhofel listed shale as an indurated, fissile and non-metamorphosed mud. Shrock (1948) later proposed a field classification whereby a fine grained rock of unknown composition and indeterminable fine grained size is designated shale; whereas a mudstone, a claystone or a siltstone are subsets of shale which slakes readily during repeated wetting and drying. Later, Ingram (1953) created a classification system which is based primarily on the layering properties of the fine grained layered rocks whilst Stow (1980) created a classification system which is based on the particle size and degree of fissility in mudrocks as shown in Table 5.1. Potter *et al.* (1980) developed a classification that uses both grain size and lamination as classification parameters (Table 5.3).

Table 5.1: Nomenclature of mudrocks.

Ingram (1953)			
Amount of silt and clay	No connotation of breaking characteristics	Fissile	Massive
Silt predominates	Siltrock	Siltshale	Siltstone
No connotation as to relative amounts	Mudrock	Mudshale	Mudstone
Clay dominates	Clayrock	Clayshale	Claystone
Stow (1980)			
Particles size and proportions	Fissile	Non-fissile	
4-63 μm >66%	Silt-shale	Siltstone	
< 63 μm no proportions	Mud-shale	Mudstone	
<4 μm >66%	Clay-shale	Claystone	

Table 5.2: Twenhofel's (1937) classification of fine grained sediments.

Unindurated	Indurated	After incipient metamorphism
	Mudstone	
Silt	Siltstone	Argillite
Mud	Shale (fissile)	
Clay	Claystone	

Table 5.3: Classification based on grain size and lamination (adapted from Potter *et al.,* 1980).

Percentage clay-size constituents (%)			0-32	33-65	66-100
Field adjective			Gritty	Loamy	Fat or slick
Nonindurated	Beds	> 10 mm	Bedded silt	Bedded mud	Bedded claymud
	Laminae	< 10 mm	Laminated silt	Laminated mud	Laminated claymud
Indurated	Beds	> 10 mm	Bedded siltstone	Mudstone	Claystone
	Laminae	< 10 mm	Laminated siltstone	Mudshale	Clayshale
Metamorphosed		Degree of metamorphism	Quartz argillite	Argillite	
			Quartz slate	Slate	
			Phyllite and/ or mica schist		

The colour of a mudrock is useful during field mapping to distinguish between various mudrock units and, it is a function of its mineralogy and geochemistry (Tucker, 2001). Boggs (2009) further stated that the colour is associated in a very general way with the type of depositional conditions. Organic matter, pyrite and the oxidation state of iron are the primary controls on the colour of mudrocks. Dark grey or black mudrocks are characterised by a high amount of organic matter and pyrite. Red and purple mudrocks results from the presence of ferric oxide and hematite. Green mudrocks arise from the ferrous iron of illite and chlorite while olive and yellow mudrocks owe their colour to a mixing of green minerals and organic matter (Tucker, 2001).

Rib and Liang (1978) described landforms associated with thick shale beds. They stated that clay shales are known for their low rounded hills, medium tones, and gullies of the gentle swale type and well integrated treelike drainage system. According to Rib and Liang (1978) interbedded sedimentary rocks show a combination of the characteristics of their component beds. When horizontally bedded, they are recognised by their uniformly dissected topography, contour-like stratification lines and tree-like drainage. When this sequence is tilted, there is evidence of parallel ridge-and-valley topography, trellis drainage and inclined but parallel stratification lines. Ray (1960) further noted that shales have relatively dark photographic tones, relatively closely and regularly spaced joints and, a fine textured drainage.

5.3.2 Laboratory tests used to classify shales

5.3.2.1 Geochemical tests

Spears (1980) developed a classification system which is based on the percentage of quartz and fissility. Spears determined the abundance of quartz using XRD tests and summarised a shale as a fissile or laminated rock whilst a mudstone is neither fissile nor laminated. Weaver (1980) proposed a classification which is based on the particle size and the percentage of phyllosilicates (clay minerals) as determined by XRD tests. Moore (2005) later devised a classification system which is based on a combination of the particle size data, pore size data and petrographic observations. Based on these

qualities, rocks are either floc-dominated whose structure is supported by the clay matrix or silt or sand-rich mudrocks whose structure are supported by a silt/fine sand framework.

5.3.2.2 Geotechnical tests

Many attempts have been made to classify argillaceous shales and predict their performance in cut slopes and embankments (Walkinshaw and Santi, 1996). The objective is to find tests that will reliably differentiate between durable shales which may be treated like a rock and to those with limited durability. Underwood (1967) suggested that shales can be grouped according to their engineering properties such as the strength, modulus of elasticity and swell potential or according to common laboratory tests such as the moisture constant, density, void ratio and permeability. Franklin and Chandra (1972), Lutton (1977), Franklin (1981) and Santi (1998) have made significant contributions to establishing specific tests for the slaking of shales. Santi (2006) determined a field method of characterising weak rocks for engineering design. In this research, Santi (2006) related laboratory tests such as the Uniaxial Compressive Strength (UCS) test and the jar slake test to field based tests such as the Point Load Strength test. The common laboratory tests that were used for proposed classification systems and slope stability evaluations consists of the Atterberg limits, the jar slake test, the slake durability test, the Point Load Strength test and the Shear Box test (Walkinshaw and Santi, 1996).

I) Particle size

According to Taylor and Spears (1981) and Tucker (2001), the geological classifications of sedimentary rocks are based predominately on the grain size of the constituent materials. Blatt *et al*. (1980) stated that mudrocks are made up of 15 % sand, 45 % silt and 40% of clay when compared to siltstones which contain 25 % of clay (Stow, 1980). Spears (1980) stated that the amount of quartz should be used as a method of classification because the ratio of quartz:/ to clay increases as the ratio of silt:/ to clay increases. Ideally, this serves as an important classification for engineers. However; certain minerals would have undergone diagenesis and will not reflect its original distribution (Hardwick, 1992). The three fold classification subdivision characterises the particle size where rock that contains particle size > 2/3 silt is a siltstone, 2/3 – 1/3 silt is a mudstone or mudshale and rocks with particle size < 1/3 silt is a claystone or is a clayshale. A sediment ternary classification after Folk (1974) which is based on the grain size is shown in Figure 5.1.

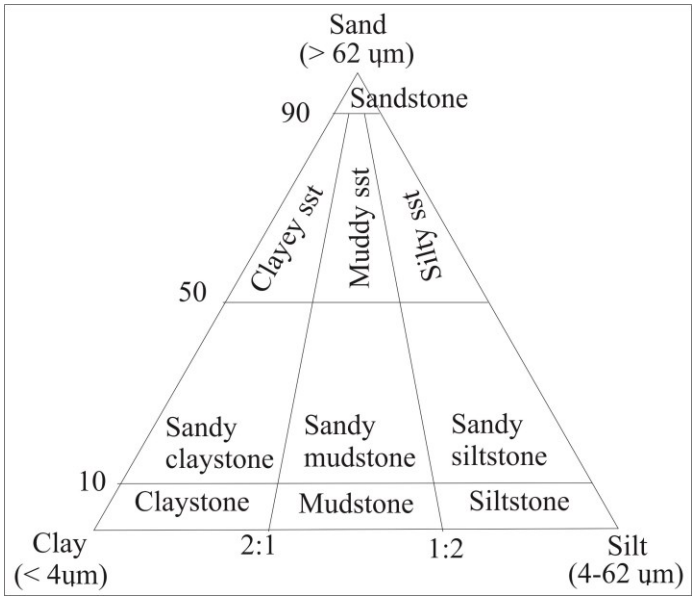

Figure 5.1: Sediment ternary diagram (adapted from Folk, 1974).

The main problem that is associated with particle size classification is that it requires experimental work which is time consuming (Hardwick, 1992). The minerals present could have undergone diagenesis which may be have altered the grain size distribution and is therefore of limited use in determining the initial environment. However, these analyses are adequate for engineering purposes as stated by Hardwick (1992).

II) Slaking tests

Slake tests were developed to provide an indication of material behaviour during the change of stresses due to alternate wetting and drying, which, to some degree, stimulate the effects of weathering (Walkingshaw and Santi, 1996). Slaking refers to the durability of a material during its interaction with water after a period of drying (Santi, 1998). Several authors such as Morgenstern and Eigenbrod (1974) and Santi (1996) have proposed that slaking should be used as a diagnostic method to distinguish between soil-like materials and rock-like materials. Burwell and Moneymaker (1950) earlier noted that slaking occurs more strongly in compacted shales than in cemented shales. The lithological factors which govern the durability of mudstones include the degree of induration, the degree of fracturing, the grain size distribution and the mineralogical composition (Bell *et al.,* 1996). Olivier (1979) considered changes in humidity and temperature to be the main causes of disintegration of mudrock. Brink (1983) suggested that dissolution of the cementing material, air breakage or the development of internal pressures due to the suction of water into the material is responsible for the slaking process.

Moriwaki and Mitchell (1977) suggested four common modes of slaking namely: dispersion slaking, swelling slaking, body slaking and surface slaking. Dispersion slaking results from the formation of a

cloudy residue as air bubbles are released from a completely submerged shale sample and occur when Na-kaolinite is abundant. Swell slaking occurs during the disintegration of a shale sample in response to a change in volume of clay minerals such as Na-montmorillonite. Body slaking refers to the macroscopic disintegration of shale material as it fractures into irregular blocks. They expect this mode to dominate when Ca-kaolinite and Ca-illite are abundant in the shale materials. Lastly, surface slaking occurs as a shale sample begins to slake from the surface inwards which is followed by the development of parallel thin plates. This mode of slaking occurs when Ca-montmorillonite is abundant.

Venter (1980) recognised three responses to slaking. These responses include the durable mudrocks that show very little breakdown, disintegrating mudrock which breaks into hard fragments of various shapes and sizes and slaking mudrock which breaks down to clay or silt sizes. Brink (1983) stated that although there is no sharp division between these types of behaviour in practise, it is useful to distinguish between them as a test suitable for classifying "slaking behaviour" is not necessarily suitable for classifying "disintegrating behaviour".

Later, Mitchell (1993) identified three mechanisms which leads to slaking. These mechanisms as stated by Mitchell (1993) include slaking which occurs as a result of the dispersion of soil particles; by stress relief and water absorption and; by tensile stresses which results from the compression of entrapped air as water is absorbed. Perry and Andrews (1982) observed three modes of slaking that corresponds well to the observations of Moriwaki and Mitchell (1997). These modes of slaking include ice block slaking, chip slaking and slaking to inherent grain sizes.

Several types of slaking tests such as the jar slake test, the slake durability test and the slake index test have been developed and used to assess the slake potential of shales (Wood and Deo, 1975; Chapman *et al.*, 1976; Oakland and Lovell, 1982; Withiam and Andrews, 1982; Santi, 1995). The Jar Slake test is performed by immersing a piece of oven dried shale in 15 ml of water to assess the degradable behaviour of the shale sample (Wood and Deo, 1975). The behaviour is described in relation to the visual appearance of its physical disintegration (Walkinshaw and Santi, 1996) (Table 5.4).

Table 5.4: Jar Slake categories based on the behaviour of the material under investigation (after Walkinshaw and Santi, 1996; Santi, 1998).

Jar Slake Index (I_j)	Material behaviour
1	Degrades to a pile of flakes or mud
2	Breaks rapidly, forms many chips or both
3	Breaks slowly, forms few chips or both
4	Breaks rapidly, develops several fractures, or both
5	Breaks slowly, develops few fractures, or both
6	No change

The disadvantages of the jar slake test are that it provides ambiguous descriptions of the results observed and fails to effectively distinguish between the slight and extreme cases of each mode (Santi, 1998). Also, the categories do not progress from the weakest reaction to the strongest reaction, for example, a sample that shows a weak slaking reaction and forms few fractures would be given a jar slake Index (I_j) of 5. Conversely, a sample which shows a weak slaking reaction but forms a few chips rather than fractures would be classified as a 3; which indicates a stronger reaction than observed. The ambiguity in the descriptions does not provide a standardised understanding by technicians when performing this test (Santi, 1998). The jar slake test was improved by performing a large number of tests on shales to reduce the variability of the descriptions that are given by technicians. (Santi, 1998). Also, schematic drawings and additional verbal descriptions were incorporated into jar slake test by Santi (1998) to improve the quality of the jar slake test.

Santi and Koncagul (1996) linked the jar slake categories to the types of slaking that were observed by Perry and Andrews (1982) and Moriwaki and Mitchell (1977). Category 1 represents dispersion slaking or slaking to inherent grain size whilst categories 2 and 3 represent chip or surface slaking. Categories 4 and 5 represent body or block slaking. Santi and Koncagul (1996) have stated that materials which exhibit block slaking tend to weather slowly at first and then speed up as compared to materials that experience chip slaking which tend to weather rapidly at first and then slow down.

The slake index test is another test which is used to determine the durability of shales. Santi (1998) highlighted general weaknesses that occur during this test. Firstly, differences in the degree of weathering in each of the samples will cause materials to pass through the 10 mm sieve. Secondly, technicians are generally inconsistent in their laboratory techniques to ensure that certain samples are not washed more rigorously than others. Santi (1998) further proposed a standardised and detailed set of test instructions to improve the accuracy of the slake index test by focusing particularly on the sieve washing portion of the test.

The slake durability test was originally developed by Gamble (1971) and Franklin and Chandra (1972) to assess the rocks resistance to weakening and disintegration when subjected to cycles of wetting and drying (ISRM, 2000). The advantages of this test are that the test is accurate, reproducible and standardised (Santi, 1998). Also, the slake durability test is the most appropriate test to use to determine the durability of shales (Santi, 1995). Other durability tests such as the Los Angeles test and the freeze/thaw or wetting/drying tests are either too rigorous for shale materials or do not accurately mimic the anticipated field conditions (Santi and Higgins, 1998). The proposed modification of this test by Santi (1998) is that the second cycle of this test is not necessary and that the first cycle of the slake durability test can be used to predict the remainder of the slaking cycles.

According to Hopkins and Beckham (1998), weak degradable materials such as weathered shales are usually defined by very high moisture content (> 10%), a slake durability index (SDI) of < 90% and materials which contain > 10-15 % of clay minerals. High moisture content indicates a high degree of fracturing, disintegration and disaggregation (Santi, 2006). Materials which have a significant amount of matrix have a much lower strength than materials which contain less matrix. Shales can be classified as mechanically hard when the SDI > 95% and can be used as rockfill. Shales are classified as soft and nondurable if the SDI < 50% and the $I_j \leq 2$ whilst intermediate shales are classified as hard and nondurable when 50% < SDI < 95% and I_j of 3-5 (Strohm, 1978; Hopkins and Beckham, 1998) (Table 5.5). Under some circumstances, some shale materials which are used in the construction of embankments require compaction by heavy equipment (Hopkins and Beckham, 1998).

Table 5.5: Description of the shear strength properties of shale depending on the slake durability and the description of shales (modified after Hopkins and Beckham, 1998).

Slake durability index (SDI) (%)	Description of shale	Shear strength parameters	
		φ'	c' (kN/m^2)
SDI < 50	Soil-like shale	20-25°	9.6
50 < SDI < 95	Intermediate shale	26-30°	9.6
SDI > 95	Hard shale	35-45°	0

III) Point Load Strength test

The Point Load Strength test was developed principally to be used in the field on rock cores or on irregular samples. The principal advantage of this test is that it can be performed in the field, irregular samples can be tested with minimum preparation and it is cost-effective (ASTM, 2010). Welsh *et al.* (1991) proposed a strength durability classification system that includes the Point Load Strength to clearly differentiate between strong - durable and weak or nondurable materials. A strength durability classification has been designed by Welsh *et al.* (1991) which was based on the work of Olivier (1979). Welsh *et al.* (1991) created a dual-index system to characterise degradable rocks into three

classes (Class I, Class II and Class III). This dual-index system consists of the jar slake test, the Free Swell test and the Point Load strength test (Figure 5.2).

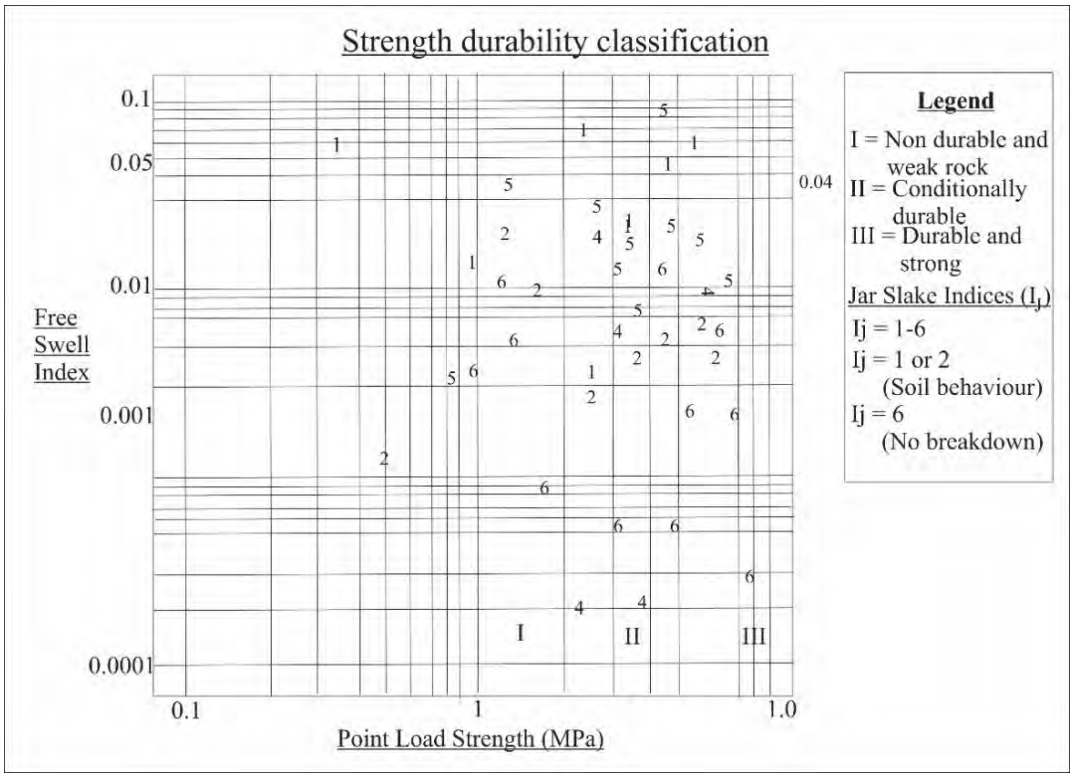

Figure 5.2: Strength durability classification of jar slaking (adapted from Welsh *et al.,* 1991).

Jar slake indices (I_J) are given according to the behaviour of a rock when immersed in water from 1-6. A jar slake index of 6 implies no change in a rock whilst an I_J of 5 implies that the rock breaks slowly and develops a few fractures. An I_J index of 3 and 4 denotes the formation of several chips and the formation of several fractures respectively. In addition, an I_J of 2 is given to the rapid disintegration of the rock material whereas an I_J of 1 is given to a rock which degrades to a pile of flakes or mud. Using the classification system which is shown in Figure 3.12, Class I materials fails the jar slake test and this material also fails during sample preparation for either the Point Load Strength test or the free swell test. It also has a free-swell > 4 % and has a Point Load Strength of < 2 MPa. Class II materials are conditionally durable and its suitability is dependent on the environmental conditions and its use. Conversely, durable and strong rocks as denoted by Class III, have a rock strength ≥ 6 MPa, a swell of 4 % and exhibits rocklike behaviour during the jar slake test. Shales with properties < Class III should not be used in drain applications and particular care is necessary when placing these materials in or near drainage features during landslide mitigation works (Walkinshaw and Santi, 1996).

The Point Load Strength test, the Free swell test and the jar slake test are basic indicator tests which are used to assess the settlement of shales when used as fill materials (Walkinshaw and Santi, 1996). The free-swell test is used to measure the uniaxial swell of core samples when immersed in water.

This test plays a pivotal role during the construction of roads and buildings, particularly when made up of swelling minerals such as smectites.

5.4 Settlement

5.4.1 Introduction

It is only with the advent of heavy foundations that the deformation performance of mudrocks which is used in foundations have been studied in detail (Hobbs, 1973; Hayden and Hobbs, 1977). Taylor and Spears (1981) stated that mudrocks pose fewer deformational problems than over consolidated clays. Settlement refers to the vertical displacement (lowering) of the surface (Craig, 2004). The average values of settlement beneath a structure together with the individual settlements experienced by its various parts influence the degree to which a structure serves it purpose (Bell, 1993). The damage due to settlement ranges from the complete failure of a structure to slight disfigurement (Bell, 1993). Settlement, especially in clayey soils, continues invariably after the construction period which makes it necessary to determine the amount of settlement (Bell, 1993). The rate of settlement in clays depend on the rate at which the void space is reduced by expelling the pore water which is induced by a structural load. Thereby allowing the structural load to be supported entirely by the soil skeleton. The measurement of settlement is rarely a limiting condition in foundations and does not entail a special study except in the case of low grade compaction shales where appreciable settlements may occur (Bell, 1993). As weathering causes mudrocks to return to a normally consolidated clay (Cripps and Taylor, 1981; Taylor and Spears, 1981; Bell, 1993), settlement of buildings constructed on normally consolidated clays are more severe (Bell, 1993).

The settlement of mudrocks can be determined from consolidation testing in a laboratory and by field tests. The settlement of embankments which are constructed using shale materials is a common problem and is often difficult to predict and control Hopkins (1988). In the laboratory, the use of conventional consolidation testing to define the deformational properties of shales are generally not applicable because of the large particle sizes of shale (Hopkins and Beckham, 1998). Consolidation rings used in the Odeometer test are usually too small to accommodate for the larger particles (Hopkins, 1988). In the field, inclinometers, piezometers and extensometers are geotechnical/ structural techniques of measuring ground deformation (subsidence) (Craig, 2004).

Conversely, land surveying techniques have been used in recent years as a basic tool to measure settlement. Land surveying is a technique, profession and science which use precision to measure, record and map the physical environment (Schofield and Breach, 2007). It makes all essential measurements to determine the relative position of points on, above or beneath the earth's surface. These measurements are used to create land maps, demarcating boundaries for land ownership and in civil law purposes. In engineering surveying, these techniques are used for planning, design and construction works both on the surface and underground (Schofield and Breach, 2007). In the field of

geology, it is a simple field method which is used to monitor ground deformation called settlement (Schofield and Breach, 2007). The traditional way of monitoring settlement is to either periodically survey the vertical movements of the markers installed on the wall of the monitored building relative to the referenced local points and identify any changes or by transmitting the geodetic coordinates from the Survey and mapping office (SMO) benchmark positions to locally defined points (Dai and Lu, 2010). Therefore, land surveying techniques are useful for the monitoring of settlement (Schofield and Breach, 2007).

5.4.2 Techniques used to measure ground deformation

Surveying instruments that are used in the field consists of precise geodetic levelling, geodetic façade monitoring or using geotechnical instruments such as electronic liquid level gauges, precise taping and crackmeters (Kavvadas, 2003). Ground deformation can be measured using geodetic surveys which include conventional measurements (precise levelling), angle and distance measurements, photogrammetric techniques and satellites (Isioye and Musa, 2007).

Precise levelling and façade monitoring are the most common methods for monitoring displacements at the ground surface in the horizontal and vertical direction (US Army Corps of engineers, 1994). They may be used in the construction industry such as in deformation monitoring, the provision of precise height control for large engineering projects such as long-span bridges and dams, and, to determine mining subsidence (Schofield and Breach, 2007). The accuracy of these measurements are typically ± 0.2 mm / 100 m distances or < 4 mm / 1 km as stated by the US Army Corps of Engineers (1994). Precise spirit levelling is used to determine the elevation of vertical control points and other points throughout the survey may be determined from these vertical control points.

By using a digital camera, photogrammetry allows engineers to easily acquire photographs on site and interpret data at the office by employing two images which cover the same content but are taken from different perspectives to compute the spatial information of a measured object (Dai and Lu, 2010). This method also improves instrument portability and reduces the amount of time and crew that are required in the field. Photogrammetry has been applied to the modelling component provision for visualisation, progress assessment (Quinones-Rozo *et al.,* 2008; Kim and Kano, 2008; Golparvar-Fard *et al.,* 2009) and for dispute resolution (Luhmann and Tecklenburg, 2001).

Ground based laser scanning allows for rapid, remote measurement of millions of points. Thus, providing an unprecedented amount of spatial information (Isioye and Musa, 2007). The Global positioning system (GPS) can also be used to measure the vertical ground deformation (Isioye and Musa, 2007). However, the accuracy of each type of technique applied depends on the technique chosen, type of instrument, the nature of the terrain and the purpose of the work (Isioye and Musa, 2007).

5.4.3 Using surveying techniques to measure ground deformation.

For building sites in dense areas such as Hong Kong, it is necessary to measure the settlement of adjacent buildings in the course of foundation excavation to minimise disturbances to surrounding buildings (Dai and Lu, 2010). Isioye and Musa (2007) have used levelling techniques to measure the amount of deformation (settlement) of some benchmarks on the main campus of the Ahmadu Bello University in Zaria and on areas surrounding the University's dam. From this study, it was found that soil erosion, the weight of the dam and variations in the water pressure and stability problems caused by high pressures. The high pressures were responsible for instabilities along the embankments of dams.

The settlement of embankment fills are often very difficult to predict because they are affected by a variety of factors such as the moisture content, depth to water table, the slope angle, volume and height of the embankment and by the degree of compaction (Hopkins, 1988; Hopkins and Beckham, 1998; Lenke, 2006; Geng and Dou, 2012). Due to these reasons, the precise levelling technique was used to monitor settlement at the Cornubia development as it is a simple, cost effective technique which involves the measurement of the vertical distance relative to a horizontal line of sight (Schofield and Breach, 2007). However, the disadvantage of using this technique is that errors can occur from collimation errors (if the line of sight is not perfectly horizontal), parallax errors (poor focusing of the cross hairs), errors arising from the incorrect reading of graduated staffs due to wear and tear, and loose fixing of the tripods cause movement of the tripod head resulting in incorrect readings to be observed (Schofield and Breach, 2007). The methodology used for the monitoring of settlement at the Cornubia housing development using the precise levelling technique is presented in Chapter 6.

5.5 Developing a rating system

The highly degradable nature of argillaceous materials such as shales and mudrocks during the sampling process makes it very difficult to obtain representative samples to perform laboratory tests. These materials disintegrate easily when cored which makes it very difficult to obtain core samples for the Uniaxial Compressive Strength test (UCS), the Brazillian Disc Strength test and the Point Load Strength test. Hajdarwish and Shakoor (2006) stated that it is very difficult to obtain undisturbed samples of mudrocks to determine its shear strength properties. The nature of argillaceous materials such as shales and mudrocks has necessitated for researchers such as Deo (1972; 1973), Chapman *et al.* (1976), Morgenstern and Eigenbrod (1974), Shamburger *et al.* (1975), Lutton (1977), Strohm (1978), Franklin (1981), Santi and Rice (1991) Welsh *et al.,* (1991), and engineers to develop methods of predicting and estimating the index and shear strength parameters (c' & φ') of these materials. Attempts are often made to estimate the shear strength from their lithological characteristics

such as the clay content and clay mineralogy or other engineering properties such as the void ratio, Atterberg limit and slake durability (Walkinshaw and Santi, 1996).

Due to the development of areas which are underlain by shale thus being characterised as unsuitable, there is a need for a shale classification system that is capable of distinguishing the grade of shale which is based its exposure to weathering. This problem can be overcome by developing an indirect method of estimating the shear strength properties of shales using simple index tests. The commonly used index tests are the Atterberg limits test, the slake durability test and the Point Load Strength test (Deo, 1972; Morgenstern and Eigenbrod; 1974; Chapman, 1975; Shamburger *et al.*, 1975).

5.5.1 Predicting the shear strength of shales

There have been numerous attempts in the past to link the shear strength of materials with various geotechnical properties (Hardwick, 1992). These attempts include linking properties such as the residual strength with the clay fraction, residual strength with the plasticity index and the residual strength with the liquid limit. Lupini *et al*. (1981) noted that the residual strength does not significantly change with an increase in the clay content. Similarly, Kenny (1968) attempted to link the residual shear strength to the plasticity index and with grain size.

Hawkins and Privett (1985) later suggested that these correlations can be made under certain stress conditions. Additionally, they observed that there is a low scatter in the observed data and that the residual angle of friction is low provided that the clay fraction exceeds 60% and that the plasticity exceeds 45%. However, if the clay fraction in a sample is between 35-60% and the plasticity index is between 25-45% then Hawkins and Privett (1985) found that there is a wide scatter in the observed data. They concluded that it is inappropriate to employ the use of these correlations as they are characteristic of British soils.

Hajdarwish and Shakoor (2006) investigated the predictability of the shear strength from the lithological characteristics and the engineering properties of mudrocks using the direct shear box method. These tests showed that better statistical analyses of the results were achieved by performing several tests to compensate for the geological variations within individual mudrocks. Bivariate analyses showed the strongest correlations between the friction angle and the chemistry of the materials (expandable clays, slake durability index, nonexpendable clays, mixed layer clay) and between cohesion and slake durability (Hajdarwish and Shakoor, 2006). Multivariate regression analyses showed no strong correlation between the cohesion and the angle of friction of all mudrocks. This study concluded that no single geological property could be used to predict the shear strength of all mudrocks due to their highly variable nature (Table 5.6).

Table 5.6: Summary of the friction angles for all mudrocks and lithological subgroups (Hajdarwish and Shakoor, 2006).

Lithological Group	Sample number	Minimum	Maximum	Mean	Variance	Standard Deviation
All Mudrocks	45	10.9°	35.8°	24.9°	60.1	7.8
Claystone	10	10.9°	30.9°	22.4°	59.2	7.7
Mudstone	10	13.2°	29.6°	19.1°	33.3	5.8
Siltstone	12	22.0°	35.8°	32.4°	15.3	3.9
Shale	13	13.8°	34.3°	24.4°	41.4	6.4

5.5.2 The shale rating system

Several classification systems have been developed by many authors such as Chapman *et al.* (1976), Franklin (1981), Perry & Andrews (1982), Hudec (1982), Withiam and Andrews (1982), Hopkins (1988), Santi & Rice (1991), Santi (1998), Koncagul and Santi, (1999) and Santi (2006) that aim to assist engineers to group degradable materials when encountered in the field. This is done by comparing field and laboratory strength tests to the chemical composition of these materials. For example, Franklin (1981) designed a shale rating system for the construction of embankments, excavating methods and for the foundation properties and this rating system will be discussed later.

However, there is no correct method for characterising these materials. These rating systems, as identified by Chapman *et al.* (1976), fall into three categories: systems developed by geologists who emphasize genesis, classification systems developed by engineers who emphasize quantitative laboratory tests and systems which are developed by agencies to a specific application or region. Santi (2006) stated that the field recognition of degradable materials and the use of field instrumentation are crucial for characterising these materials. There are many problems that arise when dealing with weak rocks. These problems include poor field data, the lack of recognition of the sensitivity to water and by the underestimation of the influence of the rock mass properties such as remnant bedding planes (Santi and Shakoor, 1997).

Strohm (1978) developed a design criteria for the use of a particular material which is based on the slake durability index (I_D) and the jar slake test. Often, a large fraction of fine material causes settlement and prevents the required rock-to-rock contact. Hard, nondurable and intermediate shales require special treatment such as a high degree of compaction. Soils ought to be compacted for lifts when $I_D < 60$, $I_j \leq 2$ and hard, nondurable intermediate shales which require special treatment have a slake durability index (I_D) between 60-90 % and a jar slake (I_J) index of 3-5. Materials can be used in rock fill on condition that sand and gravel size ($I_D > 90$, $I_j = 6$) materials do not exceed 20-30 % of the total lift. Similarly, Lutton (1977) used the slake durability index to provide an estimate of the allowable lift thickness.

The shale rating system that was designed by Franklin (1981) groups the shale rock material or residual mass according simple index tests such as the slake durability index (SDI), the Atterberg limits and the Point Load strength test (Figure 3.13). Using the rating system shown in Figure 5.3, Franklin (1981) used the Point Load Strength test to further characterise a shale provided that it has an SDI greater than 80%. Additionally, Franklin (1981) used the Atterberg limits test to rate shales if these materials have a slake durability index that was less than 80%.

After the shale rating has been determined using Figure 5.3, Franklin (1981) uses this rating (R), to predict the shear strength parameters (i.e. the effective cohesion (c′) and effective angle of internal friction (φ′)) as shown in Figure 5.4. The individual rating (R) is plotted on this chart to determine the c′ & φ′ of the shale material. Using a slake durability index of 84 % and a Point Load Strength of 0.6 MPa, an example using the rating system is shown in Figure 5.3 and Figure 5.4.

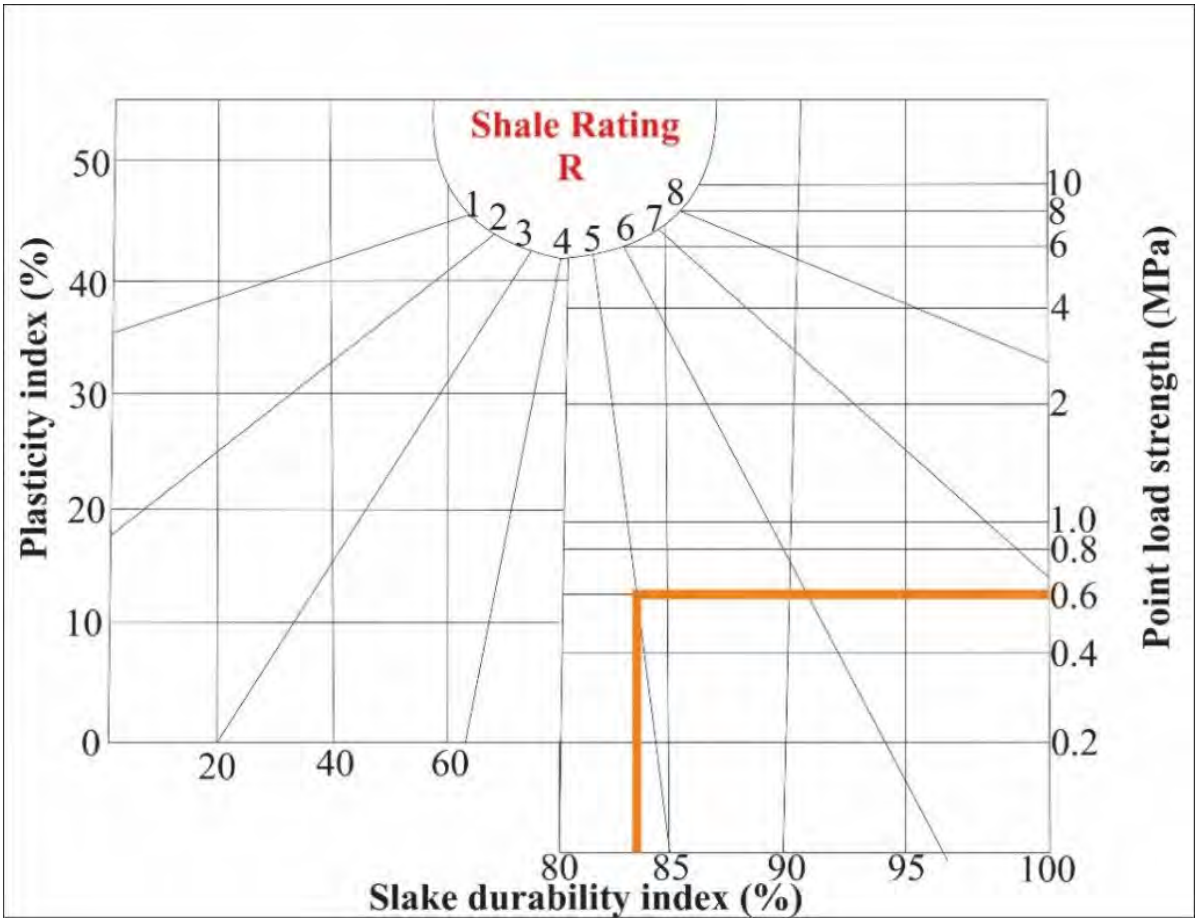

Figure 5.3: Shale rating chart (modified after Franklin, 1981).

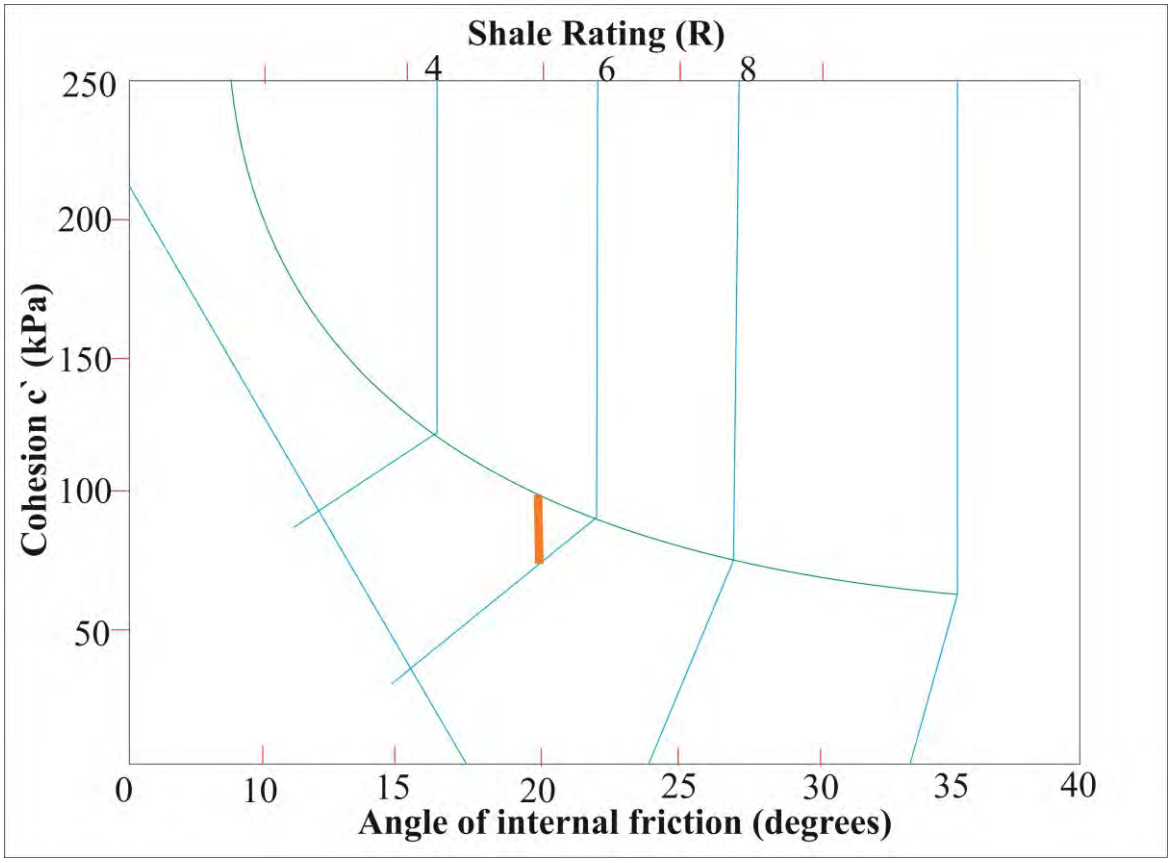

Figure 5.4: Trends in shear- strength parameters of compacted shale fills as a function of the quality of shales (modified after Franklin, 1981).

Based on tests conducted on Kentucky shales, Hopkins (1984) tried to correlate slake durability to the California Bearing Ratio for the design of pavements using Kentucky Shales. A method was developed to define suitable relationships for these designs and to convert three different indexes of slake durability to predictions of the Kentucky California Bearing Ratio (CBR) values (Walkinshaw and Santi, 1996). Perry and Andrews (1982) related the mode of slaking to slope stability problems observed in mine spoils ranging in age from 2-10 years and by relating slaking to erosion problems. Sheet erosion was controlled from the formation of a pebble pavement by armouring the surface with resistant small chunks of material. Hopkins (1988) further found that, after testing twenty samples of shale, the natural water content of unweathered shales was a good predictor of important engineering properties.

A modification of the slake index was made by Santi and Rice (1991) to provide a classification of degradable materials. Santi and Rice (1991) showed the implications and the influence of slake differential partitioning by plotting the one-cycle slake value against the difference between the five-cycle and one-cycle values. This was done to determine the expected behaviour of a particular material by comparing the current state of weathering against the difference between the first and fifth cycle of slaking (Figure 5.5). This proposed chart also indicates the subsequent laboratory tests that are likely to further characterise the material.

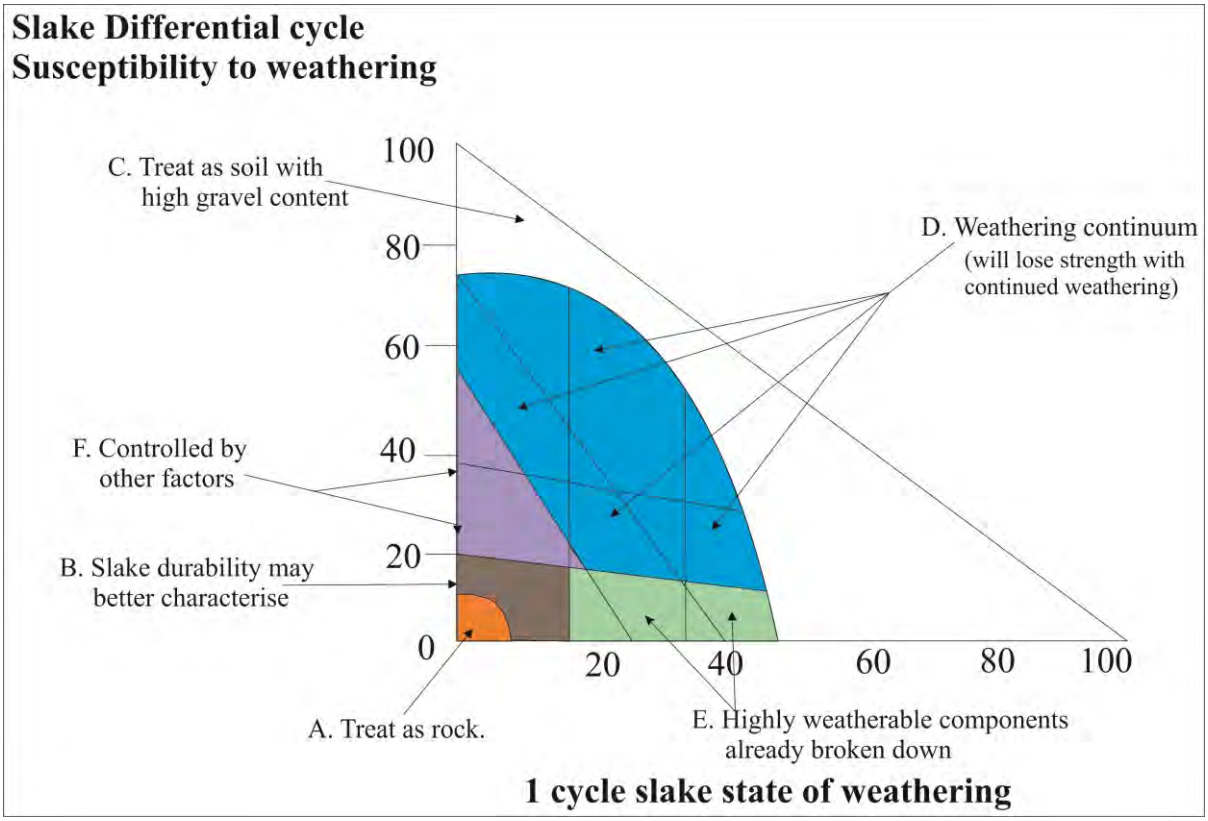

Figure 5.5: Implication of slake differential partitioning (adapted from Santi and Rice, 1991).

Franklin's (1981) shale rating chart which uses geotechnical tests such as the Atterberg limit, the Point Load Strength test and the slake durability test is used to predict the shear strength properties of shales for the purpose of excavation methods, foundation design with emphasis on the construction of embankments. However, Franklin's (1981) shale rating chart is deficient as it does not incorporate the geochemical analyses of shales as it was found that weathering causes a reduction in the strength of shales and mudrocks as they weather to a fine grained soil mass (Cripps and Taylor, 1981; Bell *et al*., 2006). In addition, Franklin (1981) did not use the jar slake test as part of the rating system despite the jar slake test being a simple, cost effective and quick test to perform. This study therefore focuses on modifying Franklin's (1981) shale rating chart to incorporate the geochemical data and the jar slake index and to develop a simple shale rating system to be used by geotechnical engineers.

5.5.3 Applications of the rating system: The design of embankments

One of the main tentative applications of Franklin's (1981) shale rating system is for the design of embankments when using shale materials. Trends in the embankment side slopes as a function of embankment height and the quality (rating) of shale construction materials are shown in Figure 5.6. A general increase in the side slope angle is apparent with increasing the shale rating to a maximum angle of 35 ° for shale rock fills that have ratings in the range of 8-9 (Franklin (1981). The side slope angle is also affected by the embankment whereby small embankments have flatter slopes thus

making it easier to maintain. As the embankment height increases, geotechnical considerations are necessary to ensure that the slopes are designed effectively and safely. The side slope angle decreases in high embankments thus reflecting the importance of embankment stability and need to maintain acceptable safety factors.

Shale embankments and platforms should be designed and constructed to have a factor of safety ≥ 1.5. When durable rock and durable shales are placed as clean rock, the amount of soil should be limited to ≤ 20 % of the fill material. Laboratory moisture-density tests are necessary to control the field compaction of shales. During the early design phases, surface structures should be constructed to convey surface runoff from the shale embankments (Hopkins and Beckham, 1998). These structures will aim to minimise seepage of water and hence reduce settlement. Additional compaction can reduce settlement whilst flatter slopes can reduce instabilities. Table 5.7 provides an indication of estimated and measured settlements when using shales as fill material. One of the major pitfalls of embankments constructed of shale is the lack of proper compaction near the edges. This often happens because compaction equipment cannot operate properly near the edge of the shale filled slope and results in a zone of weak material in the slope (Hopkins and Beckham, 1998).

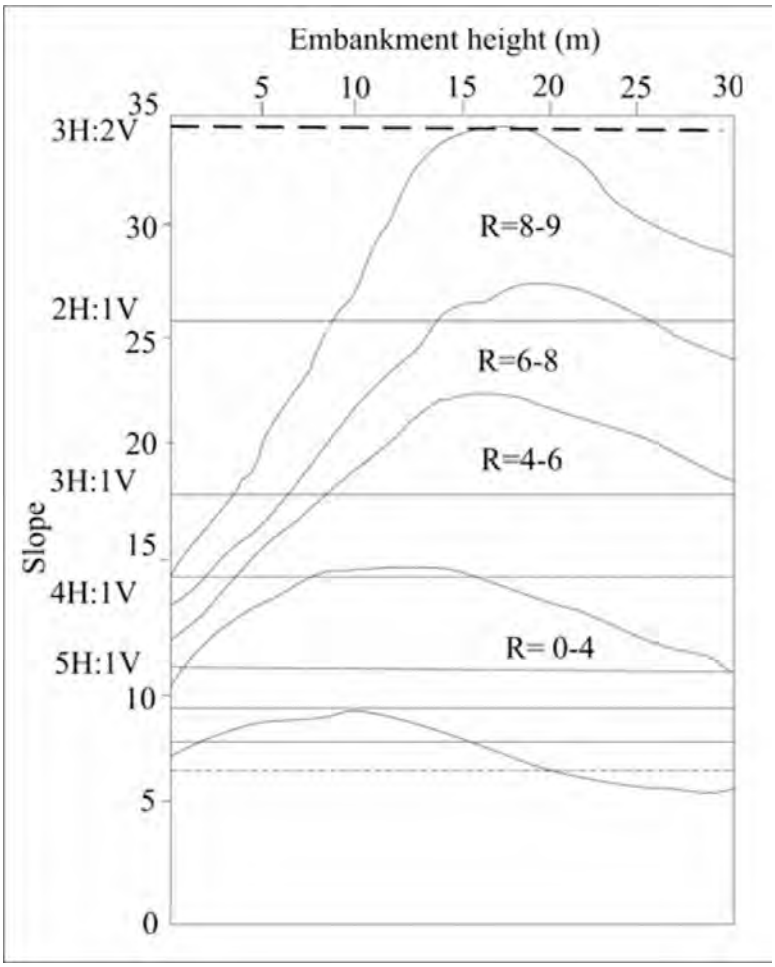

Figure 5.6: Trends in stable embankment slope angle as a function of embankment height and quality of the shale fill (modified after Franklin, 1981).

Table 5.7: Showing the estimated and measured settlements of test stations which consists of Kentucky shales (modified after Hopkins and Beckham, 1998).

Fill Height (m)	Reported Factor of Safety	SDI of Shale Fills (%)	Long-Term Settlement (m) NAVFAC (1982)	Hopkins (1985)	Measured	Strohm et al (1981)
16.76	1.4	69	0.050-0.101	0.096	-	0.076-1.27
19.81	1.5	48	0.058-0.117	0.132	0.122-0.173	0.050
19.81	1.6	89	0.634-0.127	0.119	-	0.102-0.127
15.24	1.5-1.75	-	0.046-0.091	0.053-0.076	0.074-0.081	-

Many measures can be adopted to prevent infiltration or the instabilities that are caused by water. The use of drainage blankets and filter fabrics at the base of the shale embankments can prevent the infiltration of subsurface water from deep residual soil overburdens and seepage from rock formations. Designers of shale embankments should consider the use of geosynthetic materials which are spaced at appropriate heights throughout to reinforce the outer slope of the shale fill. Hopkins and Beckham (1998)

5.6 Summary

This chapter has provided a detailed description of the various classification systems for shales and these which include field methods and laboratory tests. This chapter also presented the rating systems which are used to characterise shales and their deficiencies with emphasis on Franklin's (1981) shale rating system. The next chapter provides a description of the geology at each sampling site and the methodology which was used to monitor settlement.

Chapter 6

Fieldwork: Geotechnical sampling and monitoring of settlement.

6.1 Introduction

Fieldwork facilitates the ability to understand and visualise the complexities of geology in three dimensions (McCaffrey *et al*., 2005; Whitmeyer *et al.,* 2009). This chapter focuses on the fieldwork which was undertaken, the procedures and methods adopted in taking samples for laboratory testing and the problems encountered during the sampling process. A description of the geographical location and geological conditions of each sampling locality is given. Furthermore, the methodology used to monitor settlement of platforms comprising shale material is also presented.

6.2 Geotechnical sampling

Sampling techniques affect the quality of the results obtained from laboratory testing (Schoenleber, 2005). The grab sampling technique was chosen as the sampling technique and grab samples of the shale rock materials were obtained from each locality. A grab sample is a discrete aliquot which is representative of one specific sample site at a specific point in time (Schoenleber, 2005). The representative sampling technique was used to sample the soil material. This sampling technique was used to obtain samples which are believed to be representative of the soil materials for each sampling site (Christopher *et al.*, 2006). The purpose of using these sampling techniques to obtain geological materials was to perform laboratory tests.

A shovel was used to collect disturbed soil samples for soil index tests and placed in a plastic sampling bag. Approximately 5 kg each of soil materials were sampled from each locality. Disturbed soil samples were taken and used to conduct soil classification tests (Craig, 2004).

Fresh and weathered shale block samples were sampled using a 10 kg hammer and chisel. The shale rock materials which were sampled had a minimum dimension of 0.3 m in length and 0.1 m wide to cater for the coring process. Whilst using the hammer to obtain the block samples, care was taken to avoid creating additional fractures in the shale samples as suggested by Nandi *et al.* (2009). Fresh shale materials were sampled at approximately 0.3 m into the shale outcrop to obtain samples. According to Hopkins (1988), this method was used to minimise the effects of surface weathering on the shale samples. These materials were also placed in air-tight plastic bags and sealed to prevent any loss of moisture and transported to the Engineering Geology laboratory at the University of KwaZulu-Natal, Westville campus.

Fresh shale materials were collected and tested from each locality to determine the strength and durability of the unweathered shale materials. The weathered shale materials were sampled and tested to examine the effects of weathering on the strength and durability of the weathered shale materials in

relation to the unweathered (fresh) shales. Also, these materials were analysed to determine the type and amount of clay minerals which are present in the weathered shales as compared to the unweathered shale material. Approximately 300 kg of fresh shale material and 300 kg of weathered shale materials were sampled from each locality. A large amount of shale material was required to obtain rock cores for Point Load Strength tests as well to perform the large scale shear box tests at the University of Witwatersrand which is discussed in Chapter 7.

6.3 Sampling site

Four areas of shale outcrops were sampled within KwaZulu-Natal. These sites were chosen for sampling because of the very good exposures and accessibility of the shales of the Pietermaritzburg Formation. These shale exposures allowed for the sampling of fresh and weathered shale material as well as the sampling of the residual material. They were also chosen because they were not affected by major structural discontinuities such as faults or intrusions. Geographically, three of the four localities are found within the Pietermaritzburg metropolitan area whilst the other locality is in the Cornubia development area situated in Verulam, KwaZulu-Natal. The geographical position of each locality is shown in Figure 6.1. Figure 6.2 (a) and (b) show the distribution of shales of the Pietermaritzburg Formation found in Verulam and Pietermaritzburg area respectively.

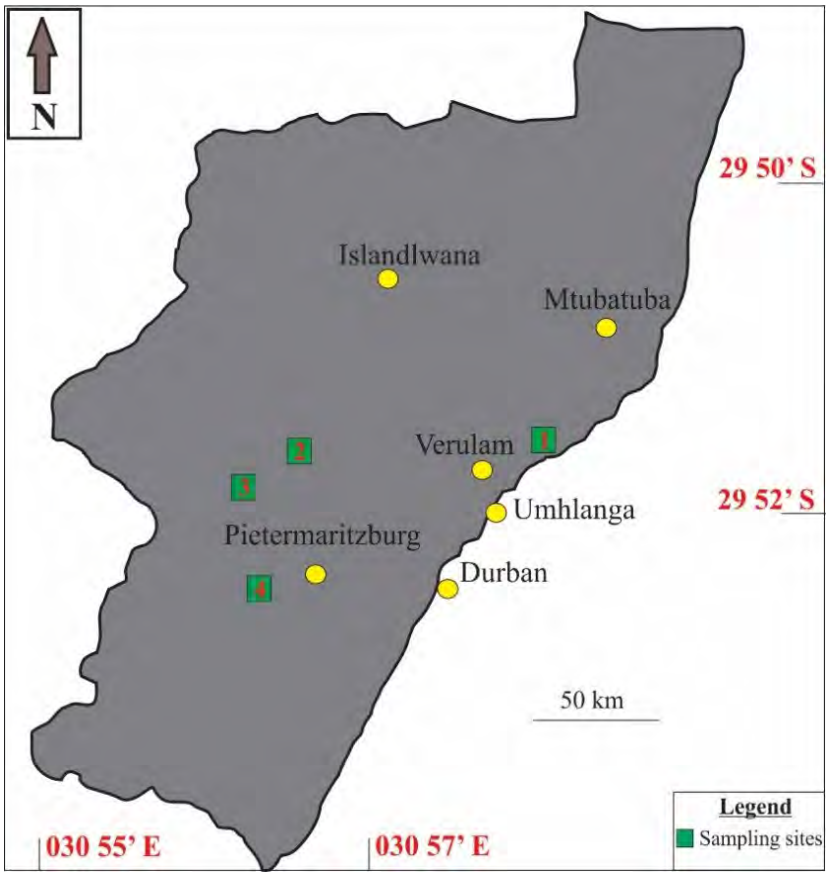

Figure 6.1: Location of the sampling sites.

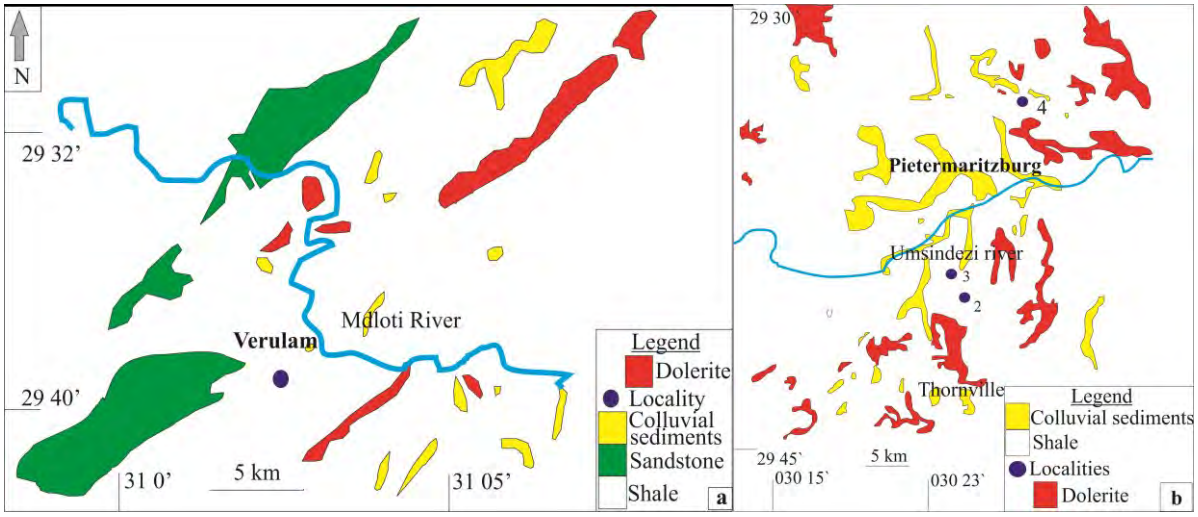

Figure 6.2: Distribution of shales of the Pietermaritzburg Formation in (a) Verulam, (b) Pietermaritzburg.

6.3.1 Locality 1: The Cornubia housing and industrial development

Locality 1 is the Cornubia housing and industrial estate area which is a multi-billion rand government funded project and aims to provide housing for the underprivileged, serve as a platform for large businesses, uplift local communities and develop the surrounding towns such as Verulam, Ottawa, Phoenix and Mount Edgecombe. Figure 6.3 (a) shows a map of Verulam and a satellite image (b) of the Cornubia housing and industrial development.

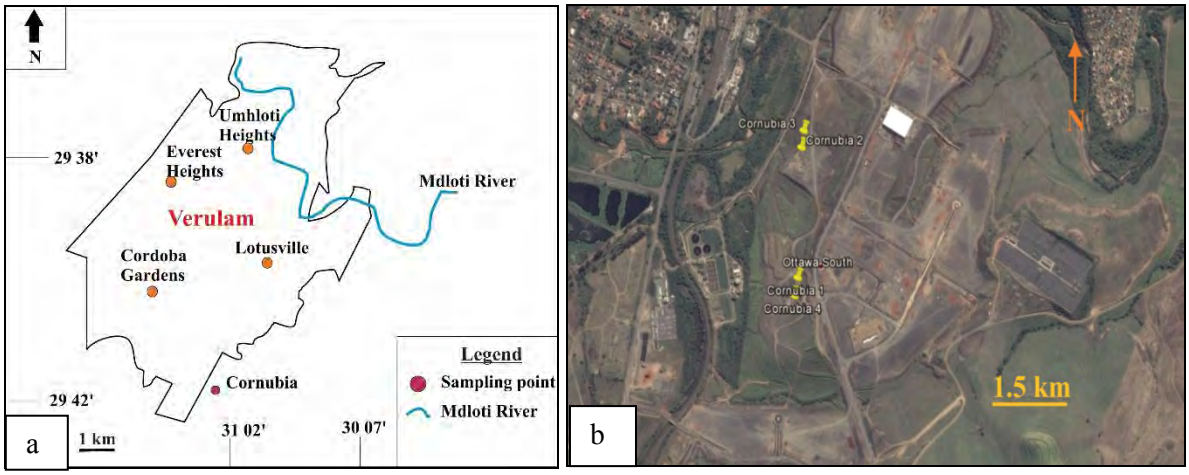

Figure 6.3: (a) The area sampled within Verulam, (b) satellite image of the Cornubia housing and industrial development

At this particular locality, the shale outcrop extends over 200 m^2 and is found at 29° 40'15.5'" S, 031° 02' 8.67" E and at an altitude of 79 m above mean sea level (MSL). Generally, the geology at the Cornubia housing and industrial development consists of sandstones, siltstones, shales, dolerite and residual soil. The siltstones and shales which are found at the Cornubia development are underlain by sandstones and capped by brown, colluvial, very sandy clays and clayey sands. These soil materials

have an average thickness of 0.5 m. The bedding of the sedimentary bedrock is generally dipping 10° in a south westerly direction in the northern and eastern part of the Corunbia development. The dolerite intrusions occur in the form of dykes and sills. They are moderately to completely weathered and are covered by residual clays or clayey sandy soils and have an average thickness of 3 m.

This particular site is underlain by shales of the Pietermaritzburg Formation and the shale bedrock is overlain by residual soils of the *in situ* shales and colluvial soils. The shale beds in this area dip at an angle of 8-10°. The laminations of the shale materials dip in the same direction as these sedimentary units. The upper "highly weathered shale" is brown in colour and breaks easily along the horizontal lamination planes. These materials are highly jointed, contain two major joint sets and the joints are partially filled with the residual soil material of the shale bedrock. The lower "less weathered shale" is dark grey in colour and is less jointed than the weathered shale. The shale banks as shown in Figure 6.4 consists of two horizons; namely the weathered horizon and the less weathered horizon.

Figure 6.4: The shale horizons at the Cornubia development.

This site is a desirable sampling locality due to the good exposures of fresh and weathered shale material, the residual soil material and the ease of obtaining shale samples. The residual soil materials consists of dark brown sandy clays and clayey sands which extends up to 0.5 m (Drennan, Maud and Partners, 2010) and were sampled from this locality to perform soil index tests. Large (> 0.3 m) shale rock samples representing the fresh and weathered material were also sampled from this locality. The *in situ* fresh and weathered shale materials are being used as fill material to create platforms for the construction of housing and industry. These materials are being removed by drill and blast techniques.

6.3.2 Localities 2, 3 and 4

Localities 2, 3 and 4 are situated in Pietermaritzburg, KwaZulu-Natal. Figure 6.5 shows a map of the Pietermaritzburg area depicting the location of these sampling sites as well as satellite images of the different sampling sites.

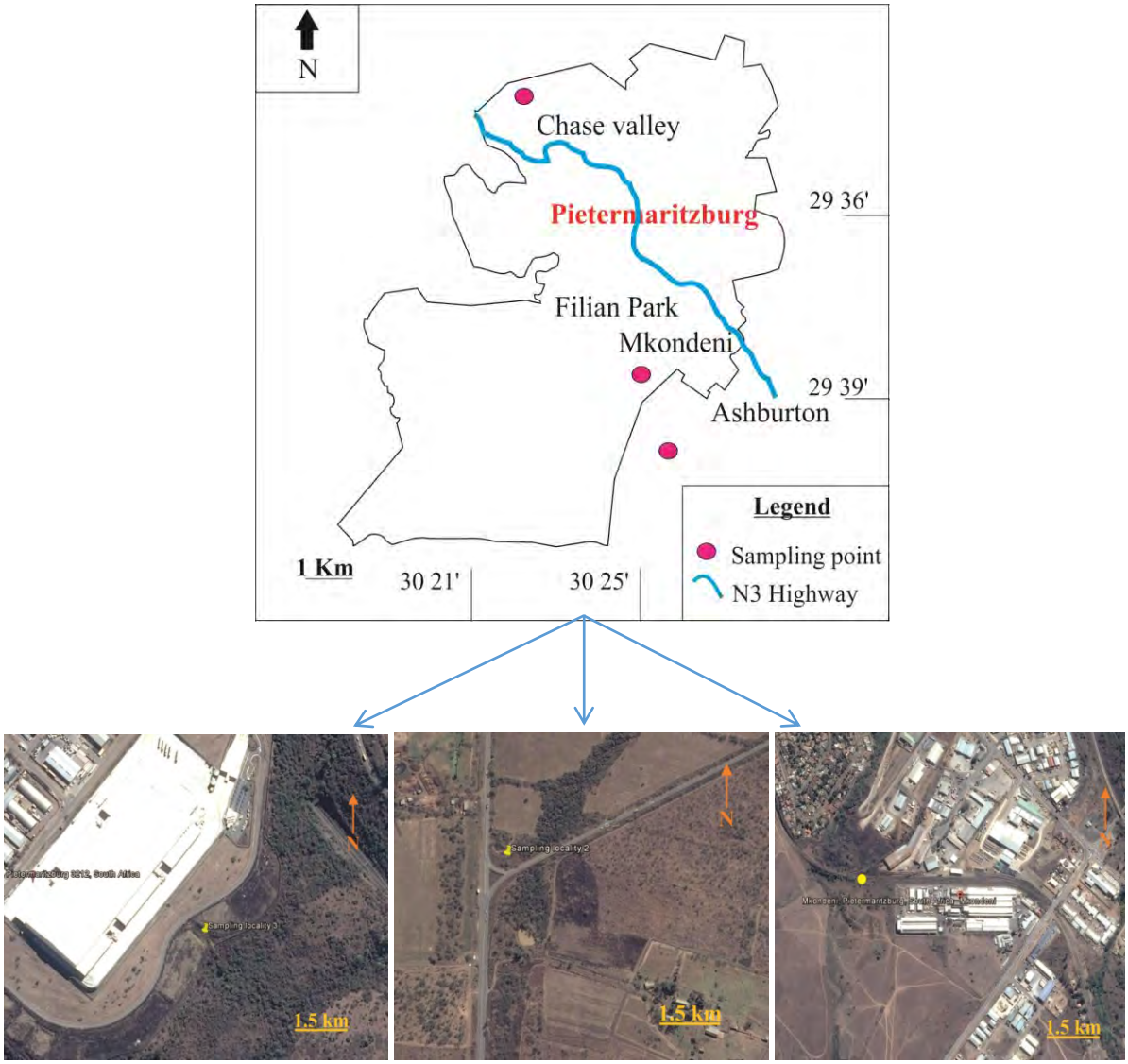

Figure 6.5: Sampling sites in the Pietermaritzburg area.

6.3.2.1 Locality 2-Ashburton

Locality 2 is situated along the railway track between Ashburton and Watsonia Drive with co-ordinates: 29° 28’ 59” S, 30° 25’ 21” E and at an elevation of 748 m above sea level. The shale outcrop at this locality appears as isolated *in situ* outcrops of fresh shale material with minor exposures of weathered shale material. The weathered shale is brown in colour whilst the less weathered (fresh) shale is dark-grey to black in colour. The poorly exposed shale outcrops made it

very difficult to obtain the orientation of this sedimentary bed. The fresh shale material is less jointed and less fractured as compared to weathered material which made sampling very difficult. At this site, a railway line was constructed on the shale outcrops (Figure 6.6). Dolerite fill has been used to stabilize this slope and surrounds the shale outcrop. This increased the difficulty in obtaining the weathered shale materials as the dolerite materials were mixed with the weathered shale material. As the weathered shale materials were sampled, they began to break into smaller pieces due to their highly fissile nature. This site was chosen as a result of the hard fresh material which was labour intensive in sampling and thus required a lot of effort to sample.

Figure 6.6: Exposure of the shales at Locality 2.

6.3.2.2 Locality 3- Mkondeni

This locality is located at 29 39’ 31” S, 30 25’ 33” E and at an elevation of 729 m. The shale outcrop appears on both banks alongside a valley and dips at angle of 11° towards north and the laminations are parallel to the shale beds. The fresh shale material at this site is more weathered than the fresh material at Locality 2. At this locality, the fresh and weathered shale materials are well exposed (Figure 6.7). The weathered shale material is brown in colour and is highly weathered. The shale is very friable and is highly jointed. The joints are partially filled and contain one major joint set. It was difficult to obtain large block sizes (> 0.3 m^2) of the weathered shale materials because samples broke easily along the lamination planes. The fresh shale material is dark grey in colour and did not disintegrate as easily as compared to the weathered material. This area was selected as a sampling site due to the ease in obtaining fresh and weathered shale rock materials and residual soil samples of the shale material.

Figure 6.7: Exposures of the fresh and weathered shales at Locality 3.

6.3.2.3 Locality 4- Chase Valley

Locality 4 is located at 29° 34’ 2, 25” S, 30° 21’ 15. 3” E and at an elevation of 686 m. This outcrop dips at 14° towards north and the laminations are parallel to the dip of the shale beds. Similar to Localities 1, 2 and 3, both the weathered shale material and fresh shale materials were sampled. The weathered shale material in this area is highly jointed and less fractured than the weathered shale materials in Locality 3. The joint surfaces are smooth and contain very little infilling. Fresh shale samples were obtained at a depth of 0.3 m. The fresh shale rock materials are medium to dark grey in colour and were less fractured and less jointed than the weathered materials. The dense vegetation at this site made sampling very difficult to obtain large shale samples for coring (Figure 6.8). Furthermore, the soil samples contained a lot of plant material and insects, in particular, ants.

Figure 6.8: Exposure of the shale materials at Locality 4.

6.4 Problems encountered during sampling

The removal of the overburden is accompanied by the vertical expansion of joints and the preferential development of horizontal fissures and can enhance the effects of vertical anisotropy (Cripps and Taylor, 1981). For this reason, it was easier to sample the weathered shale material as compared to the fresh shale material. Shale materials are also able to withstand higher forces perpendicular to laminations. As a result, more effort was required to hammer and collect representative (large) shale samples.

During the sampling process, a hammer and a chisel was used to obtain representative fractions for each laboratory test. With every strike of the hammer, the shale outcrops began to disintegrate into thin slabs of material. The disintegration of the shale material made it difficult to sample large shale materials which were required for coring. Furthermore, despite using care to sample the shale block samples as prescribed by Nandi *et al.* (2009), when using the hammer and chisel additional factures formed in the shale samples. The fractures caused the shale material to break along its planes of laminations.

To obtain fresh samples which were not affected by weathering, sampling depths of 0.3 m were required as suggested by Hopkins (1988). The sampling of shales at a greater depth instead of sampling materials at the surface, especially in Localities 1, 2 and 4, made it very difficult as the fresh material contained less fractures and joints and the materials were harder to sample.

Conversely, since mudrocks are easily weathered, they are frequently covered in vegetation (Tucker, 2001). Vegetation was found growing within the fractures of the shale outcrops as seen in Localities 3 and 4 and made it easier to obtain weathered shale samples from these localities as compared to Localities 1 and 2.

Fortunately, it was very easy to obtain representative fresh and weathered samples from Localities 1 and 3 for geochemical and geotechnical testing. In Localities 2 and 4, only a small amount of weathered shale materials were obtained. These materials were used for geochemical analyses and for geotechnical tests such as the slake durability test and the jar slake test.

6.5 Field measurement of settlement

6.5.1 Field monitoring of settlement at the Cornubia housing and industrial development

Shales, siltstones and dolerite, are being used as fill material to construct platforms at the Cornubia housing and industrial development. These platforms are being generated for the construction of housing and industrial buildings. The objective of this investigation was to measure the natural settlement of platforms which consists of shale fill. Furthermore, this investigation was conducted to determine whether the amount of settlement is proportional to rainfall. It is expected that during the

progressive weathering of the shale materials which has been exposed to the physical environment, settlement of these platforms would occur.

Two areas within the Cornubia housing and industrial development were selected for the monitoring of settlement. Within these areas, individual platforms were chosen for settlement monitoring since they represent areas of deepest fill (between 5-8 m). In addition, it is expected that the greatest amount of settlement would occur within these areas as these areas contain a large volume of shale material. Furthermore, these areas were selected as they were set aside as areas of minimal activity, so that the surveying monitoring pegs would not be damaged by construction workers or vehicles.

Three sites were selected within the two areas in the Cornubia development for the monitoring of settlement i.e. the Fountains site (Figure 6.9), and the Vumani Site and the Gralio site (Figure 6.10). At the Fountains site, shale is the major constituent fill material. At the housing sector of the Cornubia development, shales, siltstones and dolerite were used to construct platforms at the Vumani and Gralio site. Surveying pegs were used to monitor the change in the vertical height of the platforms from each area. At the Fountains site, four platforms were chosen and two surveying pegs were installed on each platform and monitored over a twelve month period. At the Vumani site, five surveying pegs were installed and monitored over a three month period whilst two surveying pegs were installed at the Gralio site and monitored over a period of four months.

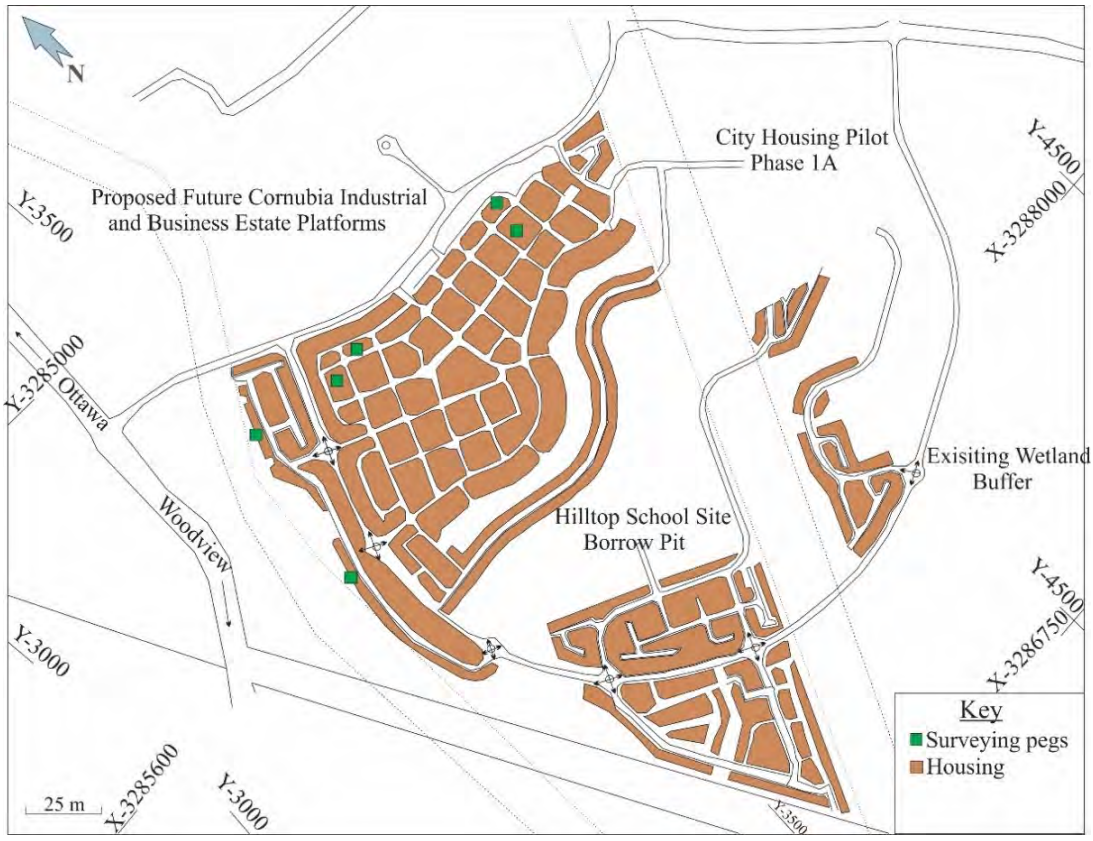

Figure 6.9: Site plan showing the location of the surveying pegs at the industrial sector of the Cornubia Housing and Industrial development (modified after Drennan, Maud and Partners, 2010).

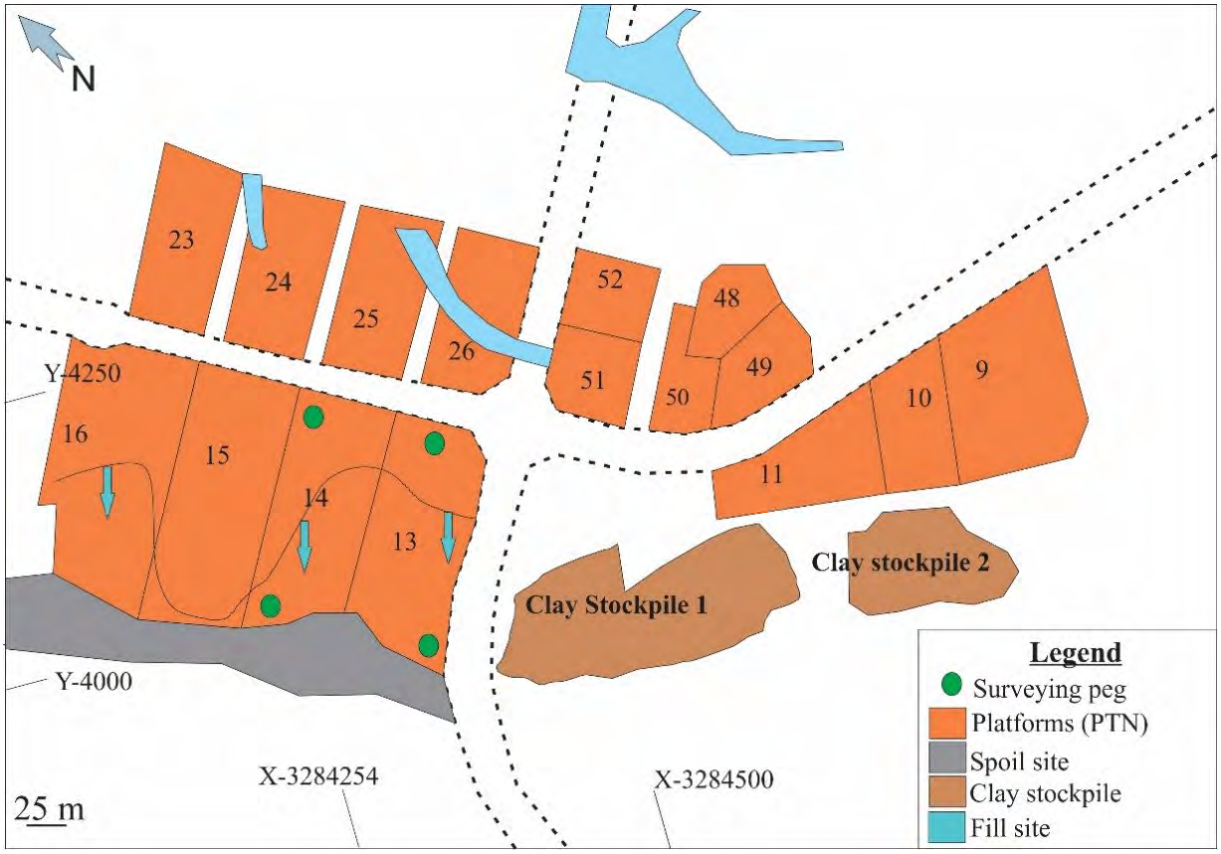

Figure 6.10: Site plan showing the location of the surveying pegs at the housing sector of the Cornubia Housing and Industrial Development (modified after Drennan, Maud and Partners, 2010).

Surveying pegs were installed on each of the specified platforms by hammering them into the ground. The geographic coordinates and the elevation of each surveying peg were then recorded. Although being labour intensive, the precise levelling technique was used to monitor settlement at the Cornubia housing and industrial development. Surveying equipment were borrowed monthly from the land surveying department from the University of KwaZulu-Natal (Howard campus) to monitor settlement. The surveying equipment which was used is shown in Figure 6.11 and it consists of a precise level which is attached to a tripod, a graduated levelling staff and a change plate. Firstly, the tripod was raised to eye level and the precise level was attached to the tripod. Thereafter, the tripod and the precise level were levelled by using the spirit bubbles which is situated on the precise level. The change plate was then placed on the floor next to the surveying peg and the levelling staff placed on top of it. Again, the levelling staff had to be levelled by using the levelling device which rests on the levelling staff.

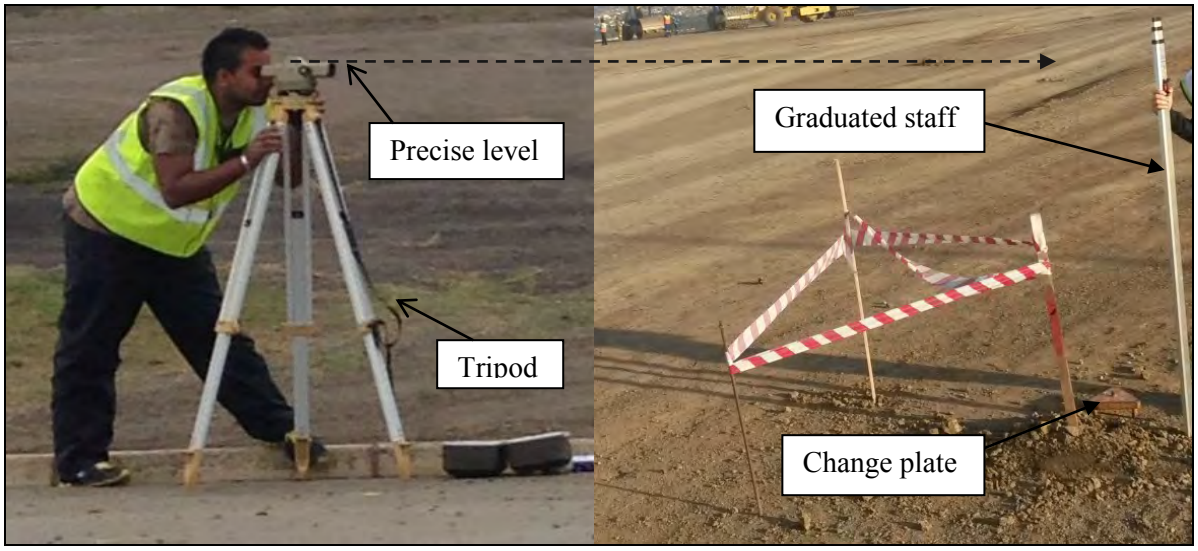

Figure 6.11: Monitoring of settlement of the shale platform using a precise level and a survey peg.

The cross-hairs which are etched onto a circle of a fine glass plate in the precise level is brought into focus by the eyepiece by the focusing screw prior to commencing observations. As pointed out by Schofield and Breach (2007), this process is necessary to remove any cross-hair parallax caused by the image of the staff being brought to a focus in front of or behind the cross-hair. Settlement readings were recorded from the highest point of the surveying peg in relation to the position which it rests onto the graduated levelling staff. Thereafter, the height of the surveying peg was measured relative to a fixed reference point to ensure that collimation errors do not occur. Collimation errors occur if the line of sight is not truly horizontal (Schofield and Breach, 2007). For the purpose of this study, street light poles were used as these reference points because they represent stationary objects which serve as fixed points (Figure 6.12). This procedure was done repeatedly for the monitoring of settlement of each peg at the respective sites. The settlement readings were taken to three decimal places from the graduated staff and were recorded to the nearest millimetre as prescribed by Schofield and Breach (2007). The accuracy of these measurements using the precise levelling technique is typically ± 0.2 mm / 100 m distances or < 4 mm/ 1 km as stated by the US Army Corps of Engineers (1994).

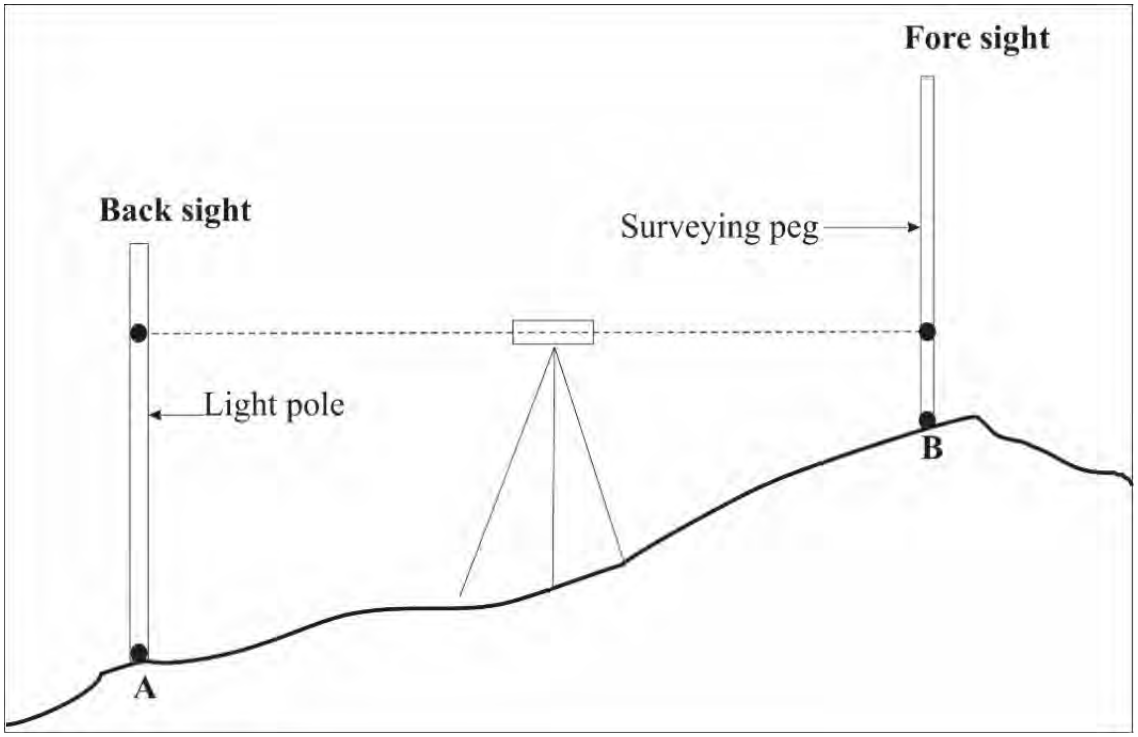

Figure 6.12: Showing the principle of precise levelling used to monitor settlement (modified after Schofield and Breach, 2007).

As a safety precaution, each surveying peg was surrounded by additional surveying pegs and wrapped with danger tape to ensure that construction vehicles would not drive over them. This precaution was also done to inform site workers that these pegs should not be tampered with since several other pegs which looked similar to the settlement pegs, are found throughout each platform.

Several difficulties were experienced during the field monitoring of settlement. Despite installing the surveying pegs in "open areas" of minimal activity and protecting the surveying pegs by additional pegs, many pegs were destroyed or broken. These pegs were continually damaged by site activity such as by construction vehicles and many surveying pegs had been removed as these areas were later categorised as areas of development. The removal of these pegs has had a significant influence on the monitoring of settlement as new pegs were required to be installed continuously. The installations of new pegs were of a different height to the original pegs and constantly required height corrections. These height corrections have made it difficult in evaluating the settlement readings.

Lastly, a graphical representation was created and was based on the amount of settlement which occurred monthly for the duration of the settlement monitoring of each site. These readings were compared to the average rainfall which occurred over the Verulam area.

6.6 Summary

This chapter presented a geographical and geological description of each Locality and the problems which were encountered during the sampling of shales. Furthermore, it also focused on the methodology which was used to monitor the natural settlement of platforms consisting of shale fill. The next chapter provides a detailed methodology and description of the laboratory tests which were performed to determine the geochemical and geotechnical properties of the shale materials from each sampling site.

Soil samples representing the completely weathered residual products were collected from the Cornubia development and from Locality 3 from the Pietermaritzburg area. At Locality 2, the *in situ* shale materials were overlain by dolerite fill, the dolerite fill material was used to stabilize and protect the railway line which was constructed on the top of that slope. The shale outcrop at Locality 4 was highly vegetated. Soil samples were taken from this Locality. However, it was very difficult to remove these organic substances.

Chapter 7

Laboratory testing

7.1 Introduction

Laboratory testing is a crucial aspect in any development as it describes the physical and chemical properties of geotechnical materials for the analysis and design of structures and, it has provided the lifeblood for the advancement in modern geotechnical engineering (Marr, 2000). Laboratory testing shows the modes in which a sample fails, it helps to explain the anomalies experienced during testing and enables us to control the stress, strain and drainage conditions (Marr, 2000; Head, 2006). This chapter describes the methodology which was used to perform the geochemical analyses and geotechnical tests. The chapter also highlights the advantages and weaknesses of each test performed. The aim of the laboratory tests were to determine the geochemical and geotechnical properties of the shale materials from each locality. These properties will later be used to develop a modified shale rating system which is the aim of this study.

7.2 Geochemical analyses

Geochemical tests were performed on the shale material from each locality in order to provide information on the chemical composition and the mineralogical composition of the shale materials. The fresh and weathered shale samples from each locality were analysed using X-ray diffraction (XRD).

7.2.1 Sample preparation in accordance with the International Atomic energy agency (IAEA, 1997)

Fresh and weathered shale material, each weighing approximately 1 kg, were sampled from each locality and transported to the Engineering Geology Laboratory at the University of KwaZulu-Natal. The impurities and weathered rinds from each of the fresh and weathered samples were removed using the serrated rock saw (Figure 7.1a). Thereafter, each sample was placed in the jaw-crusher (Figure 7.1b.) to reduce the size of the material to < 2 cm.

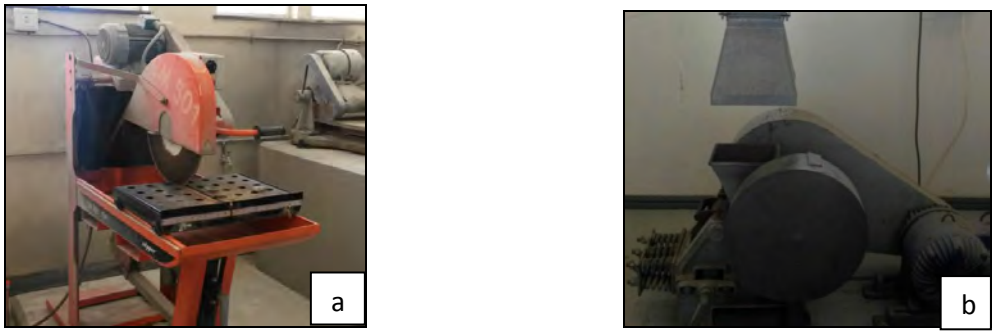

Figure 7.1: a) Rock-saw; b) Jaw-crusher apparatus.

After subjecting each sample to the jaw-crusher, the coning and quartering process was used to obtain a representative sample (approximately 80 g) for the milling phase (Figure 7.2). The selected 80 g of sample was milled in a steel mill (Figure 7.3a) to produce a fine powder (Figure 7.3b). Powdered quartz was used to clean the mill and to prevent caking from its previous use. In addition, quartz was used to clean the steel mill after milling each sample to prevent cross contamination between each sample. Acetone and tissue paper were also used to clean the mill after each milling phase.

Figure 7.2: The use of the coning and quartering technique of the shale material after using the jaw-crusher.

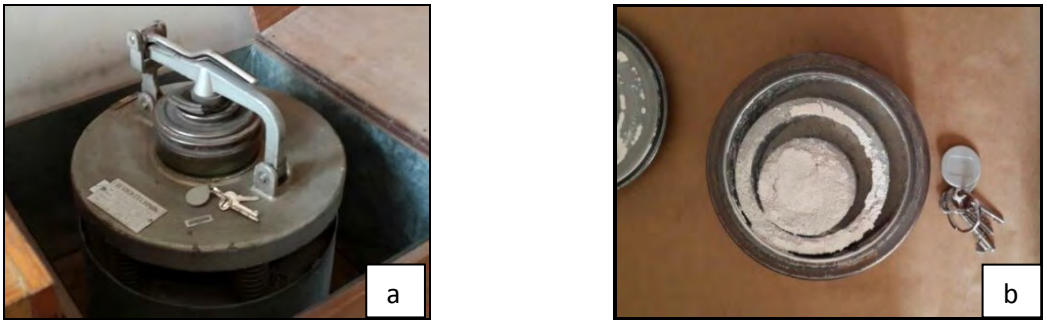

Figure 7.3: a) Vibratory disc mill and the steel mill which was used to mill the shale material; b) use of quartz after milling each sample.

7.2.2 X-Ray diffraction

The discovery of X-rays by Wilhelm Rontgen in 1895 has paved the way for major scientific discoveries. The analytical technique called X-ray diffraction (XRD) is used to identify the crystal system, the lattice constant and to identify the planes or orientations of a specimen (Nuffield, 1966). Also, this technique is used to identify the phases of a crystalline material (Dutrow, 2007). It uses monochromatic X-rays to provide information on the mineralogical composition of a specimen (Nuffield, 1966).

As primary X-rays hit the sample, the specimen diffracts these X-rays and the detector detects the position of the diffracted X-rays (Poppe *et al.*, 2002). The detector measures the two theta (2θ) angles of the X-rays which reflects off the unknown crystal. This analytical technique is regarded as an attractive and non-destructive technique because of its ease and speed of performance. It requires a

small amount of material and it can be used to perform semi-quantitative analyses on poly-mineralic mixtures (Poppe *et al.,* 2002).

Fresh and weathered shale materials from each locality were analysed using this analytical technique to determine the mineralogical composition of each sample. The weathered material was analysed to determine the change in mineralogy of the fresh shale material, particularly due to the weathering (alteration) of the major component minerals. This analytical technique as stated by Boggs (2009), allows for the identification of the minerals which are present in highly degradable materials, in particular, it allows for the identification of clay minerals.

Approximately 10 g of each sample was used for this analysis. The powdered sample was placed in a sample holder and compacted to ensure that it had a perfectly flat surface. A flat surface is required so that the 2θ angles can be measured accurately. These samples were then placed in the PANalytical Emprean XRD machine which was used to perform the XRD analyses (Figure 7.4). The PANalytical Emprean XRD machine generates a file which contains a list of the positions of the deflected X-rays for each sample tested.

Figure 7.4: PANalytical Emprean XRD machine. Inset shows the canister which contains the milled shale material.

7.2.3 Using PANalytical Highscore Plus for XRD

Once the XRD machine has analysed the samples, it is then exported as an xrdml file. This file is then imported into a computer program called Highscore plus so that the minerals found in each sample can be identified. After importing the data, the identify tab is used to begin the analyses by selecting individual minerals. These minerals are selected to determine whether their peaks match the peaks which have been identified by the XRD machine (Figure 7.5). Thereafter, a special tool incorporated within Highscore Plus called the Rietveld Analysis method was used to determine the percentage of the individual minerals found within each sample. The Rietveld method refines the user-selected parameters to minimise the difference between the observed data (experimental pattern) and a calculated pattern (Speakman, 2012). This tool matches the attributes of the observed data such as the crustal structure, preferred orientation and peak functions to the selected minerals to determine whether the attributes of the observed data matches the calculated patterns. This method was applied to the fresh and weathered shale materials from each locality. The procedures used in Highscore Plus to analyse the shale samples from the different localities were performed as suggested by Speakman (2012).

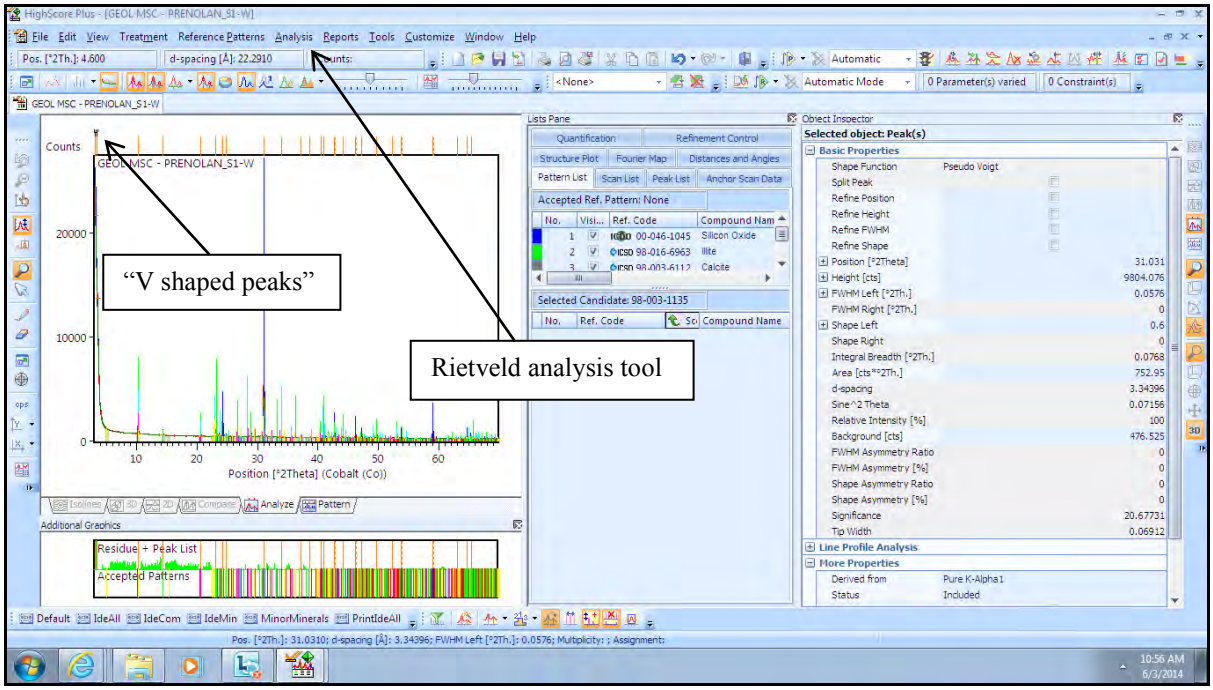

Figure 7.5: Highscore Plus computer software.

The value of these analyses depends on the knowledge of the user. According to the IAEA (1997), the user is required to have the necessary competency and to have an idea of the type of minerals which should be present in the sample under investigation as this computer software will generate many potential candidate minerals. These "v shaped" peaks will then disappear if the minerals which are chosen, match. The Richveld analysis tool is used to display the relative proportion of each mineral

and to assist in determining whether a certain mineral is actually present without performing XRF analyses.

7.3 Geotechnical testing

A series of laboratory tests were performed to determine the index properties of the residual soil material and the physical properties of the shale rock samples from the four localities. These tests comprise the Moisture Content test, the Particle Size Distribution, the Atterberg limits test, the Jar slake test, the slake Durability test, the Point Load Strength test and the Shear Box test (Table 7.1). The residual soil material from the Cornubia development and Locality 3 were subjected to the Particle Size analysis and the Atterberg limits test. The fresh and weathered shale samples from each locality were subjected to the slake durability test and the jar slake test. The Shear Box and Point Load Strength tests were performed on the fresh and weathered material from the Cornubia development and from Locality 3 from the Pietermaritzburg area. In addition, the Shear Box test was also done on the fresh material from Localities 2 and 4 from the Pietermaritzburg area. The purpose of these tests were done to geotechnically characterise the shale materials from each locality. In addition, it is hoped that the shale material from each locality will be characterised more effectively by performing a variety of index tests, durability tests and shear strength tests.

Table 7.1: Type of laboratory test performed on the fresh and weathered samples from each locality.

Type of test performed								
	Locality 1		Locality 2		Locality 3		Locality 4	
	F	W	F	W	F	W	F	W
Moisture content	Yes	Yes	Yes	Yes	Yes	Yes	Yes	Yes
Atterberg limit	Yes	No	No	No	Yes	No	No	No
Jar slake	Yes	Yes	Yes	Yes	Yes	Yes	Yes	Yes
Slake durability	Yes	Yes	Yes	Yes	Yes	Yes	Yes	Yes
Point Load Strength	Yes	No	No	No	Yes	No	No	No
Shear box	Yes	Yes	Yes	No	Yes	Yes	Yes	No

F: Fresh; W: Weathered

7.3.1 Moisture content

Head (1982) defined the moisture content of a soil or rock as the amount of water present in its pore spaces. A soil's moisture content affects behavioural properties such as the consolidation, its shear strength and the degree of swelling and shrinkage whilst the moisture content in a rock affects

properties such as inhomogeneity and anisotropy, the deformability and compressive strength (Hudson and Harrison, 1997). The moisture content has a profound effect on the behaviour of a soil and the natural moisture content gives an indication to a soil's water retention. Also, Hoek *et al.* (1998) stated that in weaker sedimentary rocks such as shales and siltstones, sample preparation for triaxial testing is difficult as they tend to de-laminate and slake when subjected to changes in the moisture content. The moisture content is determined according to Equation 7.1:

$$Moisture\ content\ (\%) = (m_W / m_S) \times 100 \qquad 7.1$$

7.3.2 Particle size distribution

Soils consist of an assemblage of discrete particles of many shapes and sizes (Craig, 2004). A particle size analysis is done to group these particles into separate range of sizes, and to determine the relative proportions, by dry weight, of each size range (Head, 1982). Soil material were sampled and analysed from the Cornubia development and Locality 3 from Pietermaritzburg in accordance with the British Standard (BS) 1377: 1975. These samples were passed through six sieves for 10 minutes. The sieve sizes used were: 2000 μm, 425 μm, 250 μm, 125 μm, 93 μm and 63 μm (Figure 7.6) and the mass retained was calculated and given as a percentage as shown in Appendix B. The mechanical sieve shaker was used to ensure that a uniform sieving procedure was used and to relieve the operator of physical effort (Head, 2006).

Figure 7.6: Sieve Shaker showing the sieves used.

Wet sieving was done as prescribed by Head (1982) to analyse the percentage of finer material (< 2 mm). These analyses were done using the Malvern Mastersizer 2000 apparatus (Figure 7.7), particularly to determine the amount of fine particles such as the amount of clay particles present. This instrument uses a laser and light diffractometer to generate a graphical representation of the "fine

particle" analysis (Head, 1982). According to McCave *et al.* (1986) a narrow beam of monochromatic light from an He-Ne laser is passed through a sediment suspension and the diffracted light is focused onto a detector. The individual particles of a given grain size diffracts light through a given angle, whereby the angle increases with a decrease in the size of the particles (Boggs, 2009). Thus, a stream of particles can be passed through the beam to generate a stable diffraction pattern. Fortunately, this instrument is equipped with a laser ablation feature which allows for the analysis of fine particles despite their tendency to stick together.

Figure 7.7: Malvern Mastersizer 2000 apparatus.

7.3.3 Atterberg limits

The liquid limit, the plastic limit and the shrinkage limit are collectively known as the Atterberg limits and was first used to classify agricultural soils in 1911 (Head, 2006). The Atterberg limit is also known as the consistency limits of a soil where consistency of a soil refers to a physical state which is indicative of a particular moisture content (Head, 1982). There are four consistency states that exist for cohesive soils which depend on their moisture content. These states consist of solid, semi- plastic, plastic and liquid. The boundaries between each state are known as the shrinkage limit, plastic limit and the liquid limit respectively (Head, 1982) and these boundaries are shown in Figure 7.8.

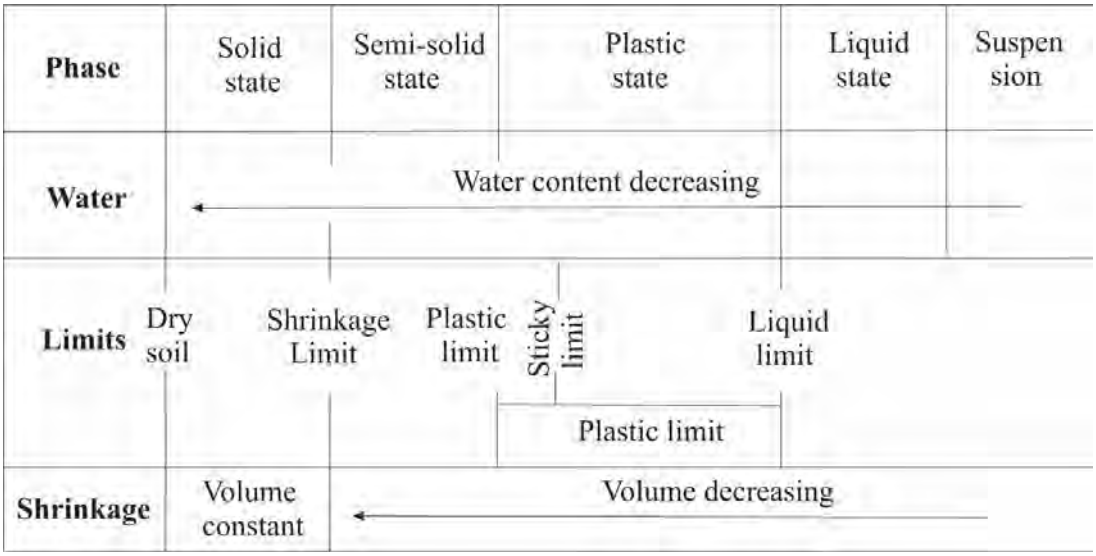

Figure 7.8: The consistency phases of cohesive soils (modified after Head, 2006).

Soil samples were tested from the Cornubia development and Locality 3 from the Pietermaritzburg area in accordance with Head (1982), (BS): 1377: 1990 and Verwaal (2005). Soil samples could not be obtained from Locality 2 because dolerite was used to stabilize the railway track which was built on the shale outcrop and, the dense vegetation in Locality 4 did not allow for the sampling of soil material.

The preparation of the soil samples from both localities commenced by dry sieving 1 kg of material through a 0.425 mm sieve for five minutes. The materials which passed through this sieve were placed in a glass bowl and mixed with de-ionised water until a slurry paste was formed. The glass lid was placed over the bowl to prevent any loss of moisture and to allow the soil material to mature for a 24 hour period. The Atterberg limits tests were done soon after the 24 hour drying period has occurred.

7.3.3.1 Liquid limit

The change between the plastic state and the liquid state of a soil as the moisture content changes is known as the liquid limit and is given as a percentage (Head, 1982). The Casagrande test was done to determine the liquid limit using an ELE Casagrande apparatus. After the 24 hour drying period, the soil material was placed in the brass bowl and a grooving tool was used to produce a groove through the centre of the soil sample (Figure 7.9). The Casagrande apparatus was switched on until the two portions of the adjacent soil material flowed together under its own weight. As soon as the adjacent soil material touched over a distance of 12.5 mm, the Casagrande apparatus was switched off and the number of taps (blows) was recorded. This procedure was done five times for each soil sample which was taken from each locality.

Figure 7.9: Casagrande test used to determine the Liquid Limit.

Thereafter, a small portion of soil material (approximately 50 g) was oven dried for 24 hours to determine the moisture content of that material. The moisture content was recorded after each step. Once the moisture content has been recorded after each step, the liquid limit was determined from plotting the number of blows against the relevant moisture content. The liquid limit is the moisture content at 25 blows from the flow curve and is shown in Figure 7.10.

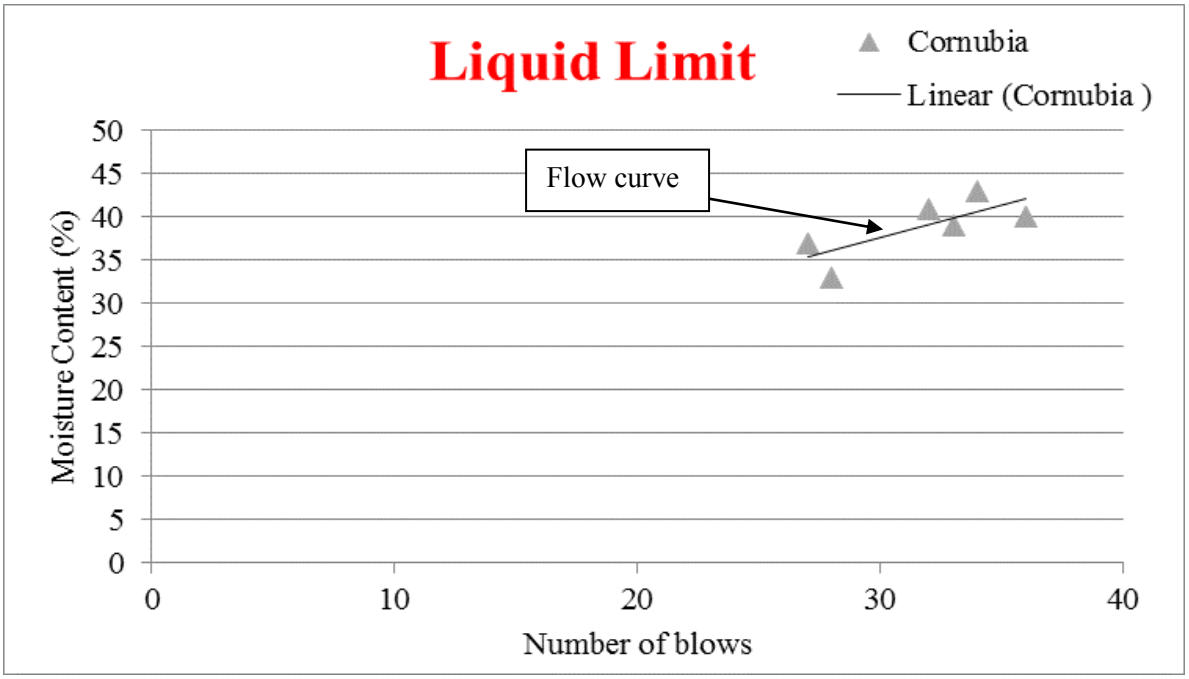

Figure 7.10: Determining the liquid limit using the Casagrande test.

7.3.3.2 Plastic limit

The plastic limit is the moisture content at which a soil passes from the plastic state to the solid state and becomes too dry to be in a plastic condition (Craig, 2004). This test is performed to determine the lowest moisture content at which a soil is plastic (Head, 2006). After sieving soil through the 0.425 mm sieve, 20 g of the sample is split into two 10 g balls. The individual 10 g balls are rolled into 3 mm threads (Figure 7.11) until the individual threads begins to break. Once all the material from the 10 g balls have been rolled into threads, the moisture content of these threads are determined. The plastic limit is the moisture content of the 3 mm threads from the 10 g ball and is given as a percentage.

Figure 7.11: Plastic limit.

Crumbling refers to shearing in the longitudinal and transverse direction as the thread is rolled and the crumbling point refers to the first sign of the thread breaking. When performing the plastic limit test, care is required to ensure that the individual threads remain intact and homogeneous.

The plasticity index refers to the difference between the plastic limit and the liquid limit respectively as shown by Equation 7.2. The plasticity index indicates the moisture content that a soil can remain in a plastic condition (Head, 1982).

$$\text{Plasticity Index} = \text{Liquid limit} - \text{Plastic limit} \qquad 7.2$$

7.3.3.3 Linear shrinkage

The linear shrinkage test was used to determine the percentage linear shrinkage of the soil material (Head, 1982). This test can be used for soil of low plasticity and includes silts and clays (Head, 2006). The soil material was placed in a mould which is lined with grease to prevent the sample from adhering to the sides (Figure 7.12).

A Venier calliper was used to measure the change in length of the soil material after oven-drying for 24 hours (Head, 1982). The linear shrinkage test is done by measuring the change in length of a soil mass after oven drying for 24 hours. The linear shrinkage was then calculated as:

$$Linear\ shrinkage = (1 - \frac{L_d}{L_o})\ x\ 100 \qquad 7.3$$

Where L_d refers to the change in length of the sample material after drying and L_o refers to the original sample length.

Figure 7.12: Linear shrinkage test.

7.3.4 Slake tests

Shales and other weak rock types are subjected to loading failure and abrasion failure (Santi and Higgins, 1998; Santi, 1998). The ability of this material to resist wear, abrasion and breakdown with time is referred to as its durability (Santi, 1998). Durability is particularly important for the construction of embankments using shales and other weak materials (Oakland and Lovell, 1982). For example, the extent of weathering is a time dependent process and the changes which are caused are

often difficult to determine (Shamburger *et al.*, 1975). Apart from visually determining the relative rates of weathering from an outcrop, laboratory tests can be done to assess the degree of weathering. The durability of shales strongly depends on its interaction with water (Hudec, 1982) which is known as slaking and often results in flaking, fracturing and the dissolution of particles (Santi and Koncagul, 1996). Due to the physical interdependence between durability and slaking, the durability of the fresh and weathered shale material from each locality was determined using the jar slake test and the slake durability test.

7.3.4.1 Jar slake test

The jar slake test is a simple durability test which does not require much sample preparation and is used to observe the physical reaction when a shale sample is immersed in water. The testing procedure commences, as developed by Wood and Deo (1975), by oven-drying a sample weighing 30-50 g for 16 hours. Lutten (1977) stated that oven dried samples are necessary since damp material is relatively insensitive to degradation. Once the samples have been oven-dried, each sample was immersed in 15 ml of distilled water. Two fresh samples and two weathered samples from each locality were used to perform the jar slake test.

Observations of the physical changes during the jar slake test were recorded after 10 minutes, 30 minutes and a final observation was recorded after 24 hours. The physical changes which were observed are given a particular Jar Slake index (I_j) as shown in Table 7.2. Each jar slake index (I_j) describes the behaviour of the shale material during the jar slake test. The weakness of this test is that it fails to distinguish between the slight and extreme cases of each mode (Santi, 1998). Therefore, Santi's (1998) proposed modification includes a visual description of the behaviour of the shale materials and additional verbal descriptors to assist in consistent classification, was applied during the jar slake test (Figure 7.13).

Table 7.2: Jar Slake index categories (adapted from Walkinshaw and Santi, 1996 after Wood and Deo, 1975).

Jar Slake Index (Ij)	Material behaviour (after Wood and Deo, 1975)	Material behaviour (after Santi, 1998)
1	Degrades to a pile of flakes or mud	Mud-degrades to a mud-like consistency
2	Breaks rapidly, forms many chips or both	Flakes- sample totally reduced to flakes. Original outline for sample not discemible.
3	Breaks slowly, forms few chips or both	Chips-chips of material fall from the sides of the sample. Sample may also be fractured. Original outline of sample is barely discernible.
4	Breaks rapidly, develops several fractures, or both	Fractures-sample fractures throughout, creating a chunky appearance.
5	Breaks slowly, develops few fractures, or both	Slabs- sample parts along a few planar surfaces.
6	No change	No discernible reaction

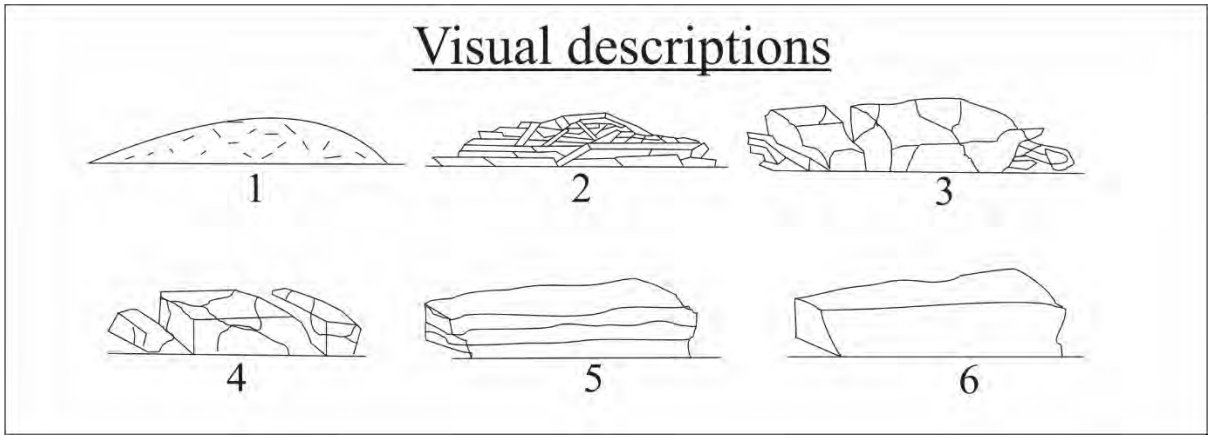

Figure 7.13: Visual descriptions for the jar slake test (adapted from Santi, 1998).

However, when using the jar slake test as a field indicator test, results can be obtained easier and is easier to perform than the standard slake durability test (Santi and Higgins, 1998). The jar slake test is done as a qualitative screening test and for materials which have a jar slake index higher than 2, slake durability tests are done to determine its suitability in the construction of embankments (Colorado Laboratory manual, 2014).

7.3.4.2 Slake durability test

Slaking of a rock material occurs after subsequent saturation, as the fluid traps air and causes the rock fabric to break up from within. This disintegration of the rock material from within is caused by the stress applied (ASTM, 2010). Commonly, this test is performed on argillaceous material such as shales, siltstones and mudrocks. The slake durability test is a simple indicator test and is used to estimate and assign the durability of weak rocks qualitatively and quantitatively in the service environment (ASTM, 2010). The slake durability test is the most appropriate test to use to determine the durability of shale (Santi, 1995). Furthermore, the test combines the effects of both soaking and abrasion in order to accelerate the rate of weathering that can be attained by water immersion alone (D'Appolonia Consulting Engineers, 1980). However, for rocks which have low permeability, the Shore Hardness test is better suited than the slake durability test because a 10 minute wetting cycle is not long enough for water to enter the rock and trigger the slaking mechanisms (Koncagul and Santi, 1999). Consequently, the slake durability indices come out very high. The two most important factors which affect a rocks resistance to slaking are its mineralogy and textural properties (ISRM, 2000). This test was done in accordance with the procedures listed by Head (1982); Santi (1998); ISRM (2000) and the ASTM (2010) procedures.

Seven sets of samples of fresh and weathered gravelly sized material from Localities 1 and 3, six sets of fresh samples and 5 sets of weathered samples from Locality 2 and four sets of fresh and weathered samples from Locality 4, each weighing ± 400 g (eight pieces), were placed in steel baskets at their

natural moisture content. The weight of the steel basket containing the samples were weighed and then placed in the slake durability apparatus as shown in Figure 7.14.

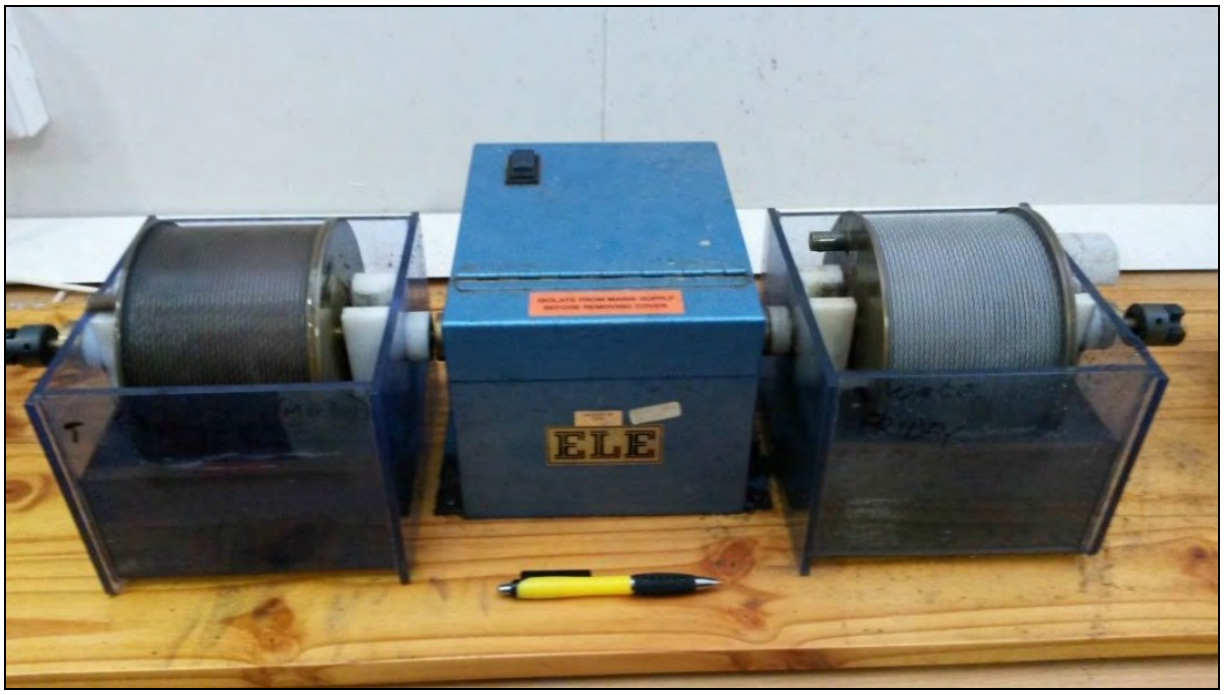

Figure 7.14: The slake durability apparatus.

Two mediums were used to assess and enhance the possibility of slaking; one basket was slaked in water while the other was slaked in ethylene glycol respectively (Head, 1982). Ethylene glycol was used due to its ability to accelerate the deterioration in rocks which contain smectite clays. It also causes rocks to disintegrate by absorbing water (Green, 2007). After slaking both samples for 10 minutes each day over a five day period, the samples were placed in the oven for 24 hours and then weighed. During the slake durability test, neither the interior drum nor the mesh should be obstructed by any support mechanism. The slake durability test was performed on fresh and weathered shale samples from each locality to assess the effects of weathering (particularly due to the exposure to water) on the weathered material relative to the fresh shale material. Since the slake durability test is used to determine the durability of shales and weak rocks when used as fill materials (Santi and Higgins, 1998), this test will be important in assessing the durability of the shale fill materials which was used to construct the platforms at the Cornubia development for housing and industry.

Slake durability indices were calculated using Equation 7.4 to determine the degradable nature of each of the shale samples tested. The slake durability index refers to the percentage by dry mass of a collection of shale pieces which are retained on a 2 mm sieve after cycles of oven drying and 10 minutes of soaking in water with a standard tumbling apparatus (ASTM, 2010). The proposed modification by Santi (1998) and by the ASTM (2010) of conducting 2 slaking cycles to predict the durability of shales was not applied during the slake durability test. Bell (1997) indicated that the 2

slake cycle often does not indicate the durability of weak rocks such as shales. Instead, he suggested that the 4 cycle slake durability test provides more accurate results (Gokceoglu *et al.* 2000; Gemici, 2001). The slake durability index (I_D) is given by:

$$\text{Slake durability Index:} \quad I_D = \frac{Weight\ of\ sample\ remaining\ in\ basket}{Orginal\ sample\ weight} x\ 100 \qquad 7.4$$

7.3.5 Point Load Strength test

The Point Load Strength test is used as an index test for the strength classification of rock materials (ISRM, 2000). It is a simple and portable test which can be carried out in the field. The test does not require extensive sample preparation and samples can be collected within a short time frame (ASTM, 2010).

The sample material to be tested can be in the shape of cores, cut blocks or irregular lumps (ISRM, 2000). Core samples from the Cornubia development and Locality 3 from the Pietermaritzburg area were obtained using the Rothenberger core-drill as shown in Figure 7.15 (a). During the sampling process, it was not possible to obtain large samples from Localities 2 and 4 for the Point Load Strength test. The core dill which was used to obtain the core samples has a diameter of 56 mm. During the coring process, the highly degradable and fissile nature of the shale material made it very difficult to obtain a large number of cores (Figure 7.15 b) for Point Load Strength testing. Taylor and Spears (1981) further stated that it is very difficult to obtain cores for laboratory tests especially for cores which are 54 mm and greater. Franklin (1981) earlier stated that shale is a difficult material to study because it is easily disturbed during drilling and sampling which affects the laboratory analyses of shales such as its strength.

The test apparatus consists of platens, ram, loading frame and a pump as shown in Figure 7.16. The concentrated load is applied through co-axial, truncated conical platens as shown in Figure 7.17. This test is performed by subjecting a rock specimen to an increasing concentrated load until failure occurs, which is seen by the break-up of the core sample.

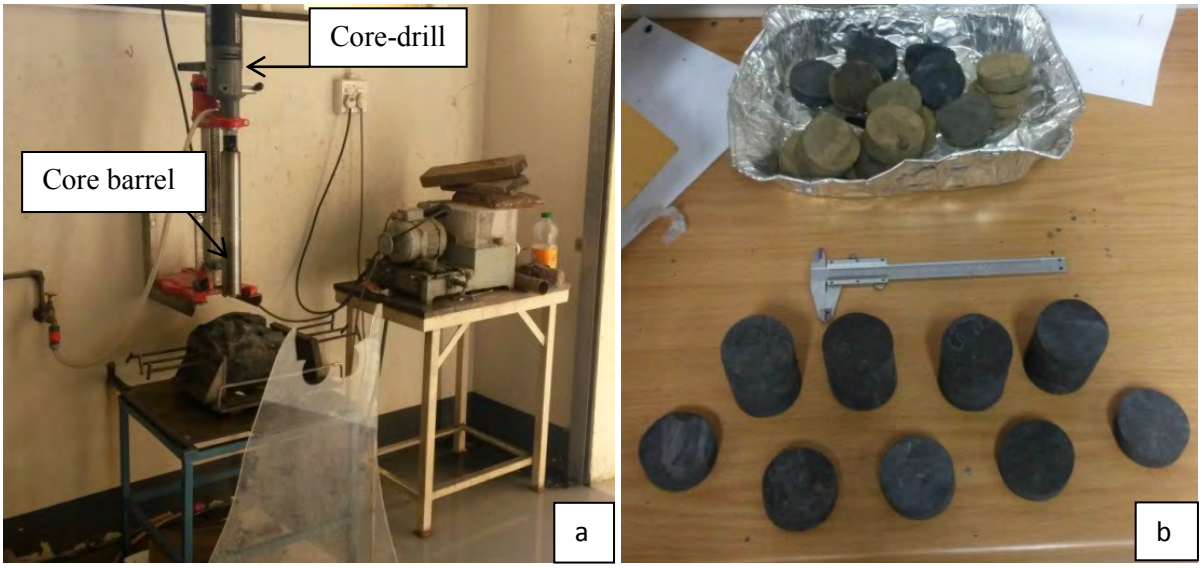

Figure 7.15: a) Core-drill used to obtain core samples for the Point Load Strength test. b) Core samples used for Point Load Strength tests.

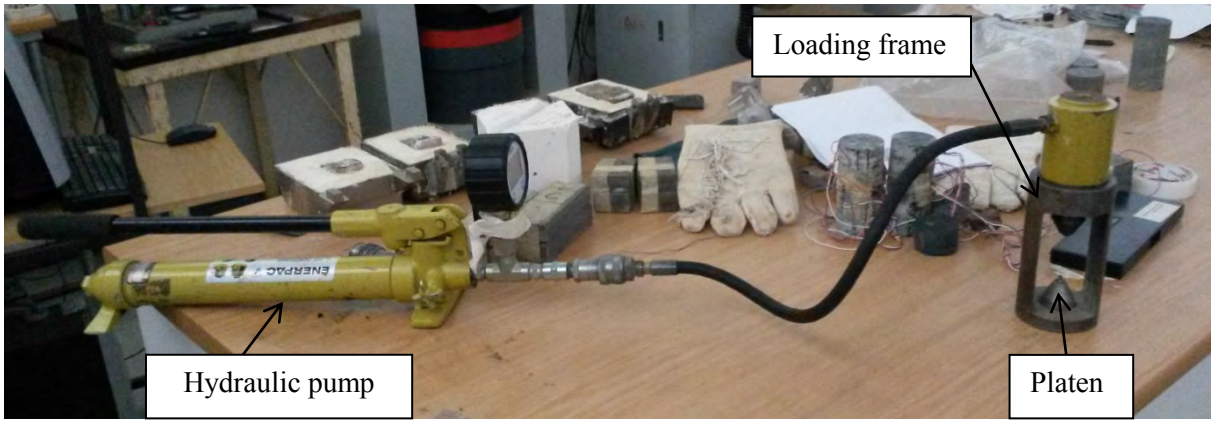

Figure 7.16: Point load apparatus.

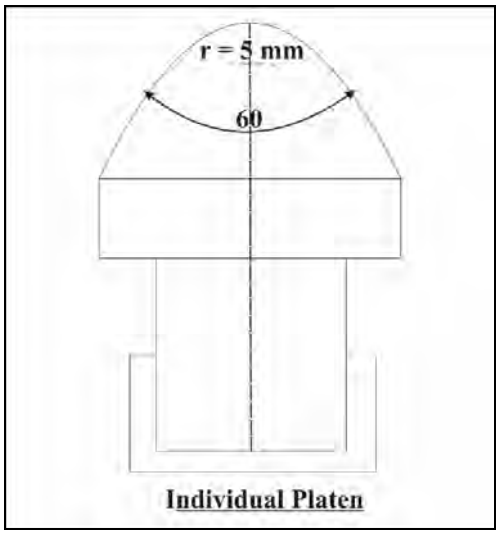

Figure 7.17: Schematic section illustrating the load applied from the shape and tip of the platens (ISRM, 2000).

Five core samples were tested axially and diametrically to determine the axial strength and the diametrical strength of the samples taken from the two localities. This test measures the pressure at failure and is used to calculate the Point Load Strength (ISRM, 2000). When performing the Point Load Strength test, the diametrical strength of a core specimen is usually lower than its axial strength (Bieniawski, 1975). Bell *et al.* (1996) showed in their investigations that the diametrical strength of the mudrocks are lower than the axial strength because these mudrocks have failed when the pressure was applied parallel to the lamination planes. Failure usually occurs along these planes of weakness during loading due to the alignment of grains which form laminations (Koncagul and Santi, 1999). The load was applied along a single plane of weakness using the hydraulic pump to compress the platens and, the pressure at failure when the sample broke was recorded. The Point Load strength was calculated as follows:

Uncorrected Point Load strength: $$I_s = \frac{P}{D_e^2} \quad (7.5)$$

P is the load at failure and D_e is the equivalent core diameter.

Load at Failure (P): P = Pressure at failure x ram area (kN/ m^2) (7.6)

Where the ram area of the apparatus used is 1.782 x 10^{-3} m^2

For diametrical tests: $D_e^2 = D^2$ (m^2) (7.7)

Where D is the diameter of the core

For axial tests: $$D_e = \frac{4A}{\pi} (mm^2) \quad (7.8)$$

Where A = W.D (W is the width and D is the diameter) and is the area of the core specimen, the size correction factor

For cores which are greater than 50 mm:

$$F = \sqrt{D_e / 50} \quad (7.9)$$

Thus, the corrected Point Load Strength for a 50 mm core is given by:

$$I_{s\,(50)} = F \times I_s \quad (7.10)$$

7.3.6 Shear box test

The Shear Box test is also called the direct shear test and one of many tests which is used to determine the shear strength of a soil or rock (Head, 1984; Craig, 2004). The shear strength of a rock or soil is one of the most important geotechnical properties as it determines the shearing resistance of a

particular soil or rock material. The determination of the shear strength of a rock is an important aspect in the design of structures such as rock slopes, dam foundations, tunnels, shafts and caverns (ASTM, 2010). Shear tests using a large shear box (300 mm x 300 mm) are often used to test fills, road construction materials, coillery spoils and industrial rubble (Hardwick, 1992).

Shear Box tests were performed at the University of Witwatersrand on the shale rock material during the winter vacation in 2014. The shear apparatus which was used is a modified and larger version of the conventional shear apparatus. These modifications were made after many years of experience by a geotechnical engineer named Mr. Norman Alexander who has worked for many years in the field of geotechnical engineering. Mr. Norman Alexander converted the manual shear system into a hydraulic system as shown in Figure 7.18. However, the basic testing procedure was done in accordance with Head (1984) and the ISRM (2000).

As part of these modifications, manual dial gauges were replaced by electronic dial gauges called Linear Variable Differential Transformers (LVDT's) as shown in Figure 7.19. The LVDT's were used instead of manual gauges as they provide more precise and continuous displacement measurements than the manual dial gauges (Hencher and Richards, 1989). The shearing system is linked to a computer system and consists of hydraulic controls, a hydraulic piston and a shear piston. The normal force is applied hydraulically using electronic signals. These "electronic signals" are converted from kilonewtons (kN) to millivolts (mV).

Figure 7.18: Modified shear apparatus showing the hydraulic controls.

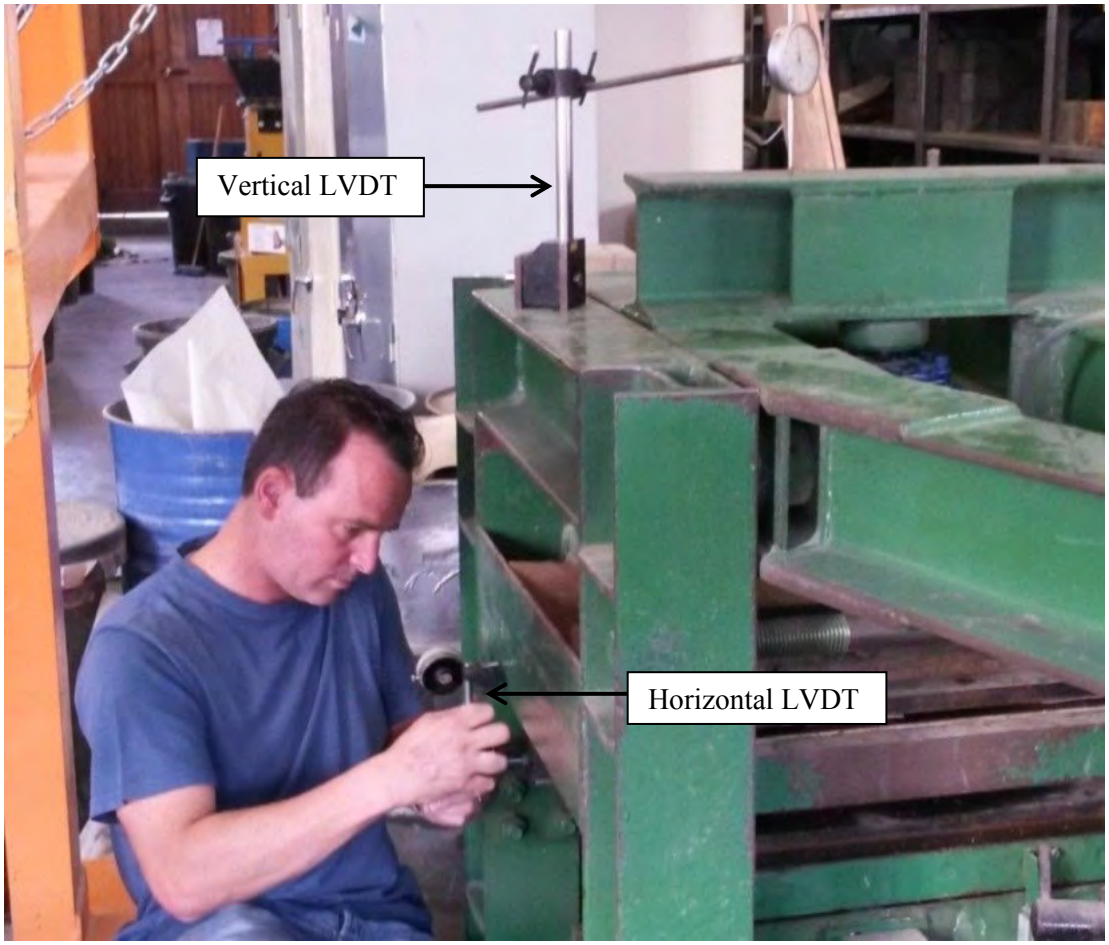

Figure 7.19: The horizontal and vertical LVDT's.

Shear box tests were performed individually on the fresh shale rock material and on the weathered shale rock material from the Cornubia development and from Locality 3 in Pietermaritzburg. Shear box tests were also done on the fresh shale rock material from Locality 2 because adequate weathered samples to perform the shear box test could not be obtained as a result of the poorly exposed outcrop. Similarly, it was only possible to obtain fresh shale material from Locality 4 from the Pietermaritzburg area due to the highly vegetated nature of this outcrop.

7.3.6.1 Sample preparation

In the first stage of sample preparation, rocks were crushed to gravel size using a hammer. These samples were then put into a rock crusher to ensure uniformity in grain size. The shear box has and equates to an area of 0.12 m^2 (300 mm x 300 by a height of 400 mm of both halves of the box). The size of the material should not exceed 10 % of the height of the shear box therefore gravel sized particles were used as prescribed by Verwaal (2005) and by Mr. Norman Alexander. Fines (< 2.5 mm) were not removed to prevent any bias and to ensure that the samples tested represent field conditions (Figure 5.20).

Figure 7.20: The size of the shale material used in the shear box.

7.3.6.2 Test setup

Mr. Andrew Hendricks, a laboratory technician at the Civil Engineering department at the University of Witwatersrand has recommended that the shear apparatus and hydraulic system should be switched on 24 hours before testing so that the hydraulic fluid can be heated. Heated hydraulic fluids ensure that air is minimized within the system so that accurate results can be obtained. Once the samples have been prepared to the required size, the shear box was assembled. The bottom half of the shear box (300 mm x 300mm) is pushed against the shearing piston and is followed by placing the top half of the shear box, Pieces of teflon sheets (5 cm in length and 2 cm wide) were added between the upper box and the lower box to reduce the friction between the steel boxes. The shale material was added in layers and compacted using a tamper to a required density (Figure 7.21). After filling the shear box with the shale material, the load cell was placed on the upper plate. Flat weights were used to raise the loading cell to the loading arm (Figure 7.22). The normal stress was applied by the loading arm to the required load using the computer system.

Figure 7.21: Compaction of the shale materials.

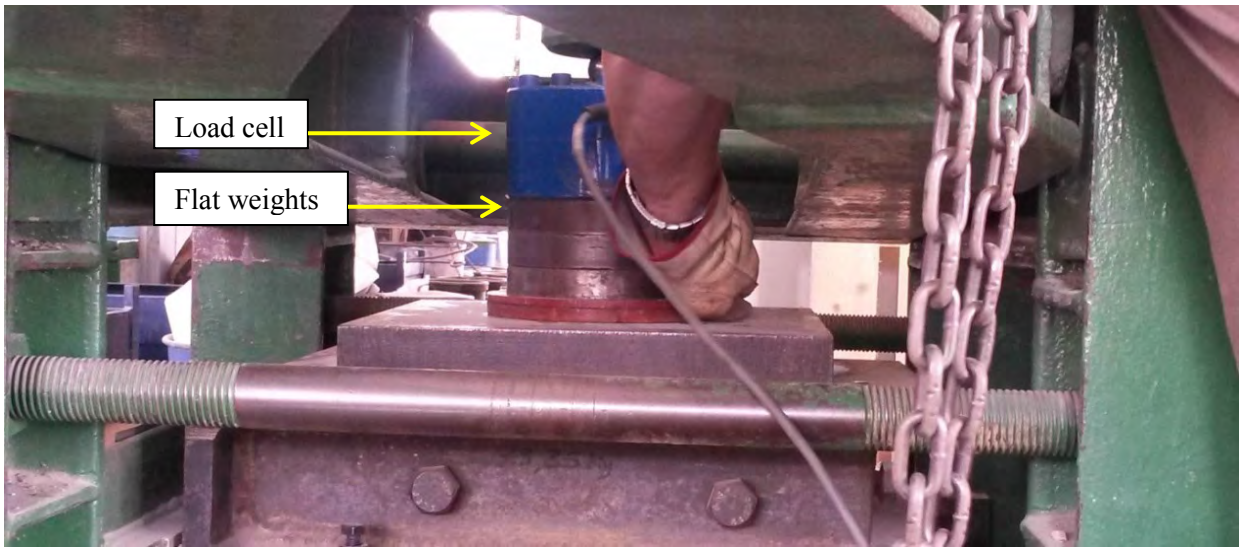

Figure 7.22: Lowering the loading arm onto the load cell which rests on flat weights.

7.3.6.3 Testing procedure

Once the shearing apparatus has been assembled and ready for shearing, the hydraulic controls were then calibrated. Firstly, the static strain indicators were zeroed and the voltage on the ammeter set to 10 V. The metal bolts that once held both boxes together were removed and the samples were sheared at a rate of 5-6 mm/min as recommended by Mr. Norman Alexander. This was done to prevent the build-up of pore water pressures. Shearing at a rate >10 mm/min will cause the rock material to bounce off each other and will cause several peaks in the shear stress versus displacement graph.

Furthermore, a high rate of shear will cause a higher measured strength due to the strain effects between the individual particles (Duncan and Wright, 2005). Initial dial gauge readings were recorded and additional dial gauges were used as a precautionary measure in the event of a power failure since electronic equipment was used. The computer software called Agilent Plus was used.

Shale samples from all four localities were subjected to a normal stress of 75 kPa, 150 kPa and 300 kPa respectively and the equivalent normal load is 8.25 kN, 16.5 kN and 33 kN respectively as prescribed by Mr. Norman Alexander. Unconsolidated undrained tests were done to determine the shear strength of the shale material from each locality. These tests were done as a result of time constraints since consolidated tests could have taken up to a week per sample to consolidate and become saturated. The fully assembled large scale shear apparatus is shown in Figure 7.23. Shearing (using the hydraulic piston) commenced by sliding one portion of the rock material over the other along a pre-determined failure plane. During the duration of shear, vertical measurements of the loading arm and the horizontal displacement of the bottom box were recorded using the LVDT's.

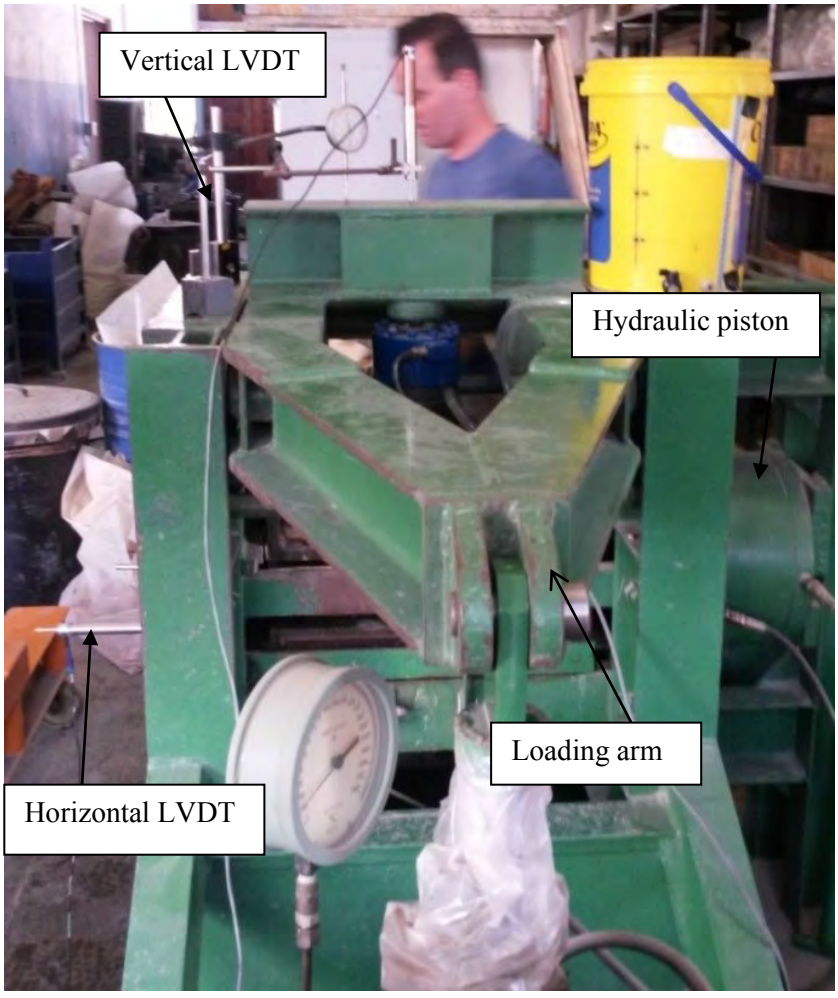

Figure 7.23: Fully assembled shear apparatus.

7.3.6.4 Post failure analysis

The shear test at a particular load is complete once a definite peak is seen from the shear stress vs horizontal displacement graph (Figure 7.24). Once this peak is seen, the hydraulic pressure is released and direction of the shearing piston is reversed. The shale material is removed from both boxes and the boxes are realigned and cleaned for the next test. Unlike the triaxial apparatus, the shear box includes no means of either pore-water pressure measurement or drainage from the box. Hence, the pore-water pressure can assumed to be zero, the test can be considered to be fully drained and effective stress numerically equal to the total stress (Duncan and Wright, 2005) (Equation 7.10).

$$\sigma = \sigma' + u \qquad u = o,\ \sigma' = \sigma \tag{7.10}$$

The shear strength parameters which are calculated from these tests are the effective angle of friction (φ′) and the effective cohesion (c′). The effective peak shear parameters are often used for the design when shales are used as fills or for shale embankments (Taylor and Spears, 1981). The maximum shear stress at failure as depicted by Figure 7.24 is plotted against the load at failure for each test. The angle of friction is calculated by determining the gradient of the line of best fit as shown in Figure 7.25. The cohesional component is the value where the line of best fit intersects the y-axis.

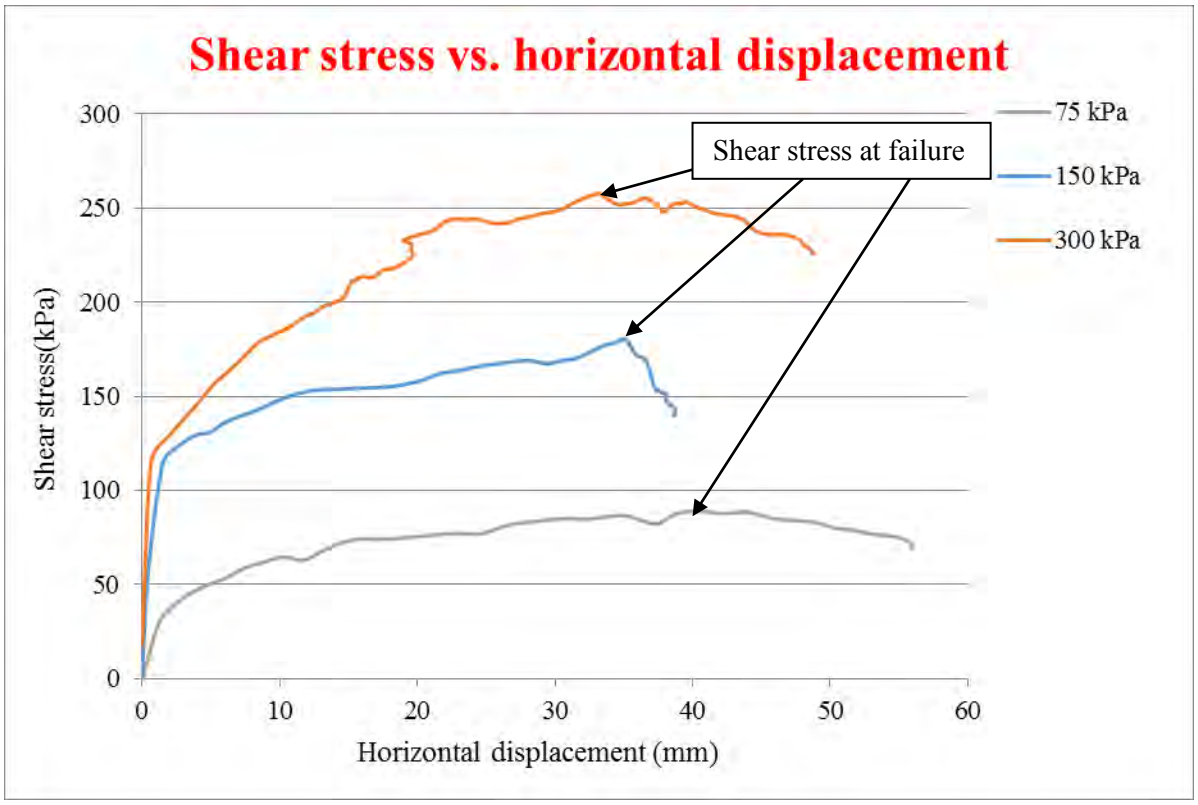

Figure 7.24: Shear stress vs horizontal displacement curve.

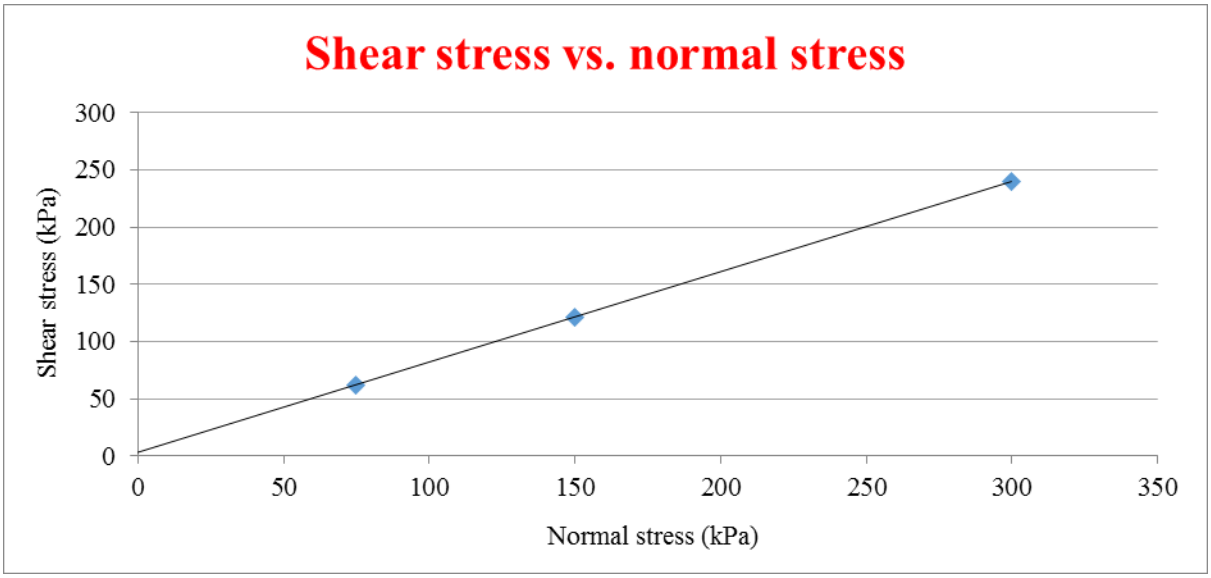

Figure 7.25: Shear stress vs. normal stress curve.

7.3.6.5 Limitations of the shear box test

The Shear Box test is a useful test in determining the shear strength parameters (c & φ) of soil and rock materials. Despite the simplicity of this test, there are several disadvantages. Firstly, drainage conditions within the sample cannot be controlled (Hardwick, 1992; Craig, 2004). As a result, a low shear rate was applied to prevent the build-up of pore pressures within the sample. Since the shear force is applied to the lower box, the shear direction can only be applied in one direction. Once the normal force is applied via the loading arm, it does not distribute this force evenly throughout the sample (Hardwick, 1992). The stress-strain distribution is not applied uniformly throughout the sample. Therefore the term normal force is given instead of normal load (ASTM, 2010). The area of contact also decreases between the two sample halves during the course of a test which causes the stress values to constantly increase (Hardwick, 1992).

During shear testing, only the boundary displacements of the box can be observed. The exact volume of the shear zone undergoing deformation is unknown and this makes it difficult to identify the position of the materials undergoing failure. The strain calculated from the applied loads therefore represents average values (Hardwick, 1992). Since only the boundary displacements of the box can be observed and the exact volume of the shear zone to which the deformation is restricted, the calculated strains represent average values and describes that part of the soil which is undergoing failure (Hardwick, 1992). Craig (1983) stated that the stress concentrations start to build up at the edge of the boxes and move towards the centre. The shear box test also has a maximum displacement limit which is determined by the size of the box.

Furthermore, despite having improved sensitivity of recording measurements from the automation of laboratory equipment, several drawbacks can occur. The automation this equipment requires high up-front costs and cost of repairing this equipment is high. Technicians or individuals are required to know how to use this equipment and to have an understanding of the soil/ rock behaviour. This will enable the user to determine whether the results obtained can be accepted or if these tests should be repeated (Marr, 2000). Also, the large scale shear box is an expensive and time consuming test which did not allow for repetitive tests to be undertaken on the shale materials.

7.4 Summary

A description of the methodology used to perform the geochemical tests has been given in this chapter. This chapter explained the importance of effective sample preparation and provided insight into the methodology used to perform X-ray diffraction tests. It also highlighted the testing procedures used to perform the various geotechnical tests on the residual soil and shale rock material. Chapter 8 presents and discusses the results of the geochemical and geotechnical tests and highlights some of the weaknesses from conducting these tests.

Chapter 8

Laboratory results and discussion

8.1 Introduction

This chapter presents and discusses the results obtained from the geochemical analyses of the samples collected and the geotechnical tests conducted on the shale rocks and the residual materials. Furthermore, it provides a discussion on the results from the settlement monitoring of platforms comprising shales which was monitored at the Cornubia housing and industrial development.

8.2 Geochemical analyses

8.2.1 X-Ray Diffraction (XRD)

The results obtained from the XRD analyses using the Richveld analysis tool in Highscore Plus are shown in Table 8.1 and the diffraction peaks are presented in Appendix A. The common minerals are shown to be quartz and muscovite mica. Quartz was identified as being the most abundant non-clay mineral which was present in the fresh and weathered shale materials from each locality. The fresh shale material analysed from the Cornubia development contained almost all of the minerals shown in Table 8.1 with the exception of nacrite. The minor minerals present are nacrite, siderite and dickite.

Table 8.1: The percentage of minerals found in each sample using Highscore Plus from the XRD analyses.

X-ray diffraction tests (XRD), Fresh (F) Weathered (W)								
Locality	(1) Cornubia		Locality 2		Locality 3		Locality 4	
Percentage (%)	F	W	F	W	F	W	F	W
Quartz	44.0	44.3	53.4	53.9	57.7	58.4	54.7	50.7
Mica (Muscovite)	25.1	31.3	21.2	17.2	28.6	18.4	17.8	22.2
Siderite (carbonate)	3.8	-	0.1	0.4	-	0.1	-	0.4
Chamosite	5.0	-	-	-	-	-	-	0.5
Dickite (Kalolinte group)	0.2	1.1	-	-	0.2	0.1	0.9	-
Sericite	14.5	-	1.7	5.8	0.2	13	23.1	-
Nacrite (Kaolinite group)	-	-	1.3	-	1.9	2.0	0.3	18.8
Illite	0.9	23.1	20.4	19.4	9.3	9.6	2.1	0.9
Montmorillonite	1.9	0.2	-	0.1	0.1	-	-	-
Kaolinite	0.1	-	1.9	3.4	2.0	2.0	-	6.6
Chlorite	6.2	-	-	-	-	-	-	-

The weathered shale material from the Cornubia development contained almost double the amount of muscovite mica as compared to shale materials from Localities 2 and 4. The fresh material is expected to have a lower amount of clay minerals than the weathered shale samples as pointed out by Nandi *et*

al. (2009). However, with the exception of the fresh material from Locality 2, the shales from each locality do not confirm to this expected behaviour (Table 8.1). It is expected that a higher percentage of clay minerals should be found in the weathered shale samples from each locality due to the alteration of muscovite to clay minerals (Nandi *et al.,* 2009). However, this was not observed by the XRD analyses. The composition of the shale samples analysed from the Cornubia development are similar to the studies performed by Wilson (1983) and Bell and Maud (1996) on the shales of the Pietermaritzburg Formation.

Illite is the dominant clay mineral which was found in all of the shale samples analysed. The weathered shales from the Cornubia development contained the highest percentage of illite as compared to the weathered shale samples from the Pietermaritzburg area. The higher amount of illite in the weathered shales from the Cornubia development could have formed from the alteration of the muscovite mica from the fresh shale material from this locality (Deer *et al*., 1992). Illite could also have formed from the weathering of muscovite and kaolinite as stated by Deer *et al.* (1992) and Bell (1993). The higher percentage of illite observed by the shale materials from Localities 1 and 2 could have formed in a weakly acidic or alkaline environment (Hardwick, 1992). The higher amount of illite as compared to the amount of montmorillonite observed in the fresh and weathered shale samples from each locality could have formed by the expense of montmorillonite. This means that the conversion of smectites to illites occurs under a low temperature environment (Ramseyer and Boles, 1985; Whitney, 1990). Drennan (1963) stated that the percentage of illite in the Ecca shales usually falls within the range of 20 - 40 % and the XRD analyses of the fresh shales from the Cornubia development and the fresh and weathered shales from Locality 2 supports this finding.

The minerals constituting the kaolin group are kaolinite, dickite and nacrite. Kaolinite, is the second prevalent clay mineral which is found in most of the shale materials with the exception of the weathered shales from the Cornubia development and the fresh shales from Locality 4 but occurs in low percentages (<10%). Based on the XRD analyses, there is no common trend in the abundance of kaolinite between the fresh and weathered shale samples from each locality. Although very unlikely, the increase in kaolinite by the decrease illite can be attributed to a change in environment from an alkaline or a weakly acidic environment to a moderately acidic environment (Hardwick, 1992) as seen by the weathered shale samples from Locality 4. Dickite and nacrite are clay minerals which form part of the kaolin group (Poppe *et al.*, 2002). Their presence in the fresh and weathered shale samples from each locality, except for the weathered material from Locality 4, are very low or absent.

Powell (2010) stated that the swelling behaviour of expansive soils is directly related to the clay mineralogy, particularly the presence of montmorillonite. Montmorillonite is absent in most of the shale samples and also occurs as a minor clay mineral, especially in the shale samples from the Cornubia development (<2%). The low amount of montmorillonite implies that the shale samples are

potentially not expansive (Hardwick, 1982). The occurrence of chamosite in the Ecca shales forms from a reducing depositional environment at a pH ranging from 6-8 (Drennan, 1963). Even in the absence of CO_2, chamosite will be leached at a moderate acidity, leaving behind a clay residue (Drennan, 1963). The behaviour of these minerals reflects the changes in the Eh-pH of this formation (Johnson *et al.,* 2006).

The other minor minerals are chlorite and siderite and are present in some of the shale samples. In the Cornubia development, chlorite is only found in the fresh samples and absent in the rest of the shale samples. The high percentage of chlorite observed by the fresh shales from the Cornubia development could have formed from the alteration of kaolinite to chlorite as the clastic material is eroded off the source area (Taylor and Spears, 1981). However, chlorite forms in weakly acidic or alkaline environment during diagenesis, at the expense of smectites (Hardwick, 1992). If the latter was considered, then there should be an increase in the percentage of montmorillonite in the weathered material of the shales from the Cornubia development due to the absence of chlorite. However this was not observed. Siderite is an unstable mineral as stated by Taylor and Spears (1981) and is found in low percentages in the shale samples analysed.

a major limitation of XRD tests are that it cannot determine the chemical composition of a particular mineral. Although X-ray fluorescence (XRF) could have been used to identify the chemical composition of each sample by identifying the individual elements, it was not possible to perform these analyses because the department of Geological Science at the University of KwaZulu-Natal lacks a technician to operate the XRF equipment.

8.3 Geotechnical tests (Raw data is provided in Appendix B and C)

8.3.1 The moisture content test

The results from the moisture content tests of the shale materials from each locality are shown in Table 8.2 and the calculations are shown in Appendix B. The natural moisture content of the fresh material, except for Locality 2, is lower than the weathered material of the shale materials from each locality. Bell (1993) stated that the moisture content of most shales are between 5-35 % and that the moisture content of the weathered material is usually higher than the fresh material.

Table 8.2: Results of the moisture content test.

Moisture content test (%) (Rock material)								
Locality	Cornubia (1)		Locality 2		Locality3		Locality 4	
Material	Fresh	Weathered	Fresh	Weathered	Fresh	Weathered	Fresh	Weathered
Moisture content (%)	5.9	7.1	4.5	4.1	5.0	5.4	5.4	9.9
Residual material								
	Cornubia				Locality 3			
Moisture content (%)	12.6				9.9			

8.3.2 Particle size distribution

The results from the particle size distribution performed on samples from the Cornubia development and Locality 3 using the sieve shaker are shown in Figure 8.1 and the calculations are shown in Appendix B.2. The particle size distribution curves show the grading of each soil sample by dry weight into separate ranges based on the size of the individual grains (Head, 1982). The results of the soil samples taken from the Cornubia development and from Locality 3 in the Pietermaritzburg area show uniform grading curves. The soil samples are dominated by fine sand sized particles (0.63 mm – 2 mm) with minor amounts of clay. According to the particle size distribution curves, the two samples analysed could be classified as clayey SAND. The effective size (D_{10}) is 130 for the soil material from Locality 3 in Pietermaritzburg and D_{60} is 780 compared to the soil samples from the Cornubia development which has a D_{10} of 140 and D_{60} of 800. The soil samples analysed from the Cornubia development and Locality 3 from the Pietermaritzburg area are well graded.

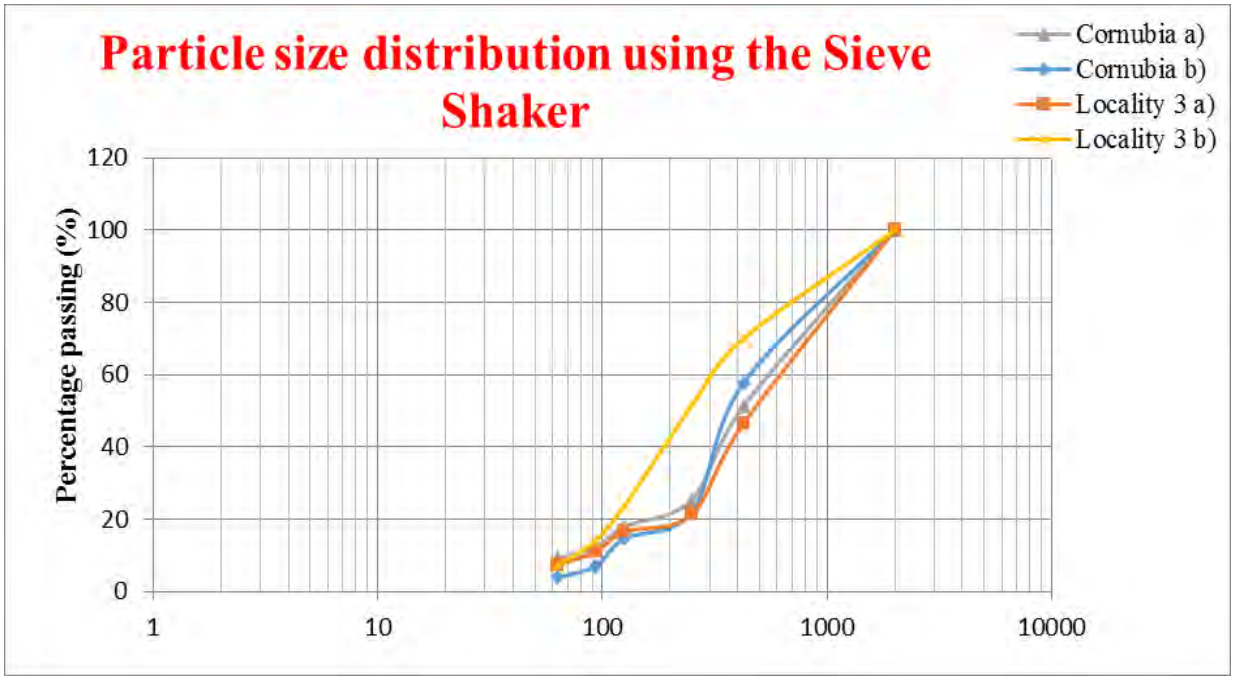

Clay	Fine	Medium	Coarse	Fine	Medium	Coarse	Gravel
	Silt			Sand			
(µm)							

Figure 8.1: Particle size distribution.

The Malvern Diffractometer test was performed to determine the percentage of clay fraction in each of the soil samples. These tests revealed that the soil samples contain a low clay fraction (<15 %) and further supports the particle size analyses performed by the sieve shaker (<10 %) from Locality 3 from the Pietermaritzburg area and from the Cornubia development (Figure 8.2).

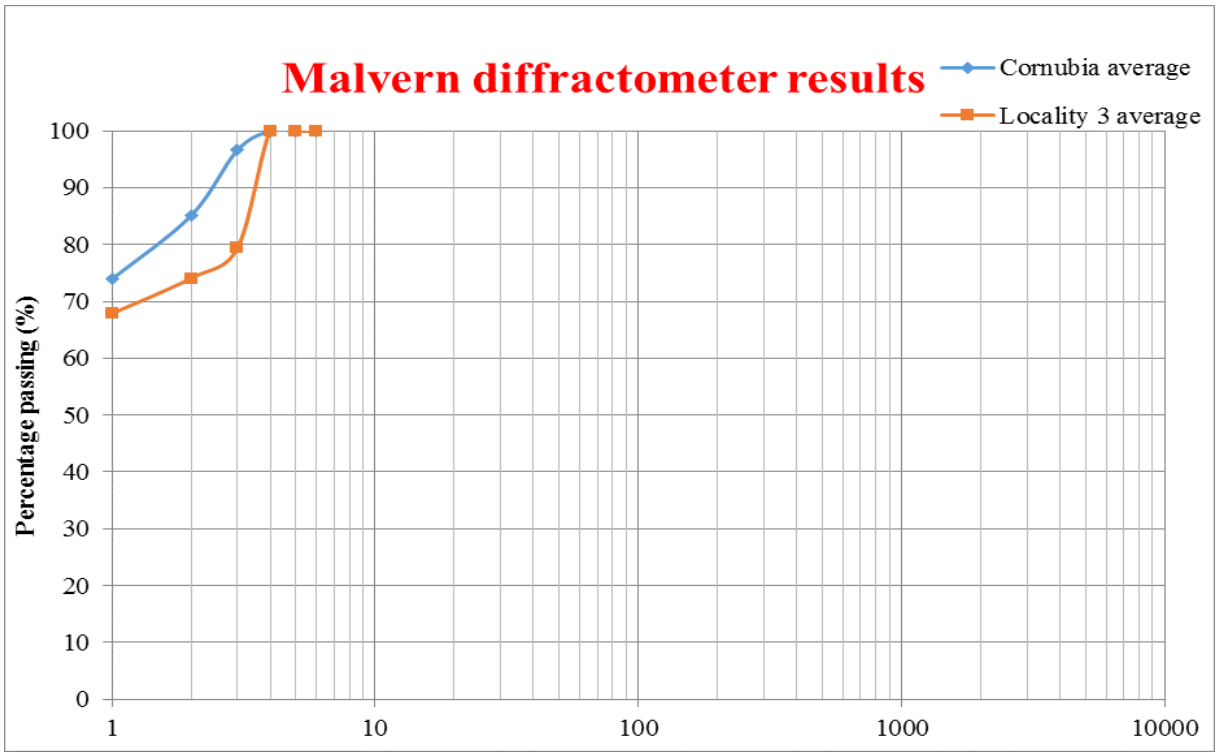

Figure 8.2: Results from the Malvern Mastersizer 2000.

8.3.3 Atterberg limits

A summary of the results of the Atterberg limits of the soil materials from the Cornubia development and Locality 3 are presented in Table 8.3 and the calculations are shown in Appendix B.3. The average liquid limit of the soil samples from the Cornubia development is 37% whilst the average liquid limit of the soil at Locality 3 in Pietermaritzburg is 26%. The average liquid limit of the soil material from Locality 3 in the Pietermaritzburg area (26 %) is considerably lower than the average liquid limit of the soil material from the Cornubia development (37 %). The liquid limit of the soil material from these localities lies within a similar range of liquid limits (i.e. 35-70) when compared to the studies performed by Bell and Maud (1996) on shales of the Pietermaritzburg Formation. The plastic limit of the soil material from the Cornubia development is also higher than the plastic limit of the residual material from Locality 3. The plasticity index of the soil samples from the Cornubia development is 14 whilst the plasticity index of the soil sample from Locality 3 from the Pietermaritzburg area is 7. In addition, the plasticity index of the soil material from the Cornubia development and Locality 3 from the Pietermaritzburg area falls within a similar range of the plasticity indices of the shales of the Pietermaritzburg Formation which were investigated by Bell and Maud (1996).

Table 8.3: Atterberg limits of the soil material analysed from Localities 1 and 3.

Atterberg limits			
Locality	**Cornubia**	**Locality 3**	**Classification of swell potential according to O'Neil and Poormoayed, 1980)**
Liquid limit (%)	(33-40) 37*[3]	(22-30) 26*[3]	Low
Plastic limit (%)	(20-25) 23*	(15-23) 19*	Low
Plasticity index (%)	14	7	Low
Linear shrinkage (%)	4	3	Low

Range: (); Average: *; Number of tests: []

Based on the BS (1999) soil classification scheme the residual material are categorised as CL type soils as shown in Figure 8.3 whereby the residual material from the Cornubia development has intermediate plasticity (LL: 35-50) whilst soils from Locality 3 have low plasticity (LL < 35). The relationship of the moisture content to the liquid and plastic limits can be expressed numerically by calculating its liquidity index (LI). The liquidity index of Locality 3 in Pietermaritzburg was lower (LI = -1.27) as compared to the liquidity index from the Cornubia development (LI = -0.71). The negative liquidity index values indicate that the soils are desiccated and that these soils are drier than their plastic limits (Assaad *et al.*, 2004).

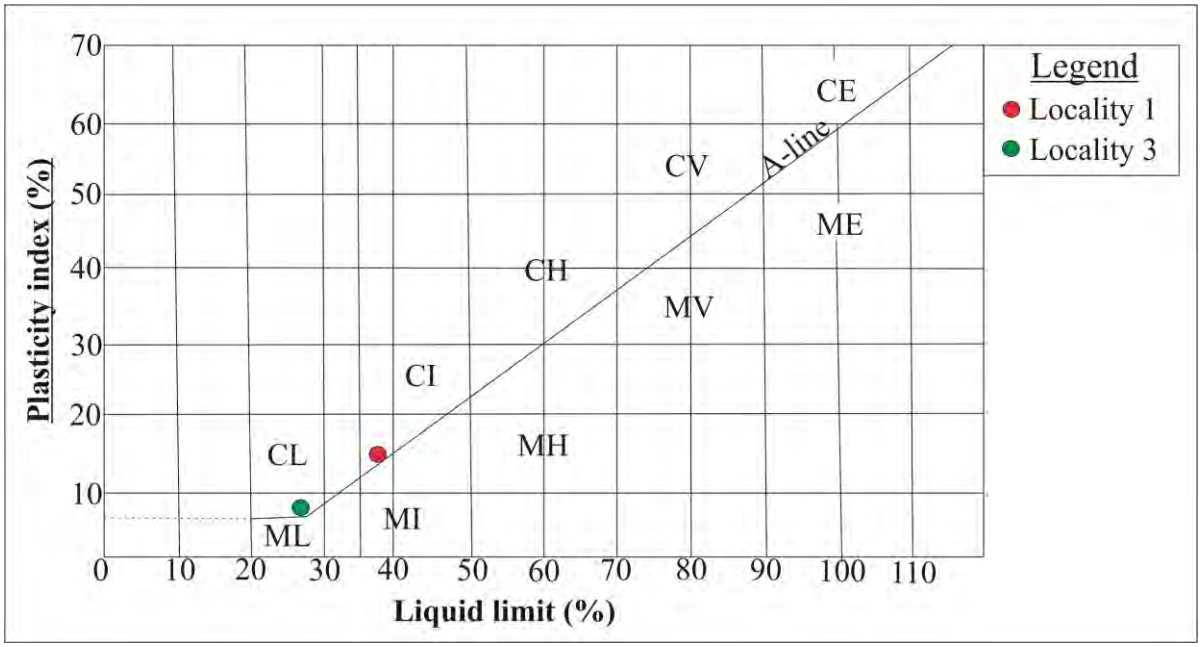

Figure 8.3: Plasticity chart used to classify the soil material from Localities 1 and 3 (modified after BS 5930: 1999).

8.3.4 Jar slake test

A summary of the observations made during the jar slake test is shown in Table 8.4.

Table 8.4: Description of the observations during the jar slake test.

Jar Slake Test								
	Locality 1		**Locality 2**		**Locality 3**		**Locality 4**	
Time	Fresh	Weathered	Fresh	Weathered	Fresh	Weathered	Fresh	Weathered
10 Minutes	Forms a few chips (5)	Develops several fractures and water turned milky (4)	No change (6)	No change (6)	Forms few fractures (5)	Forms few fractures (5), water turned milky	No change (6)	Forms few chips (5)
30 Minutes	No change (6)	No change (6)	No change (6)	No change (6)	No change (6)	No change (6)	No change (6)	No change (6)
24 Hours	No change (6)	No change (6)	No change (6)	No change (6)	No change (6)	No change (6)	No change (6)	No change (6)

The numbers 1 to 6 describes a particular jar slake index where 1 indicates that a shale degrades to a pile of mud whilst 6 indicates no observable reaction

The fresh and weathered samples from the three localities within the Pietermaritzburg area showed a slight physical change over the duration of the jar slake tests. On the other hand, the shale material examined from the Cornubia development showed the most distinctive observation from all the shale materials tested. Small chips (< 2 mm) began to break-off during the first fifteen minutes from the fresher (dark) shale material from the Cornubia development and caused a decrease in visibility in the beaker. After 24 hours, the pieces of the shale material from this locality settled and the water was clear once again. The weathered shale sample from the Cornubia development turned the water milky and formed a few chips during the jar slake test. After a 24 hour period, the water remained milky well after the larger chips of shale material had settled to the bottom of the beaker (Figure 8.4). The shale material from the three localities within the Pietermaritzburg area showed very little change during the jar slake test. Very few chips (one or two) formed from the fresh shale samples from Locality 3 during this test. The shale samples from the Pietermaritzburg area were much more intact and did not react as vigorously as compared to shale samples from the Cornubia development when submerged in water. Generally, the reaction of all the shale materials tested occurred within the first 30 minutes of the test after immersion and in many cases, after 10 minutes.

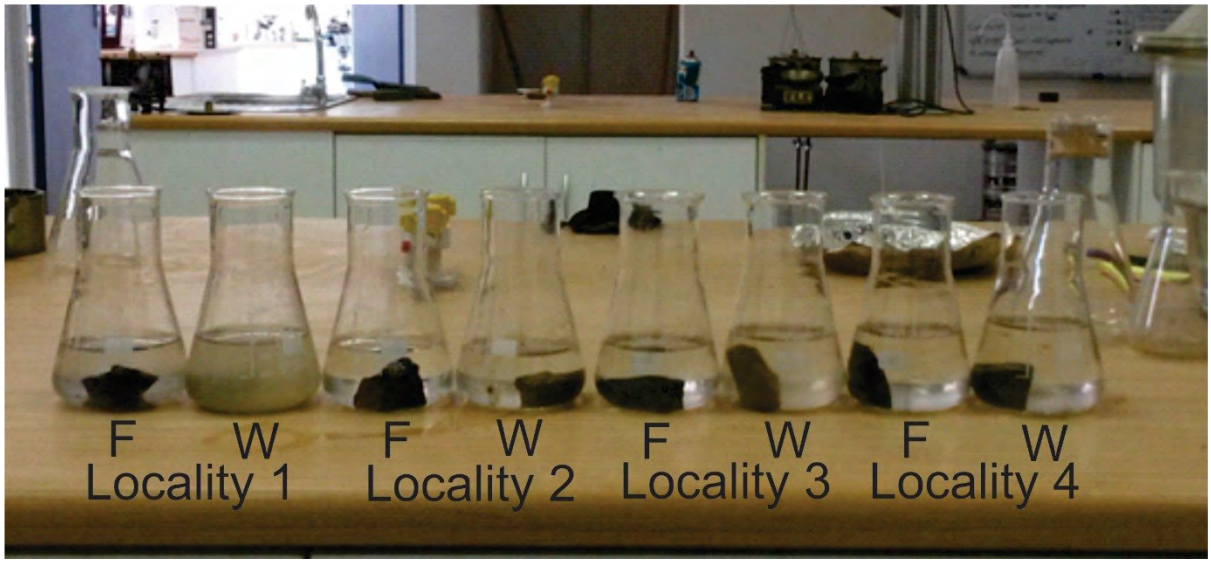

Figure 8.4: Jar slake observations (from left to right, the fresh (F) and weathered (W) shales from Localities 1 - 4 respectively).

The jar slake indices were related to the mode of slaking of the shale materials tested as suggested by Santi and Koncagul (1996). Jar slake indices of 4 and 5 suggest that body slaking has caused the observable changes of the fresh and weathered shales from Localities 1 and 3 and to the weathered shales from Locality 4. Moriwaki and Mitchell (1977) suggested that body slaking occurs when Ca-illite are abundant in a particular material. However, the XRD analyses do not support their findings. Perry and Andrews (1982) stated that materials which show block slaking during the jar slake test produce stable embankments and pose minor erosional problems. A weakness with the jar slake test is that the categories do not necessary progress from the weakest reaction to the strongest reaction. For example, a sample which shows a weak slaking reaction that forms a few chips rather than fractures as seen by the fresh shales from Locality 1 and the weathered shales from Locality 4, should have a jar slake index of 3. However, a jar slake index of 3 was not given to these shale materials because their visual changes did not match Santi's (1998) proposed modification of the jar slake test. Furthermore, the jar slake methodology fails to provide an umambiguous description between each category. For example, the distinction between many fractures and few fractures or between many chips and few chips may be different for different technicians (Santi, 1998). Thus, the results of the jar slake test could be very subjective as it entirely depends on the ability to distinguish between the jar slake indices.

8.3.5 Slake durability test

The results obtained from the slake durability tests for each locality are shown in Table 8.5 and Appendix B.4.

Table 8.5: The slake durability results of the shale material from each Locality.

Slake durability index (%)								
	Locality 1		Locality 2		Locality 3		Locality 4	
Medium	F (7#)	W (7#)	F (6#)	W (5#)	F (7#)	W (7#)	F (4#)	W (4#)
Water SDI (%)	(93-97) 95*	(91.-95) 93*	(95-98) 97*	(91-97) 94*	(94-98) 96*	(92-97) 95*	(95-97) 96*	(94-98) 96*
Ethylene Glycol SDI (%)	(95-99) 97*	(87.-91) 89*	(96-98) 97*	(92-97) 95*	(95-98) 97*	(94-98) 96*	(96-98) 97*	(96-98) 97*

F: Fresh; W: Weathered; Range: (), Average:*; Number of samples tested: #

The fresh materials from each locality are durable as shown by their high slake durability indices (SDI) in Table 8.5. The fresh shale material from the Cornubia development disintegrated much more when slaked in water than in ethylene glycol. However, the weathered material from this locality disintegrated significantly when slaked in ethylene glycol (having an average slake durability index of 89 %) as compared to water. This could be as a result of a higher clay fraction in the weathered shales as compared to the fresh shales from this locality. Chapman (1975) stated that shales which contain a low percentage of montmorillonite show less slaking in ethylene glycol than when slaked in water. This could be the reason that the average SDI of the fresh and weathered shale samples from Localities 3 and 4 and the weathered shale material from Locality 2 is lower when slaked in water than in ethylene glycol. However the fresh shale material from Locality 1 has the highest percentage of montmorillonite than all the fresh samples tested from each locality therefore supporting Chapman (1975) findings. Also, the weathered material from the Cornubia development has the lowest average slake durability index when slaked in water as compared to the three other localities. This observation is probably due to the shale samples having a higher percentage of illite and muscovite mica and a lower percentage of quartz than the shale samples from the other localities.

The fresh shale material from Localities 3 and 4 from the Pietermaritzburg area disintegrated more when slaked in water (96% and 96% respectively) as compared to ethylene glycol (97% and 97% respectively). It is expected that ethylene glycol would penetrate the shale samples much easier due to the presence of the clay minerals however the geochemical results that are presented in Table 8.1 showed that there was a low percentage of expanding clay minerals. The weathered materials from all three localities within the Pietermaritzburg area have higher slake durability indices than the weathered material from the Cornubia Development when slaked in water and ethylene glycol. Water was able to cause the weathered shale samples from the Cornubia development to disintegrate much easier than the samples which were immersed in ethylene glycol. Bell *et al.* (1996) pointed out that the durability of shales are often controlled by the constituent fine particles and by the composition of each sample. As seen from Table 8.5, the lower SDI of the weathered shales from the Cornubia

development could be attributable to its higher percentage of illite and lower amount of quartz as compared to the other sampling sites. Although the weathered material has a lower slake durability index than the fresh material from each locality, it still has a high slake durability index after the 4 cycle slake durability test. The slake durability index of the shale materials from Localities 2, 3 and 4 from the Pietermaritzburg area are higher than the shale materials from the Cornubia development and this could be as a result of the higher amount of quartz and lower clay content as suggested by Koncagul and Santi (1999). The lower slake durability indices of the weathered shales from Localities 2 and 4 are possibly due to the higher amount of kaolinite present than the fresh shales from these localities. Moriwaki and Mitchell (1977) stated that rocks which contain kaolinite slake faster when submerged in water as a result of pore air compression.

Based on the classification system by Hopkins and Beckham (1998) and Broch and Franklin (1972), the shales from each locality could be regarded as having high to extremely high slake durability indices and as hard shales respectively as shown in Table 8.6.

Table 8.6: Slake durability classification.

Slake durability classification (modified after Hopkins and Beckham, 1998)		
Slake durability index SDI) (%)	Jar slake Index	Description of shale
SDI < 50	≤ 2	Soil-like shale
-50 < SDI > 95	3 – 5	Intermediate shale
SDI > 95	6	Hard shale
Slake durability classification (adapted from Broch and Franklin, 1972)		
Slake durability index		Description
25-50 %		Low
50-75 %		Medium
75-90 %		High
90-95 %		Very high
> 95 %		Extremely high

Hopkins (1988) suggested that oven drying samples prior to performing slake durability tests, as compared to air-drying sometimes produces higher slake durability indices. However, the predominant degradation mechanism of the shales could be as a result of pore air compression which takes place when the shales are immersed in water and this results in the development of capillary suction pressures. The entrapped air exerts tension on the solid skeleton causing the material to fail in tension. Pore air compression could be the dominant slaking mechanism in the non-expansive clay minerals. Comparatively, clay surface hydration by ion adsorption could be the slaking mechanism of swelling clays such as montmorillonite (Andrews *et al.*, 1980).

Since the weathering of shales is a time dependant process, the multi stage (4 cycle) slake durability test was used to determine the degree of weathering (Figure 8.5). The effects of weathering was seen particularly after the second cycle of the slake durability test and further slaking cycles of the shales showed that the degree of weathering becomes constant after the second cycle of weathering. The rate of the disintegration of these materials begins to decrease after the first cycle and follows a steady rate of disintegration during each slaking cycle. The most significant trend in these slaking cycles is seen by the weathered shale material from the Cornubia development as the shale material continuously degrades at a higher rate as compared to the shales from the other localities. This could be as a result of the lower percentage of quartz and a higher percentage of illite as evident from the XRD results.

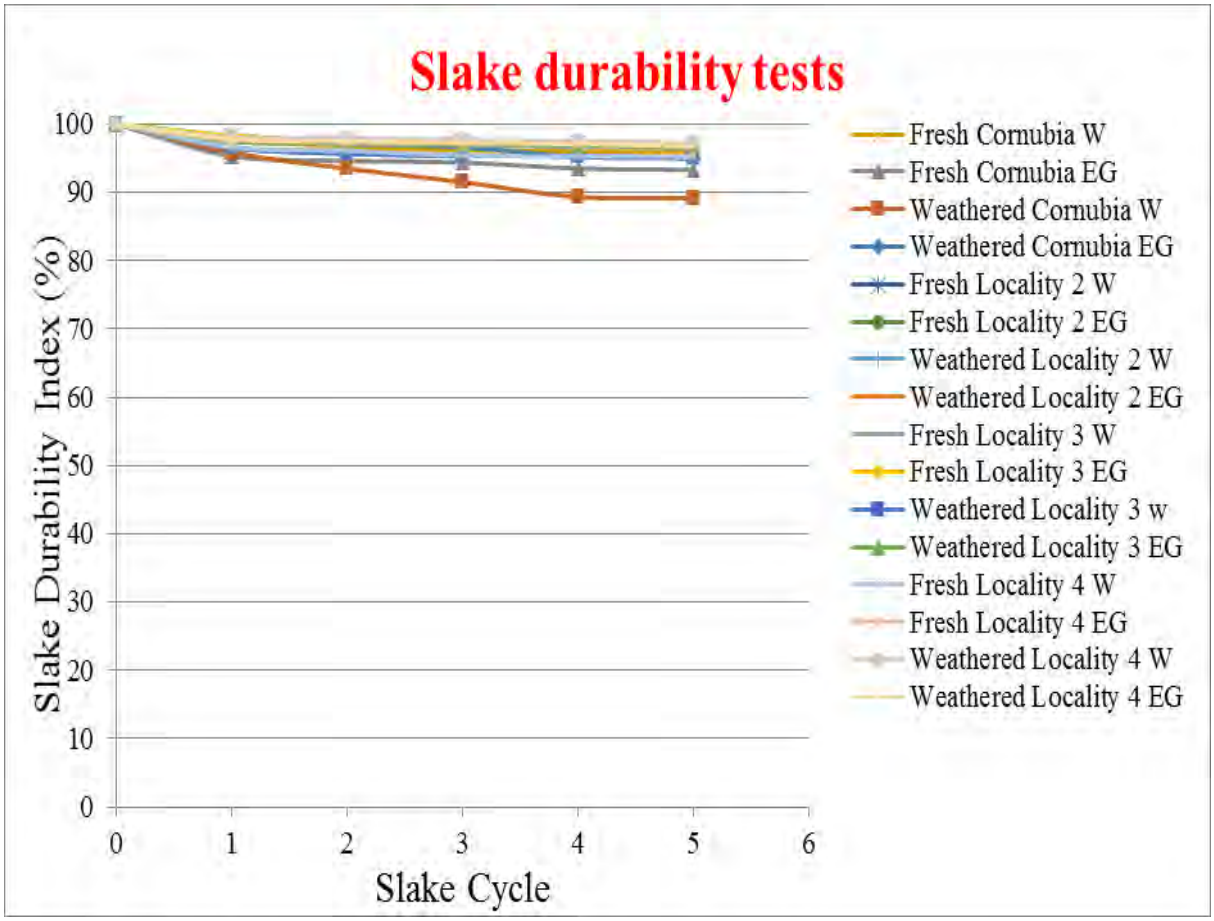

Figure 8.5: Change in the slake durability index from a change in the slaking cycle of the samples from each locality.

The results further support Santi's (1998) proposed modification of characterising a material after a single cycle of slaking. However, the results also show the necessity of conducting more slaking cycles because the first slaking cycle shows the greatest decrease in the materials slake durability and will therefore over-estimate the predictions of the degradable nature of a material. In addition, this proposed modification would not be applicable for predicting the further slaking cycles for the shale

materials from the Cornubia development as their rate of degradation was not uniform during subsequent cycles.

8.3.6 Point Load Strength test

The results from the Point Load Strength tests conducted on the shale samples from Localities 1 and 3 are presented in Table 8.7 and the calculations are shown in Appendix B.5. Additionally, due to the limited point load strength values that are available on shales of the Pietermaritzburg Formation, the point load results that were obtained by Toniolo (2012) are also shown in Table 8.7.

Table 8.7: Point Load test results from the Cornubia development and from Locality 3 from the Pietermaritzburg area.

Point Load Strength test				
Locality	**Type of material**	**Point Load Strength (MPa)**	**Point Load Strength index (after Franklin and Broch, 1972)**	**Toniolo (2012)**
Axial				
1	Fresh	(3.06 – 3.25) 3.15* [5]	High strength (1-3 MPa)	**Locality 1** (1.86-2.26) 2.04* [5] **Locality 2** (3.10-4.75) 3.83* [5] **Locality 3** (5.84-7.33) 6.50* [5]
	Weathered	(2.00-2.62) 2.31* [5]	High strength (1-3 MPa)	
3	Fresh	(3.00-4.11) 3.00*[5]	High to very high strength (3-10 MPa)	
	Weathered	(2.61-3.43) 3.56*[5]	High strength (1-3 MPa)	
Diametrical				
3	Fresh	(1.48 – 1.67) 1.58*[5]	High strength (1-3 MPa)	**Locality 1** (0.70-1.00) 0.88 [5] **Locality 2** (1.35-1.61) 1.50 [5] **Locality 3** (4.16-5.30) 4.64 [5]
	Weathered	(1.01 – 1.18) 1.12*[5]	High strength (1-3 MPa)	
1	Fresh	(1.33 – 1.64) 1.49*[5]	High (3-10 MPa)	
	Weathered	(0.95 – 1.10) 1.04*[5]	High strength (1-3 MPa)	

Number of samples tested: []; Range: (); Average*

Based on the Point Load Strength test results, it was observed that the Point Load Strength is much higher for the darker, fresher shale material as compared to the weathered shale materials. The average Point Load Strength values of the fresh and weathered material were higher for Locality 3 from the Pietermaritzburg area as compared to the shale samples tested from the Cornubia development. The Point Load Strength test could not be performed on the shale materials from Localities 2 and 4 because the core samples began to break easily during coring. Furthermore, it was only possible to obtain a few core samples from Localities 1 and 3 as a result of the fissile nature of the shale samples whilst sampling.

The axial strength of the shale samples tested from each locality are higher than the diametrical strength. When failure is initiated parallel to the bedding planes (anisotropy) of sedimentary rocks, the resulting diametrical strength is lower than the axial strength (Broch, 1983; ISRM, 2000). The observed diametrical strength is lower than the axial strength since the force applied by the individual platen are parallel to the lamination planes and to the degree of fissility which reduces the force which is required to break shales (Bell and Maud, 1996; Bell *et al.,* 1997). Based on the Point Load Strength index after Brock and Franklin (1972), the shale materials have a high Point Load Strength. Table 8.7 further presents the results obtained from the study performed by Toniolo (2012) due to the scarcity of the Point Load Strength test results on shales of the Pietermaritzburg Formation from the literature. According to the axial and diametrical Point Load Strength, the results from this study are similar to the Point Load Strength results as determined by Toniolo (2012) on shales of the Pietermaritzburg Formation.

8.3.7 Shear Box test

For each shear box test conducted, shear stress versus horizontal displacement curves were drawn for each normal stress. Thus, 3 sets of graphs were plotted for each set of test conducted for the materials tested. Examples of these graphs are shown in Figure 8.6 – Figure 8.9 and the calculations of the shear stresses are shown in Appendix C. The remainder of the shear stress versus horizontal displacement curves and the shear stress versus normal stress curves are shown in Appendix C.

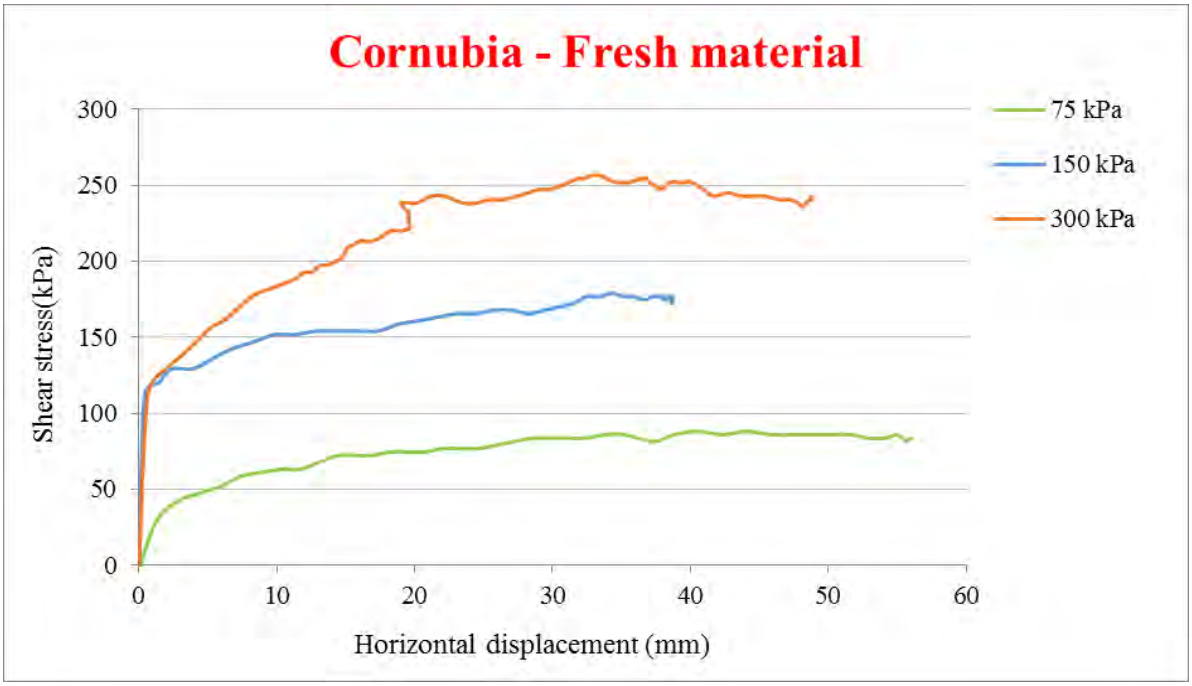

Figure 8.6: Shear stress vs horizontal displacement curves for the fresh material from the Cornubia development.

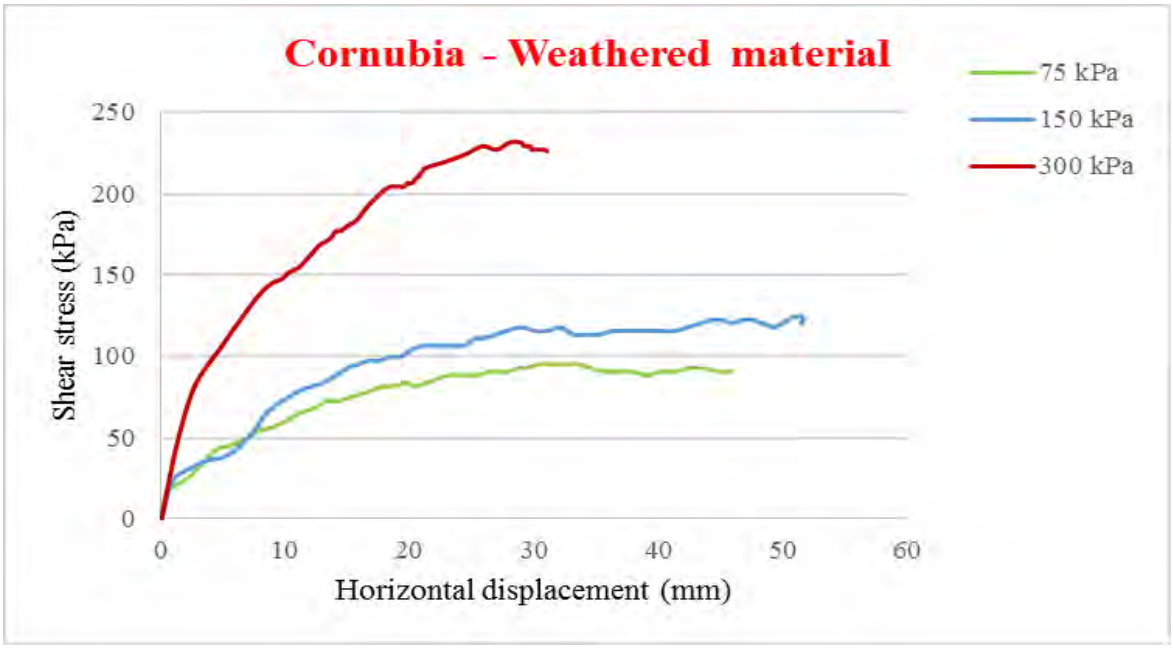

Figure 8.7: Shear stress vs horizontal displacement curves for the weathered material from the Cornubia development.

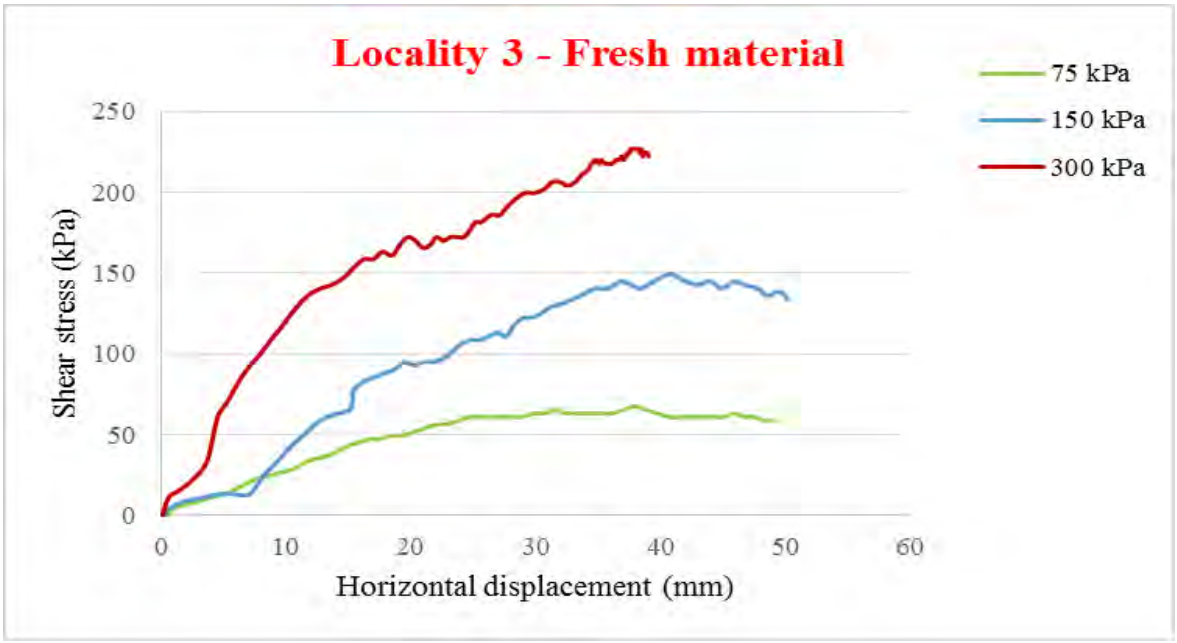

Figure 8.8: Shear stress vs horizontal displacement curves for the fresh material from Locality 3 from the Pietermaritzburg area.

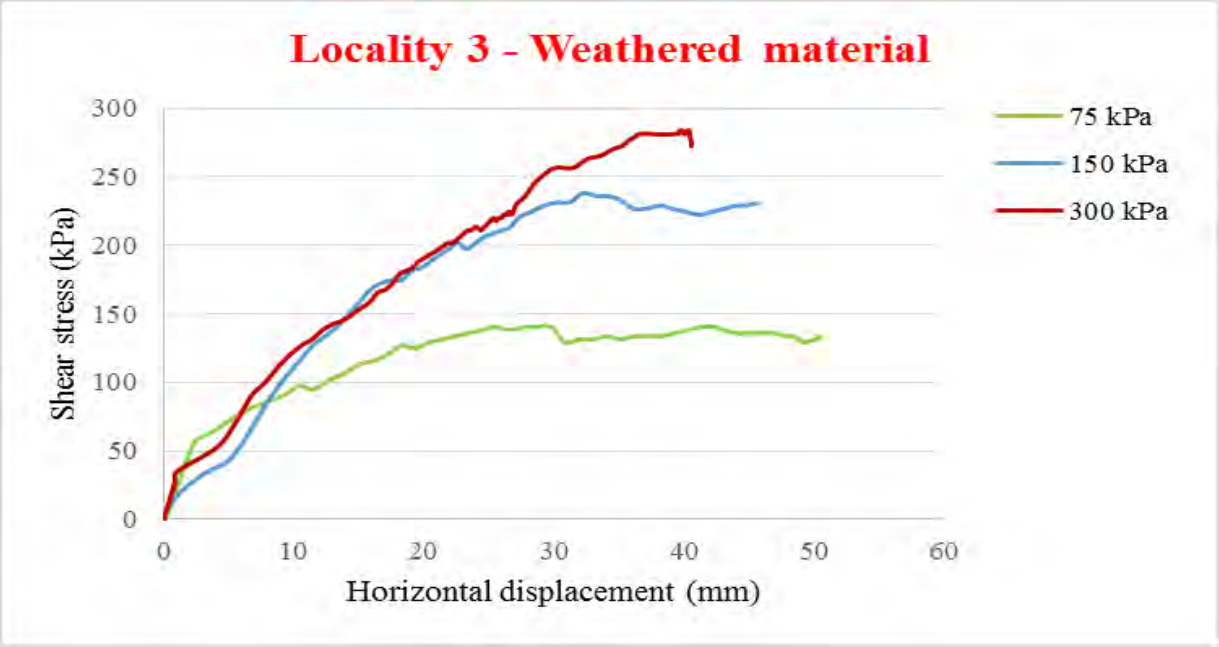

Figure 8.9: Shear stress vs horizontal displacement curves for the weathered material from Locality 3 from the Pietermaritzburg area.

The shear stress versus horizontal displacement graphs of the shear box tests are curvilinear as shown in Figure 8.6 – Figure 8.9. The shear stress versus horizontal displacement curves of the fresh shale samples from Localities 1 and 3 display a sharp linear shape at the start of the shear box test as shown in Figure 8.6 and Figure 8.8 and these curves resemble a typical shear stress profile of loosely compacted sand (Craig, 2004). The attrition of the angular and tabular particles to the corners of the shear box during the shear box tests possibly causes the curvature and the step-like pattern in the curves.

The shear stress versus horizontal displacement curves of the weathered material show greater curvature than the fresh shale material tested. The greater curvature shown by the weaker shale materials (i.e. the weathered shale samples) are more prone to particle breakdown during the shear box test since movement is forced along a defined shear plane of the shale samples (Hardwick, 1992). The peak shear stress at each increment of normal stress (except for the normal stress of 75 kPa) are much higher for the fresh shale samples than for the weathered shale samples tested from the Cornubia development. However, the peak shear stress at each increment of normal stress are much higher for the weathered shale samples than for the fresh shale samples tested from Locality 3.

The weathered material from the Cornubia development failed much sooner than the fresh shale material from this locality (Figure 8.6 and Figure 8.7). However, this pattern was not seen whilst testing the fresh and weathered shale material from Locality 3 in the Pietermaritzburg area (Horizontal displacement > 40 mm). A similar pattern of the loading curves were also seen during the

shear box test of the fresh material from Localities 2 and 4 from the Pietermaritzburg area. The mixture of the fresh and weathered shale materials from the Cornubia development failed at a lower shear stress than the mixture of the fresh and weathered shale materials from Locality 3 from the Pietermaritzburg area. The fresh shale material from the Cornubia development reaches its peak stress sooner (at a shorter horizontal displacement) than the fresh shale samples from localities 2, 3 and 4.

The shear stress versus horizontal displacement curves shown in Figure 8.6 - Figure 8.9 do not show distinct peaks to differentiate between the peak strength and the residual strength. Therefore, where a definite peak was not seen, the peak shear stress at failure of each curve was taken at the highest point from the shear stress versus horizontal displacement curve and these values were recorded at a horizontal displacement of less than 50 mm. A failure envelope was then produced using the peak shear stress at failure at each normal stress as presented in Table 8.8 to obtain the effective shear strength parameters, c′ and φ′ for each set of tests conducted. Using a line of best fit as shown in Figure 8.10, c′ was recorded as the intercept of this line with the y axis and φ′ was determined from the gradient of the line of best fit. Examples of the failure envelopes are shown in Figures 8.10 - 8.13 and the remainder of the failure envelopes are shown in Appendix C.

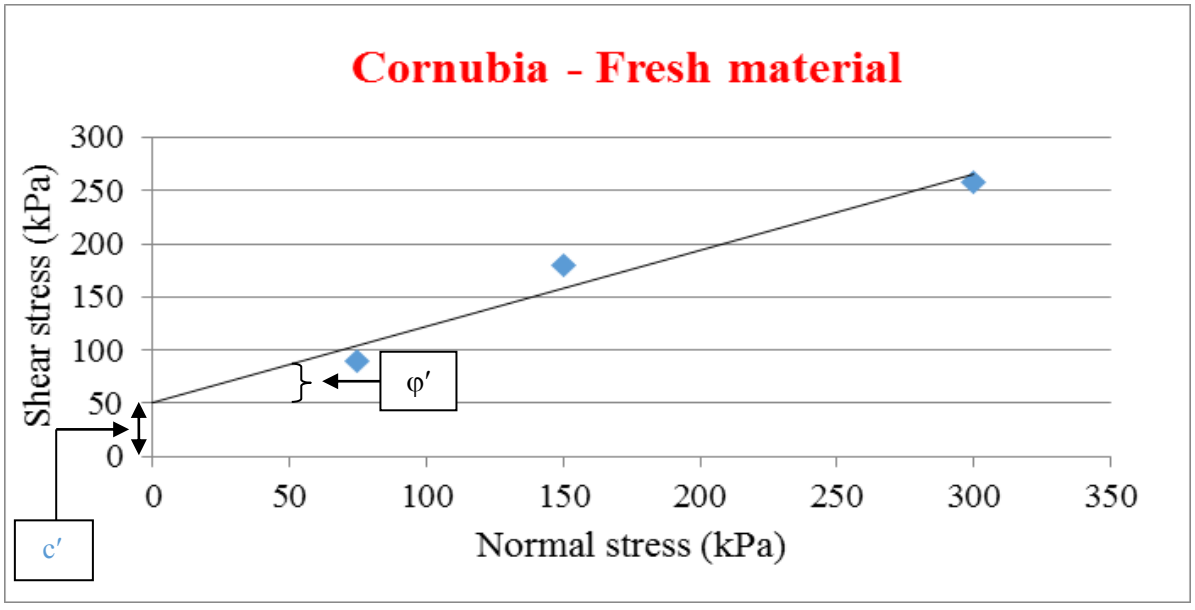

Figure 8.10: Shear stress vs normal stress for the fresh material from the Cornubia development.

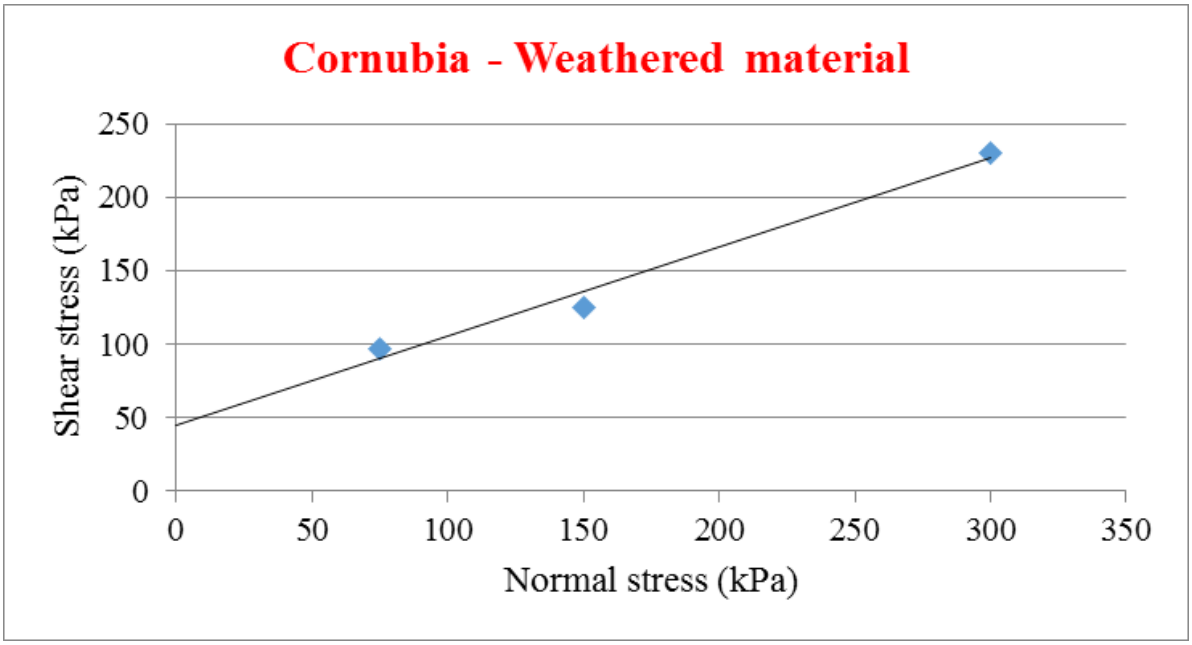

Figure 8.11: Shear stress vs normal stress for the weathered material from the Cornubia development.

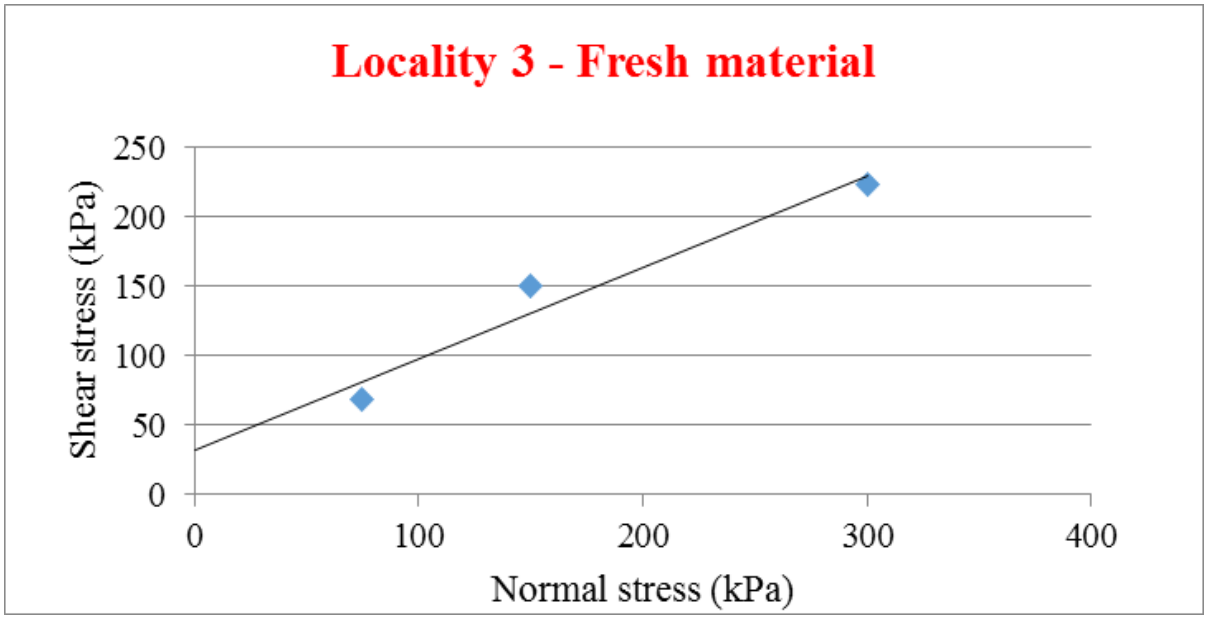

Figure 8.12: Shear stress vs normal stress for the fresh material from Locality 3.

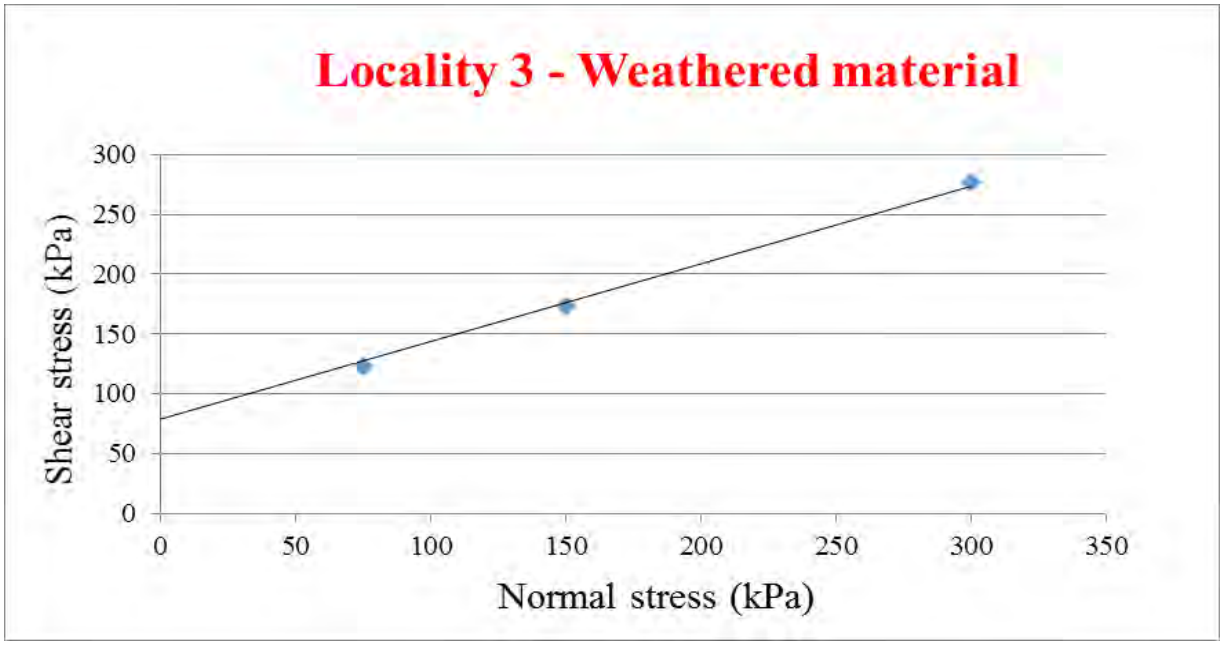

Figure 8.13: Shear stress vs normal stress for the weathered material from Locality 3.

Table 8.8: The peak shear stress at failure at each normal stress of the shale materials tested for each locality.

Shear stress (kPa)								
Locality	Locality 1: Cornubia development			Pietermaritzburg area				
				Locality 2	Locality 3			Locality 4
Normal stress (kPa)	Fresh	Weathered	Mixture	Fresh	Fresh	Weathered	Mixture	Fresh
75	89	95	75	61	68	141	95	52
150	179	125	129	145	150	238	168	120
300	256	238	231	229	227	284	247	240

A summary of the effective shear strength parameters (i.e. c′ and φ′) obtained from the failure envelopes in shown in Table 8.9. It was observed that the shear strength properties of the weathered shale samples from the Cornubia development are lower than the weathered shale material from Locality 3. Furthermore, the effective cohesion of the weathered sample from Locality 3 in the Pietermaritzburg area was very high as compared to the weathered materials from the other localities. Despite observing this anomaly (i.e. high cohesion), it was not possible to perform an additional shear box test on this sample because the shear box test is very laborious and there was a limited time available to perform the shear test. Furthermore, it was difficult to transport a large quantity of material which is required to conduct the shear box test.

The weathered shale samples that were tested from the Cornubia development has the lowest φ′ value than from all of the shale materials tested and has a lowest c′ from all the shales tested with the

exception of the fresh material from Localities 2 and 4. The fresh shale material tested from Locality 4 has a higher φ′ but has the lowest c′ as compared to the fresh shale material from the Cornubia development and Localities 2 and 3 from the Pietermaritzburg area. A mixture of the fresh and weathered material from the Cornubia development and Locality 3 showed that the shear strength parameters, c′ and φ′ fell in between the shear strength parameters of the fresh and weathered material. In addition, it was found that c′ of the weathered material from the Cornubia development, consistent with the other laboratory tests which were performed, were much lower from the Cornubia development than the shale material tested from Locality 3 from the Pietermaritzburg area. Gartung (1986) suggested that the friction angle usually decreases during weathering thus the weathered material showing a lower φ′ than the fresh samples. However, the shale samples tested from Locality 3 do not support his findings.

Table 8.9: The effective shear strength parameters obtained from the unconsolidated undrained shear box tests.

Locality								
	Cornubia development			**Pietermaritzburg**				
	1			**2**	**3**			**4**
Parameter	Fresh	Weathered	Mixture	Fresh	Fresh	Weathered	Mixture	Fresh
Effective friction angle (φ′)	36°	32.2°	34.7°	37°	33°	34.4°	33.4°	39°
Effective cohesion (c′) (kPa)	51	30	48.1	21.5	38	71	51.3	9.7

The effects of weathering are observed by the large difference in the φ′ between the fresh and weathered shale samples. Wan and Kwong (2004) showed that during their laboratory investigation of materials which contained a high percentage of clays, the cohesion of these materials can be very high (up to 50 kPa). They stated that the high cohesion is as a result of the strong inter-particle bonds of the amorphous clay materials. Furthermore, it is possible for c′ to vary significantly, when materials are well compacted (Hopkins, 1988). Hajdarwish and Shakoor (2006) stated that the cohesion of fresh shales can range from 240 kPa- 7850 kPa.

The high cohesion observed from the weathered material from Locality 3 from the Pietermaritzburg area can be regarded as an outlier as compared to the shear tests conducted on the weathered shale samples from the Cornubia development. It is generally expected for the fresher materials to have a higher cohesion than weathered materials because weathering often reduces the shear strength of an argillaceous material. This behaviour was observed by the shear tests performed on the shales from the Cornubia development with the exception of the shale samples from Locality 3. In the weathered shale material of Locality 3, the compaction of the shale sample into the shear box could have created

hard layers within the sample tested which could also have caused the high cohesion as stated by Hardwick (1992). Additionally, the weathered sample from this locality contained more fines than the weathered shale samples from the Cornubia development. The greater amount of fines would have increased the packing density of the weathered shales from this locality and could be the reason for the high c′ value.

The shear strength properties of Underwood (1967) classification system as shown on Table 8.10 was used to describe the shale samples from each locality since the information regarding shales of the Pietermaritzburg Formation is very limited. Using this classification, all of the shale samples tested are characterised as being favourable according to their φ′. However, the shale samples from Localities 1 to 4 are characterised as being unfavourable according to their c′ despite that these samples have a high frictional component.

Table 8.10: Using Underwood (1967) shale classification system to classify the shales tested.

Physical properties						
Shear strength parameter	**Average range of values (Underwood, 1967)**		Cornubia	Locality 2	Locality 3	Locality 4
	Unfavourable	Favourable				
Effective friction angle (φ′)	10 - 20°	20 – 65°	32.2-36°	37°	33 – 34.4°	39°
Effective cohesion (c′) (kPa)	37 – 700	700-10500	30-51	21.5	38 - 71	9.7

The large scale shear box test is a costly, time consuming and a very laborious laboratory test to perform to determine the shear strength of a material. Firstly, time is required to ensure that the samples are of the same size and thickness as stated by Norman Alexander (2014). The setup of the testing equipment is a lengthy process and time is required to perform the shear test of each material under a particular load. Due to these limitations and as a result of the large number of samples that were tested, it was only possible to perform a single test per fresh or weathered sample from each locality. These limitations did not allow for the repetition of any tests even if an anomaly was observed such as the c′ of the weathered shales of Locality 3. Furthermore, the shear box test is a very expensive test to perform and labour intensive as stated by Marr (2000) which are limiting factors in the commercial environment. A further disadvantage is that the only known stresses known to be imposed on the samples are the normal stress and shear stress and that the stress distribution throughout the sample is not uniform as stated by Atkinson and Bransby (1978). Additionally, a major problem of the shear box test is that the split nature of the box imposes a location and direction of the shear plane upon the sample. Additionally, the loss of material between the halves of the shear box is

a common problem as stated by Hardwick (1992) thus making it very difficult to obtain a true measurement of dilation.

8.4 Settlement analyses

When shales are used to construct embankments consisting of gravel sized materials and greater, these materials are expected to settle about 1% of the fill height (Ribbink, K., pers. comm., 2015). Using the precise levelling technique that was discussed in Chapter 6 to obtain the monthly observed settlement from each site from the Cornubia development such as the Fountains site (Figure 8.14), the Gralio (8.16) site and the Vumani site (8.18), a prediction was made to determine the total expected settlement which equates to 1 % for each platform. Each prediction was calculated using the average settlement at a particular site (i.e. Fountains, Gralio, and Vumani) to determine the time taken for the fill to settle approximately 1% of its fill height. The readings that were recorded monthly are presented in Appendix D.

In the industrial sector which was prepared by Fountains Civil Engineering, each platform consists of a mixture of the *in situ* fresh and weathered shale material. At this site, settlement analyses from platforms 10 to 14 showed that the annual settlement is approximately 74 mm (Figure 8.14). The results show that the settlement is less than 1 % of the fill height whereby the maximum fill height is 8 m. Based on the rainfall data, it was seen that most of the settlement occurred during the rainy months, that is, in September and between the months of November to January (Figure 8.15). Despite the high amount of rainfall in January and February, the rate of settlement decreased.

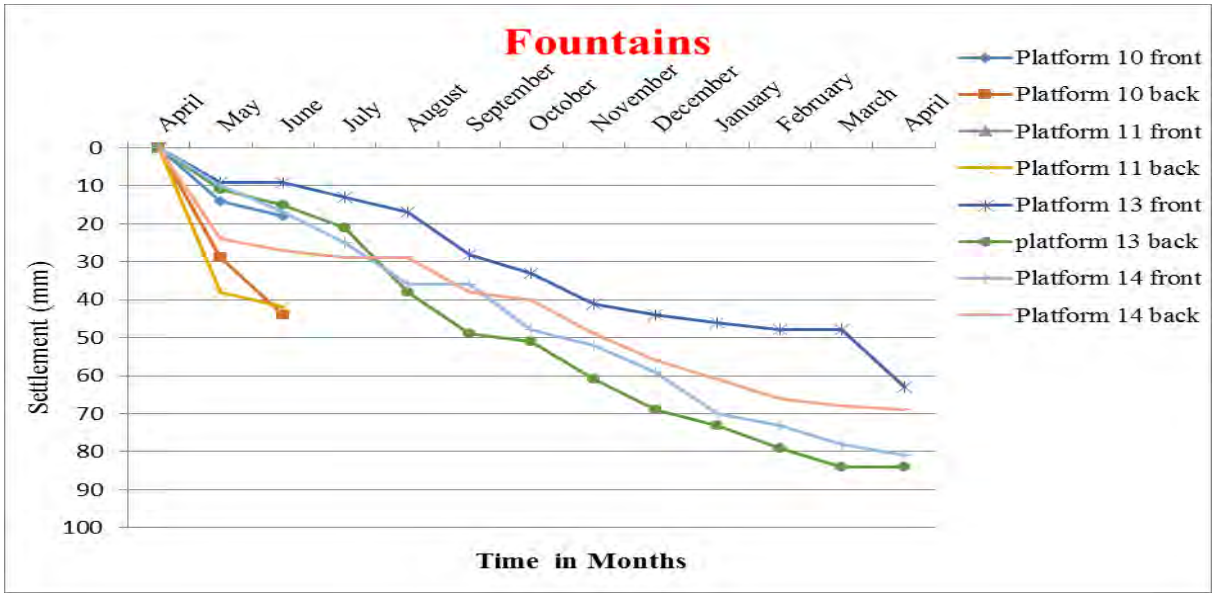

Figure 8.14: Settlement plot over a one year period at the Fountains site in the industrial sector of the Cornubia Housing and Industrial development.

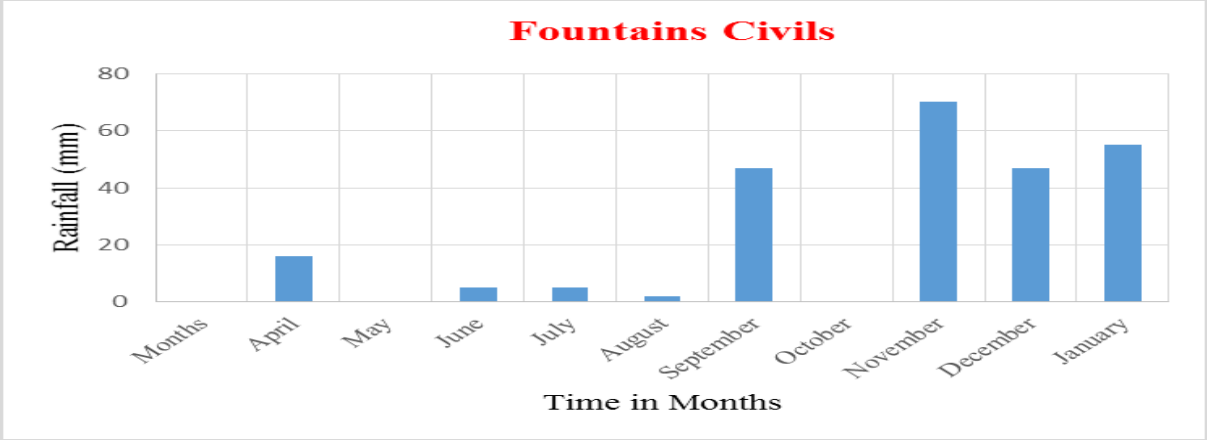

Figure 8.15: Amount of rainfall during the settlement monitoring period at the Fountains site.

The monitoring of settlement was also done over two sites in the housing sector of the Cornubia housing and industrial development; the Vumani Site and the Gralio Site. At the Vumani Site, dolerite was used as the major constituent fill material in conjunction with a thin layer of shale material (which was approximately 300 mm thick). Based on the settlement readings, this site was estimated to settle approximately 1 % of the fill height whereby the maximum fill height is 7 m and equates to 70 mm of settlement (Figure 8.16). If it was considered that the highest rate of settlement of 7 mm/ month (average settlement for the 3 month monitoring period), it is expected that most of the settlement will occur within ten months (Ribbink, K., pers. comm., 2015). By assuming that the platforms were completed in August 2014 and that the monitoring of settlement began in September 2014 and was stopped in December 2014, it should take approximately seven months more (i.e. July 2015) for most of the settlement to occur. The amount of settlement which occurred during September 2014 to December 2014 is shown in Figure 8.16 and the rainfall received during the monitoring period is shown in Figure 8.17.

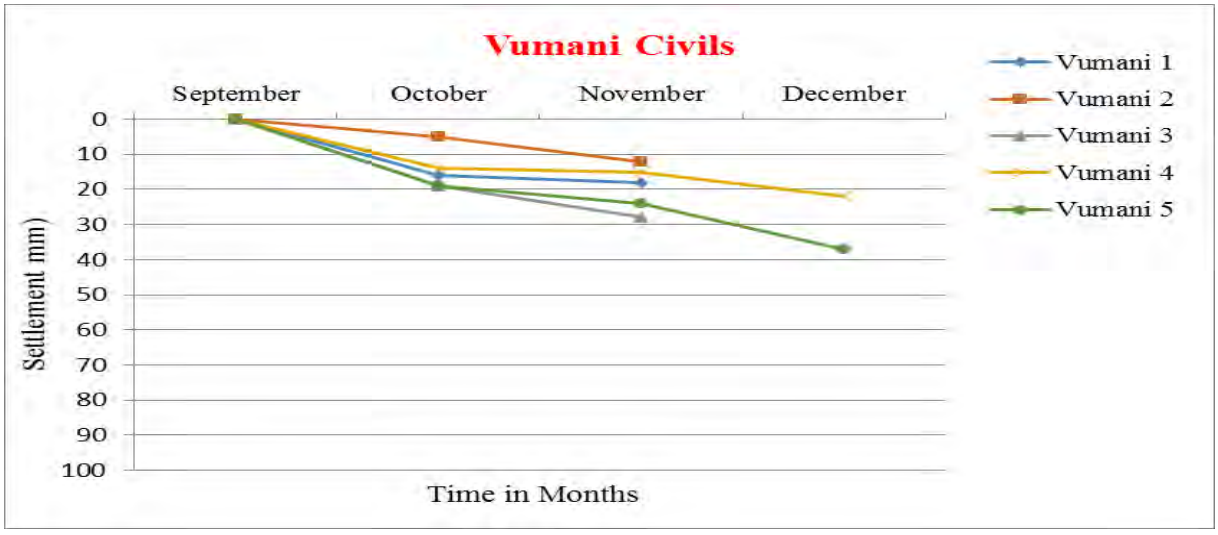

Figure 8.16: Settlement plot over a four month period at the Vumani site in the housing sector of the Cornubia development.

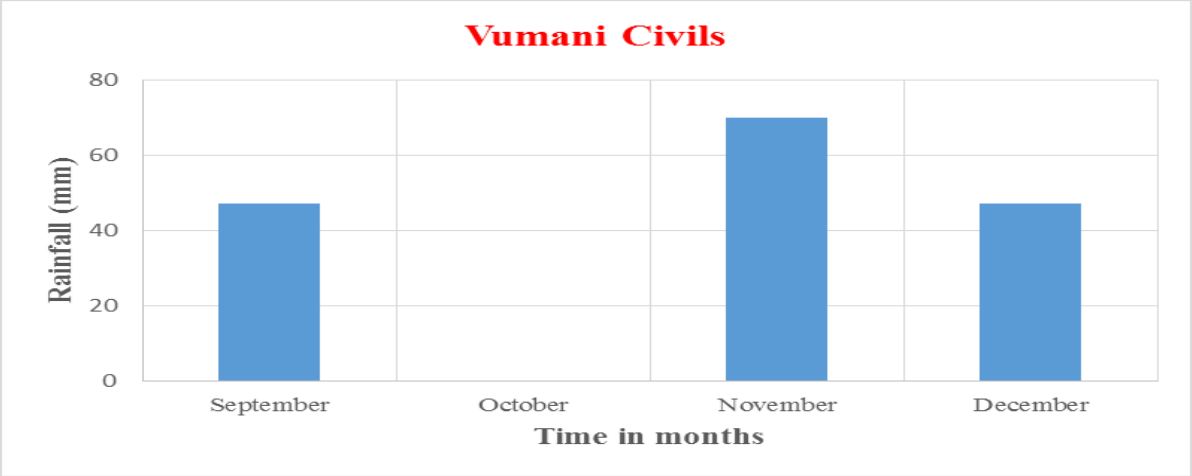

Figure 8.17: Amount of rainfall during the settlement monitoring period at the Vumani site.

The Gralio Site comprises siltsone fill which is approximately 6 m thick. It was observed that this site settled by approximately 28 mm over a 4 month period (i.e. from September 2014-January 2015). It is estimated that this site will settle approximately two percent of the fill height which equates to 120 mm of settlement and this prediction is based on the initial high rate of settlement (Figure 8.18). Considering that the highest rate of settlement is 7 mm/ month (using an average settlement of 7 mm/ month during the 4 month monitoring period), it is expected that the total amount of settlement will occur within a period of seventeen months. Therefore, by assuming this site has been completed in August 2014 and that the monitoring of settlement commenced from September 2014 and stopped in January 2015, the majority of the settlement should occur within the next thirteen months. The amount of rainfall which occurred during the settlement monitoring period is shown in Figure 8.19.

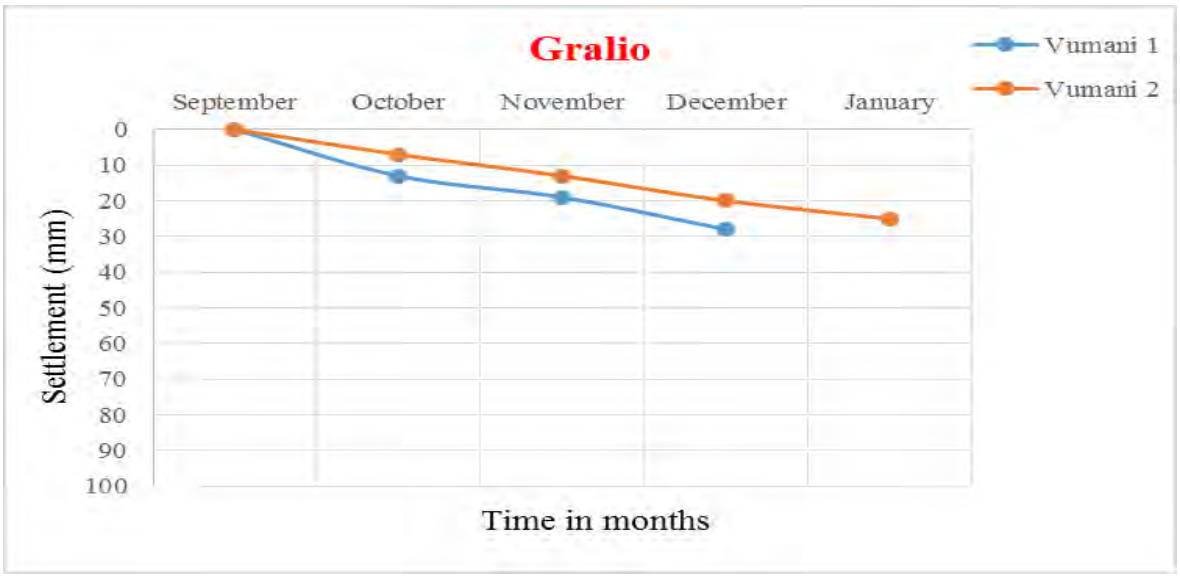

Figure 8.18: Settlement plot over a six month period at the Gralio site in the housing sector of the Cornubia development.

Figure 8.19: Amount of rainfall during the settlement monitoring period at the Gralio site.

The monitoring of settlement at the Cornubia development was a time consuming and difficult task to perform. Surveying pegs for the monitoring of settlement were frequently destroyed and were constantly required to be replaced. As a result of continual peg destruction, especially at the Vumani Site and the Gralio Site, the average rate of settlement was estimated from the amount of settlement which occurred over the stipulated period of time. The rate of settlement from each Site which ranges from 1-2%, is higher than the usual expected amount of settlement as stated by NAVFAC (1982) (Table 8.11). The above straight line assessment (using a projected/ estimated amount of settlement) has not accounted for the initial rapid settlement on completion of the platforms since the monitoring of settlement commenced approximately 2 months after. Also, the settlement analyses presented only represents 80-90 % of the settlement which excludes future long-term settlement or differential settlement beneath the building footprints which will be exerted by the structure to be built on these platforms (Ribbink, K., pers. comm., 2015).

Table 8.11: Comparison between the monitored settlements with values from the literature.

Long term settlement (mm)						
	Cornubia development			Station no. (adapted from Hopkins and Beckham, 1998)		NAVFAC
Locality	Fountains	Vumani	Gralio	Station 498+50	Station 317+50	-
Fill height (mm)	8000	7000	6000	19812	15240	-
Settlement (mm)	74	70	120	120-170	70-80	-
Settlement of fill (%)	<1	1	2	0.61-0.86	0.46-0.52	0.3-0.6

The settlement analyses of the fill material used to construct platforms at the Cornubia development each had different rates of settlement. Surprisingly the platforms at the Gralio Site consisting of siltstone fill had a higher rate of settlement (7 mm/ month) than the shale material (which is expected

to be highly degradable and have a higher rate of settlement) that has been used at the Fountains Site. The settlement analyses at the Gralio site began during the rainy months of 2014 (i.e. October-November) and could be the result of the higher amounts of settlement than the Fountains site. Hopkins and Beckham (1998) have stated that shales may exhibit large and excessive settlement rates when soaked during rainy months. However, the platforms at the Fountains Site were completed in early 2014 which implied that the expected initial rapid settlement would have occurred long before the monitoring of settlement and that the rate of settlement could have decreased. Also, the thickness of the fill material at the Fountain's Site is 2 m greater than at the Gralio Site whereby a higher rate of settlement was expected to occur at the Fountain's site. However, this was not observed. The increase of settlement during September (2014) to January (2015) of the platforms during this period could also be due to the load imposed by the large machinery onsite. The prediction of the future settlement is a difficult task since the settlement of embankments are affected by a variety of factors. The factors that affect the settlement of an embankment include the dry density, the moisture content, the type of material and the degree of compaction.

8.5 Summary

This chapter presented the results obtained from performing a series of index and strength tests on the residual soil and the shale rock materials. Soil index tests and rock strength tests were done to identify and determine the nature and strength of the materials from each locality. The shales have a low clay content and are considered as being non expansive. The shales tested are characterised as being mechanically hard according to Hopkins and Beckham (1998) and are very hard and have a high Point Load Strength according to Broch and Franklin (1972). Settlement monitoring was done to assess the amount of settlement over a one year period. These analyses showed that the amount of settlement monitored falls within acceptable limits (1%) for the settlement of an embankment fill comprising shale material. Based on the results obtained from all the geotechnical tests, the fresh and weathered shale samples from each locality are suitable for construction and should exhibit few problems if compacted correctly. The next chapter will provide an indirect method of predicting the shear strength parameters of shale using a shale rating system which will be crucial to geotechnical engineers in the construction industry.

Chapter 9

Development of a modified rating system for shales

9.1 Introduction

Shales pose difficulties during the sampling process for laboratory testing as pointed out by Hopkins (1988) and Nandi *et al.* (2009). Fam *et al.* (2003) further stated that this happens because these materials are weak and are sensitive to changes in moisture and time. Therefore, information regarding the shear strength for engineering projects involving these materials are scarce or assumed (Hajdarwish and Shakoor, 2006). There is thus a need for a shale classification system that is capable of distinguishing all grades and qualities of shales which allows for a correlation between the type of shale and its performance on engineering projects. This can be accomplished by developing an indirect method of predicting the shear strength properties of these materials using simple index tests. These index tests include geochemical analyses and the use of common geotechnical tests such as the Atterberg limits, the slake durability test, the jar slake test and the Point Load Strength test (Deo, 1972; Morgenstern and Eigenbrod, 1974; Chapman *et al.*, 1976; Hajdarwish and Shakoor, 2006).

This chapter uses the information from the laboratory results presented in Chapter 8 and from a compilation of the literature on shales to modify Franklin's (1981) shale rating chart. Firstly, the chapter focuses on a robust method of rating shales, which is followed by a simple method which can be used directly by geotechnical engineers in the construction industry to categorise shales and predict their shear strength parameters by performing simple index tests. The proposed modified shale rating chart will serve as an effective method of estimating the shear strength properties of shales, using shales of the Pietermaritzburg Formation as a case study. It is envisaged that this method will be very useful in the construction industry as it offers a quick method for estimating the shear strength properties of shales.

9.2 The development of a modified shale rating system

Several researchers (e.g. Deo, 1973; Lutton, 1977; Strohm *et al*., 1978; Franklin, 1981; Santi and Rice, 1991; the U.S. Office of Surface Mining Reclaimation and Enforcement, 1991; Hopkins and Beckham, 1998; Hajdarwish and Shakoor, 2006) have proposed procedures for the design and construction of embankments by performing laboratory tests on highly degradable materials (Walkinshaw and Santi, 1996). These procedures were initially created and designed for shales especially when shales and mudrocks were used in the construction of embankments and pavements (Walkinshaw and Santi, 1996). Thus, the use of shales such as for the stability design of an engineered fill embankment and for road layerworks requires knowledge of the anticipated long term shear strength properties of the fill. Therefore, it is very important to be aware of these aspects because shales exhibit geotechnical properties which range from low strength, low durability fissile

materials to hard rock materials (Dick *et al.,* 1994; Yasar and Erdogan, 2004; Santi, 2006). Thus, the nature of shales will affect the long term shear strength and post construction settlement characteristics of an engineered fill. However, a major disadvantage of the methods which were previously designed to rate shales by Franklin (1981) and by Santi and Rice (1991), was that minimal attempts were made to integrate the geochemical properties of a material to its geotechnical properties.

These shale rating and classification systems focused on the geotechnical properties of shales and the overlying residual soil material. Hajdarwish and Shakoor (2006) showed in their laboratory investigations, that it is not possible to use a single geological property such as lamination or engineering property such as the void ratio, specific gravity and dry density to predict the shear strength of shales. For example, shales which have a high slake durability index does not necessary imply that it has a high shear strength. They suggested that a variety of engineering properties such as the slake durability index (SDI), Point Load Strength and Atterberg limits should be used to predict the shear strength parameters of these materials. The following sections present a method of graphically integrating the geochemical analyses and the geotechnical properties from the laboratory results that are presented in Chapter 8 and from the relevant literature on shales to modify Franklin's (1981) shale rating chart using shales of the Pietermaritzburg Formation as a case study.

Franklin (1981) developed a shale rating chart to rate shales by assigning shale ratings from 1 – 9 which are based on geotechnical tests such as Atterberg limit, the Point Load Strength test and the slake durability test for the construction of embankments. In Franklin's (1981) shale rating chart, the Point Load Strength test and slake durability test were used to obtain a shale rating if the shale sample has an SDI that is greater than 80 whilst the Atterberg limit and the slake durability test were used if the shale sample has an SDI that is less than 80 %. In this study, Franklin's (1981) original shale rating chart (using shale ratings from 1-9) was modified to incorporate the geochemical analyses and the geotechnical properties. For the purpose of this study, Franklin's (1981) shale rating chart was modified to incorporate the jar slake test and to use three shale ratings (i.e. R, 1-3) instead of using nine shale ratings. The reasons for using fewer shale ratings will be discussed in further sections. The modifications will enable for the shear strength parameters (c' & φ') of shales to be predicted within reasonable limits and to provide an indication of settlement and clay content when shales are used as fills.

Using the jar slake index which is a modification to Franklin's (1981) shale rating chart, a shale sample is first assigned a rating by measuring its fourth cycle slake durability index. Hard, rocklike shales which have an SDI greater than 80 % and a jar slake index greater than 4 will be further characterised using the Point Load Strength test. The shale rock material or residual material which

has an SDI lower than 80 % and a jar slake index less than 4 will be characterised using their Atterberg limits.

9.2.1 Using Franklin's (1981) shale ratings from 1-9 to characterise shales

Based on the test results and using Franklin's (1981) shale ratings from 1-9, shales which have a shale rating from 1-3 will be regarded as highly weathered clay shales. These materials would have a low slake durability index, a jar slake index less than 3 and a Point Load Strength less than 1 MPa. Shales which have a rating of 6-9 will be considered as slightly weathered to fresh shales, have a high slake durability index, a jar slake index greater than 4 and a high Point Load Strength (> 2.5 MPa). Shales which show characteristics between class 1 and class 3 will have a shale rating of 4-5, a medium to high slake durability index and a Point Load Strength between (1-2.5 MPa). The shale ratings from 1 - 9 and their descriptions according to their current state of weathering and simple index tests are shown in Table 9.1.

Table 9.1: Description of the shale ratings (R) using Franklin's (1981) shale ratings (1-9) according to simple index tests and their degree of weathering which are based on literature and the results presented in Chapter 8.

Shale rating (R)			
Description	1-3	4-5	6-9
Degree of weathering	Highly weathered and clay shales	Moderately weathered	Fresh to slightly weathered
Atterberg limit (LL; PI)	LL >55; PI>26	LL: 55-34; PI: 26-16	LL: <34; PI: <16
Slake durability index (SDI) (%)	SDI < 60	SDI 60-88	SDI > 88
Jar slake index	< 3	3-4	5-6
Point Load Strength (MPa)	< 1	1-2.5	> 2.5

9.2.2 Rating system based on geochemical data using shales of the Pietermaritzburg Formation

During weathering, shales weather to form a fine grained mass of soil as stated by Hopkins (1988). While weathering degrades the shale rock material into a soil mass, it undergoes an overall reduction in its shear strength (Cripps and Taylor, 1981; Bell *et al*., 2006). Franklin's (1981) shale rating chart which is based on using simple index tests to determine the shear strength of shales does not account for geochemical analyses. Thus, Franklin's (1981) shale rating chart was modified using the geochemical analyses that are presented in Chapter 8 to incorporate the mineralogy of the shale samples which is based on the quartz content and the clay content.

Figure 9.1a shows Franklin's (1981) original shale rating chart which was used to predict the shear strength properties ($c' \ \& \ \varphi'$) of shales using simple index tests for the construction of embankments. Figure 9.1b shows the modification of Franklin's (1981) shale rating chart which incorporates the geochemical data to rate shales using the clay content and the quartz content. A major benefit of

incorporating the geochemical data is that shales suffer from a loss of shear strength as weathering alters this material into a fine grained mass of soil.

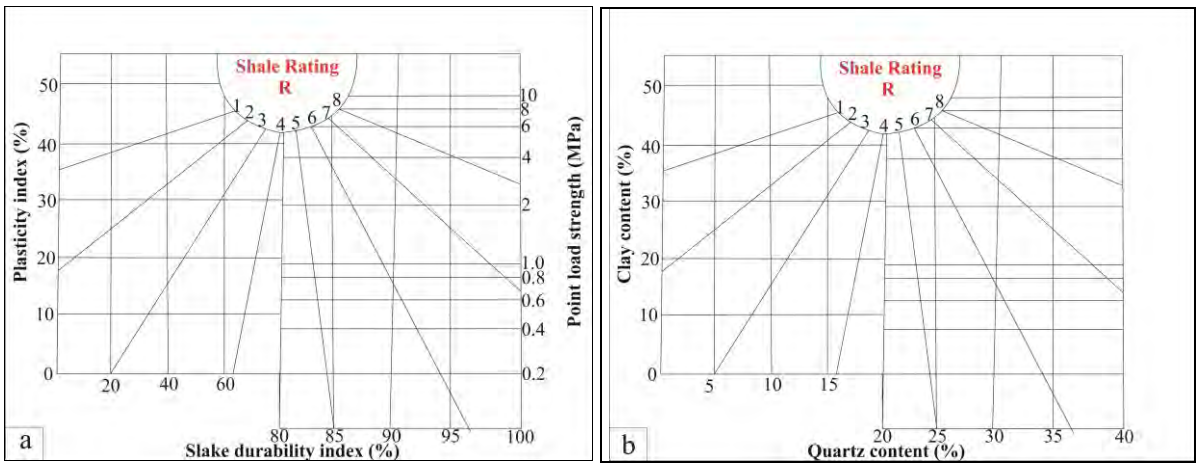

Figure 9.1: Rating system based on the chemical composition of the shale material (modified after Franklin, 1981); a: Franklin's (1981) original shale rating chart, and b: modified version of Franklin's 1981) shale rating chart.

As a result of the degradable nature of shales, it seems appropriate for the less durable shales to have a lower shale rating (R) as compared to the durable shales which should have a higher shale rating. Figure 9.1b shows that the shale ratings which are used to describe the shale material decreases with an increase in the clay mineralogy and a decrease in the quartz content. For example, weathered shales that contain a high clay content are expected to have a low quartz content and will plot towards the left of Figure 9.1.b therefore these materials will have a shale rating of less than 4. Comparatively, shales that have a low clay content are expected to have a high quartz content and will plot towards the right hand side of Figure 9.1b thus having a shale rating that is greater than 4. Therefore, using Table 9.1, shales which have a shale rating of less than 4 are considered to be highly weathered and very weak.

The geochemical analyses of the shale material from the Cornubia development in Chapter 8, showed an increase in the clay content from the fresh and weathered material to support the modification of Franklin's (1981) shale rating chart. The weathered shale material sampled from the Cornubia development contained a higher clay content than the fresh material and further displayed a lower Point Load Strength and slake durability index to the shale samples from Localities 2, 3 and 4 within the Pietermaritzburg area and will be discussed in future sections in this chapter.

9.2.3 Shale rating system based on geotechnical data

Previously, all proposed methods of rating shales such as by Lutton (1977), Franklin (1981) and Santi and Rice (1991) focused on the index properties of the soil and rock material. In particular, Franklin (1981) grouped and assigned shale ratings according to the quality of shales which were based on the

plasticity index, the slake durability index and the Point Load Strength. However, Franklin (1981) did not use the jar slake test as part of the rating system despite the jar slake test being a simple, cost effective and quick test to perform. The jar slake test was incorporated into Franklin's (1981) shale rating chart to provide an additional test to better characterise the shale materials and the results that were used to incorporate the jar slake test were obtained from Chapter 8 and from the relevant literature (e.g. Hopkins and Beckham, 1998). For example, using Figure 9.2, a high jar slake index (6) will correlate well with a high slake durability index (SDI = 95 %) and Point Load Strength (2.5 MPa) and this will produce a shale rating of 6-9. Conversely, a low jar slake index (2) will correlate well with a low slake durability index (SDI = 40) and low plasticity index (< 20) and will result in a shale rating of 1-3.

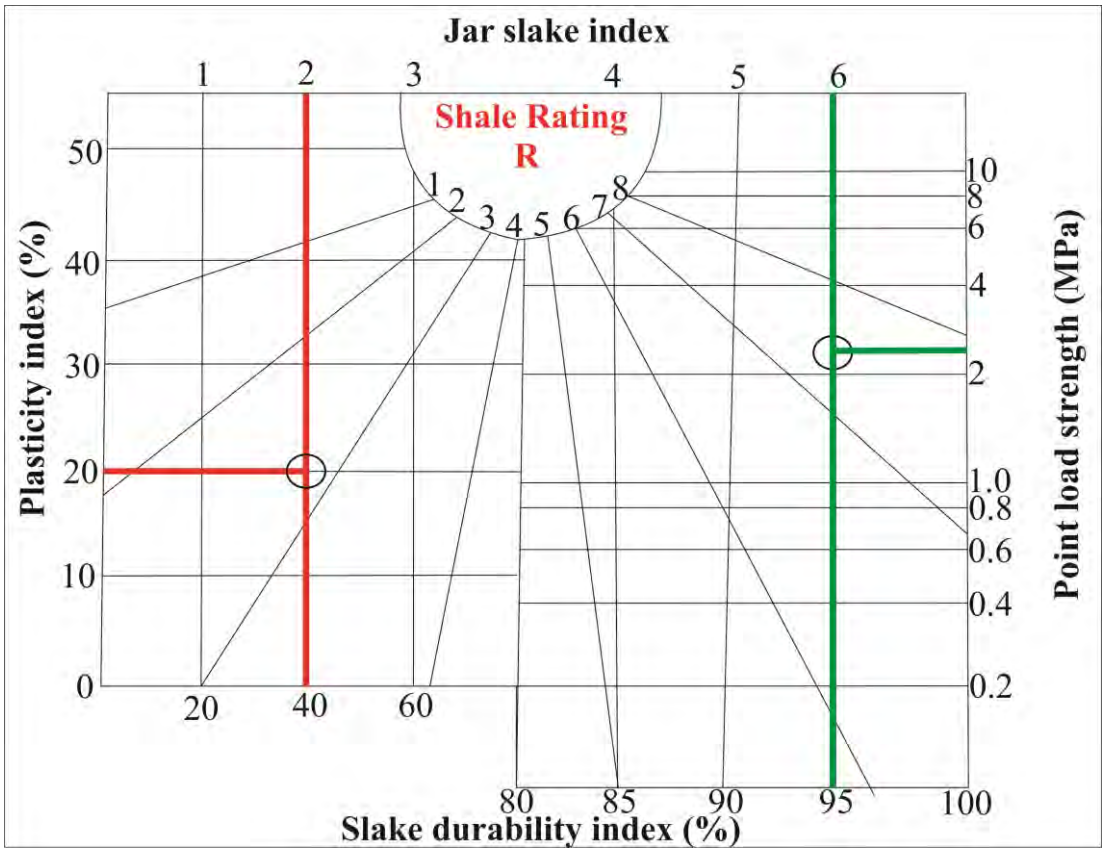

Figure 9.2: Shale rating chart as a function of the Plasticity Index, Jar Slake index, Slake Durability and the Point Load Strength (modified after Franklin, 1981).

9.2.4 Ratings based on integrating the geotechnical tests, the geochemical analyses of the shale materials and settlement

The settlement of embankment fills are often very difficult to predict because they are affected by a variety of factors such as the moisture content, depth to water table, the slope angle, volume and height of the embankment and by the degree of compaction (Hopkins, 1988; Hopkins and Beckham, 1998; Lenke, 2006; Geng and Dou, 2012). An attempt was made to incorporate the settlement

predictions into Franklin's (1981) shale rating chart using the settlement monitoring that was performed at the Cornubia development. Despite the difficulties that were experienced during the monitoring of settlement at the Cornubia development such as the continual peg destruction, these results were combined with results from the literature such as the results obtained by Hopkins and Beckham (1998) on the monitoring of testing fill stations comprising shales to provide an estimation of the potential settlement when using a shale of a certain quality. The modified rating system as shown in Figure 9.3, combines the geochemical data i.e. the clay content, the jar slake test and the slake durability test to provide an estimation of the potential settlement for a shale material of a certain quality. For example, if a shale sample contains 18 % clay minerals, a jar slake index of 5 and has an SDI of 90 %, the potential settlement can be estimated by constructing a horizontal line from the point of intersection from the test data to the settlement axis as shown in Figure 9.3.

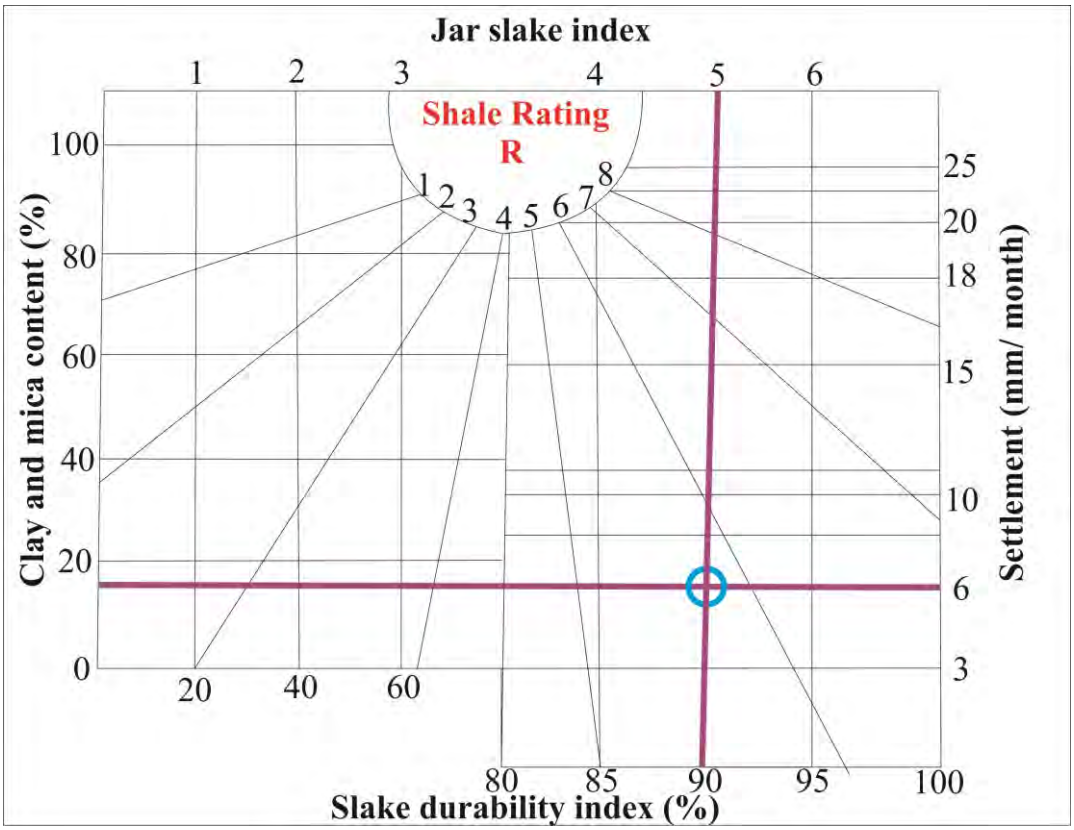

Figure 9.3: Shale rating chart based on slake durability tests, X-ray diffraction tests and the settlement.

Using the shale ratings that are obtained from Figure 9.1 - Figure 9.3, it is possible to determine the effective shear strength parameters (c′ & φ′) of a shale material using Figure 9.4. Figure 9.4 presents the second part of Franklin's (1981) shale rating chart which is used to predict the shear strength parameters of shales, particularly for the construction of well compacted embankments. Franklin (1981) stated that after a shale rating (R) is obtained, the shear strength parameters of well compacted embankments should be obtained from "area one" as depicted in Figure 9.4. This chart essentially

indicates that as the shale rating increases, the shale fill that is used in an embankment becomes progressively more frictional (i.e. the effective friction angle increases), until at high ratings, the shale behaves as a granular fill with limited cohesion and with an angle of friction that is greater than 25 °.

Although Figure 9.4 provides a method of estimating the effective shear strength parameters of shales, it is ambiguous as it provides a range of the effective cohesion rather than a single value. An example of this limitation using a shale rating of 6 is shown in Figure 9.4. This shows that the estimated c′ value can range from 60 - 90 kPa (the shaded area represents Franklin's chart without any modifications thus showing the estimated range of c′ values). Thus, Franklin (1981) stated that "Area 1" should be used for well compacted embankments to determine the shear strength properties of shales as it is expected that a mixture of fresh and weathered shale materials will be used. In comparison, "Area 2" should be used to predict the shear strength of very fresh shales that are expected to have a smaller percentage of fine materials thus expected to have a higher friction angle.

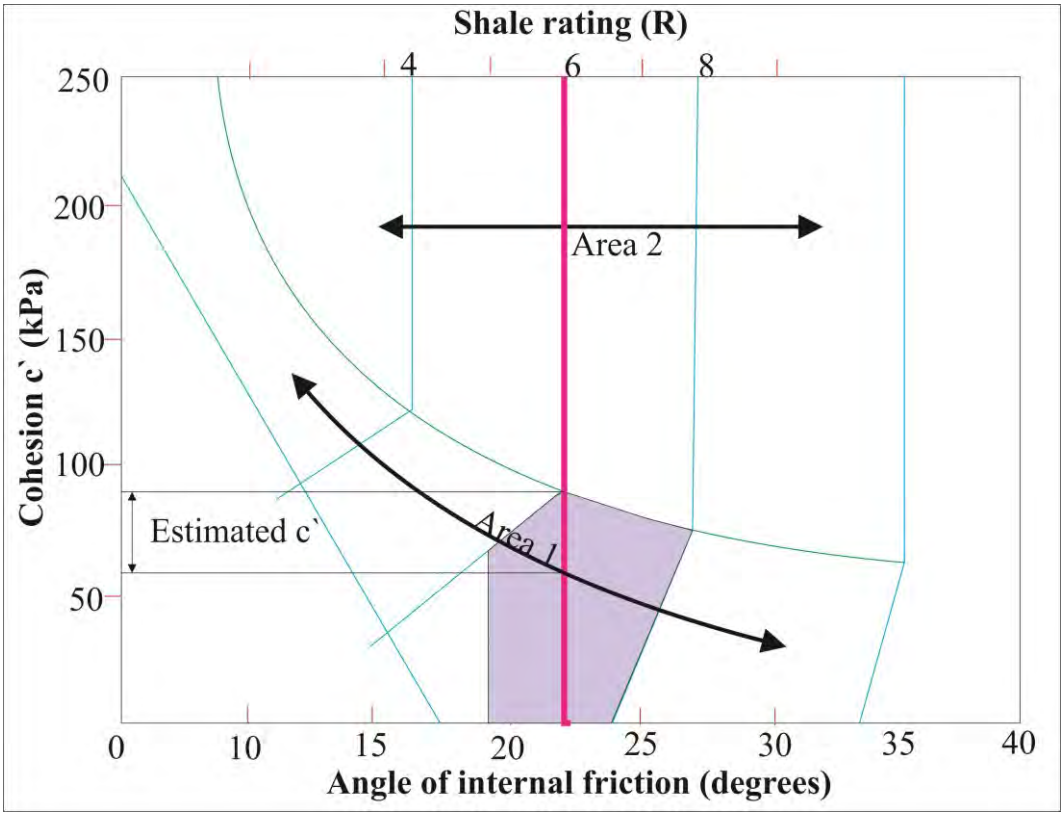

Figure 9.4: Shale rating chart that shows the trends in the shear strength parameters of compacted shales (modified after Franklin, 1981).

9.3 The development of a simple shale rating system to be used by geotechnical engineers.

The previous sections focused on the addition of the results from the geochemical analyses and the geotechnical tests such as the jar slake test to modify Franklin's (1981) shale rating chart. Additionally, the proposed modified shale rating chart further incorporates an aspect of estimating the

settlement of shales of a particular rating (R). Franklin's shale ratings from 1-9 make using the shale rating chart complicated because the geotechnical data sometimes plots between two ratings thus making it very difficult to obtain the shear strength parameters (c′ & φ′) using Figure 9.4.

Thus, Franklin's (1981) shale rating chart of using simple index tests was adopted and modified to include the jar slake test to provide an additional test to rate shales. Additionally, this study modified Franklin's (1981) shale ratings from 1-9 to 1-3 as it serves a simpler and easier method for the characterisation of shales. The fewer shale ratings caters for a broader range, which better mimics the geotechnical and geochemical properties of shales during weathering. The modified method also provides an estimation of the shear strength parameters for a particular shale rating and reduces the time spent and costs endured by companies on performing large scale shear box tests on shales to determine their shear strength properties. It is hoped that such a rating system will serve as an easier and faster method for the characterisation of shales especially for geotechnical engineers. Figure 9.5 presents the 3 broader shale ratings instead of the 9 shale ratings, and further incorporates the jar slake index into Franklin's (1981) shale rating chart.

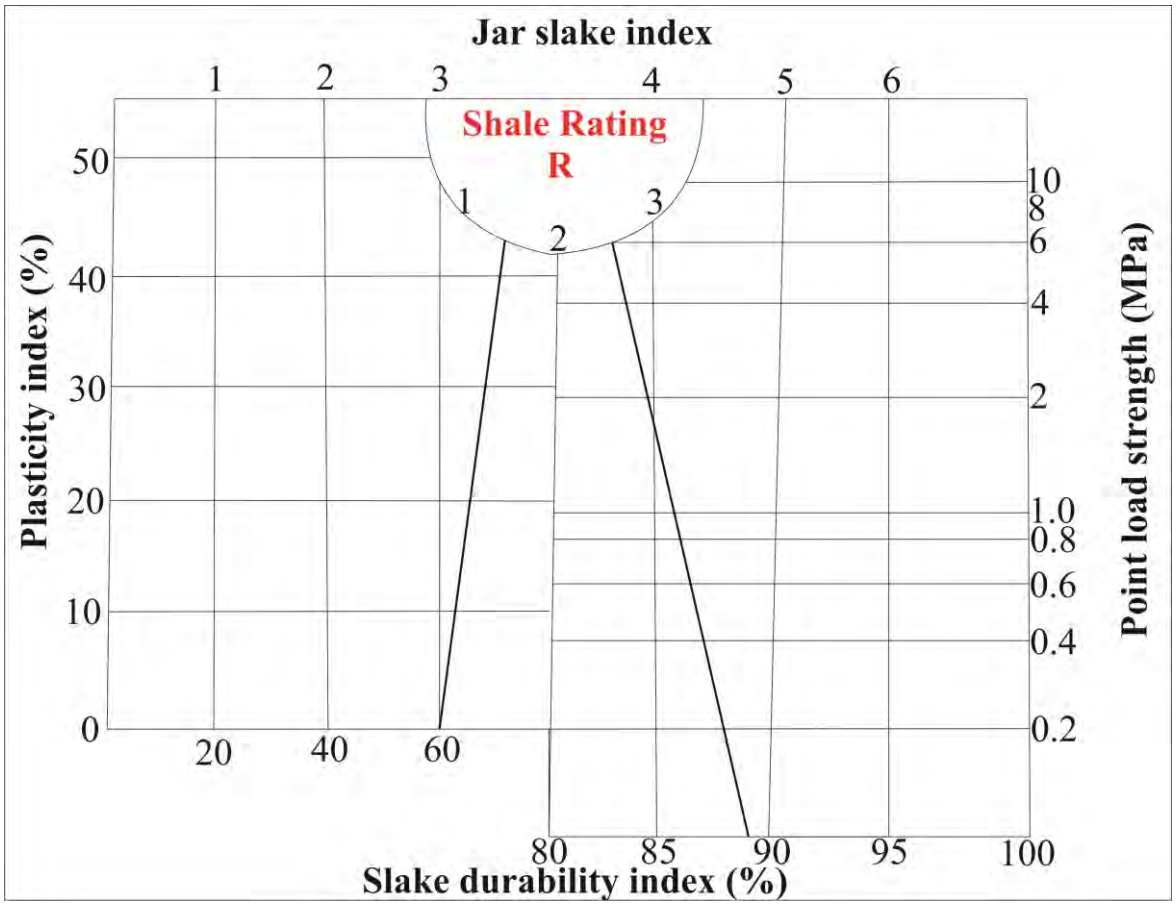

Figure 9.5: Broader groups for rating shales based on the Plasticity Index, the slake durability index, the jar slake test and the Point Load Strength test (modified after Franklin, 1981).

The shale ratings from 1-3 were based on the laboratory results that are presented in Chapter 8 and from the results from various researchers as listed in Table 9.2. The shale rating of 1 was given to highly weathered shale materials and is characterised by an SDI of less than 60 % and a jar slake index of less than 3. These materials would represent the residual clays and gravel material which have formed from the progressive weathering of the shale rocklike material. On the other hand, the shale rating of 3 is given to shale materials with an SDI which is greater than 88 % and a jar slake index greater than 4. These materials will represent the *in-situ* fresh shale materials. The shale rating of 2 refers to shales that often behave between R1 and R3 which is in response to their reaction to the physical environment and exhibit a variation in their geotechnical properties. This means that depending on their exposure to the environment, the prevailing environmental conditions such as high rainfall and the amount of vegetation present, shales will be subjected to varying degrees of weathering and by an expected change in their geotechnical properties. The broader shale rating of 2 also caters for shales which have high slake durability indices but are difficult to predict their shear strength parameters when used in a fill embankment (see Table 9.4). The shale rating of 2 is a suitable representation when shales are used in the construction environment as shale materials that are used comprise a mixture of soil and rocklike (granular) material thus having a variation in their engineering properties.

As a result of the limited information that is available on shales of the Pietermaritzburg Formation, Table 9.2 presents a compilation of a range of geochemical and geotechnical properties of shales from the literature whilst Table 9.3 presents a summarised version of the laboratory results from Chapter 8. After a geotechnical engineer has conducted the various index tests (such as the Atterberg limits, slake durability test, jar slake test) on shales to obtain the index values, the geotechnical engineer should then compare their results with the values in Table 9.4 to determine the rating (e.g. R1/ R2/ R3). For example, shales which display an SDI of 80 %, an I_j of 4 and a Point Load Strength of 2 MPa will be awarded a shale rating of 2. Thereafter, Table 9.5 provides an estimation of the effective shear strength parameters of a shale material which is based on the shale rating (R1/ R2/ R3) from Table 9.4. The range of c' and φ' have been grouped according to the laboratory results presented in Chapter 8 and from a literature search by authors such as Underwood (1967); Cripps and Taylor (1981); Wilson (1983); Hopkins (1988); Bell and Maud (1996; 1997); Hopkins and Beckham (1998); Hajdarwish and Shakoor (2006); Drennan, Maud and Partners (2010); Aghamelu *et al.* (2010) and Toniolo (2012).

Table 9.2: Geochemical and geotechnical information on shales compiled from the literature to support the shale rating chart.

Author(s)	Clay mineralogy	Atterberg limit (%)	SDI (%)	Point Load Strength (MPa)		Shear strength parameters		Settlement (%)
				Ax	Dia	Cohesion (kPa)	Friction angle	
Underwood (1967)	Montmorillonite, illite, kaolinite,	-	-	-	-	35-10500	10-65°	-
* Wilson (1983)	Illite, chlorite	-	-	-	-	-	15-25°	-
Hopkins and Beckham (1998)	-	PL: 1-18 LL: 19-40	1-99	-	-	1-56.8	22.7-45°	0.4-0.9
* Bell and Maud (1996; 1997)	Illite, chlorite	PL: 18-35; LL: 25-70	-	-	-	0	16.6°	-
Bell *et al.* (1997)	Kaolinite, illite	PL: 12-25 LL: 27-41	80-96		1.22-2.59	0.09-0.37	-	-
* Drennan, Maud and Partners (2010)	-	-	-	-	-	10-23	13-28°	0.5-2%: gravelly clays, 2-4%:fat clays
Aghamelu *et al.* (2010)	-	PL: 17-26 LL: 53-65	-	-	-	48-55	23-31°	-
* Toniolo (2012)	Kaolinite, illite	-	91.5-99	1.86-7.33	0.70-5.30	-	-	-

* Shales of the Pietermaritzburg Formation.

Table 9.3: Summary of the Laboratory results which are presented in Chapter 8.

Test		**Locality 1**		**Locality 2**		**Locality 3**		**Locality 4**	
		F	W	F	W	F	W	F	W
	Soil material								
Atterberg limit		LL: 33-40 , PL: 20-25, PI: 14		-		LL: 22-30, PL: 15-23, PI: 19		-	
Rock material									
Jar slake		5-6	4-6	6	6	5-6	5-6	6	5-6
SDI	W	93-97	91.-95	95-98	91-97	94-98	92-97	95-97	94-98
	F	95-99	87.-91	96-98	92-97	95-98	94-98	96-98	96-98
Point Load Strength	Ax	3.06–3.3	1.33-1.64	-	-	3.00-4.11	1.48-1.67	-	-
	Dia	2.0-2.62	0.95-1.10	-	-	2.61-3.43	1.0–1.18	-	-
Shear box	c′	51	30	21.5	-	38	71	9.7	-
	φ′	36°	32.2°	37°	-	33°	34.4°	39°	-

F: Fresh, W: Weathered; W.: Water; EG: Ethylene glycol; Ax: Axial tests, Dia: Diametrical tests.

Table 9.4: Using simple index test results from the literature to characterise the shale material according to shale ratings.

Shale Rating (R)				
Index test		R1	R2	R3
Atterberg limit	Liquid limit	>55	55-34	<34
	Plastic limit	>26	26-16	<16
	Plasticity index	>29	29-18	<18
Jar slake (I_j)		<3	3-4	5-6
Slake durability (SDI) (%)		< 60	60-88	> 88
Point Load Strength (MPa)		< 1	1-2.5	> 2.5

Table 9.5: Using shale ratings (R) to predict the shear strength of shales and associated settlement.

Shale Rating (R)			
	1	**2**	**3**
Description	Highly weathered	Moderately weathered	Fresh to slightly weathered
φ′	< 19°	19 - 33°	> 33°
c′ (kPa)	0-4	5-19	> 19
Settlement (%)	> 3 (< 5 years)	1.1-3 (5 years)	< 1.1 (5 years)
Mineralogy (%)	Quartz content: < 30, Clay minerals: > 40	Quartz content: 30-60, Clay minerals: 30-60	Clay minerals: < 30, Quartz content: > 40

In the event of using shales as fill material, a prediction of the estimated settlement is also provided in Table 9.5. The estimated range of settlement values that are presented in Table 9.5 have been determined from the monitoring of settlement of the shale platforms from the Cornubia development and from the available literature (e.g. NAVFAC, 1982; Hopkins and Beckham, 1998). All values presented below are reasonable estimates particularly when using shales of the Pietermaritzburg Formation.

In the design of slopes for highway shale embankments, Hopkins and Beckham (1998) stated that a knowledge of the effective stress parameters (c′ & φ′) is essential to determine the stability of slopes. In addition, the long term durability of shales is one of the basic requirements for the design of shale embankments (Hopkins and Beckham, 1998). For example, shales that are classified as hard and durable (SDI > 90; I_j = 6) can be used as rockfill (Hopkins and Beckham, 1998). However, intermediate shales which are classified as hard and non-durable (50 < SDI < 90; I_j = 3-5) are difficult to compact and require heavy machinery (Hopkins and Beckham, 1998). Thus, a variation of shear strength parameters are used during slope stability studies to determine the stability of a slope. Using the shear strength parameters of R2 shale rating as an example, a best case scenario (c′ = 19 kPa & φ′ = 33°) should be used in conjunction with the worst case scenario (c′ = 5 kPa & φ′ = 19°) to perform the slope stability analyses. Furthermore, the average shear strength values should be used (c′ = 12 kPa & φ′ = 26) as this would account for the variability in material properties.

Franklin (1981) stated that a maximum friction angle of 35° should be used for slopes that are 10-15 metres in height. Smaller embankments composed of shales of 5-10 metres in height are usually designed to have flatter slopes so that these embankments can be easily maintained. However, the slope angle is reduced (i.e. < 35°) for embankments that are greater than 15 metres to ensure that acceptable safety factors are reached hence reflecting the growing importance of embankment stability (Franklin, 1981). However, the design of high shale embankments requires the use of shale materials which have an R3 shale rating as defined in Table 9.5

The laboratory results presented in Chapter 8 support the "R3" shale rating with the exception of the φ′ of the weathered material from the Cornubia development and c′ of the fresh material from Locality 4, whilst the "R1" and "R2" rating were deduced from the literature. The largest range of cohesion values (as shown in Table 9.4) for the shale rating of 2 as compared to the shale rating of 1 or 3 were chosen because the shale rating of 2 is representative of the behaviour of shales which are used in the field environment. Engineers rarely encounter very fresh and competent shale material and if fresh shale samples are used, these materials will weather easily when exposed to the physical environment hence the narrow range in the shear strength parameters of R3. Also**,** they will not use highly weathered shale materials as shales sometimes weather to a fine grained mass (R1). An estimation on the clay content and quartz content is provided in Table 9.3. It is expected that highly weathered shales would have a high percentage of clay minerals and a low percentage of quartz whilst fresh rocklike shales is expected to have a high quartz content and low clay content.

9.3.1 Testing the validity of the modified rating system

The results obtained from the index tests which were performed on the shale samples from the different localities in this study were used to test the validity of the modified rating system. This was done in order to validate whether the shear strength parameters obtained from the laboratory testing are within the range of values of the predicted shear strength parameters based on the rating system. Firstly, using Figure 9.6, the index properties were used to determine the rating of the shale samples from the different localities. For example, the SDI was used in conjunction with the I_j values and Point Load Strength results of the shale materials from Localities 1 and 3 whilst the SDI and the I_j values were used from Localities 2 and 4 to determine the shale rating R using Figure 9.6. The Atterberg limit results from Localities 1 and 3 were not used as the SDI of the shale samples is greater than 80 % as suggested by Franklin (1981). Thereafter, the predicted shear strength values of a particular shale rating that is presented in Table 9.5 was compared to the shear box results from Chapter 8 which are summarised in Table 9.6.

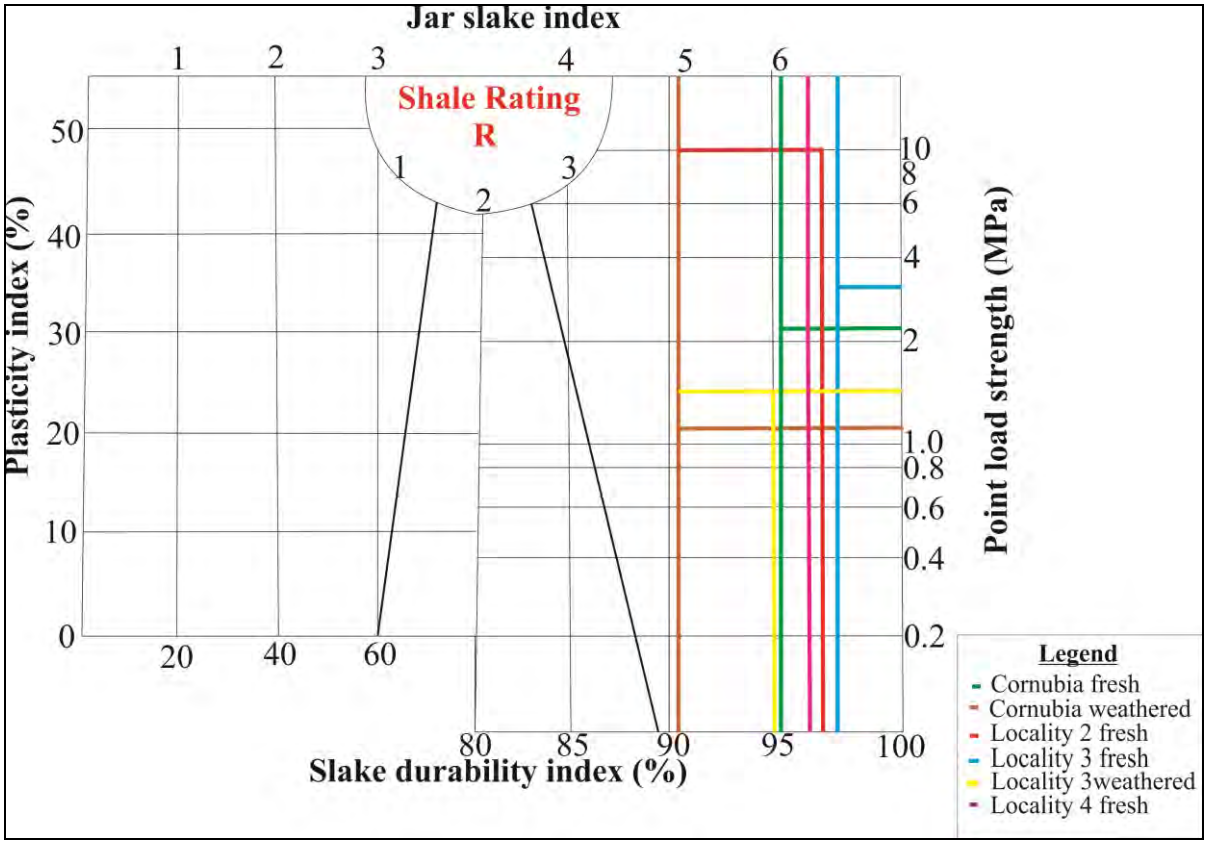

Figure 9.6: Predicting the shale rating of the shales from the four sampling sites.

Table 9.6: Using the geotechnical properties of the shale material from each locality to obtain a shale rating to determine whether the shear box results matches the shear strength parameters presented in Table 8.5.

	Locality 1			Locality 2	Locality 3			Locality 4
	Fresh	Weathered	Mixture	Fresh	Fresh	Weathered	Mixture	Fresh
Rating	3	3	3	3	3	3	3	3
Shear box results	c′:51 φ′ : 36°	c′ : 30 φ′ : 32.2°	c′ : 48.1 φ′ : 34.7°	c′ : 21.5 φ′ : 37°	c′ : 38 φ′ : 33°	c′ : 71 φ′ : 34.4°	c′ : 51.3 φ′ : 33.4°	c′ : 9.7 φ′ : 39°
Table 8.5	c': >19 φ′:> 33°	c': >19 φ′: > 33°	c': >19 φ′: > 33°	c': >19 φ′: > 33°	c': >19 φ′: >33°	c': >19 φ′: > 33°	c': >19 φ′: > 33°	c': >19 φ′: > 33°
Validity	Yes for c′ & φ′	Yes for c′ No for φ′	Yes for c′ & φ′	Yes for c′ & φ′	Yes for c′ & φ′	Yes for c′ & φ′	Yes c′ & φ′	No for c′ Yes for φ′

Using Figure 9.6 and Table 9.4, the results show that the shale samples tested from the different localities are categorised as having a rating (R) of 3. The predicted values of c′ and φ′ using the modified shale rating chart were found to be similar or within the range of values that were obtained from the shear box tests as presented in Table 8.9 with the exception of the c′ value of the fresh shale samples from Locality 4, and the φ′ value of the weathered material from Locality 1. Thus, there is a slight difference between the predicted shear strength results using the modified shale rating system to

the shear box results. For example, there is a slight difference in φ′ between the predicted value of > 33° using the rating system to the shear box test result of 32.2° of the weathered shale sample from the Cornubia development. However, there is a large difference in the c′ value between the predicted value using the modified rating system and the shear box value of the fresh shale sample from Locality 4. Since index tests were not done on the mixture of the shale samples from Localities 1 and 3, the results obtained using Table 9.5 showed that the predicted shear strength parameters are within the values that were obtained from the shear box tests for a shale rating of 3. It is expected that the mixture of the fresh and weathered shale samples From Localities 1 and 3 should represent the shale materials that are used in the construction environment and should have a shale rating of two. However, the results revealed that the "mixture" of the shale samples fall within a rating of 3 and could be due to the mixture of the shale sample containing more fresh shale materials than weathered shale materials. Thus, it is important to consider the current state of weathering of a shale sample as Cripps and Taylor (1981) stated that the greatest variation found in the engineering properties of mudrocks can be attributed to the effects of weathering. Although Hajdarwish and Shakoor (2006) revealed that there are strong correlations between the friction angle and mineralogy and between the cohesion and SDI of mudrocks respectively, this relationship was not observed by the shale samples in this study. This emphasises that a single lithological characteristic or engineering property cannot be used as an independent value to predict the shear strength property of shales or mudrocks and that there are a variety of factors to be considered.

In addition to rating the shale materials from each of the four localities, the geotechnical properties of the Kentucky shales from the Kentucky area in the U.S.A were subjected to the modified shale rating system. The index test results which include the Atterberg limits, the I_j values and SDI values were used to obtain a shale rating (R) for the Kentucky shales. Using the modified shale rating system as shown in Figure 9.7, a shale rating (R) of 2 and 3 was obtained for the Nancy and Drakes shales and, Hance shales from the Kentucky area respectively from the index test results. Thereafter, the estimated range of φ′ for a shale rating of 2 which are presented in Table 9.5 were similar to the φ′ values which were determined by Hopkins and Beckham (1998). However, the maximum values of c′ which were determined by Hopkins and Beckham (1998) were higher than the predicted values of c′ for a shale rating of 2 for the Nancy shales and Drakes shales which are shown in Table 9.5. Thus, the shale rating chart was successful in predicting the φ′ values for the Nancy and Drakes shale samples using the results from the index tests but the values for c′ were higher than the range of values that are presented in Table 9.5. Although the range of c′ for a rating of 2 as suggested by Table 9.5 was not sufficient for c′ for the Nancy and Drakes shales, a rating of 2 should be used to rate these shales, as it will cater for the variability in the material properties of the shales in general.

The results from the monitoring of settlement over 3 years which was undertaken at two shale fill test stations in the Kentucky area are presented in Table 9.7. Table 9.5 further provides an estimated percentage of settlement for a 5 year period of a particular shale rating when used for the construction of shale embankments. For example, the test fill station 498+50 in the Kentucky area settled approximately 0.9 % of its fill height over a 3 year period as shown in Table 9.7. Thus, if the monitoring peg was not destroyed at the test fill station in the Kentucky area and the settlement monitoring continued for a five year period, the amount of settlement could have increased therefore falling into the shale rating of 2 as proposed in Table 9.5. Furthermore, there is a small difference between the predicted amount of settlement for a shale rating of 2 (1-1.3 %) as shown in Table 9.5 to the measured amount of settlement from the test fill stations (0.5-0.9 %) as shown in Table 9.7.

Table 9.7: The geotechnical properties that were used to obtain a shale rating for the Kentucky shales (modified after Hopkins and Beckham (1998).

	Plasticity index	Jar slake index	SDI	Measured shear strength parameters		Shale rating	Predicted shear strength parameters	
				c′	φ′		c′	φ′
Unweathered Kentucky shales								
Drakes	7	4	65	9.62-53.3	26.8-32.6°	2	5-19	19-33°
Hance	5	5	93	23.9-87.8	25.9-31.7°	3	> 19	>33°
Nancy	9	3	62	10-46.2	25.5-29.5°	2	5-19	19-33°
Settlement (using Kentucky shales)								
Test station no.	Fill height (mm)		Settlement (3 years)				Settlement prediction from Table 9.5 for R2	
			Measured (mm)		%			
498+50	19180		120-170		0.9		1.1-3 (5 years)	
317+50	15240		70-80		0.5		1.1-3 (5 years)	

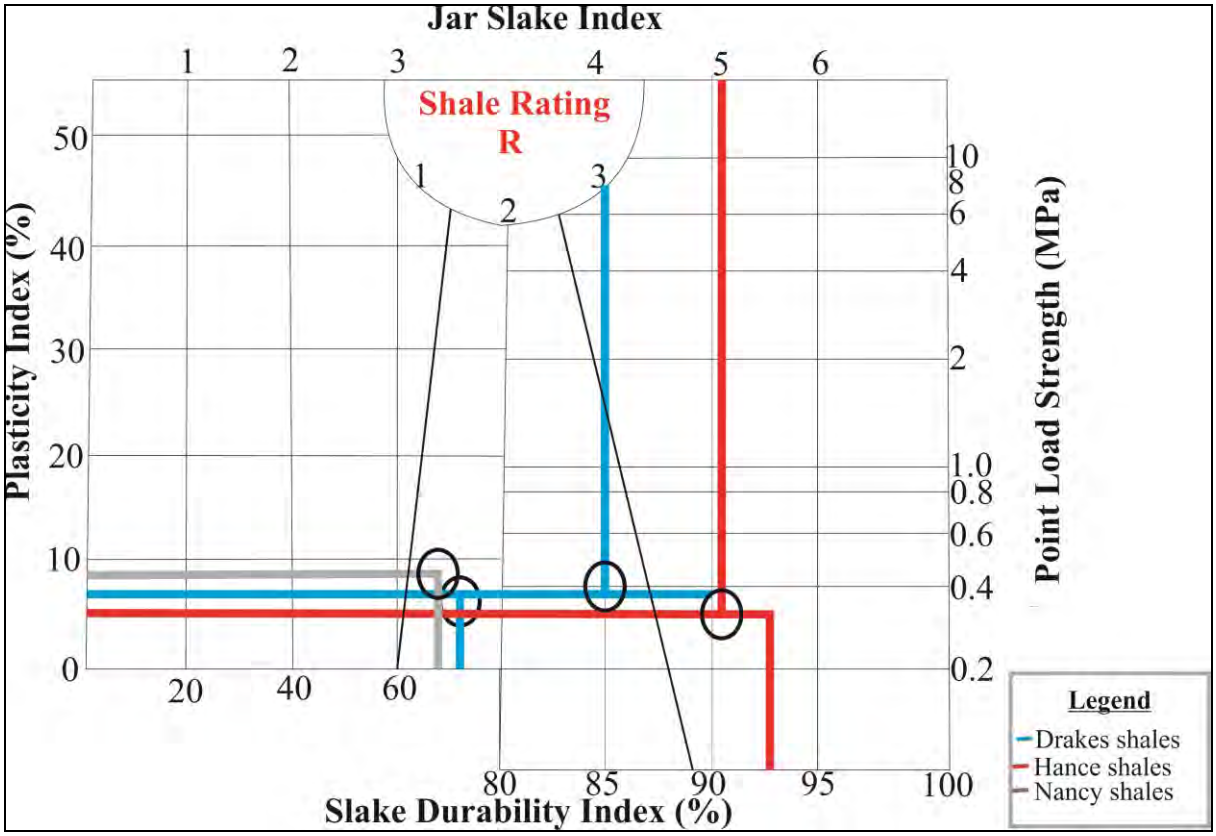

Figure 9.7: Testing the proposed field rating system for engineers on shales and mudrocks.

9.4 Limitations of the proposed shale rating system

The modified shale rating chart presented in Figure 9.7 showed that occasionally it is not possible to get a single point of intersection of three geotechnical tests. For example, a shale rating of 2 was given to the Drakes shale sample from Kentucky as presented in Figure 9.7 despite that the 3 geotechnical tests which were used did not intersect at a single point as a result of three tests being used. To avoid the problem of obtaining two shale ratings for a particular sample, the Atterberg limits test should only be used if the slake durability index of a shale material is less than 80 % as suggested by Franklin (1981) whilst the Point Load Strength test should be used to rate shales if the slake durability index is greater than 80 %.

It is important to remember that the proposed rating system provides a simple and cost effective way of indirectly predicting the shear strength properties of shales. In addition, it would be necessary to consider the current state of weathering of shales in relation to the predicted values of the shear strength parameters and also the proportion of fresh to weathered materials. For example, the results obtained from the shear box test for the mixture of the fresh and weathered material from Locality 3 displays c′ and φ′ values which are in between the shear box results of the fresh and weathered shale samples respectively.

9.5 Summary

This chapter presented a modification of Franklin's (1981) shale rating chart that is used to predict the shear strength parameters of shales. As part of the modifications, the geochemical analyses were combined with the geotechnical properties and integrated into the modified shale rating system. In addition, the laboratory results which were presented in Chapter 8 were combined with an extensive literature research to produce three shale ratings (R1, R2 & R3) instead of nine which makes it easier to categorise shales. Furthermore, the modified shale rating system provides a method of estimating the associated settlement for shales of a particular quality. By subjecting the shale rating system to the shale samples from each locality, the laboratory results and the shale ratings that were obtained from the shale rating chart support the "R3" rating. The next chapter presents a summary of the main findings of this dissertation and highlights the need for further research.

Chapter 10

Conclusion

10.1 Introduction

The objective of this study was to undertake a multidisciplinary method of indirectly determining the shear strength properties of shales. During the course of this research, laboratory tests were done to determine the geochemical and geotechnical properties of shales of the Pietermaritzburg Formation. The outcome of these tests has led to the development of a modified method of predicting the shear strength of shales using shales of the Pietermaritzburg Formation as a case study which involves using simple index test and associated settlement. Furthermore, the validity of the proposed rating system was verified with values obtained previously from the literature. This chapter presents the main findings of this dissertation and highlights the possibilities for further research.

The main findings of this study are:

a) The Pietermaritzburg Formation is exposed in many areas in the Durban and Pietermaritzburg area. The shale beds of the Pietermaritzburg Formation dip between 8-15 ° in these two areas and have random joint orientations. The sampling of shale material to obtain representative samples to conduct laboratory testing was difficult as they break down very easily during the sampling process due to the high fissility. The sampling sites were chosen because they were easily accessible.

b) Field monitoring of settlement was done at the Cornubia development on shale fills to determine the amount of settlement over a particular time period using the precise levelling surveying technique. The settlement analyses showed that very little settlement occurred in the absence of rain. However during the rainy season, there was much more settlement. The monitoring of settlement thus showed that the settlement of these shale platforms during the monitoring period were within an acceptable range, that is, the average settlement of each platform was less than 1 % of the fill height.

c) Geochemical analyses using the X-ray diffraction technique was performed on shale materials from each sampling site to determine the minerals that are found in each sample. These analyses revealed that the dominant non-clay minerals are quartz and muscovite mica and that the dominant clay mineral that was observed in each sample is illite.

d) A geotechnical investigation that involved using simple index tests such as the particle size distribution analysis, the Atterberg limits, the jar slake test, the slake durability test, the Point

Load Strength test and the large scale shear box test were performed to determine the geotechnical properties of the shale materials from each locality. The particle size analyses showed that the residual soil is characterised as a clayey SAND and has a very small percentage of clay materials. The Atterberg limits test showed that the soil material from the Cornubia development has a higher plasticity index than soil material from Locality 2 from the Pietermaritzburg area.

Slaking tests comprising the jar slake test and the slake durability test were performed on the fresh and weathered shale samples from each locality to determine its resistance to weathering. The results of the jar slake tests showed that there was no observable reaction of samples analysed, with the exception of the weathered material from the Cornubia development. Similarly, the slake durability tests showed that the fresh and weathered material from each locality are characterised as hard and durable shales and have high slake durability indices. However, the weathered material from the Cornubia development had the lowest slake durability index from all 4 localities when slaked in ethylene glycol.

The Point Load Strength test was done to determine the Point Load Strength of the shale samples from Localities 1 and 3. It was only possible to obtain core samples for the Point Load Strength test from Localities 1 and 3 because they began to disintegrate very easily during the coring process. In addition to the slake durability results, the fresh and weathered shale material showed a lower Point Load Strength than shale samples from Locality 3 in the Pietermaritzburg area. Furthermore, the axial tests showed a higher Point Load Strength than the diametrical tests which is consistent with the literature.

Unconsolidated undrained large scale shear box tests were done at the University of Witwatersrand using an in-house modified shear box apparatus to determine the shear strength parameters of the shale materials from each of the respective localities. The shear box test results showed that the shale materials have high shear strength properties (i.e. high effective cohesion and effective angle of friction). The weathered shale samples from the Cornubia development followed a similar trend and has the lowest effective angle of friction as compared to the other samples tested.

Based on the results obtained, the fresh and weathered shales of the Pietermaritzburg Formation are highly durable and are characterised as being a hard rock.

e) The shale rating chart developed by Franklin (1981) was modified using the results that were presented in Chapter 8 and from an extensive literature review on previous work done on shales.

The shale rating chart uses the geochemical analyses and simple index tests such as the Atterberg limits, slake durability index and the jar slake index to indirectly predict the shear strength properties of shales. The modified system focuses on three broad shale rating instead of Franklin's (1981) shale rating chart which contains nine ratings and provides a table that denotes a range of shear strength parameters for a particular shale rating. Shales of the Pietermaritzburg Formation was used as a case study to design this rating system. The results of the laboratory tests performed on shales of the Pietermaritzburg area which was used for this study supports the "R3" groupings of the rating system with the exception of c′ for the fresh shale samples from Locality 4 and, φ′ of the weathered material from Locality 1. The broader groupings of the modified shale rating chart reduces the time spent on performing lengthy tests by geotechnical engineers in the construction industry as they are often bound by financial limitations and time constraints.

10.2 Further studies

This dissertation focused on the nature of shales and their geochemical and geotechnical properties. As a result, the recommendations listed below will be of great interest as this rating system is a work in progress and improvements are recommended:

i) As a result of the numerous problems which were encountered during sampling, a new method of sampling should be adopted. This would ensure that more representative samples of shale can be obtained for laboratory testing. Furthermore, it would be beneficial to conduct more than one shear box test and to test shale samples which contain different proportions of fresh and weathered material.

ii) Further research should be continued into selecting more sites and less durable shales of the Pietermaritzburg Formation to further this research to confirm the "R1" and "R2" groupings.

iii) Possible future research can be undertaken to determine the geotechnical and geochemical behaviour of siltstones and shales of the Dwyka Group. Furthering this research will be beneficial as it enables geotechnical engineers to easily classify/ rate argillaceous materials.

iv) In addition to shales; claystones, mudstones and siltstones should be tested and used to create a robust rating system.

Shales of the Pietermaritzburg Formation are competent when not exposed to the physical environment but degrades easily when exposed to water. Continuing this research based on the above recommendations would make this rating system more robust and applicable to a wider range of

degradable materials and further research will be beneficial to geotechnical engineers in the construction environment and to future researchers (academics).

References

Agbede, I.O. & Smart, P., (2007). Geotechnical properties of Makurdi shale and effects on foundations. *Nigerian Journal of Technology*, Vol. 26, pp. 63-73.

Aghamelu, P.O., Nnabo, P.N. & Ezeh, H.N., (2010). Geotechnical and Environmental problems related to shales in the Abakaliki area, South-eastern Nigeria, *African Journal of Environmental Science and Technology*. Vol. 5, 2, pp. 80-88.

Alexander, N., (2012). Techniques used to conduct shear box tests. [conversation] (Personal communication, June 2014).

American Society for testing and materials (ASTM), (2010). In ASTM, Book of standards.

Anderson, A.M. & McLachlan, I.R., (1976). The plant record in the Dwyka and Ecca Series (Permian) of the southwestern half of the Great Karoo Basin, South Africa. *Palaeontology of Africa*, 19, pp .31-42.

Andrews, D.E., Withiam, J.L., Perry, E.F. & Crouse, H.L., (1980). Environmental effects of slaking of surface mine spoils: Eastern and Central United States. Final report, U.S. Department of the Interior, Bureau of Mines, Denver.

Anon, (1977). Working partly report on the description of rock masses for engineering purposes. The Engineering Group of the Geological Society. *Quarterly Journal of Engineering Geology.* London. pp. 355-388.

Assaad, F.A., Lamoreaux, P.E. & Hughes, T.H., (2004). Field methods for geologists and hydrogeologists. Springer-Verlag, Berlin, Heidelberg.

Atkinson, J.H. & Bransby, P.L., (1978). *The Mechanics of Soils: An introduction to critical state soil mechanics*, McGraw-Hill, London, England.

Attewell, P. & Farmer, I.W., (1976). *Principles of Engineering Geology*, Chapman and Hall, London, pp. 1045.

Barbour, T.G., Atkinson, R.H. & Ko, H.Y., (1979). Relationship of mechanical, index and mineralogical properties of coal measure rock. *20th Symposium on Rock Mechanics*, Austin, Texas, pp.189-198.

Bates, R.L. & Jackson, J.A., (1980). Glossary of geology, *American Geology Institute,* 2nd Edition, Falls Church, VA.

Bell, F.G., Entwisle, D.C. & Culshaw, M.G., 1996). A geotechnical survey of some British Coal Measures mudstones, with particular emphasis on durability, *Engineering geology*, Elsevier, 46, pp. 115-129.

Bell, F.G., (1978). The physical and mechanical properties of the fell sandstones, Northumberland, England. *Engineering Geology*, pp. 55-71.

Bell, F.G., (1993). Engineering Geology. Blackwell Scientific Publications, Oxford.

Bell, F.G., (2007). Engineering Geology. 3rd Edition. Oxford, Elsevier Ltd.

Bell, F.G. & Lindsay, P., (1998). Durability of shales of the Pietermaritzburg Formation, greater Durban area, South Africa. *Proceedings 8th Congress on International Association of Engineering Geology,* Vancouver, M. D.P. & Hungr, O. (Eds.), Balkema, A.A., Rotterdam, pp. 275-282.

Bell, F.G. & Maud, R.R., (1996). Examples of landslides associated with the Natal Group and Pietermaritzburg Formation in the greater Durban area of Natal, South Africa. *Bulletin of the International Association of Engineering Geology*, Paris, 53, pp. 11-20.

Bell, F.G. & Maud, R.R., (1997). Case histories of landslides in residual soils on the Pietermaritzburg Formation, Greater Durban area, South Africa. *Engineering Geology and the Environment.* pp. 519-524.

Bell, F.G. and Maud, R.R., (2000). Landslides associated with the Colluvial the Natal Group in the Greater Durban Region of Natal, South Africa. In: *Environmental Geology,* Vol. 39, Issue 9, Springer-Verlag, pp. 1029-1038.

Bhatia, M.R., (1985). Composition and classification of Paleozoic flysch mudrocks of eastern Australia: Implications in provenance and tectonic setting interpretation. *Sedimentary Geology*, 41, pp. 249-268.

Bieniawski, Z.T., (1975). The Point-load test in geotechnical practice, *Engineering Geology*, Vol. 9, Issue 1, pp. 1-11, Elsevier.

Birkeland, P.W., (1974). *Pedology, weathering, and geomorphological research*. New York, Oxford University Press, London.

Bishop, A.W., Green, G.E., Garga, V.K., Anderson, A. &Brown, J.D., (1971). A new ring shear apparatus and its application to the measurement of residual strength. *Geotechnique*, 21, pp. 273-329.

Bjerrum, L., (1967). Progressive failure in slopes of overconsolidated plastic clay and clay shales. *ASCE (Soil Mechanics and Foundations Division),* pp. 1-49.

Blatt, H., Middleton, G. & Murray, R.C., (1980). *Origin of Sedimentary Rocks.* Prentence-Hall Incorporated, New Jersey.

Blatt, H., (1982). *Sedimentary Petrology,* Freeman, New York.

Boggs, S. Jr., (2009). *Petrology of sedimentary rocks*. 2nd Edition, Cambridge University Press.

Brace, W.F., (1961). Dependence of fracture strength of rocks on grain size. *Proceedings of the 4th Symposium on Rock Mechanic.* University Park, Penn, pp. 99-103.

Brink, A.B.A., (1983). *Engineering Geology of Southern Africa.* The Karoo Sequence. Building Publications, Cape Town. Vol. 3.

Brink, A. B. A. (1985). *Engineering Geology of Southern Africa*, Vol. 4: Post-Gondwana Deposits, Building Publications, South Africa.

British Standards Institution, (1975). BS 1377, *Methods of test for soils for Civil Engineering Purposes.* B.S.I., London.

British Standards Institution, (1990). BS 1377, *Methods of test for soils for Civil Engineering Purposes.* B.S.I., London.

British Standards Institution, (1999). BS, 5930, *Code of Practice for Site Investigations*, British Standards Institution, London.

Broch, E., & Franklin, J.A., (1972). The Point-Load Strength test. *International Journal of Rock Mechanics and Mining Sciences,* Vol.9, pp. 669-697.

Broch, E., (1983). Estimation of strength isotropy using the Point-Load test. *International Journal of Rock Mechanics, Mining Sciences and Geomechanics Abstracts*. Vol. 20, No. 4, pp. 181-187.

Bryson, L.S., Gomez, I.C. & Hopkins, T.C., (2011). Correlations between Durability and Geotechnical Properties of compacted shales. Geo-Frontiers, *Advances in Geotechnical Engineering,* pp. 4109-4118.

Buhmann, C., (1992). Smectite-to-illite conversion in a geothermally and lithologically complex Permian sedimentary sequence, *Clays and Clay Minerals,* Vol. 40, pp. 53-64.

Burnett, A.D. & Fookes, P.G., (1974). A regional engineering geological study of the London Clay in the London and Hampshire Basins, Quarterly Journal of Engineering Geology, London, Vol. 7, pp. 257-295.

Burwell, E.B. & Moneymaker, B.C., (1950). *Geology in dam construction*. In Paige, S. (Eds.) (Chairman). *Application of geology to Engineering Practice:* Berkey vol.: The Geological Society of America, Boulder. pp, 11-43.

Carter, P.G & Mills, D.A., (1976). Engineering geology investigations for the Kielder Tunnels. *Quarterly Journal of Engineering Geology*, London, 2, pp. 161-181.

Chandler, R.J., (1969). The effect of weathering on the shear strength of the Keuper Marl. *Geotechnique,* 19, pp. 321-334.

Chandler, R.J., (1972). Lias clay: Weathering processes and their effect on shear strength, *Geotechnique,* 22, pp. 403-431.

Chandler, R.J., Pachakis, M., Mercer, J. & Wrightman, J., (1973). Four long-term failures of embankments found on areas of landslip. *Quarterly Journal of Engineering Geology.* London, 6, pp. 405-422.

Chapman, D.R., (1975). Shale classification tests and systems: A comparative study. *Joint Highway Research Project,* JHRP-75-11. Purdue University, Indiana.

Chapman, D.R., Wood, L.E., Lovell, C.W. & Sisiliano, W.J., (1976). A comparative study of shale Classification tests and systems. *Bulletin of the Association of Engineering Geologists,* Vol. 13, No. 4, pp. 247-266.

Christopher, B.R., Schwartz, C. & Boudreau, R., (2006). *Geotechnical aspects of pavements*. Report no. NHI-05-037, National Highway institute, U.S department of Transportation, Washington, D.C.

Clarke, F.W., (1924). *Bulletin, United States Geological Survey*, 700, pp. 29.

Colorado Laboratory Procedure, (2014). Determining the durability of shales for use as embankments.

Craig, R.F., (1983). *Soil Mechanics*. 3rd Edition. Van Norstrand Reinhold, United Kingdom.

Craig, R. F., (2004).*Craig's Soil Mechanics*.7th Edition. Spon Press, London.

Cripps, J.C. & Taylor, R.K., (1981). The engineering properties of mudrocks. *Quarterly Journal of Engineering Geology*, Vol. 14, pp. 325-346.

Cripps, J.C. & Taylor, R.K., (1986). Engineering Characteristics of British Over-consolidated Clays and Mudrocks, Tertiary deposits. *Engineering Geology,* No.22, pp. 349- 376.

Curtis, C.D., Lipshie, S.R., Oertel, G. & Pearson, M.J., (1980). Clay orientation in some Upper Carboniferous mudrocks, its relationship to quartz content and some inferences about fissility, porosity, and compaction history: *Sedimentology*, 17, pp. 333-339.

D'Appolonia Consulting Engineers, (1980). Environmental effects of slaking of surface mine spoils Eastern and central United States. Final report, J0285024. Prepared for: *U.S.D.I. Bureau of Mines,* pp.232.

Dafalla, M.A and Al-Shamrani, M.A., (2014). Swelling characteristics of Saudi Tayma Shale and consequential impact on light structures, *Journal of Civil Engineering and Architecture,* Vol. 8, pp. 613-623.

Dai, F. & Lu, M., (2010). Evaluation of photogrammetry for monitoring settlement of building adjacent to foundation jobsite. *Proceedings of the International Conference on Computing in Civil and Building Engineering*, Nottingham University Press.

Deere, D.U. & Miller, R.P., (1966). *Engineering classification and index properties for intact rock*. Department of civil engineering, University of Illinois, Urbana, pp. 90-101.

Deer, D.U., Howie, R.A. & Zussman, J., (1992). *An introduction to the rock forming minerals*. 2nd Edition, Pearson Education Limited, Essex.

Deo, P., (1972). *Shales as Embankment Materials*: Unpublished PhD. Thesis, Purdue University, West Lafayette, pp. 201.

Deo, P., (1973). *Use of shale in embankments*, Joint Highway Research Project, Purdue University, West Lafayette, report no. 14.

Dick, J.C., Shakoor, A. & Wells, N., (1994). A geological approach towards developing a mudrock durability classification system. *Canadian Geotechnical Journal*, Vol. 31, pp. 17-27.

Ding, W., Li, C., Jiu, K., Zeng, W & Wu, L., (2012). Fracture development in shale and its relationship to gas accumulation. *Geoscience Frontiers*, Vol. 3, pp. 97-105.

Drennan, J.A., (1963). An unusual occurrence of chamosite. *Clay Mineral Bulletin.* Vol 5, pp. 382.

Drennan, Maud and Partners, (2010). *Report to Tongaat Hulett development on the detailed geotechnical investigation, Cornubia*, Reference no: 21368.

Drnevich, V.P., Hopkins, T.C., Allen, D.L. & Hale, S.S., (1976). Engineering properties. Chapter 4 of a technical report, *The Chemical and Engineering Properties of Eastern Oil Shale*, Robl, T.L., & Koppenaal, D.W. (Eds.), Institute for Mining and Minerals Research, University of Kentucky.

Dube, A.K. & Singh, B., (1972). Effect of humidity on tensile strength of sandstone. *Journal of Mines Metals and Fuel,* pp. 8-10.

Duncan, J. M. & Wright, S.G., (2005). *Soil Strength and Slope Stability.* Wiley and Sons, New Jersey.

Dutrow, B.L., (2007). *Geochemical Instrumentation Analysis- X-ray Diffraction (XRD)*, Science Education Resource Centre.

Fam, M.A., Dusseault, M.B. & Fooks, (2003). Drilling in mudrocks: Rock behaviour issues. *Journal of Petroleum Science and Engineering,* Vol. 38, pp. 155-166, Elssevier.

Fityus, S.G., Jeffrey, M., Aglias, K.J., Johnson, J, A. & Simmons, J.V., (2015). Weathering and degradation of shales and mudrocks. *International Symposium on Rock Mechanics.* The 13th International Congress on Rock Mechanics, Montreal, Canada.

Folk, R.L., (1974). *Petrology of Sedimentary rocks*. 3rd Edition, Hemphill's Bookstore, Austin.

Franklin, J.A., (1981). A shale rating system and tentative applications to Shale Performance. *In Transportation Research Record 790*, TRB, National Research Council, Washington, D.C., pp. 2-12.

Franklin, J.A. & Chandra, R., (1972). The slake durability test. *International Journal of Rock Mechanics and Mining Science*. Vol.9, pp. 325-341.

Gamble, J.C., (1971). *Durability- Plasticity classification of shales and other argillaceous rocks:* Unpublished PhD. Thesis, University of Illinois, Urbana-Champaign, IL, pp. 161.

Gartung, E., (1986). Excavation in hard clays of the Keuper Formation, *Proceedings of Symposium, Geotechnical Engineering Division,* Seattle, Washington.

Gemici, U., (2001). Durability of shales in Narlidere, Izmir, Turkey, with emphasis on the impact of water on slaking behaviour. *Environmental Geology,* No. 41, pp. 430-439.

Geng, M. & Dou, Y., (2012). Analysis of the influence factors of differential settlement of high embankment in mountain area. *Open Journal of Civil Engineering,* Vol.2, pp. 214-217.

Geological Survey, (1988). 1:250 000 Geological Series 2730 Vryheid. Geological Survey, Pretoria.

Gokceoglu, C., Ulusay, R. & Sonmez, H., (2000). Factor affecting the durability of selected weak and clay-bearing rocks from Turkey, with particular emphasis on the influence of the number of drying and wetting cycles. *Engineering* Geology, 57, pp. 215-237.

Golparvar-fard, M., Pena-mora, F. & Savarese, S., (2009). Application of D4AR- A 4-dimedel for automating construction progress monitoring data collection, processing and communication. Special issue next generation construction IT: technology foresight, future studies, road mapping, and scenario planning. *Journal of Information Technology in Construction*. Vol.14, pp. 129-153.

Green, P.P., (2007). Durability testing of basic crystalline rocks and specification for use as road base aggregate, *Bulletin of Engineering Geology and the Environment*, 66, pp. 431-440.

Griffiths, J.C., (1967). *Scientific method in the analysis of sediments*. McGraw-Hill, New York.

Gutierrez, M., Nygard, R., Hoeg, K. & Beere, T., (2008). Normalised undrained shear strength of clay shales, *Engineering Geology*, Vol. 99, No 1-2, pp. 31-39.

Hajdarwish, A. & Shakoor, A., (2006). *Predicting the shear strength parameters of mudrocks*. The Geological Society of London, IAEG paper no. 607, pp. 1-9.

Handlin, J. & Hager, R.W., (1957). Experimental deformation of sedimentary rock under a confining pressure. *Journal of American Association of Petrographic Geology*, pp.1-50.

Hardwick, A. M., (1992). *Weathering and brittleness in shale fill dams and embankments,* Durham MSc theses, Durham University, pp. 24-26

Hawkins, A. B. & Privett, K.D., (1985). Measurement and use of residual shear strength in soils. *Ground Engineering*, 18, pp. 22-29.

Haydon, R.E.V. & and Hobbs, N.B., (1977). The effect of uplift pressures on the performance of a heavy foundation on a layered rock. *Proceedings of the Conference on Rock Engineering*, Newcastle, pp. 457-472

Head, K.H., (1982). *Manual of Soil Laboratory Testing*, Vol. 1, *Soil Classification and Compaction Tests,* Pentech Press, London.

Head, K.H., (1984). *Manual of Soil laboratory testing*, Vol. 2, Wiley & Sons, London.

Head, K.H., (2006). *Manual of Soil Laboratory Testing,* 3rd Edition, Vol. 3, Whittles Publishing, Scotland.

Hencher, S.R. & Richards, L.R., (1989). Laboratory direct shear testing of rock discontinuities. *Ground Engineering*, pp.21-34.

Hobbs, D.W., (1966). A study of the behaviour of a broken rock under triaxial compression, its application to mine roadways. *International Journal of Rock Mechanics and Mineral Sciences*, 3, pp. 11-43.

Hobbs, D. W., (1970). The behaviour of broken rock under triaxial compression. *International Journal of Rock Mechanics and Mineral Sciences,* 7, pp. 125- 148.

Hobbs, N.B., (1973). Effects of non-linearity on the prediction of settlements of foundations on rock. *Quarterly Journal of Engineering Geology,* London, pp. 153-168.

Hobday, D.K. & Von Brunn, V., (1979). Fluvial sedimentation and paleogeography of an early Paleozoic failed rift, southeastern margin of Africa. *Palaeogeography, Palaeoclimatology and Palaeoecology,* 28, pp. 169-184.

Hoek, E., Kaiser, P.K. & Bawden, W.F., (1998). *Support of underground excavations in hard rock*, A.A. Balkema, Rotterdam.

Hopkins, T.C., (1984). *Relationship between Kentucky CBR and Slake Durability*. University of Kentucky Research Report UKTRP-84-24, Lexington.

Hopkins, T.C., (1988). *Shear strength of Compacted Shales*. University of Kentucky Research Report. UKTRP-88-1, Lexington.

Hopkins, T.C. & Beckham, T.L., (1998). *Embankment construction using shale*. Research Report: KTC-98-2. Kentucky Transportation Centre, University of Kentucky, pp.1-41.

Horsrud, P., (2001). *Estimating mechanical properties if shale from empirical correlations*. Society of Petroleum Engineers (SPE), pp.1-6.

Huang, W.T., (1962). *Petrology.* McGraw- Hill, New York.

Hudec, P. P., (1982). Statistical Analysis of Shale Durability Factors. *Transportation Research Record* 873, Transportation Board, Washington D.C., pp. 28-35.

Hudson, J.A. & Harrison, J.P., (1997). *Engineering rock mechanics: An introduction to the principles*, Pergamon, Elsevier.

Ingram, R.L., (1953). Fissility of mudrocks. *Bulletin of the Geological Society*, 64, pp. 869-878.

International atomic energy agency (IAEA), (1997). *Sampling, Storage and sample preparation procedures for X-ray fluorescence analysis of environmental materials*, Vienna, Austria, pp. 8-54.

International Society for Rock Mechanics (ISRM), (2000). *Suggested methods for Laboratory testing*.

Irsyam, M., Susila. E., & Himawan, A., (2008). Slope failure of an embankment on clay shale at KM 97 + 500 of the Cipularang Toll Road and the selected solution, *International Symposium on Geotechnical Engineering, Ground Improvement and Geosynthetics for Human Security and Environmental Protection,* Bangkok, Thailand, pp. 531- 540.

Isioye, O.A. & Musa, A.A., (2007). The use of geodetic levelling for crustal motion and deformation studies: A 30 year case study in Ahmadu Bello University, Zaria, *The Information Manager,* Vol. 7 (2),

Jackson, J.O. & Fookes, P.G., (1974). The relationship of the estimated former burial depth of the lower Oxford Clay to some soil properties. *Quarterly Journal of Engineering Geology*, London, Vol.7, pp. 137-179.

Johnson, M.R., Hunter, D.R., Anhaeuser, C.R., and Thomas, R.J., (2006). Sedimentary rocks in the Karoo Supergroup. *In:* Johnson, M.R., Anhaeusser, C.R., and Thomas, R.J. (Eds.), *The Geology of South Africa,* Geological Society of South Africa, Johannesburg/ Council for Geoscience, Pretoria, 461-470.

Kanitpanyacharoen, W., Wenk, H. R., Kets, F., Lehr, C. & Wirth, R. (2011). Texture and anisotropy analysis of Qusaiba Shales. *Department of Earth and Planetary Science*, University of California, Vol. 59, pp. 536-556.

Kavvadas, M.J., (2003). Monitoring and modelling ground deformations during tunnelling. *11th FIG. Symposium on Deformation Measurements*, Santorini, Greece, pp. 1-19.

Kenny, T.C., (1968). Residual strength of fine grained materials and mineral mixtures. *Norwegian Geotechnical Institute,* pp. 53-58.

Kim, H. & Kano, N., (2008). Comparison of construction photograph and VR image in construction progress. *Automation in Construction.* 17 (2), pp.137-143. New York: Elsevier Science.

Koncagul, E.C. & Santi, P.M., (1999). Predicting the unconfined compressive strength of the Breathitt shale using slake durability, shore hardness and rock structural properties, *International Journal of Rock Mechanics and Mining Sciences*, pp. 139-153.

Krinsley, D.H., Pye, K., Boggs Jr, S. & Tovey, N.K., (1998). *Backscattered scanning electron microscopy and image analysis of sediments and sedimentary rocks,* Cambridge University Press, Cambridge.

Krynine, P.D., (1948). The megascopic study and field classification of sedimentary rocks. *Journal of Geological Science,* 56, pp.130-165.

Kuenen, P. H., (1959). Experimental abrasion, part 3, fluviatile action on sand. *American Journal of Science,* 257, pp. 172-190.

Kuenen, P. H., (1960). Experimental abrasion, part 4, Eolian action. *Journal of Geology*, 68, pp.427-449.

Lashkaripour, G.R. & Dusseault, M.B., (1993). A statistical study on shale properties: Relationships among principal shale properties. *Probabilistic methods in Geotechnical Engineering.,* Li and LO (Eds.), Balkema, Rotterdam, the Netherlands.

Lenke, L.R., (2006). Settlement issues-Bridge approach slabs. *Report no. NM04MNT-02*, New Mexico, Department of Transportation.

Liu, K.W., (2002). Deep burial diagenesis of the siliclastic Ordovician Natal Group, South Africa. *Sedimentary Geology*, Vol 1154, pp. 177-189.

Luhmann, T. & Tecklenburg, W., (2001). Hybrid photogrammetric measurement and geodetic surveillance of historical buildings for an urban tunnel construction. *International Workshop on Recreating the Past Visualisation and Animation of Cultural Heritage,* Ayuttaya, Thailand.

Lundegard, P.D. & Samuels, N.D., (1980). Field classification of fine-grained sedimentary rocks. *Journal of Sedimentary Petrology,* 50, pp. 781-786.

Lupiui, J.F., Skinner, A.E. & Vaughan, P.R., 1981). The drained residual strength of cohesive soils. *Geotechnique,* 31, pp. 181-213.

Lutton, R.J., (1977). Slaking Indexes for design (Report FHWA-RD-77-1). *Design and Construction of compacted Shale Embankments, U.S. Department of Transportation*, Vol. 3, pp. 94.

Marr, W.A., (2000). *Advances and retreats in geotechnical measurements*. ASCE GSP No. 111, Silva, F. & Kavazanjian, E. Jr., (Eds.).

Marques, E.A.G., Vargas, E.D.O & Antunes, F.S., (2005). A study of the durability of some shales, mudrocks and siltstones from Brazil. *Geotechnical and Geological Engineering,* 23, pp. 321-348.

Marshall, J.E.A., (1994). The Falkland Islands: A key element in Gondwana paleogeography. *Tectonics.* Vol. 13, pp. 499-514.

Marshall, C.G.A. & Von Brunn, V., (1999). The stratigraphy and origin of the Natal Group. *South African Journal of Geology.* Vol. 102, pp.15-25.

Marshall, C.G.A., (2006). The Natal Group. *In:* Johnson, M.R., Anhaeusser, C.R., and Thomas, R. J. (2006; Eds.). *The Geology of South Africa,* Geological Society of South Africa, Council for Geosciences, Pretoria, pp. 431-441.

Mccaffrey, K.J.W., Jones, R.R., Holdsworth, R.E., Wilson, R.W., Clegg, P., Imber, J., Holliman, N. & Trinks, I., (2005). Unlocking the spatial dimension: digital technologies and the future geoscience fieldwork. *Journal of the Geological Society,* London, Vol. 162, pp. 1-12.

McCave, I.N., Bryant, R.J., Cook, H.F. & Coughanowr, C.A., (1986). Evaluation of a laser-diffraction size analyser for use with natural sediments. *Journal of Sedimentary Petrology,* 56, pp. 561-564.

McLachlan, I.R. & Anderson, A.M., (1977). Fossil insect wings from the early Permian White Band Formation, South Africa. *Palaeontology. Afr.,* Vol. 15, pp. 37-64.

Merriman, R.J., Highley, D.E. & Cameron, D.G., (2003). *Definition and characteristics of very-fine grained sedimentary rocks*: clay, mudstone, shale and slate. *British Geological Survey. Commissioned Report,* CR/03/281N, pp. 1-22.

Meth, D.L., Uken R. and Whitmore, G.P., (2002). *Promoting our local geological heritage*. KwaZulu-Natal: 3500 million years of geological history. *Proceedings.* Regional Workshop on Tertiary Sector Geoscience Education in Southern Africa. Building regional networks on local expertise, Vasconcelos, L. (Eds.), Maputo, Mozambique, Nov. 2000, pp. 49-52.

Mitchell, J.K., (1993). *Fundamentals of Soil Behaviour*. John Wiley and Sons, New York.

Moore, J., (2005). *Integration of the sedimentological and petrophysical properties of mudstone samples*. Unpublished PhD thesis. School of Civil Engineering and Geosciences, University of Newcastle.

Morgenstern, N.R. & Eigenbrod, K.D., (1974). Classification of argillaceous soils and rocks. *Geotechnical Division* (ASCE), Vol. 100, pp. 1137-1156.

Moriwaki, Y. & Mitchell, J.K., (1977). The role of dispersion in the slaking of intact clay. In: *Dispersive Clays, Related Piping and Erosion in Geotechnical Projects*, Sherard, J.L. & Decker, R.S. (Eds.), ASTM STP 623: *American Society for Testing and Materials*, Philadelphia, pp. 287-302.

Nandi, A., Liutkus, C.M. & Whitelaw, M.J., (2009). *Geotechnical characterization of Sevier and Rome Shale, East Tennessee*. Department of Geosciences, East Tennessee State University, John City, USA, pp. 1-8.

National Building Research Institute (NBRI), (1967). *Handbook of South African natural building stone*. National Development Fund for the Building Industry, Johannesburg.

NAVFAC, (1982). *Foundations and Earth Structures*. DM-&.2, Department of Navy, Naval Facilities Engineering Command.

Nicols, G., (2009). *Sedimentary and Stratigraphy*. 2nd Edition. West Sussex, Wiley and Blackwell.

Nuffield, E.W., (1966). *X-Ray Diffraction methods*, Wiley.

O' Neil, M.W. & Poormoayed, A.M., (1980). Methodology for foundations on expansive clays. *Proceedings of the American Society for Civil Engineers, Journal of the Geotechnical Division,* Vol. 106, pp. 1245-1367.

Ola, S.A., (1980). Some Foundation design problems in Sokoto area of North-Western Nigeria. *7th Regional conference for Africa on S.M.F.E*. Accra, pp. 269-275.

Oakland, M.W. & Lowell, C.W., (1982). Standardised tests for compacted shale highway embankments. In: *Transportation Research Record*, 873, *TRB, National research Council*, Washington, D.C, pp.-15-22.

Olivier, H.J., (1979). Applicability of geomechanics classification to the Orange-Fish tunnel rock masses. *Transactions of the Southern African Institution of Civil Engineers,* Vol. 21, **8**, pp. 179-185.

Oliver, M., Bell, F.G. & Jeremy, C.A., (1994). The effect of rainfall on slope failure, with examples from the greater Durban area. *Proceedings of Seventh Congress of the International Association of Engineering Geology, Lisbon, A.A.* Balkema, Rotterdam, Vol. 3, pp. 1629-1639.

Ollier, C., (1984). Weathering. *Geomorphology texts*. Longman, London and New York.

Page, T.C. & Solesbury, F., (1983). Proposed railway tunnel in the Pietermaritzburg shale Formation in KwaZulu-Natal. In*:* Brink, A.B.A., (1983). *Significance of the rock fabric of mudrocks in determining the rock mass classification for tunnelling*. *Engineering Geology of Southern Africa*, *the Karoo Sequence.* Vol. 3, Building Publications, Cape Town.

Parry, R.H.G., (1972).Some properties of heavily over-consolidated Lower Oxford Clay at a site near Bedford. *Geotechnique.* Vol. 22, pp. 485-507.

Perry, E.F. & Andrews, D.E., (1982). Slaking Modes of geologic materials and their Impacts on Embankment Stability. In: *Transportation Research Record 873, TRB, National Research Council*, Washington, D.C., pp. 22-28.

Pettijohn, F.J., (1957). *Sedimentary Rocks*, Harper, New York, pp. 348.

Pettijohn. F.J., (1967). *Sedimentary Rocks.* Harper Brothers, New York.

Pettijohn, F.J., (1975). *Sedimentary Rocks,* 3rd Edition, Harper and Bros, New York.

Picard, M.D., (1971). Classification of fine grained sedimentary rocks. *Journal of Sedimentary Petrology,* 41*,* pp. 179-195.

Pidwirny, M., (2006). *Weathering*. *Fundamentals of Physical Geography.* 2nd Edition.

Poppe, L.J., Paskevich, J.C., Hathaway & Blackwood, D.S., (2002). A laboratory manual for X-ray powder diffraction. *U.S. Geological Survey Open File Report* 01-041, pp. 1-88.

Potter, P.E., Maynard, J.B. & Pryor, W.A., (1980). *Sedimentology of shale*. Springer- Verlag, New York, pp. 332.

Potter, P.E., Maynard, J.B. & Depetris, P.J., (2005). *Mud and Mudstones*: Springer-Verlag, Berlin.

Powell, J.S., (2010). *Geotechnical Characterisation of the Bearpaw Shale*. Queen's University, Kingston, Ontario, Canada.

Price, N.J., (1960). The compressive strength of coal measure rocks. *Coillery Engineering*, 37, pp. 283-292.

Quinones-Rozo, C.A, Hashhash, Y.M.A. & Liu, L.Y., (2008). Digital image reasoning for tracking excavation activities. *Automation in Construction,* 17 (5), pp. 608-622.

Ramseyer, K. & Boles, J.R., (1985). Mixed layer illite/ smectite minerals in Tertiary sandstones and shales, San Joaquin Basin, California, *Clays and clay minerals,* Vol. 34, pp. 115-124.

Ray, A.G., (1960). *Aerial Photographs in Geologic Interpretation and Mapping.* U.S. Geological Survey Professional Paper, 373, pp. 230.

Rib, H.T. & Liang, T., (1978). Recognition and identification. In: *Special Report 176: Landslides: Analysis and control. TRB, National research Council*, Washington, D.C., pp. 34-80.

Ribbink, C., (2015). The approach used to modify the shale rating system using laboratory results and the monitoring of settlement at the Cornubia development. [conversation] (Personal communication, January 2014-October 2015), Geotechnical Engineer of Drennan, Maud and Partners, Durban, South Africa.

Richards, N.P., (2006). Engineering geological mapping in Pietermaritzburg South Africa: Constraints on development, The Geological Society of London, International Association for Engineering Geology, 407, pp. 1-11.

Rowe, H., Hughes, N. & Robinson, K., (2012). The quantification and application of handheld energy dispersive X-ray fluorescence (ED-XRF) in mudrock chemostratigraphy and geochemistry. *Chemical Geology*, 324-325, pp. 121-131.

Rowsell, D.M. & De Swardt, A.M.J., (1976). Diagenesis in Cape and Karoo sediments and its bearing on their hydrocarbon potential. *Transactions of the Geological Society of South Africa*, Vol. 79, pp. 81-153.

Russell, D.J. & Parker, A., (1979). Geotechnical, mineralogical and chemical inter-relationships in weathering profiles of an over-consolidated clay. *Quarterly Journal of Engineering Geology*, London, Vol. 12, pp. 107-16.

Samuels, S.G., (1975). Some properties of the Gault Clay from the Ely-Ouse Essex Water tunnel. *Building research Establishment*, pp.19.

Santi, P.M. & Rice, R.H., (1991). Preliminary Classification of Transitional Materials. Proceedings of the *27th Symposium on Engineering Geology and Geotechnical Engineering*, Logan, Utah, pp. 8-13.

Santi, P.M., (1995). *Classification and testing of weak and weathered rock material: A model based on Colorado shales:* Unpublished PhD. Dissertation, Colorado, School of Mines, Golden, pp. 286.

Santi, P.M. & Koncagul, E.C., (1996). Predicting the mode, susceptibility and rate of weathering of shales. In Matheson, G. (editor), *Design in residual soils: Geotechnical and environmental issues,* ASCE Geotechnical special publication, American Society of Civil Engineers, New York, p No. 62; p.37-55.

Santi, P.M. & Shakoor, A., (1997). Summary of pre-symposium questionnaire. In Santi, P.M. ad Shakoor, A. (Editors), *Characterisation of weak and weathered rock masses associated*, *Association of Engineering Geologists Special Publication, 9*: Association of Engineering Geologists, Denver, pp. 225-233.

Santi, P.M., (1998). Improving the jar slake, slake index, and slake durability tests for shales: *Environmental Engineering Geo-Science,* Vol. 4. pp. 285-396.

Santi, P.M. & Higgins, J.D., (1998). Methods for predicting shale durability in the field: *Geotechnical Testing Journal,* Vol.21, pp. 195-202.

Santi, P.M., (2006). Field methods for characterizing weak rock for engineering. *Environmental and Engineering Geoscience*, Vol 12, pp. 1-11.

Schieber, J., (1986). *Facies and origin of shales from the mid-Proterozoic Newland Formation*, Belt Basin, Montana, USA.

Schoenleber. J.R., (2005). *Field sampling procedures manual*. Department of Environmental Protection. New Jersey.

Schofield, W. & Breach, M., (2007). *Engineering Surveying*, 6th Edition, Elsevier Ltd.

Shalabi, F.I., Cording, E.J. & AL- Hattamleh, O.H., (2007). Estimation of rock engineering properties using hardness tests. *Engineering Geology,* Vol. 90, pp. 138-147.

Shamburger, H.H., Patrick, D.M. & Lutton, R., (1975). *Design and construction of compacted shale embankments, Federal Highway Administration*, D.C., Vol. 1, Report No. FHWA-RD-75-61.

Shrock, R.R., 1948. A classification of sedimentary rocks. *Journal of Geology.*, 56, pp. 118-129.

Skempton, A.W., (1964). Long-term stability of clay slopes. *Geotechnique.* 14, pp. 77-101.

South African Committee for Stratigraphy (SACS), (1980). Stratigraphy of South Africa. Part1: Lithostratigraphy of the Republic of South Africa, South West Africa/ Namibia, and the Republic of Bophuthatswana, Transkei, and Venda (L.E. Kent, comp). *Handbook for Geological Surveys of South Africa,* 8, pp. 690.

Sowers, G.B. & Sowers, G. E., (1970). *Introductory soil mechanics and foundations*. Macmillan, New York, pp. 556.

Speakman, S.A., (2012). *Introduction to PANalytical X'Pert Higscore Plus v.3.0*. MIT Centre for Material Science and Engineering, pp. 1-19.

Spears, D.A. & Taylor, R.K., (1972). Influences of weathering on the composition and engineering properties of in situ Coal Measures rocks. *International Journal of Rock Mechanics and Mineral Sciences*. Vol. 9, pp. 729-56.

Spears, D.A., (1980). Towards a classification of shales. *Journal of the Geological Society of London,* 137, pp. 128-129.

Stow, D.A.V., (1980). Fine grained sediments: Terminology. *Quarterly Journal of Engineering Geology,* 14, pp. 243-244.

Stow, D.A.V. & Piper, D.J.W., (1984). Deep water fine-grained sediments: history, methodology and terminology, in Stow, D.A.V. & Piper (Eds.), *Fine- grained sediment:* Geological Society Special Publication, 15, pp. 3-14.

Strohm, W.E., (1978). Field and laboratory Investigations, Phase III (Report FHWA-RD-78-140). *In: Design and Construction of Compacted Shale Embankments*, U.S. Department, pp.154.

Strohm, W.E., Bragg, G.H. & Ziegler, T.W., (1981). *Design and construction of compacted shale embankments*, (Technical Guidelines), U.S. Army Corp of Engineers Waterways Experiment Station, Geotechnical Laboratory, Prepared for Federal Highway Administration, Washington, Vol. 5.

Stroman, R., Beene, R.R.W, & Hull, A.M., (1984). Clay shale foundation Slide at Waco Dam, Texas. *First International conference on case Histories in Geotechnical Engineering*, pp. 579- 586.

Sudo, T., Shimoda, S., Yotsumoto, H. & Aita, S., (1981). *Electron micrographs of clay minerals*. Elsevier, Amsterdam.

Taylor, D.W., (1948). *Fundamentals of Soil Mechanics.* John Wiley & Sons, New York, pp.700.

Taylor, R.K., (1986). The Aberfan disaster: Engineering geology of mudrocks two decades later. In: *Geology in the Real World- the Kinsley- Dunham volume.* Institute of Mining and Metallurgy. (Eds.): Dunham, K.C., Nesbitt, R.C. & Nicol, I.

Taylor, R.K., (1988). Coal Measures mudrocks: Composition, classification and weathering processes. *Quarterly Journal of Engineering Geology,* London, 21, pp. 85-99.

Taylor, R.K. & Spears, D.A., (1981). Laboratory investigation of mudrocks. *Quarterly Journal of Engineering Geology*, London, Vol. 14, pp. 291-309.

Terzaghi, R. & Peck, R., (1967). *Soil Mechanics in engineering practice*. John Wiley and Sons, New York, pp. 729.

Toniolo, F., (2012). *A geological and geotechnical investigation of the Pietermaritzburg Formation shales in KwaZulu-Natal*, BSc (Hons.) Unpublished honours project, University of KwaZulu-Natal.

Tourtelot, H.A., (1960). Origin and use of the word "shale". *American Journal of Science*, 258, pp. 335-343.

Tovey, N.K., Hounslow, M.H. & Wang, J.M., (1995). Orientation analysis and its application in image analysis: *Advances in Imaging and Electron Physics*., 93, pp. 219-329.

Tucker, M.E., (2001). *Sedimentary Petrology:* An introduction to the origin of sedimentary rocks, third edition, Blackwell publishing, pp. 93- 109.

Turner, D.P., (2000). Soils of KwaZulu-Natal and Mpumalanga: Recognition of natural soil bodies. PhD thesis, University of Pretoria.

Twenhofel, W.H., (1937). Terminology of the fine grained mechanical sediments, *Report on the Committee on Sedimentation*, Natural Research Council for the Division of Geology and Geography, pp. 81-104

Underwood, L.B., (1967). Classification and Identification of shales. *Journal of the Soil Mechanics and Foundations division*. ASCE, Vol.23, pp. 97-116.

United States (U.S.) Army Corps of Engineers (2002). *Structural Deformation Surveying* (EM 1110-21009), U.S. Army Corps of Engineers, Washington, DC.

Vallejo, L.E., Robinson, M.K., Stewart, M. & Ann, C., (1994). Role of shale pores on settlement. *Proceedings for the conference in vertical and horizontal deformations of foundations and embankments*, University of Pittsburgh, pp. 1425-1434.

Venter, J.P., (1980). The engineering properties and road building characteristics of mudrocks, with special reference to Southern Africa, PhD thesis, University of Pretoria, Pretoria.

Verwaal, W, (2005). *Soil Mechanics, Laboratory Manual*. Geotechnical laboratory of DGM, Thimphu Bhutan.

Visser, J.N.J., (1989). The Permo- Caboniferous Dwyka Formation of southern Africa: Deposition by a predominantly subpolar marine ice sheet. Palaeogeography, Palaeoclimatology, Palaeoecology, Vol 70, pp. 377-391.

Walkinshaw, J.L. & Santi, P.M., (1996). Chapter 21-Shales and other degradable materials. In Turner, A. A.K. and Schuster, R.L. (Editors), *Landslides: Investigation and Mitigation*, TRB Special Report: Transportation Research Board, National Research Council, Washington, DC, pp. 555-576.

Wan, Y. & Kwong, J., (2004). Shear strength of soils containing amorphous clay-size materials I a slow-moving landslide. *Engineering Geology*, Elsevier, 4,Vol. 65, pp. 293-303.

Ward, W, H., Marsland, A. & Samuels, S.E., (1965). Properties of the London Clay at the Ashform Common Shaft: In-situ and undrained tests, *Geotechnique,* 18, 321-44.

Weaver, C.E., (1980). Fine grained rocks: shales or physilites. *Sedimentary Geology,* 27, pp. 301-313.

Welsh, R.A., Vallejo, L.E., Lovell, L.W. & Robinson, M.K., (1991). The U.S. Office of surface Mining (OSM). Proposed strength durability Classification system. In: *Practice, Symposium on Detection of and Construction at the Soil/ Rock Interface* (Eds.: W.E. Kane and B, Amadei). ASCE Geotechnical Special Publication, No. 28, American Society of Civil Engineers, New York.

Whitmeyer, S., Feely, M., De Paor, D., Hennessey, R., Whitmeyer, S., Nicoletti, J., Santagelo, B., Daniels, J. & Rivera, M., (2009). Visualisation techniques in field geology education: A case study from western Ireland, *The Geological Society of America,* Special paper 461.

Whitney, G., (1990). Role of water in the smectite to illite reaction: C*lays and Clay Minerals,* pp.343-350.

Wilkins, A.D., (2013). *Terminology and the classification of fine grained sedimentary rocks- is there a difference between claystone, a mudstone and a shale?* Department of Geology and Petroleum Geology, University of Aberdeen, pp.1-12.

Wilson, C., (1983). *Symposium on Geotechnical Engineering in areas in Natal underlain by Ecca Shale*. Durban Branch in conjunction with the Geotechnical Division of the S.A. Institution of Civil Engineers.

Withiam, J.L. & Andrews, D.E., (1982). Relevance of durability testing of shales to field behaviour: In: *Transportation Research Record,* Washington, DC*,* 873*,* pp, 36-42.

Wood, L.E. & Deo, P., (1975). A suggested system for classifying shale materials for Embankments. *Bulletin of the Association of Engineering Geologists*, 1, Vol. 12, pp. 39-55.

Wylie, D, C. & Mah, C. W, (2004). *Rock slope engineering*, Civil and Mining, 4th Edition, Spon Press, New York

Yaalon, D.H., (1961). Mineral composition of the average shale. Department of geology, The Hebrew University, Jerusalem, Department of Geology, pp. 1-6.

Yasar, E & Erdogan, Y., (2004). Estimation of rock physicomechanical properties using hardness methods. *Engineering Geology.* Vol. 71, pp. 281 -288.

Zydron, T. & Zawizsa, E., (2011). Shear strength investigation of soils in landslide areas. *Geologija,* Vol. 53, pp. 147 – 155.

Acknowledgements

This dissertation required many hours of dedication, hard work and assistance from various people. First and foremost, the author would like to thank his parents, Soonderi Naidoo and Krishnaswami Naidoo and his dearest brother, Kaveshin Naidoo, for motivating him to follow a career in geology and for their continuous guidance, love and support.

Secondly, the author extends his gratitude to the Department of Civil Engineering at the University of Witwatersrand for graciously allowing for the use of their large scale shear box which was a crucial part of this study. Also, a heart filled thanks is extended to Andrew Hendricks and Charles Macrobert for their assistance whilst the shear tests were performed.

Thirdly, Prenolan would like to thank Dr. E.D.C Hingston for his extraordinary guidance and motivation as both a supervisor and as a role model. The author is also thankful to Karl Ribbink for his gracious donation towards this study and for his help in providing vital information and assistance to complete this dissertation. The author also extends his gratitude to to Mukesh Seyambu, the laboratory technician, for all of his assistance throughout the authors university career and to P. Suthan for conducting the XRD tests.

Lastly, the author would like to thank Simone Govender for all of her love and support throughout this ordeal.

Appendix A: XRD results

Date: 3/5/2014 Time: 7:53:19 AM File: GEOL MSC - PRENOLAN_COR-B User: suthanp

Anchor Scan Parameters

Dataset Name:	GEOL MSC - PRENOLAN_COR-B
File name:	C:\XRD Data\GEOL MSC - PRENOLAN_COR-B.xrdml
Sample Identification:	COR-B
Measurement Date / Time:	3/4/2014 1:12:15 PM
Operator:	suthanp
Raw Data Origin:	XRD measurement (*.XRDML)
Scan Axis:	Gonio
Start Position [°2Th.]:	3.0003
End Position [°2Th.]:	69.9923
Step Size [°2Th.]:	0.0080
Scan Step Time [s]:	6.9850
Scan Type:	Continuous
Divergence Slit Type:	Fixed
Divergence Slit Size [°]:	0.5000
Specimen Length [mm]:	10.00
Measurement Temperature [°C]:	25.00
Anode Material:	Co
K-Alpha1 [Å]:	1.78901
K-Alpha2 [Å]:	1.79290
K-Beta [Å]:	1.62083
K-A2 / K-A1 Ratio:	0.50000
Generator Settings:	45 mA, 40 kV
Diffractometer Type:	00000000011116802
Diffractometer Number:	0
Goniometer Radius [mm]:	240.00
Dist. Focus-Diverg. Slit [mm]:	100.00
Spinning:	Yes

Graphics

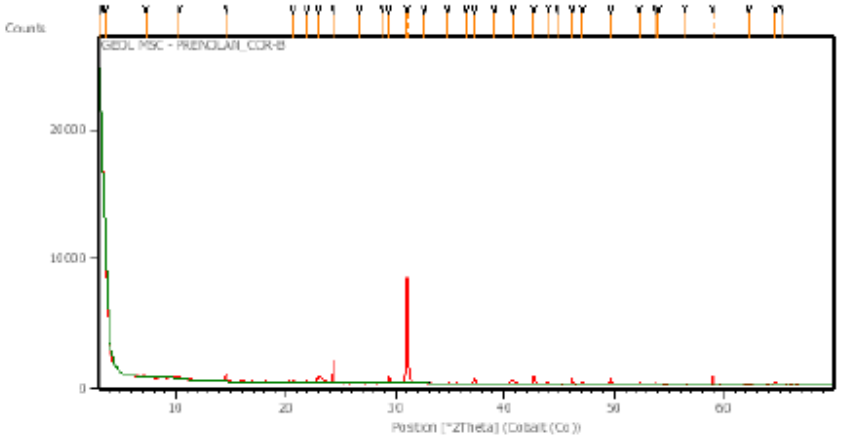

Peak List

Pos.[°2Th.]	Height [cts]	FWHMLeft[°2Th.]	d-spacing [Å]	Rel. Int. [%]
3.1756	2987.89	0.1574	32.30547	36.83
3.5450	238.62	0.4093	28.94036	2.94
7.2028	70.26	0.1889	14.25074	0.87
10.2929	162.26	0.0945	9.97919	2.00
14.5538	662.03	0.0945	7.06713	8.16
20.6060	68.52	0.4408	5.00445	0.84
21.9067	57.31	0.1889	4.71109	0.71

22.9537	360.95	0.2204	4.49869	4.45
24.2632	1603.14	0.0394	4.25944	19.76
26.6212	23.55	0.3779	3.88808	0.29
28.7898	117.52	0.1260	3.60072	1.45
29.3338	386.50	0.1102	3.53537	4.76
31.0266	8113.27	0.0672	3.34442	100.00
32.5693	97.60	0.1920	3.18999	1.20
34.8415	50.33	0.4608	2.98779	0.62
36.4874	32.52	0.4608	2.85730	0.40
37.2946	448.42	0.0672	2.79759	5.53
39.1189	26.06	0.4608	2.67188	0.32
40.8296	262.22	0.4608	2.56442	3.23
42.6984	514.28	0.0576	2.45709	6.34
44.0179	34.34	0.7680	2.38693	0.42
44.7826	61.01	0.1920	2.34822	0.75
46.1691	476.05	0.0768	2.28138	5.87
47.1225	211.91	0.0768	2.23778	2.61
49.7102	351.62	0.0768	2.12813	4.33
52.3197	111.30	0.2304	2.02892	1.37
53.7105	198.50	0.0960	1.98014	2.45
54.0791	76.47	0.1152	1.96765	0.94
56.4417	25.79	0.4608	1.89164	0.32
58.9457	670.88	0.1152	1.81806	8.27
62.2057	73.28	0.3072	1.73160	0.90
64.6949	199.40	0.0768	1.67181	2.46
65.2285	79.49	0.1152	1.65962	0.98

Anchor Scan Parameters

Dataset Name:	GEOL MSC - PRENOLAN_COR-W
File name:	C:\XRD Data\GEOL MSC - PRENOLAN_COR-W.xrdml
Sample Identification:	COR-W
Measurement Date / Time:	3/4/2014 1:46:07 PM
Operator:	suthanp
Raw Data Origin:	XRD measurement (*.XRDML)
Scan Axis:	Gonio
Start Position [°2Th.]:	3.0003
End Position [°2Th.]:	69.9923
Step Size [°2Th.]:	0.0080
Scan Step Time [s]:	6.9850
Scan Type:	Continuous
Divergence Slit Type:	Fixed
Divergence Slit Size [°]:	0.5000
Specimen Length [mm]:	10.00
Measurement Temperature [°C]:	25.00
Anode Material:	Co
K-Alpha1 [Å]:	1.78901
K-Alpha2 [Å]:	1.79290
K-Beta [Å]:	1.62083
K-A2 / K-A1 Ratio:	0.50000
Generator Settings:	45 mA, 40 kV
Diffractometer Type:	00000000011116802
Diffractometer Number:	0
Goniometer Radius [mm]:	240.00
Dist. Focus-Diverg. Slit [mm]:	100.00
Spinning:	Yes

Graphics

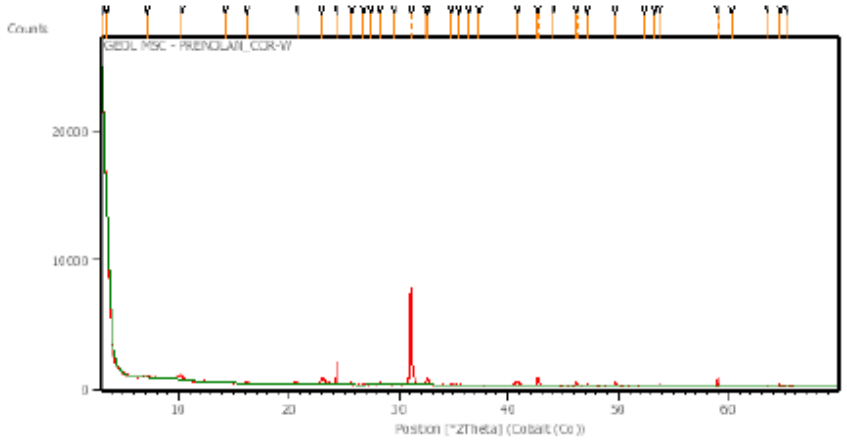

Peak List

Pos.[°2Th.]	Height [cts]	FWHMLeft[°2Th.]	d-spacing [Å]	Rel. Int. [%]
3.1452	3165.71	0.1574	32.61771	42.52
3.4975	673.43	0.2519	29.33325	9.04
7.1150	142.34	0.1889	14.42626	1.91
10.3132	502.90	0.0630	9.95965	6.75
14.1735	11.65	0.7557	7.25575	0.16
16.1358	61.77	0.2519	5.37815	0.83
20.6906	170.70	0.1574	4.98471	2.29

22.9811	367.13	0.2204	4.49361	4.93
24.2809	1650.84	0.0551	4.25638	22.17
25.6566	191.78	0.0945	4.03167	2.58
26.6867	43.50	0.3149	3.87843	0.58
27.4436	86.34	0.1260	3.77371	1.16
28.2122	92.09	0.2519	3.67290	1.24
29.5023	100.89	0.3149	3.51563	1.35
31.0453	7446.10	0.0576	3.34245	100.00
32.3368	183.56	0.1152	3.21231	2.47
32.5596	456.81	0.1344	3.19092	6.16
34.8314	79.46	0.2304	2.98863	1.07
35.5714	71.61	0.1152	2.92841	0.96
36.4681	68.26	0.3072	2.85876	0.92
37.3723	22.22	0.4608	2.79197	0.30
40.8502	263.45	0.4608	2.56318	3.54
42.7083	591.82	0.0576	2.45654	7.95
44.1506	59.96	0.5376	2.38011	0.81
46.1806	386.50	0.0480	2.28085	5.19
47.1612	213.55	0.0768	2.23604	2.87
49.7291	372.37	0.0672	2.12737	5.00
52.3591	68.16	0.2304	2.02750	0.92
53.2623	50.72	0.2688	1.99557	0.68
53.7304	182.86	0.0768	1.97946	2.46
58.9565	725.13	0.0576	1.81776	9.74
60.3188	80.10	0.1152	1.78044	1.08
63.4756	25.99	0.4608	1.70047	0.35
64.7016	211.10	0.0768	1.67165	2.84
65.2508	73.53	0.1152	1.65912	0.99

Anchor Scan Parameters

Dataset Name:	GEOL MSC - PRENOLAN_S1-B
File name:	C:\XRD Data\GEOL MSC - PRENOLAN_S1-B.xrdml
Sample Identification:	S1-B
Measurement Date / Time:	3/4/2014 1:37:38 PM
Operator:	suthanp
Raw Data Origin:	XRD measurement (*.XRDML)
Scan Axis:	Gonio
Start Position [°2Th.]:	3.0003
End Position [°2Th.]:	69.9823
Step Size [°2Th.]:	0.0080
Scan Step Time [s]:	6.9850
Scan Type:	Continuous
Divergence Slit Type:	Fixed
Divergence Slit Size [°]:	0.5000
Specimen Length [mm]:	10.00
Measurement Temperature [°C]:	25.00
Anode Material:	Co
K-Alpha1 [Å]:	1.78901
K-Alpha2 [Å]:	1.79290
K-Beta [Å]:	1.62083
K-A2 / K-A1 Ratio:	0.50000
Generator Settings:	45 mA, 40 kV
Diffractometer Type:	0000000011116602
Diffractometer Number:	0
Goniometer Radius [mm]:	240.00
Dist. Focus-Diverg. Slit [mm]:	100.00
Spinning:	Yes

Graphics

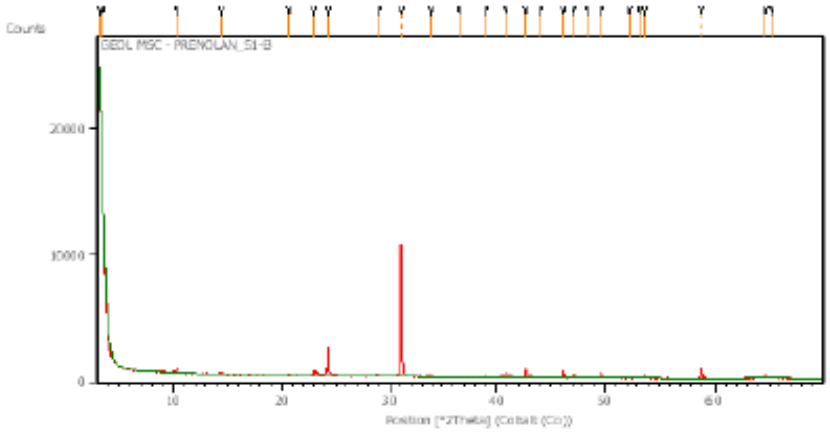

Peak List

Pos.[°2Th.]	Height [cts]	FWHMLeft[°2Th.]	d-spacing [Å]	Rel. Int. [%]
3.1601	3046.56	0.1889	32.46421	29.43
3.5006	684.39	0.1574	29.30722	6.61
10.2529	277.85	0.0945	10.01805	2.68
14.3751	78.26	0.1889	7.15451	0.76
20.6363	75.26	0.1889	4.99767	0.73
22.9557	305.46	0.1417	4.49851	2.95
24.2650	2182.62	0.0472	4.25912	21.09

29.0206	54.08	0.2519	3.57270	0.52
31.0356	10350.87	0.0576	3.34348	100.00
33.9056	54.19	0.5376	3.06775	0.52
36.5289	16.14	1.0752	2.85417	0.16
39.0532	46.73	0.6144	2.67620	0.45
40.8889	283.85	0.2304	2.56086	2.74
42.7000	720.49	0.0480	2.45700	6.96
44.0885	52.80	0.4608	2.38330	0.51
46.1703	598.76	0.0384	2.28133	5.78
47.1456	338.30	0.0384	2.23674	3.27
48.3703	28.61	0.4608	2.18339	0.28
49.7082	454.20	0.0480	2.12821	4.39
52.3204	68.44	0.1536	2.02890	0.66
53.2195	43.76	0.5376	1.99706	0.42
53.7161	270.70	0.0576	1.97995	2.62
58.9415	881.67	0.0960	1.81818	8.52
64.6974	270.22	0.0768	1.67175	2.61
65.2491	115.88	0.0576	1.65916	1.12

Anchor Scan Parameters

Dataset Name:	GEOL MSC - PRENOLAN_S1-W
File name:	C:\XRD Data\GEOL MSC - PRENOLAN_S1-W.xrdml
Sample Identification:	S1-W
Measurement Date / Time:	3/4/2014 2:11:33 PM
Operator:	suthanp
Raw Data Origin:	XRD measurement (*.XRDML)
Scan Axis:	Gonio
Start Position [°2Th.]:	3.0003
End Position [°2Th.]:	69.9923
Step Size [°2Th.]:	0.0050
Scan Step Time [s]:	6.9850
Scan Type:	Continuous
Divergence Slit Type:	Fixed
Divergence Slit Size [°]:	0.5000
Specimen Length [mm]:	10.00
Measurement Temperature [°C]:	25.00
Anode Material:	Co
K-Alpha1 [Å]:	1.78901
K-Alpha2 [Å]:	1.79290
K-Beta [Å]:	1.62083
K-A2 / K-A1 Ratio:	0.50000
Generator Settings:	45 mA, 40 kV
Diffractometer Type:	00000000111116802
Diffractometer Number:	0
Goniometer Radius [mm]:	240.00
Dist. Focus-Diverg. Slit [mm]:	100.00
Spinning:	Yes

Graphics

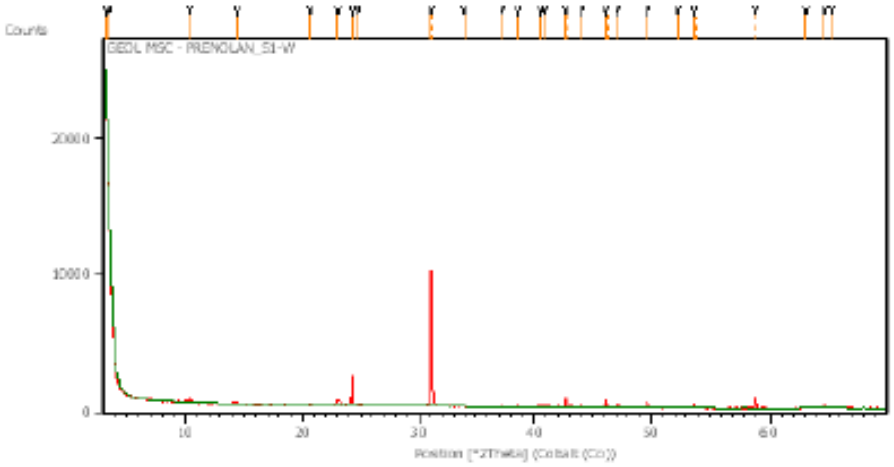

Peak List

Pos. [°2Th.]	Height [cts]	FWHMLeft [°2Th.]	d-spacing [Å]	Rel. Int. [%]
3.1843	2890.68	0.1574	32.21754	29.48
3.9810	764.63	0.1889	29.97211	7.80
10.2817	272.62	0.1260	9.99010	2.78
14.3390	86.31	0.3149	7.17242	0.88
20.6589	87.99	0.1889	4.99227	0.90
23.0186	330.66	0.1889	4.98638	3.37
24.2653	2048.30	0.0472	4.25908	20.89

24.7682	75.96	0.3149	4.17391	0.77
31.0310	9804.08	0.0576	3.34396	100.00
33.9457	44.99	0.3072	3.06423	0.46
37.2186	140.18	0.0768	2.80310	1.43
38.6270	71.50	0.1536	2.70456	0.73
40.5431	144.17	0.1152	2.58177	1.47
40.9419	297.02	0.3072	2.55768	3.03
42.6954	708.19	0.0480	2.45725	7.22
44.0965	53.92	0.3840	2.38269	0.55
46.1583	551.16	0.0576	2.28189	5.62
47.1504	291.20	0.0576	2.23653	2.97
49.7115	388.59	0.0576	2.12808	3.96
52.3326	64.52	0.2304	2.02846	0.66
53.7180	270.40	0.0768	1.97988	2.76
58.9395	863.60	0.0672	1.81823	8.81
63.0815	4.80	0.9216	1.70959	0.05
64.6986	239.26	0.0960	1.67172	2.44
65.3107	57.17	0.2304	1.65777	0.58

Anchor Scan Parameters

Dataset Name:	GEOL MSC - PRENOLAN_S2-B
File name:	C:\XRD Data\GEOL MSC - PRENOLAN_S2-B.xrdml
Sample Identification:	S2-B
Measurement Date / Time:	3/4/2014 1:29:10 PM
Operator:	sutharp
Raw Data Origin:	XRD measurement (*.XRDML)
Scan Axis:	Gonio
Start Position [°2Th.]:	3.0003
End Position [°2Th.]:	69.9923
Step Size [°2Th.]:	0.0080
Scan Step Time [s]:	6.9850
Scan Type:	Continuous
Divergence Slit Type:	Fixed
Divergence Slit Size [°]:	0.5000
Specimen Length [mm]:	10.00
Measurement Temperature [°C]:	25.00
Anode Material:	Co
K-Alpha1 [Å]:	1.78901
K-Alpha2 [Å]:	1.79290
K-Beta [Å]:	1.62083
K-A2 / K-A1 Ratio:	0.50000
Generator Settings:	45 mA, 40 kV
Diffractometer Type:	0000000011116002
Diffractometer Number:	0
Goniometer Radius [mm]:	240.00
Dist. Focus-Diverg. Slit [mm]:	100.00
Spinning:	Yes

Graphics

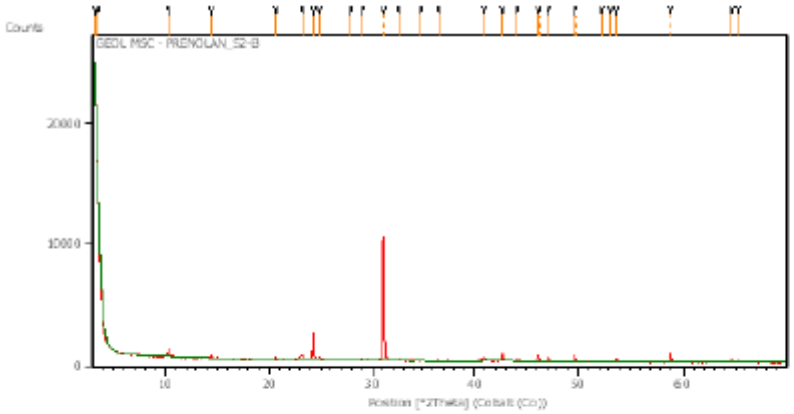

Peak List

Pos. [°2Th.]	Height [cts]	FWHM Left [°2Th.]	d-spacing [Å]	Rel. Int. [%]
3.1636	3128.11	0.0945	32.42801	30.80
3.9543	909.72	0.2834	29.69980	8.96
10.2785	599.41	0.0787	9.99321	5.90
14.3486	114.14	0.1889	7.16756	1.12
20.6314	199.47	0.0787	4.99885	1.96
23.2040	281.64	0.1102	4.45101	2.77
24.2662	2181.90	0.0472	4.25891	21.48

24.8037	52.99	0.2519	4.16803	0.52
27.8854	30.85	0.3779	3.71508	0.30
28.9943	67.02	0.1889	3.57587	0.66
31.0389	10156.37	0.0576	3.34313	100.00
32.5072	81.53	0.3072	3.19593	0.80
34.8165	53.85	0.4608	2.98987	0.53
36.4970	14.58	0.6144	2.85657	0.14
40.9570	263.27	0.2688	2.55678	2.59
42.7116	675.63	0.0576	2.45636	6.65
44.1180	39.57	0.4608	2.38178	0.39
46.1760	646.85	0.0480	2.28106	6.37
47.1591	340.26	0.0672	2.23614	3.35
49.7267	475.87	0.0576	2.12747	4.69
52.3203	38.11	0.2304	2.02890	0.38
53.1537	74.19	0.3072	1.99935	0.73
53.7181	247.83	0.0768	1.97988	2.44
58.9528	872.32	0.0768	1.81786	8.59
64.7237	235.70	0.0672	1.67115	2.32
65.3160	47.35	0.2304	1.65765	0.47

Anchor Scan Parameters

Dataset Name:	GEOL MSC - PRENOLAN_S2-W
File name:	C:\XRD Data\GEOL MSC - PRENOLAN_S2-W.xrdml
Sample Identification:	S2-W
Measurement Date / Time:	3/4/2014 2:03:04 PM
Operator:	sutharp
Raw Data Origin:	XRD measurement (*.XRDML)
Scan Axis:	Gonio
Start Position [°2Th.]:	3.0003
End Position [°2Th.]:	69.9923
Step Size [°2Th.]:	0.0080
Scan Step Time [s]:	6.9850
Scan Type:	Continuous
Divergence Slit Type:	Fixed
Divergence Slit Size [°]:	0.5000
Specimen Length [mm]:	10.00
Measurement Temperature [°C]:	25.00
Anode Material:	Co
K-Alpha1 [Å]:	1.78901
K-Alpha2 [Å]:	1.79290
K-Beta [Å]:	1.62083
K-A2 / K-A1 Ratio:	0.50000
Generator Settings:	45 mA, 40 kV
Diffractometer Type:	000000011116802
Diffractometer Number:	0
Goniometer Radius [mm]:	240.00
Dist. Focus-Diverg. Slit [mm]:	100.00
Spinning:	Yes

Graphics

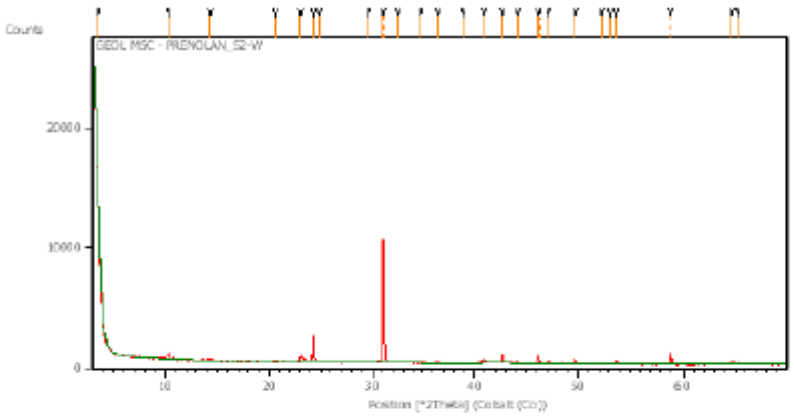

Peak List

Pos. [°2Th.]	Height [cts]	FWHMLeft[°2Th.]	d-spacing [Å]	Rel. Int. [%]
3.4993	593.89	0.1574	29.31790	5.80
10.2557	485.79	0.0472	10.01531	4.75
14.3105	79.80	0.2519	7.18661	0.78
20.5866	174.41	0.1574	5.00957	1.70
23.0323	328.78	0.2519	4.48374	3.21
24.2705	2044.88	0.0472	4.25815	19.98
24.8151	82.00	0.2519	4.16614	0.80

29.6306	71.24	0.1889	3.50074	0.70
31.0341	10235.76	0.0576	3.34363	100.00
32.4615	61.05	0.2304	3.20030	0.60
34.8290	56.82	0.3072	2.98883	0.56
36.4469	38.44	0.3072	2.86022	0.38
38.9131	19.77	0.6144	2.68546	0.19
40.9170	298.99	0.2304	2.55917	2.92
42.7082	704.11	0.0384	2.45655	6.88
44.1793	61.94	0.5376	2.37864	0.61
46.1680	621.62	0.0480	2.28143	6.07
47.1492	295.63	0.0576	2.23658	2.89
49.7391	420.08	0.0960	2.12697	4.10
52.3045	65.55	0.1536	2.02947	0.64
53.0991	34.83	0.2304	2.00126	0.34
53.7142	214.10	0.0576	1.98002	2.09
58.9529	913.04	0.0576	1.81786	8.92
64.7055	223.91	0.0768	1.67156	2.19
65.2456	77.29	0.1152	1.65924	0.76

Anchor Scan Parameters

Dataset Name:	GEOL MSC - PRENOLAN_S3-B
File name:	C:\XRD Data\GEOL MSC - PRENOLAN_S3-B.xrdml
Sample Identification:	S3-B
Measurement Date / Time:	3/4/2014 1:20:42 PM
Operator:	sutharp
Raw Data Origin:	XRD measurement (*.XRDML)
Scan Axis:	Gonio
Start Position [°2Th.]:	3.0003
End Position [°2Th.]:	69.9823
Step Size [°2Th.]:	0.0080
Scan Step Time [s]:	6.9850
Scan Type:	Continuous
Divergence Slit Type:	Fixed
Divergence Slit Size [°]:	0.5000
Specimen Length [mm]:	10.00
Measurement Temperature [°C]:	25.00
Anode Material:	Co
K-Alpha1 [Å]:	1.78901
K-Alpha2 [Å]:	1.79290
K-Beta [Å]:	1.62083
K-A2 / K-A1 Ratio:	0.50000
Generator Settings:	45 mA, 40 kV
Diffractometer Type:	00000000111116802
Diffractometer Number:	0
Goniometer Radius [mm]:	240.00
Dist. Focus-Diverg. Slit [mm]:	100.00
Spinning:	Yes

Graphics

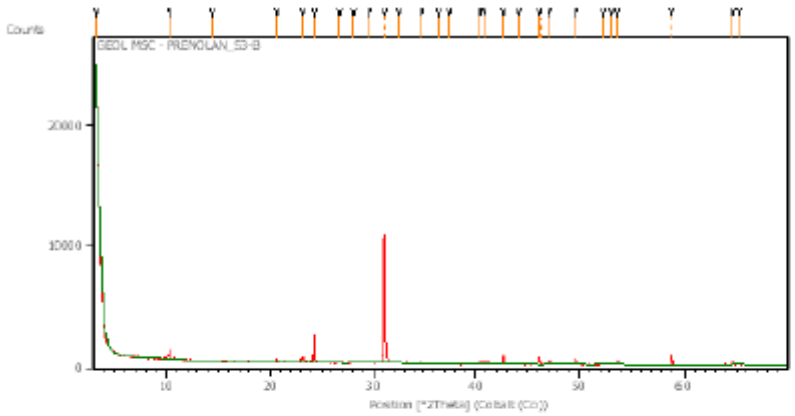

Peak List

Pos. [°2Th.]	Height [cts]	FWHM Left [°2Th.]	d-spacing [Å]	Rel. Int. [%]
3.1548	3111.22	0.1574	32.51920	29.87
10.2763	725.82	0.1102	9.99526	6.97
14.3644	54.07	0.3779	7.15979	0.52
20.6393	246.62	0.0945	4.99696	2.39
23.1522	351.32	0.2519	4.46083	3.37
24.2749	2218.04	0.0630	4.25741	21.29
26.7000	38.19	0.3779	3.87681	0.37

28.0636	79.47	0.0945	3.69196	0.76
29.6243	56.48	0.7557	3.50147	0.54
31.0376	10416.89	0.0576	3.34326	100.00
32.4519	90.21	0.3072	3.20123	0.87
34.8010	64.79	0.3840	2.99116	0.62
36.3985	36.15	0.4608	2.86404	0.35
37.9498	26.92	0.6144	2.78640	0.26
40.4309	110.53	0.2304	2.58863	1.06
40.8654	286.96	0.2688	2.56227	2.75
42.7056	709.41	0.0672	2.45669	6.81
44.1999	63.39	0.3072	2.37759	0.61
46.1742	617.39	0.0672	2.28115	5.93
47.1460	303.44	0.0768	2.23672	2.91
49.7121	454.96	0.0672	2.12805	4.37
52.3368	32.06	0.2304	2.02830	0.31
53.1359	94.70	0.2304	1.99997	0.91
53.7207	258.05	0.0768	1.97979	2.48
58.9541	955.40	0.0864	1.81762	9.17
64.6998	250.04	0.0960	1.67170	2.40
65.3039	67.98	0.3072	1.65792	0.65

Anchor Scan Parameters

Dataset Name:	GEOL MSC - PRENOLAN_S3-W
File name:	C:\XRD Data\GEOL MSC - PRENOLAN_S3-W.xrdml
Sample Identification:	S3-W
Measurement Date / Time:	3/4/2014 1:54:35 PM
Operator:	sutharp
Raw Data Origin:	XRD measurement (*.XRDML)
Scan Axis:	Gonio
Start Position [°2Th.]:	3.0003
End Position [°2Th.]:	69.9923
Step Size [°2Th.]:	0.0080
Scan Step Time [s]:	6.9850
Scan Type:	Continuous
Divergence Slit Type:	Fixed
Divergence Slit Size [°]:	0.5000
Specimen Length [mm]:	10.00
Measurement Temperature [°C]:	25.00
Anode Material:	Co
K-Alpha1 [Å]:	1.78901
K-Alpha2 [Å]:	1.79290
K-Beta [Å]:	1.62083
K-A2 / K-A1 Ratio:	0.50000
Generator Settings:	45 mA, 40 kV
Diffractometer Type:	0000000011116602
Diffractometer Number:	0
Goniometer Radius [mm]:	240.00
Dist. Focus-Diverg. Slit [mm]:	100.00
Spinning:	Yes

Graphics

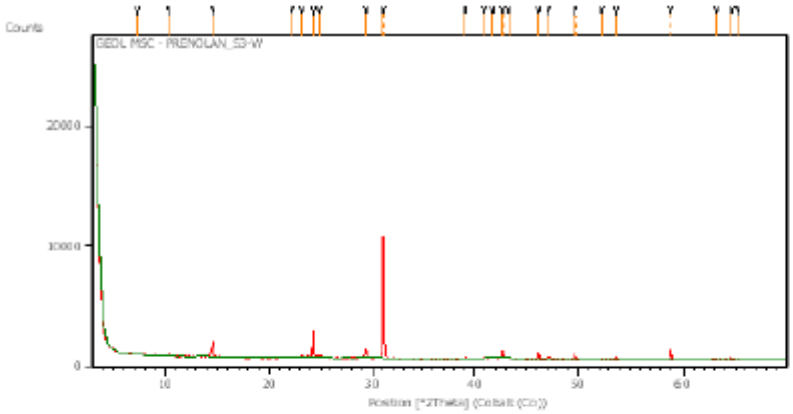

Peak List

Pos. [°2Th.]	Height [cts]	FWHM Left [°2Th.]	d-spacing [Å]	Rel. Int. [%]
7.2809	62.24	0.3779	14.09802	0.61
10.2476	100.27	0.2519	10.02322	0.98
14.5594	1362.50	0.0630	7.06441	13.38
22.1815	50.41	0.3779	4.65545	0.50
23.1412	72.26	0.3149	4.46292	0.71
24.2690	2152.91	0.0472	4.25844	21.15
24.8395	135.25	0.2834	4.16212	1.33

29.3407	720.77	0.1574	3.53456	7.08
31.0333	10180.86	0.0672	3.34372	100.00
39.1091	61.67	0.4608	2.67252	0.61
40.9382	58.69	0.3072	2.55791	0.58
41.7636	46.46	0.3840	2.50954	0.46
42.7028	647.69	0.0576	2.45685	6.36
43.2573	77.85	0.3072	2.42683	0.76
46.1624	540.50	0.0864	2.28169	5.31
47.1454	290.71	0.0768	2.23675	2.86
49.7162	446.68	0.0672	2.12789	4.39
52.3314	43.56	0.2304	2.02850	0.43
53.7110	224.05	0.0768	1.98013	2.20
58.9490	998.90	0.0672	1.81797	9.81
63.1937	17.22	0.7680	1.70727	0.17
64.6938	227.96	0.0960	1.67183	2.24
65.2331	86.33	0.1152	1.65952	0.85

Appendix B

1.1 Moisture content: Soil and Rock material

Table B.1: Moisture content.

	Tray (g)	Tray + Wet sample	Wet sample	Dry sample + tray	Dry sample	Moisture content
Cornubia Fresh	10	62	52	57.8	49.1	5.9
Cornubia Weathered	10	66	56	61.1	52.3	7.07
Locality 2 Fresh	10	61.6	51.6	59.4	49.4	4.45
Locality 2 Weathered	10	63.8	53.8	60.3	51.7	4.06
Locality 3 Fresh	12	64.4	52.4	61.9	49.9	5.01
Locality 3 Weathered	12	72.2	60.2	69.1	57.1	5.43
Locality 4 Fresh	12	70.8	58.8	65.7	55.8	5.38
Locality 4 Weathered	12	67.4	57.4	62.1	54.3	5.71
Soils						
Cornubia	12	513.6	501.6	457.5	445.5	12.59
Locality 3	12.1	524	511.9	472.1	466	9.85

2.1 Particle size: Sieve shaker

Table B.2: Particle size analyses using the sieve shaker.

			Sieve Size (mm)						
			4	2	0.425	0.25	0.125	0.093	0.063
Cornubia	a)	% Passing		53.45	25.19	4.84	5.61	3.55	7.36
		Cumulative	100	46.55	21.36	16.52	10.91	7.36	0
	b)	% Passing		48.63	25.94	7.5	5.6	3.19	9.08
		Cumulative	100	51.31	25.37	17.87	12.27	9.08	0
PMB Locality 3	a)	% Passing		42.26	35.78	7.33	7.63	3.24	3.78
		Cumulative	100	57.76	21.98	14.65	7.02	3.78	0
	b)	% Passing		42.24	34.75	8.97	7.47	4.69	1.86
		Cumulative	100	57.74	22.99	14.02	6.55	1.86	0

2.2 Malvern diffractometer

Table B.3: Malvern diffractometer results.

Size	**Cornubia development**		**Locality 3**	
	Percentage (%)	**Cumulative**	**Percentage (%)**	**Cumulative**
<63	74.01	74.01	67.80	67.80
<90	11.15	85.16	6.24	74.05
<125	11.49	96.66	5.32	79.37
<250	3.34	100	2.35	100

3 Atterberg limits

3.1 Liquid limit

Table B.4: Liquid limit of the soil samples from the Cornubia development**.**

Cornubia development					
Moisture content (%)	**No. of blows**	**Moisture content (%)**	**No. of blows**	**Moisture content (%)**	**No. of blows**
41	32	26.47	25	30	27
43	34	40	22	33	25
39	33	57.5	31	29	29
33	28	62.5	29	27	33
37	27	24.39	24	24	32
40	26	26	27	30	27

Table B.5: Liquid limit of the soil samples from Locality 3.

Locality 3					
Moisture content (%)	**No. of blows**	**Moisture content (%)**	**No. of blows**	**Moisture content (%)**	**No. of blows**
29	26	27	33	42	38
33	31	30	27	36.11	38
30	28	29.3	30	31.03	36
29	25	29.7	26	27.2	32
28	23	26.39	28	16.45	28
35	30	27.3	20		

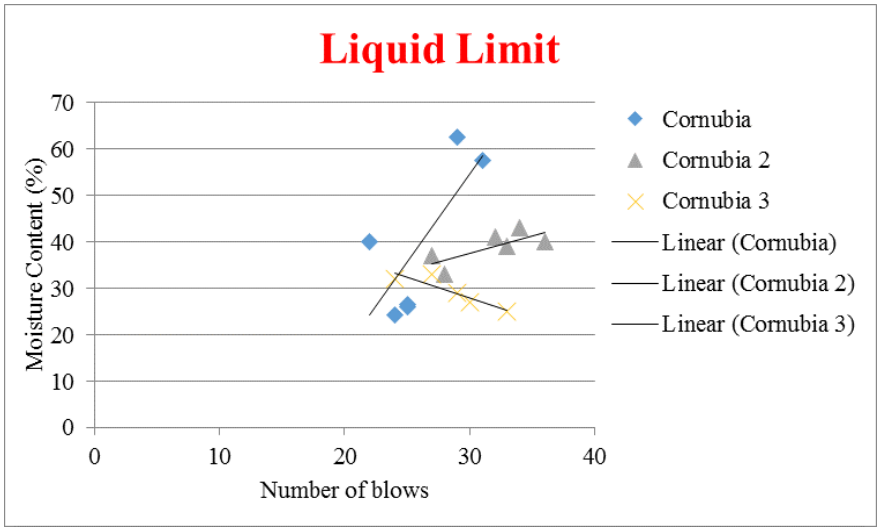

Figure B.1: Liquid limit plot of the soil samples from the Cornubia Development.

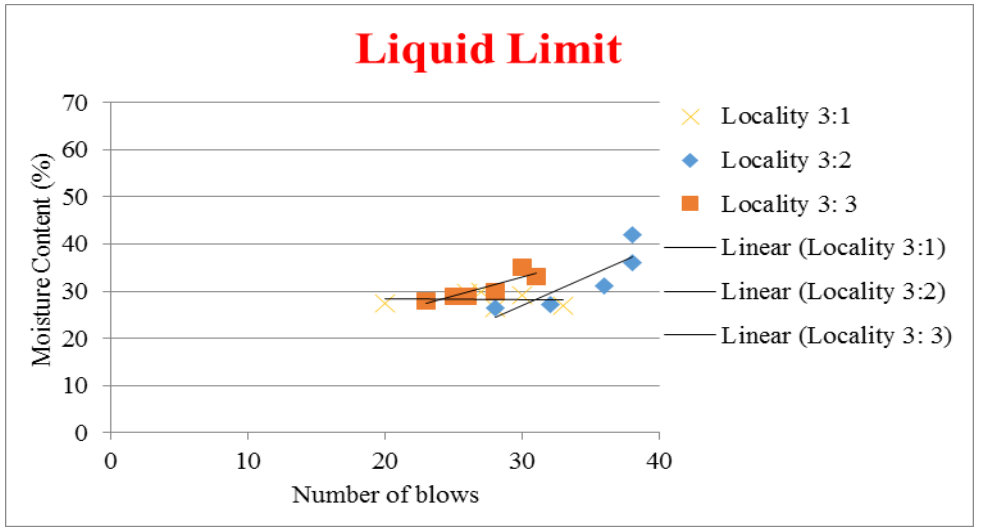

Figure B.2: Liquid limit plot of the soil samples from Locality 3.

3.2 Plastic Limit

Table B.6: Plastic limits test of the soil samples from Localities 1 and 3.

	Tray (g)	Tray + Wet Sample (g)	Wet Sample (g)	Dry sample + Tray (g)	Dry Sample (g)	Moisture content (%)	Average
PL Cor 1	2.5	13.9	11.4	11.7	9.2	23.91	
PL Cor 2	2.5	14.9	12.4	12.4	9.9	25.25	23
PL Cor 3	2.9	14.57	11.67	12.6	9.7	20.3	
PL Loc 3-1	2.4	12.65	10.25	10.2	7.96	23.49	
PL Loc 3-2	2.4	12.7	10.3	10.7	8.56	20.4	19
PL Loc 3-3	2.4	12.02	9.62	10.7	8.36	15	

B.4 Slake durability

Table B.6: Slake durability results.

Cornubia	Original weight	Day 1	Day 2	Day 3	Day 4	Day 5	SDI (%)
Fresh : Ethylene glycol							
1	449	447.2	446.1	445.2	444.4	431.6	96.12
2	443.2	433.4	432.2	430.3	428	422.5	95.32
3	417.4	408.8	408.1	412.4	411	409.1	98.81
4	406.5	394	392.1	389.7	387.7	386.8	95.15
5	408.1	398.2	399.3	394.9	392.1	387.3	94.90
6	428.5	419.5	415.2	412.7	411.6	410.2	95.72
7	408.3	398.4	395	392.1	391	390.2	95.56
Water							
1	431	425.7	422	409	405.4	401.3	93.10
2	410	396.7	396.6	395.8	394.7	394.2	96.14
3	411.5	398	397	396.7	395.4	393.9	95.72
4	413.3	398.1	397.7	397	396.6	396	95.81
5	434.4	418.3	417.3	416.5	415.6	414.8	95.48
6	407.5	394.3	393.3	392.4	391.4	389.7	95.63
7	402.8	387.5	387.2	386.3	385.9	389.2	96.62
Weathered: Water							
1	425.7	411.9	410.9	409.4	408.8	407	95.45

2	424.3	404.9	398.3	396.9	396.4	393	92.62
3	415.8	397.6	395.8	394.3	393.4	392.8	94.46
4	413.8	395.3	392.6	396.6	391	389.4	94.10
5	419.2	399	396.2	394.1	393.9	391	93.27
6	429.8	401.5	398.1	395.6	392.5	391.1	90.99
7	425.5	405	403.2	400.6	385.8	385.8	90.96
Weathered: Ethylene glycol							
1	430	429.2	421.3	402.7	391	383.4	89.16
2	411.4	387.3	375.3	382.2	372.9	372.4	90.52
3	415.5	397	391.6	377.6	362.8	362.5	87.24
4	410.8	392.1	386	379.6	363.6	363	88.36
5	402.5	393.3	384.7	378.5	363.3	362.8	90.13
6	414.1	399.2	385.2	378.4	372.1	371	89.59
7	413.8	394.1	382	365.7	367.7	367	88.69
Locality 2				**Fresh: Water**			
1	402	392.8	390.8	385.9	385	384.6	95.67
2	440.5	429.5	427.7	421.3	420.6	420	95.34
3	422.7	412.7	412.7	412.8	402.2	401.4	94.96
4	419.6	414.3	413	412.8	411.4	410	97.71
5	425.4	414.6	413.4	412.7	411.6	411.03	96.62
6	411.7	410.8	398.6	397.22	394.8	394.01	95.70

Ethylene glycol							
1	419	410.7	409.3	408.03	403.6	395	95.94
2	414.2	404.9	403.6	402.9	401.4	400.7	96.74
3	414.4	405	403.5	402.5	402.1	401	96.76
4	421.4	412.6	413.6	408.6	407.1	404	95.87
5	420.7	414.5	411.4	411	409.2	408.9	97.50
6	403.4	396.3	395.3	393.9	390.2	389.6	96.57
Weathered: Water							
1	402.6	393.8	390	389.4	389.1	388.6	96.52
2	459.7	430.7	429.7	419.3	418	417.19	90.75
3	454.8	421.6	421.4	420	419.4	419	92.12
4	427.5	418.1	417	416.5	417.4	416.53	97.43
5	442	437.3	430.6	408.2	406.8	406.3	91.92
Ethylene glycol							
1	422.8	409.3	408.4	407.3	406.8	406	96.02
2	405.9	397.2	396	395	395.1	394.6	97.21
3	418.2	406.2	404.5	403.8	402.8	402.3	96.19
4	420.8	413.2	390.7	390.6	389	388.4	92.30
5	414	412.6	410.3	408.9	408.2	402.6	97.25
Locality 3				**Fresh: Water**			
1	420.2	412.9	411.9	410.5	408.5	401	95.43
2	416.1	407.3	402.7	406.3	396.6	396	95.16

3	432	418	414.9	413.6	412.9	412	95.37
4	402.1	393.3	391	383.3	378	377.1	93.78
5	414.4	410.2	402.9	400.9	399.8	399.1	96.30
6	409.2	406.5	404.8	403.7	402.65	402	98.24
7	426.3	421.8	413.4	409.7	410.7	410.1	96.19
Ethylene glycol							
1	401.8	395.1	395.3	394	391.7	391.2	97.36
2	417.7	411.9	411.1	411.3	410.1	409.6	98.06
3	411.5	405.4	403.1	402.1	401.8	401.3	97.52
4	412.5	406.4	404.6	404.7	404	403.5	97.81
5	416.8	407.7	403	401.6	398.6	397.1	95.27
6	410.9	403	393.9	393.5	394.3	394.7	96.05
7	416.6	409.1	407	406.8	405.3	404.2	97.02
Weathered: Water							
1	443.7	420.7	411.2	411.3	411.7	410	92.40
2	428.2	416.2	412.3	411.6	409.8	409.2	95.56
3	411.1	395.9	392.4	392.5	392.3	391.4	95.20
4	423	408.6	404.9	401.4	409	408.2	96.50
5	403.2	392	390.1	390	386.7	382.6	94.89
6	428.2	413.2	412.3	408.3	399	397.8	92.90
7	420.9	409.8	406.6	406.3	404.4	401	95.27
Ethylene glycol							

1	416.6	409.2	407.6	407.9	406.8	404	96.97
2	417.3	410.5	410.1	409	408.2	407.1	97.55
3	415.8	393.1	391.9	391.1	391.6	390.23	93.85
4	427.9	418.3	415.9	414.4	408.3	406.6	95.02
5	426.2	418.9	417.9	416.5	415.8	414	97.13
6	409.3	398	394.2	395.5	393.81	393.12	96.04
7	423	415.8	414.8	407.8	402.3	401.1	94.82
Locality 4				**Fresh: Water**			
1	434.4	418.9	416.7	415.6	414.9	414	95.30
2	450.4	436	433.4	429	428.6	428.01	95.02
3	416.8	414.8	409.7	406.7	405.3	403.9	96.90
4	442.4	427.45	425.05	422.3	421.75	421	95.16
Ethylene glycol							
1	440.3	426.8	425.8	425.2	424.8	424.26	96.35
2	448.3	441.3	440.8	440.1	439.3	438.6	97.83
3	460.5	458.2	457.3	455.1	451	448.3	97.35
4	444.3	434.05	433.3	432.65	432.05	431.43	95.16
Weathered: Water							
1	423	416.4	415.9	414.8	414.2	413.4	97.73
2	411.9	402.2	402	401.2	400.6	399.7	97.03
3	426.5	417.7	416.9	414.8	515.2	413.6	96.97
4	417.45	407.8	401.6	399.2	396.9	394	94.38

Ethylene glycol							
1	434.3	427.5	423.3	420.1	418.7	418	96.24
2	432.6	424.9	425.4	424.9	424.3	422	97.54
3	407.9	402.9	400.9	399.8	397.9	397.1	97.35
4	433.45	426.2	424.35	422.5	421.5	420	96.89

B.5: Point Load strength

Table B.7: Axial Point Load Strength.

Locality	Sample	Height (mm)	Diameter (mm)	Pressure @ failure (MPa)	Area of cylinder (m^2)	Area of the core (m^2)	Load @ failure (kN)	De^2 (mm)	F	Is (MPa)	I_s50 (MPa)
Axial											
Fresh											
1	1	16	56	2.45916	0.001782	7740.88	4.38	1141.401	0.82	3.84	3.15
	2	17	56	2.54826	0.001782	7916	4.54	1212.739	0.85	3.74	3.18
	3	17	56	2.60172	0.001782	7916	4.63	1212.739	0.85	3.82	3.25
	4	18	56	2.69082	0.001782	8092.74	4.79	1284.076	0.86	3.73	3.21
	5	20	56	2.77992	0.001782	8444.60	4.95	1426.752	0.88	3.47	3.06
3	1	18	56	2.92248	0.001782	8092.74	5.20	1284.076	0.86	4.06	3.49
	2	19	56	2.61954	0.001782	8268.67	4.66	1355.414	0.87	3.44	3.00
	3	21	56	2.83338	0.001782	8620.53	5.04	1498.089	0.89	3.37	3.00
	4	16	56	3.2076	0.001782	7740.88	5.71	1141.401	0.82	5.01	4.11
	5	16	56	3.43926	0.001782	7740.88	6.12	1141.401	0.82	5.37	4.40
Weathered											
1	1	18	56	2.01366	0.001782	8092.74	3.59	1284.076	0.86	2.79	2.40
	2	20	56	1.9602	0.001782	8444.60	3.49	1426.752	0.88	2.45	2.15
	3	21	56	1.88892	0.001782	8620.53	3.37	1498.089	0.89	2.25	2.00
	4	16	56	1.97802	0.001782	7740.88	3.52	1141.401	0.82	3.09	2.53

	5	18	56	2.19186	0.001782	8092.74	3.91	1284.076	0.86	3.04	2.62
3	1	17	56	2.37006	0.001782	7916	4.22	1212.739	0.85	3.48	2.96
	2	19	56	2.24532	0.001782	8268.67	4.00	1355.414	0.87	2.95	2.57
	3	19	56	2.4057	0.001782	8268.67	4.29	1355.414	0.87	3.16	2.75
	4	20	56	2.29878	0.001782	8444.60	4.10	1426.752	0.88	2.87	2.53
	5	17	56	2.44134	0.001782	7916	4.35	1212.739	0.85	3.59	3.05

Table B.8: Diametrical Point Load Strength**.**

Locality	**Sample**	**Height (mm)**	**Diameter (mm)**	**Pressure @ failure (MPa)**	**Area of cylinder (m^2)**	**Load @ failure (kN)**	**De^2 (mm)**	**I_s (MPa)**	**F**	**I_s50 (MPa)**
Diametrical										
Fresh										
3	1	65	56	2.45916	0.001782	4.38	3136	1.40	1.06	1.48
	2	67	56	2.54826	0.001782	4.54	3136	1.45	1.06	1.54
	3	70	56	2.60172	0.001782	4.64	3136	1.48	1.06	1.57
	4	69	56	2.69082	0.001782	4.80	3136	1.53	1.06	1.62
	5	71	56	2.77992	0.001782	4.95	3136	1.58	1.06	1.67
1	1	72	56	2.56608	0.001782	4.57	3136	1.46	1.06	1.55
	2	68	56	2.72646	0.001782	4.86	3136	1.55	1.06	1.64
	3	67	56	2.19186	0.001782	3.91	3136	1.25	1.06	1.33
	4	70	56	2.38788	0.001782	4.26	3136	1.36	1.06	1.44
	5	70	56	2.45916	0.001782	4.38	3136	1.40	1.06	1.48

Weathered										
1	1	70	56	1.83546	0.001782	3.27	3136	1.04	1.06	1.10
	2	69	56	1.76418	0.001782	3.14	3136	1.00	1.06	1.06
	3	67	56	1.83546	0.001782	3.27	3136	1.04	1.06	1.10
	4	68	56	1.63944	0.001782	2.92	3136	0.93	1.06	0.99
	5	65	56	1.58598	0.001782	2.83	3136	0.90	1.06	0.95
3	1	66	56	1.81764	0.001782	3.24	3136	1.03	1.06	1.09
	2	67	56	1.9602	0.001782	3.49	3136	1.11	1.06	1.18
	3	70	56	1.67508	0.001782	2.98	3136	0.95	1.06	1.01
	4	39	56	1.88892	0.001782	3.37	3136	1.07	1.06	1.13
	5	68	56	1.94238	0.001782	3.46	3136	1.10	1.06	1.17

Appendix C: Shear box

C.1 Calculations

The following equations were used to convert the data recorded by the computer recording programme (Agilent Plus) for the shear box calculations:

Load applied: Pressure = Force/ Area

Force = 75 kN/m^2 * 0.110 m^2

= 8.18 kN Equation C.1

To convert the force to voltage: 8.18 * 4.046 mV = 33.10 Equation C.2

NB: The same procedure was applied for the shear stresses of 150 kN/m^2 and 300 kN/m^2 to calculate the normal force to be applied.

Area: 0.12 m^2, however, since the normal force is not distributed across the entire sample, an assumed contact of 95% results in an area of 0.110 m^2

Horizontal displacement: (spread sheet value * -7.6) + 25 Equation C.3

(NB. Horizontal displacement is displayed as the cumulative value which represents the actual displacement between two recordings of displacement). Furthermore, horizontal displacement values that display negative values are multiplied by -1 to obtain a positive value after the calculation is made.

Shear stress: [(spread sheet value * 1000) * (0.2501) + (-0.2989)]/ Area Equation C.4

C.2 Remainder of the shear stress vs horizontal displacement curves and the shear stress vs normal stress curves

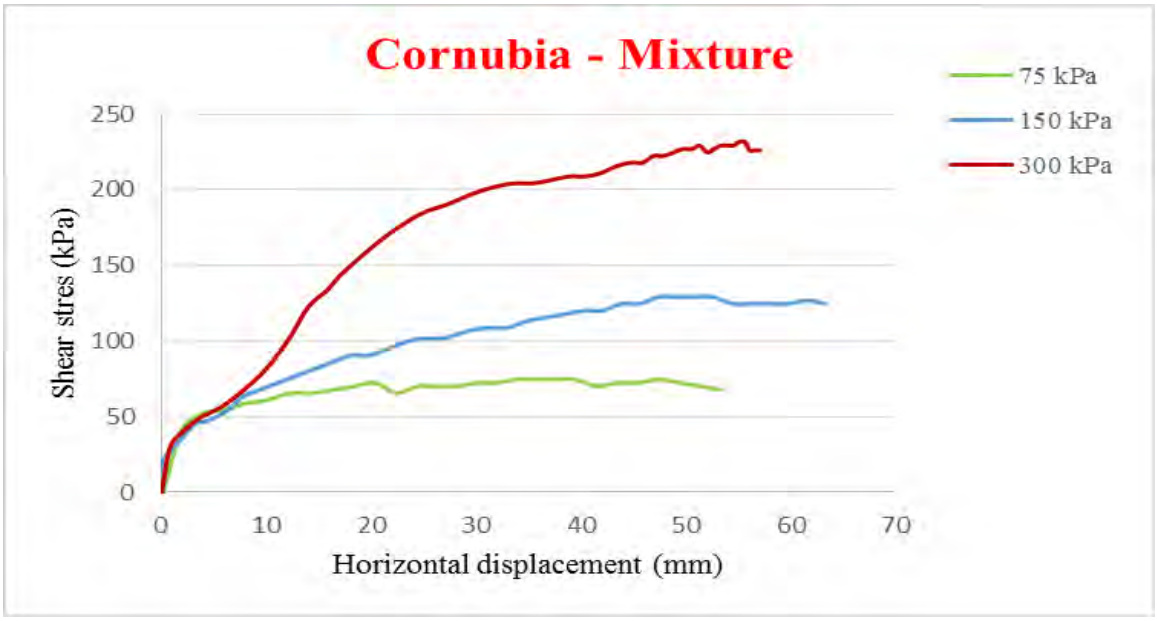

Figure C.1: Shear stress vs horizontal displacement cures for the mixed material from the Cornubia development.

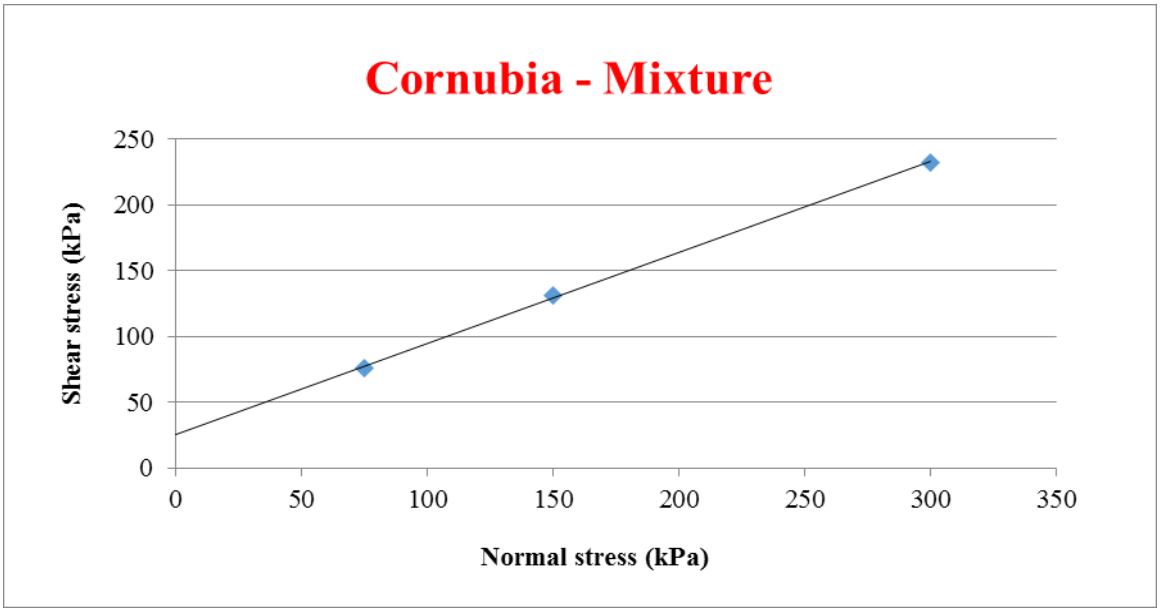

Figure C2: Shear stress vs normal stress for the mixed material from the Cornubia development.

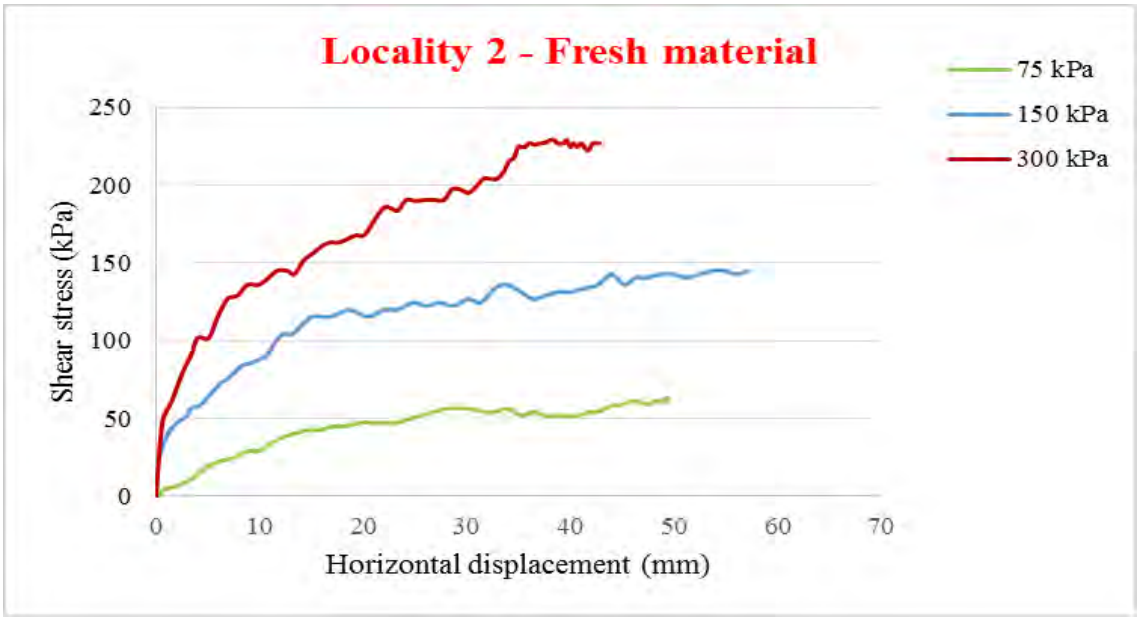

Figure C.3: Shear stress vs horizontal displacement curves for the fresh material from Locality 2.

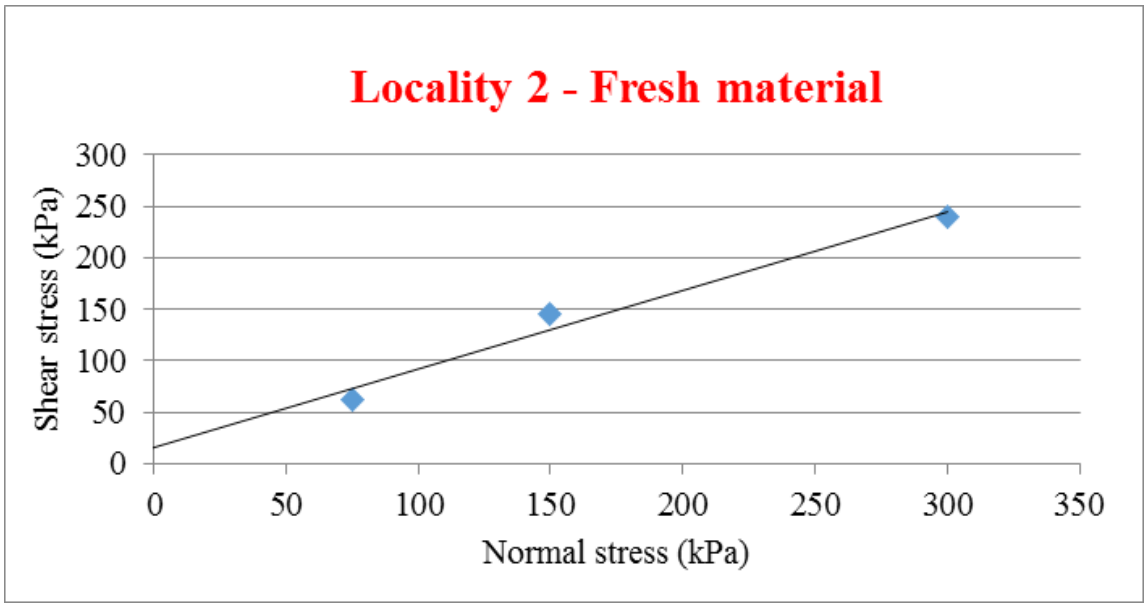

Figure C.4: Shear stress vs normal stress for the fresh material from Locality 2.

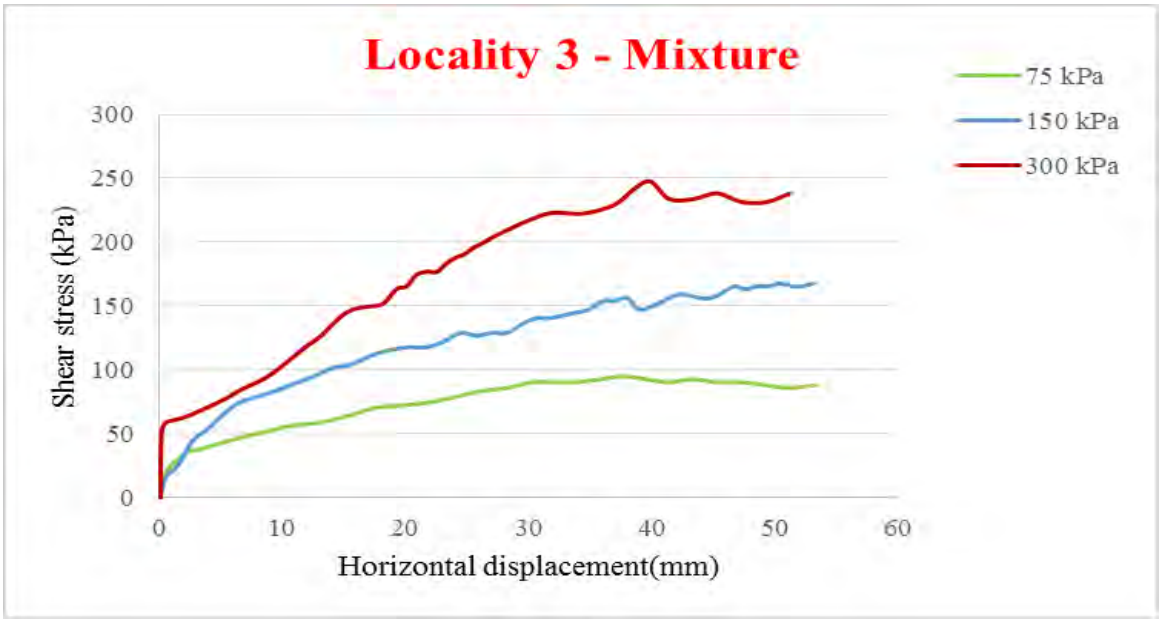

Figure C.5: Shear stress vs horizontal displacement curves for the mixed material from Locality 3.

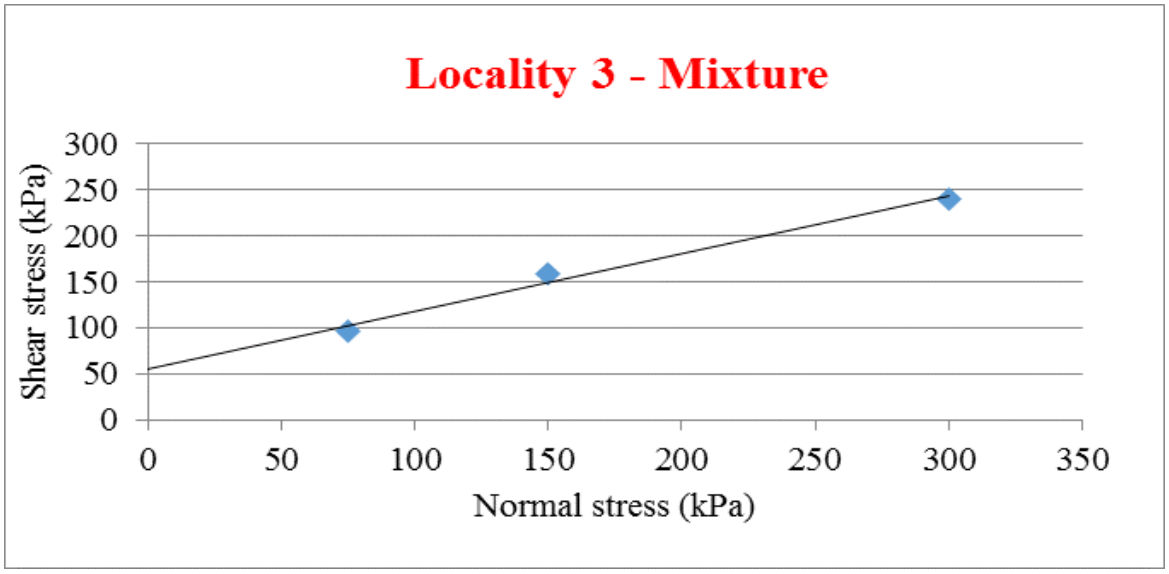

Figure C.6: Shear stress vs normal stress for the mixed material from Locality 3.

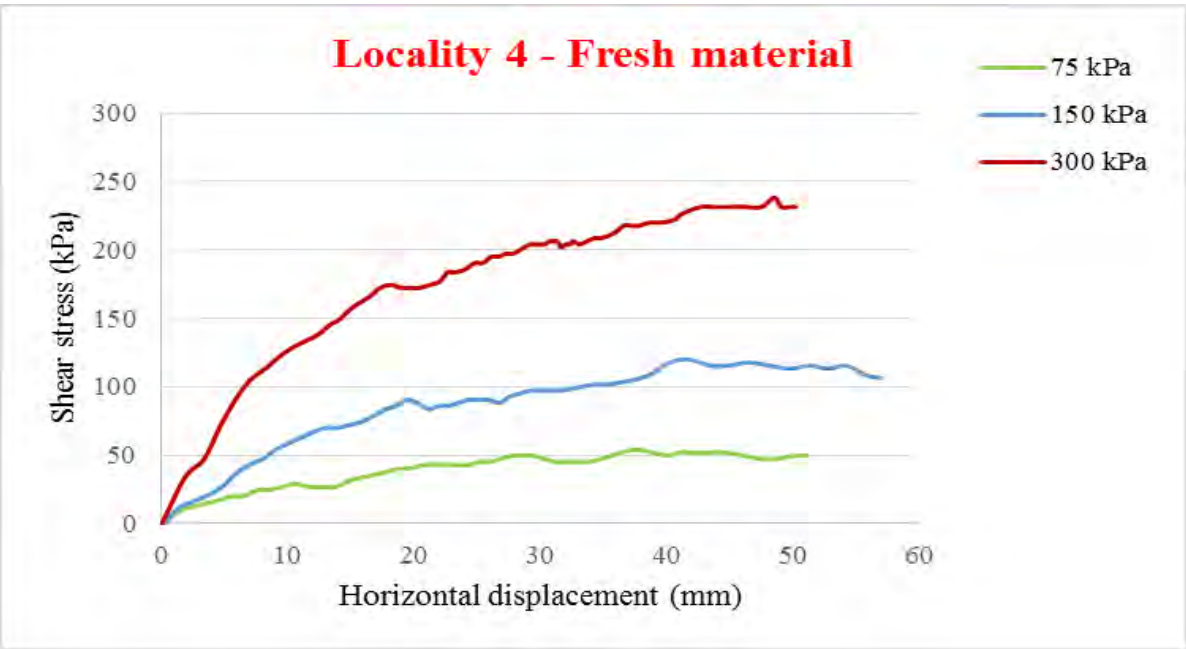

Figure C.7: Shear stress vs horizontal displacement curves for the fresh material from Locality 4.

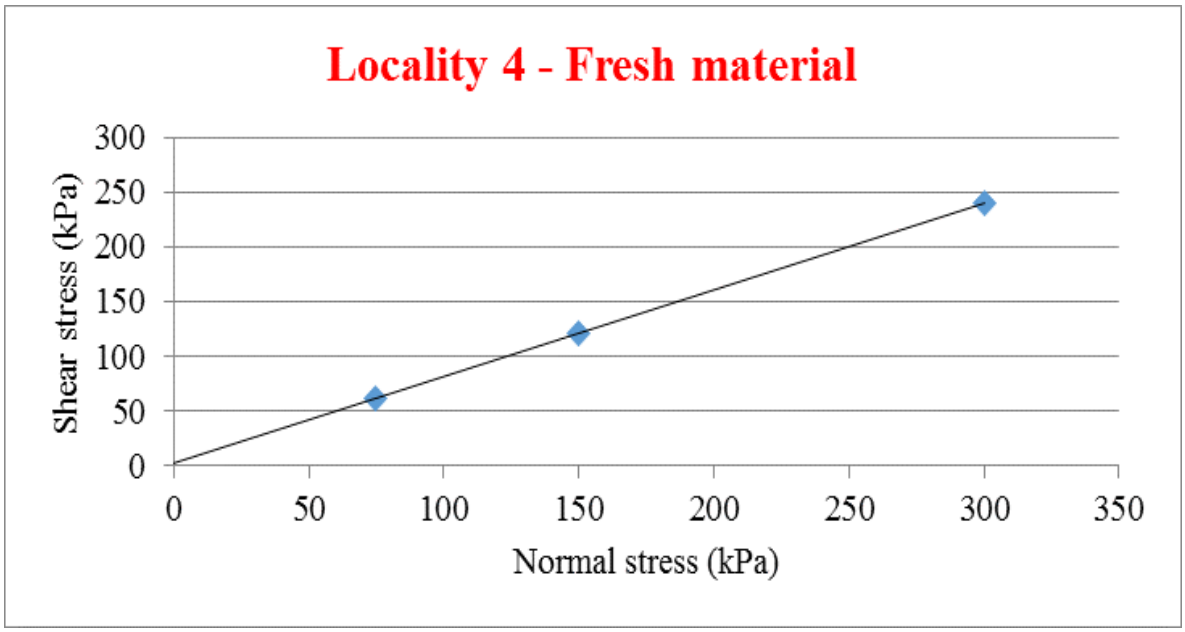

Figure C.8: Shear stress vs normal stress for the fresh material from Locality 4.

Table C.1: Shear box results for the fresh shale material from the Cornubia development.

75 kPa				150 kPa				300 kPa			
Shear load (mV)	**Shear stress (kPa)**	**Hori disp. (mV)**	**Hori disp. (mm)**	**Shear load (mV)**	**Shear stress (kPa)**	**Hori disp. (mV)**	**Hori disp. (mm)**	**Shear load (mV)**	**Shear stress (kPa)**	**Hori disp. (mV)**	**Hori disp. (mm)**
0.000	0.000	0.000	0.000	0.000	0.000	0.000	0.000	0.000	0.000	0.000	0.000
0.014	29.114	2.641	1.277	0.051	113.238	0.344	1.470	0.051	113.238	1.824	0.665

0.020	42.755	2.423	2.933	0.054	120.059	0.234	2.306	0.058	129.154	1.651	1.977
0.022	47.303	2.230	4.396	0.058	129.154	0.032	3.839	0.062	138.248	1.495	3.163
0.024	51.850	2.027	5.941	0.058	129.154	-0.114	4.948	0.066	147.343	1.353	4.246
0.027	58.671	1.835	7.400	0.060	133.701	-0.223	5.774	0.070	156.437	1.224	5.226
0.028	60.945	1.655	8.766	0.062	138.248	-0.367	6.873	0.072	160.985	1.101	6.157
0.029	63.218	1.450	10.324	0.064	142.795	-0.570	8.418	0.075	167.805	0.984	7.046
0.029	63.218	1.269	11.702	0.066	147.343	-0.769	9.927	0.078	174.626	0.877	7.864
0.031	67.765	1.094	13.032	0.068	151.890	-0.961	11.385	0.080	179.174	0.776	8.628
0.033	72.313	0.914	14.400	0.068	151.890	-1.159	12.889	0.081	181.447	0.677	9.385
0.033	72.313	0.752	15.628	0.069	154.164	-1.356	14.386	0.082	183.721	0.587	10.066
0.033	72.313	0.581	16.928	0.069	154.164	-1.554	15.892	0.083	185.995	0.500	10.727
0.034	74.586	0.416	18.187	0.069	154.164	-1.748	17.368	0.084	188.268	0.418	11.353
0.034	74.586	0.247	19.469	0.069	154.164	-1.942	18.839	0.086	192.815	0.335	11.980
0.034	74.586	0.076	20.769	0.071	158.711	-2.132	20.284	0.086	192.815	0.261	12.543
0.035	76.860	-0.091	22.040	0.072	160.985	-2.314	21.670	0.088	197.363	0.187	13.105
0.035	76.860	-0.265	23.357	0.073	163.258	-2.493	23.029	0.088	197.363	0.117	13.642
0.035	76.860	-0.433	24.634	0.074	165.532	-2.677	24.431	0.089	199.636	0.045	14.186
0.036	79.134	-0.606	25.952	0.074	165.532	-2.847	25.720	0.090	201.910	-0.022	14.693
0.037	81.407	-0.772	27.210	0.075	167.805	-3.022	27.051	0.093	208.731	-0.080	15.135
0.038	83.681	-0.943	28.515	0.075	167.805	-3.183	28.274	0.094	211.005	-0.136	15.562
0.038	83.681	-1.112	29.797	0.074	165.532	-3.326	29.364	0.095	213.278	-0.193	15.992
0.038	83.681	-1.290	31.147	0.075	167.805	-3.473	30.479	0.095	213.278	-0.248	16.415
0.038	83.681	-1.455	32.406	0.076	170.079	-3.609	31.512	0.095	213.278	-0.313	16.904
0.039	85.955	-1.641	33.816	0.077	172.353	-3.739	32.502	0.096	215.552	-0.393	17.513
0.039	85.955	-1.827	35.233	0.079	176.900	-3.871	33.504	0.098	220.099	-0.492	18.264
0.037	81.407	-2.105	37.344	0.079	176.900	-3.984	34.361	0.098	220.099	-0.611	19.172
0.039	85.955	-2.294	38.783	0.080	179.174	-4.082	35.104	0.099	222.373	-0.152	15.679
0.040	88.228	-2.521	40.509	0.079	176.900	-4.187	35.905	0.101	226.920	-0.266	16.549
0.039	85.955	-2.763	42.344	0.079	176.900	-4.280	36.614	0.103	231.467	-0.400	17.567
0.040	88.228	-2.984	44.026	0.078	174.626	-4.368	37.282	0.106	238.288	-0.591	19.016
0.039	85.955	-3.230	45.892	0.079	176.900	-4.437	37.805	0.106	238.288	-0.746	20.195
0.039	85.955	-3.459	47.637	0.079	176.900	-4.477	38.108	0.108	242.835	-0.871	21.145
0.039	85.955	-3.633	48.957	0.079	176.900	-4.465	38.016	0.108	242.835	-1.010	22.202
0.039	85.955	-3.820	50.376	0.078	174.626	-4.498	38.271	0.106	238.288	-1.183	23.521
0.039	85.955	-3.989	51.664	0.078	174.626	-4.519	38.424	0.106	238.288	-1.303	24.434
0.038	83.681	-4.153	52.907	0.079	176.900	-4.554	38.690	0.107	240.562	-1.442	25.489
0.038	83.681	-4.318	54.163	0.078	174.626	-4.555	38.704	0.107	240.562	-1.574	26.489

0.039	85.955	-4.425	54.979	0.077	172.353	-4.554	38.694	0.108	242.835	-1.699	27.443
0.037	81.407	-4.517	55.677	0.079	176.900	-4.547	38.639	0.109	245.109	-1.809	28.276
0.038	83.681	-4.548	55.908	0.078	174.626	-4.542	38.599	0.110	247.383	-1.912	29.060
0.038	83.681	-4.560	55.999	0.077	172.353	-4.550	38.665	0.110	247.383	-2.010	29.807
0.038	83.681	-4.561	56.009	0.078	174.626	-4.535	38.547	0.111	249.656	-2.107	30.543
								0.112	251.930	-2.190	31.173
								0.113	254.204	-2.267	31.754
								0.113	254.204	-2.342	32.329
								0.114	256.477	-2.396	32.739
								0.114	256.477	-2.448	33.131
								0.114	256.477	-2.497	33.503
								0.113	254.204	-2.559	33.976
								0.112	251.930	-2.633	34.542
								0.112	251.930	-2.711	35.130
								0.112	251.930	-2.789	35.721
								0.113	254.204	-2.861	36.273
								0.113	254.204	-2.927	36.769
								0.112	251.930	-2.966	37.072
								0.110	247.383	-3.075	37.894
								0.112	251.930	-3.157	38.519
								0.112	251.930	-3.230	39.074
								0.112	251.930	-3.301	39.619
								0.112	251.930	-3.367	40.116
								0.110	247.383	-3.473	40.924
								0.108	242.835	-3.571	41.666
								0.109	245.109	-3.710	42.726
								0.108	242.835	-3.832	43.652
								0.108	242.835	-3.948	44.531
								0.108	242.835	-4.065	45.425
								0.107	240.562	-4.195	46.408
								0.107	240.562	-4.304	47.240
								0.106	238.288	-4.376	47.789
								0.105	236.015	-4.418	48.107
								0.106	238.288	-4.457	48.403
								0.107	240.562	-4.490	48.651
								0.107	240.562	-4.494	48.680
								0.107	240.562	-4.497	48.704

								0.107	240.562	-4.508	48.791
								0.108	242.835	-4.511	48.808

Table C.2: Shear box results for the weathered shale material from the Cornubia development.

75 kPa				150 kPa				300 kPa			
Shear load (mV)	**Shear stress (kPa)**	**Hori disp. (mV)**	**Hori disp. (mm)**	**Shear load (mV)**	**Shear stress (kPa)**	**Hori disp. (mV)**	**Hori disp. (mm)**	**Shear load (mV)**	**Shear stress (kPa)**	**Hori disp. (mV)**	**Hori disp. (mm)**
0.000	0.000	0.000	0.000	0.000	0.000	0.000	0.000	0.000	0.000	0.000	0.000
0.0005	-1.580	3.191	-0.067	0.011	22.293	2.086	0.881	0.021	45.029	2.264	1.291
0.008	15.472	3.124	0.440	0.014	29.114	1.950	1.922	0.035	76.860	2.107	2.487
0.010	20.019	3.042	1.068	0.015	31.387	1.868	2.541	0.042	92.775	1.957	3.622
0.012	24.566	2.899	2.151	0.017	35.935	1.709	3.752	0.047	104.144	1.810	4.742
0.016	33.661	2.744	3.336	0.018	38.208	1.520	5.190	0.052	115.512	1.676	5.759
0.020	42.755	2.589	4.506	0.021	45.029	1.359	6.410	0.056	124.606	1.563	6.621
0.021	45.029	2.451	5.563	0.025	54.124	1.213	7.517	0.06	133.701	1.449	7.485
0.023	49.576	2.278	6.875	0.029	63.218	1.111	8.295	0.063	140.522	1.346	8.268
0.025	54.124	2.141	7.914	0.032	70.039	0.982	9.274	0.065	145.069	1.252	8.984
0.026	56.397	1.989	9.068	0.034	74.586	0.854	10.248	0.066	147.343	1.157	9.705
0.028	60.945	1.831	10.274	0.036	79.134	0.725	11.230	0.068	151.890	1.067	10.386
0.030	65.492	1.705	11.231	0.037	81.407	0.600	12.181	0.069	154.164	0.980	11.052
0.031	67.765	1.565	12.291	0.038	83.681	0.475	13.125	0.071	158.711	0.906	11.614
0.033	72.313	1.432	13.304	0.040	88.228	0.352	14.062	0.073	163.258	0.832	12.177
0.033	72.313	1.311	14.224	0.042	92.775	0.230	14.987	0.075	167.805	0.764	12.691
0.034	74.586	1.182	15.202	0.043	95.049	0.112	15.887	0.076	170.079	0.701	13.169
0.035	76.860	1.061	16.125	0.044	97.323	-0.002	16.753	0.077	172.353	0.642	13.619
0.036	79.134	0.946	16.999	0.044	97.323	-0.114	17.602	0.079	176.900	0.581	14.082
0.037	81.407	0.829	17.887	0.045	99.596	-0.227	18.460	0.079	176.900	0.537	14.417
0.037	81.407	0.711	18.780	0.045	99.596	-0.338	19.306	0.08	179.174	0.480	14.853
0.038	83.681	0.597	19.646	0.047	104.144	-0.450	20.161	0.081	181.447	0.422	15.292
0.037	81.407	0.484	20.509	0.048	106.417	-0.565	21.030	0.082	183.721	0.360	15.762
0.038	83.681	0.373	21.350	0.048	106.417	-0.679	21.898	0.084	188.268	0.301	16.212
0.039	85.955	0.262	22.197	0.048	106.417	-0.786	22.710	0.086	192.815	0.236	16.703
0.040	88.228	0.152	23.032	0.048	106.417	-0.896	23.547	0.088	197.363	0.158	17.300
0.040	88.228	0.043	23.863	0.048	106.417	-1.008	24.399	0.09	201.910	0.078	17.904
0.040	88.228	-0.066	24.692	0.050	110.965	-1.117	25.227	0.091	204.184	0.008	18.434
0.040	88.228	-0.176	25.521	0.050	110.965	-1.220	26.012	0.091	204.184	-0.034	18.754
0.041	90.502	-0.281	26.325	0.051	113.238	-1.331	26.853	0.091	204.184	-0.067	19.004
0.041	90.502	-0.386	27.121	0.052	115.512	-1.447	27.739	0.091	204.184	-0.102	19.277

0.041	90.502	-0.493	27.933	0.053	117.785	-1.610	28.977	0.091	204.184	-0.140	19.563
0.042	92.775	-0.601	28.754	0.052	115.512	-1.746	30.008	0.092	206.457	-0.172	19.804
0.042	92.775	-0.705	29.546	0.052	115.512	-1.890	31.103	0.092	206.457	-0.202	20.035
0.043	95.049	-0.809	30.338	0.053	117.785	-2.018	32.077	0.092	206.457	-0.229	20.240
0.043	95.049	-0.917	31.154	0.051	113.238	-2.159	33.145	0.093	208.731	-0.252	20.416
0.043	95.049	-1.019	31.933	0.051	113.238	-2.283	34.087	0.094	211.005	-0.297	20.758
0.043	95.049	-1.125	32.734	0.051	113.238	-2.432	35.220	0.096	215.552	-0.360	21.234
0.043	95.049	-1.240	33.609	0.052	115.512	-2.570	36.270	0.097	217.825	-0.476	22.115
0.042	92.775	-1.349	34.441	0.052	115.512	-2.705	37.293	0.098	220.099	-0.606	23.101
0.041	90.502	-1.492	35.527	0.052	115.512	-2.839	38.313	0.1	224.646	-0.805	24.615
0.041	90.502	-1.642	36.664	0.052	115.512	-2.971	39.320	0.102	229.194	-0.969	25.864
0.041	90.502	-1.794	37.823	0.052	115.512	-3.095	40.261	0.101	226.920	-1.113	26.958
0.040	88.228	-1.959	39.072	0.052	115.512	-3.235	41.321	0.103	231.467	-1.253	28.019
0.041	90.502	-2.103	40.167	0.053	117.785	-3.365	42.313	0.103	231.467	-1.368	28.894
0.041	90.502	-2.255	41.323	0.054	120.059	-3.496	43.310	0.102	229.194	-1.403	29.159
0.042	92.775	-2.400	42.423	0.055	122.333	-3.619	44.240	0.102	229.194	-1.424	29.318
0.042	92.775	-2.546	43.536	0.055	122.333	-3.731	45.095	0.102	229.194	-1.436	29.409
0.041	90.502	-2.698	44.689	0.054	120.059	-3.838	45.904	0.102	229.194	-1.446	29.491
0.041	90.502	-2.845	45.806	0.055	122.333	-3.937	46.659	0.102	229.194	-1.469	29.664
				0.055	122.333	-4.052	47.537	0.101	226.920	-1.479	29.739
				0.054	120.059	-4.138	48.184	0.101	226.920	-1.494	29.849
				0.054	120.059	-4.168	48.415	0.101	226.920	-1.502	29.909
				0.053	117.785	-4.267	49.167	0.101	226.920	-1.528	30.112
				0.054	120.059	-4.363	49.900	0.101	226.920	-1.533	30.148
				0.055	122.333	-4.424	50.361	0.101	226.920	-1.558	30.341
				0.056	124.606	-4.493	50.888	0.101	226.920	-1.591	30.590
				0.056	124.606	-4.519	51.083	0.101	226.920	-1.587	30.559
				0.056	124.606	-4.551	51.324	0.101	226.920	-1.592	30.600
				0.056	124.606	-4.565	51.434	0.101	226.920	-1.604	30.689
				0.055	122.333	-4.590	51.621	0.101	226.920	-1.612	30.749
				0.055	122.333	-4.584	51.575	0.101	226.920	-1.626	30.856
				0.055	122.333	-4.575	51.510	0.106	238.288	-2.047	34.053
				0.054	120.059	-4.569	51.464				
				0.054	120.059	-4.577	51.526				
				0.054	120.059	-4.574	51.499				
				0.054	120.059	-4.577	51.520				

Table C.3: Shear box results for the mixture of the fresh and weathered shale material from the Cornubia development.

75 kPa				150 kPa				300 kPa			
Shear load (mV)	**Shear stress (kPa)**	**Hori disp. (mV)**	**Hori disp. (mm)**	**Shear load (mV)**	**Shear stress (kPa)**	**Hori disp. (mV)**	**Hori disp. (mm)**	**Shear load (mV)**	**Shear stress (kPa)**	**Hori disp. (mV)**	**Hori disp. (mm)**
0.000	0.000	0.000	0.000	0.000	0.000	0.000	0.000	0.000	0.000	0.000	0.000
0.0001	-2.490	4.101	0.080	0.007	13.198	4.990	-0.035	0.014	29.114	4.746	0.820
0.019	40.482	3.854	1.957	0.010	20.019	4.982	0.030	0.019	40.482	4.579	2.089
0.024	51.850	3.610	3.809	0.011	22.293	4.960	0.192	0.023	49.576	4.354	3.798
0.025	54.124	3.344	5.836	0.013	26.840	4.874	0.849	0.026	56.397	4.101	5.722
0.027	58.671	3.066	7.944	0.017	35.93	4.736	1.899	0.031	67.765	3.816	7.890
0.028	60.945	2.784	10.089	0.021	45.02	4.567	3.181	0.037	81.407	3.541	9.982
0.030	65.492	2.501	12.242	0.022	47.303	4.400	4.454	0.046	101.870	3.245	12.232
0.030	65.492	2.225	14.341	0.025	54.124	4.154	6.320	0.055	122.333	3.013	13.993
0.031	67.765	1.946	16.461	0.029	63.218	3.963	7.776	0.060	133.701	2.770	15.838
0.032	70.039	1.690	18.406	0.031	67.765	3.751	9.382	0.065	145.069	2.575	17.321
0.033	72.313	1.425	20.420	0.033	72.313	3.529	11.072	0.075	167.805	2.073	21.138
0.030	65.492	1.164	22.404	0.035	76.860	3.302	12.794	0.082	183.721	1.610	24.656
0.032	70.039	0.910	24.335	0.037	81.407	3.070	14.563	0.085	190.542	1.249	27.396
0.032	70.039	0.660	26.235	0.039	85.955	2.841	16.300	0.088	197.363	0.946	29.701
0.032	70.039	0.405	28.174	0.041	90.502	2.614	18.024	0.090	201.910	0.670	31.797
0.033	72.313	0.155	30.069	0.041	90.502	2.375	19.840	0.091	204.184	0.428	33.637
0.033	72.313	-0.093	31.952	0.043	95.049	2.141	21.617	0.091	204.184	0.189	35.452
0.034	74.586	-0.339	33.823	0.045	99.596	1.909	23.385	0.092	206.457	-0.042	37.210
0.034	74.586	-0.586	35.702	0.046	101.870	1.692	25.031	0.093	208.731	-0.259	38.861
0.034	74.586	-0.835	37.596	0.046	101.870	1.435	26.984	0.093	208.731	-0.462	40.399
0.034	74.586	-1.087	39.507	0.048	106.417	1.158	29.087	0.094	211.005	-0.663	41.927
0.032	70.039	-1.343	41.456	0.049	108.691	0.901	31.044	0.096	215.552	-0.853	43.374
0.033	72.313	-1.606	43.453	0.049	108.691	0.652	32.939	0.097	217.825	-1.029	44.708
0.033	72.313	-1.864	45.414	0.051	113.238	0.402	34.833	0.097	217.825	-1.184	45.892
0.034	74.586	-2.121	47.371	0.052	115.512	0.158	36.688	0.099	222.373	-1.319	46.913
0.033	72.313	-2.395	49.448	0.053	117.785	-0.080	38.500	0.099	222.373	-1.447	47.887
0.032	70.039	-2.652	51.403	0.054	120.059	-0.317	40.302	0.100	224.646	-1.575	48.861
0.031	67.765	-2.905	53.324	0.054	120.059	-0.552	42.086	0.101	226.920	-1.681	49.668
				0.056	124.606	-0.785	43.855	0.101	226.920	-1.804	50.605
				0.056	124.606	-1.017	45.618	0.102	229.194	-1.897	51.312
				0.058	129.154	-1.248	47.376	0.100	224.646	-1.991	52.023
				0.058	129.154	-1.475	49.105	0.101	226.920	-2.080	52.697

				0.058	129.154	-1.705	50.850	0.102	229.194	-2.164	53.336
				0.058	129.154	-1.941	52.641	0.102	229.194	-2.249	53.986
				0.056	124.606	-2.174	54.417	0.102	229.194	-2.324	54.556
				0.056	124.606	-2.412	56.222	0.103	231.467	-2.389	55.048
				0.056	124.606	-2.655	58.071	0.103	231.467	-2.467	55.638
				0.056	124.606	-2.883	59.803	0.101	226.920	-2.524	56.070
				0.057	126.880	-3.118	61.586	0.101	226.920	-2.580	56.497
				0.056	124.606	-3.334	63.232	0.101	226.920	-2.656	57.075

Table C.4: Shear box results for the fresh shale material from Locality 2.

75 kPa				**150 kPa**				**300 kPa**			
Shear load (mV)	**Shear stress (kPa)**	**Hori disp. (mV)**	**Hori disp. (mm)**	**Shear load (mV)**	**Shear stress (kPa)**	**Hori disp. (mV)**	**Hori disp. (mm)**	**Shear load (mV)**	**Shear stress (kPa)**	**Hori disp. (mV)**	**Hori disp. (mm)**
0.000	0.000	0.000	0.000	0.000	0.000	0.000	0.000	0.000	0.000	0.000	0.000
0.004	6.377	1.8	0.727	0.015	31.387	4.5	0.623	0.022	47.303	4.717469	0.621
0.006	10.925	1.7	1.946	0.019	40.482	4.4	1.161	0.028	60.945	4.599076	1.521
0.009	17.745	1.5	3.370	0.022	47.303	4.3	2.008	0.036	79.134	4.465075	2.539
0.011	22.293	1.3	4.646	0.024	51.850	4.1	3.020	0.041	90.502	4.355565	3.371
0.012	24.566	1.1	6.064	0.026	56.397	4.1	3.357	0.046	101.870	4.269536	4.025
0.014	29.114	0.9	7.485	0.027	58.671	4.0	4.292	0.046	101.870	4.127051	5.108
0.014	29.114	0.8	8.827	0.030	65.492	3.9	5.240	0.052	115.512	4.014851	5.961
0.016	33.661	0.6	9.888	0.033	72.313	3.7	6.161	0.057	126.880	3.892946	6.887
0.018	38.208	0.5	11.041	0.035	76.860	3.6	7.183	0.058	129.154	3.763557	7.871
0.019	40.482	0.3	12.281	0.038	83.681	3.5	8.201	0.061	135.975	3.63845	8.821
0.020	42.755	0.1	13.512	0.039	85.955	3.3	9.245	0.061	135.975	3.49711	9.896
0.020	42.755	0.0	14.709	0.041	90.502	3.1	10.651	0.063	140.522	3.367333	10.882
0.021	45.029	-0.2	15.941	0.044	97.323	3.1	11.310	0.065	145.069	3.259013	11.705
0.021	45.029	-0.3	17.169	0.047	104.144	2.9	12.211	0.065	145.069	3.132427	12.667
0.022	47.303	-0.5	18.396	0.047	104.144	2.8	13.151	0.064	142.795	3.043963	13.339
0.022	47.303	-0.7	19.616	0.050	110.965	2.7	14.198	0.068	151.890	2.921012	14.274
0.022	47.303	-0.8	20.777	0.052	115.512	2.6	15.097	0.070	156.437	2.800229	15.192
0.022	47.303	-1.0	22.015	0.052	115.512	2.4	15.977	0.072	160.985	2.692243	16.013
0.023	49.576	-1.1	23.173	0.052	115.512	2.3	16.865	0.073	163.258	2.588481	16.801
0.024	51.850	-1.3	24.386	0.053	117.785	2.2	17.741	0.073	163.258	2.477071	17.648
0.025	54.124	-1.4	25.501	0.054	120.059	2.1	18.626	0.074	165.532	2.366182	18.491
0.026	56.397	-1.6	26.738	0.053	117.785	2.0	19.479	0.075	167.805	2.264778	19.261
0.026	56.397	-1.8	28.043	0.052	115.512	1.8	20.582	0.075	167.805	2.159682	20.060
0.026	56.397	-1.9	29.190	0.054	120.059	1.6	22.030	0.078	174.626	2.064492	20.783

0.025	54.124	-2.1	30.373	0.054	120.059	1.5	23.389	0.081	181.447	1.975094	21.463
0.025	54.124	-2.2	31.616	0.056	124.606	1.3	24.781	0.083	185.995	1.895158	22.070
0.026	56.397	-2.4	32.760	0.055	122.333	1.1	26.111	0.080	179.174	1.809229	22.723
0.024	51.850	-2.5	33.971	0.056	124.606	0.9	27.422	0.082	183.721	1.72648	23.352
0.025	54.124	-2.7	35.156	0.055	122.333	0.8	28.720	0.085	190.542	1.625431	24.120
0.024	51.850	-2.9	36.303	0.057	126.880	0.6	30.076	0.084	188.268	1.50387	25.044
0.024	51.850	-3.0	37.485	0.056	124.606	0.4	31.349	0.085	190.542	1.382042	25.970
0.024	51.850	-3.1	38.550	0.060	133.701	0.3	32.626	0.085	190.542	1.259748	26.899
0.024	51.850	-3.3	39.757	0.061	135.975	0.1	33.911	0.085	190.542	1.144368	27.776
0.025	54.124	-3.4	40.811	0.059	131.427	-0.1	35.183	0.088	197.363	1.044275	28.537
0.025	54.124	-3.5	41.617	0.057	126.880	-0.2	36.375	0.088	197.363	0.942183	29.313
0.026	56.397	-3.7	42.593	0.058	129.154	-0.4	37.589	0.087	195.089	0.834546	30.131
0.027	58.671	-3.8	43.319	0.059	131.427	-0.6	38.759	0.089	199.636	0.729573	30.929
0.027	58.671	-3.9	44.303	0.059	131.427	-0.7	40.064	0.091	204.184	0.644076	31.579
0.028	60.945	-4.0	44.987	0.060	133.701	-0.9	41.342	0.091	204.184	0.558889	32.226
0.028	60.945	-4.1	45.730	0.061	135.975	-1.1	42.639	0.091	204.184	0.468202	32.915
0.027	58.671	-4.2	46.577	0.064	142.795	-1.2	43.921	0.093	208.731	0.388979	33.517
0.028	60.945	-4.3	47.373	0.061	135.975	-1.4	45.174	0.096	215.552	0.318397	34.054
0.028	60.945	-4.4	47.809	0.063	140.522	-1.5	46.209	0.097	217.825	0.255342	34.533
0.028	60.945	-4.4	48.379	0.063	140.522	-1.7	47.341	0.100	224.646	0.202193	34.937
0.029	63.218	-4.5	48.731	0.064	142.795	-1.9	48.682	0.100	224.646	0.158679	35.268
0.029	63.218	-4.5	49.153	0.064	142.795	-2.0	49.882	0.100	224.646	0.11289	35.616
0.028	60.945	-4.6	49.262	0.063	140.522	-2.2	51.171	0.101	226.920	0.073556	35.915
0.028	60.945	-4.5	49.103	0.064	142.795	-2.4	52.432	0.101	226.920	0.034673	36.210
0.028	60.945	-4.6	49.296	0.065	145.069	-2.5	53.604	0.097	217.825	-0.01304	36.573
0.029	63.218	-4.6	49.305	0.065	145.069	-2.7	54.838	0.099	222.373	-0.06468	36.965
								0.100	224.646	-0.11347	37.336
								0.099	222.373	-0.16378	37.718
								0.102	229.194	-0.20793	38.054
								0.102	229.194	-0.25052	38.377
								0.101	226.920	-0.28996	38.677
								0.101	226.920	-0.3295	38.978
								0.101	226.920	-0.37351	39.312
								0.102	229.194	-0.41114	39.598
								0.100	224.646	-0.45938	39.965
								0.101	226.920	-0.50018	40.275
								0.100	224.646	-0.54516	40.617

								0.101	226.920	-0.59341	40.983
								0.100	224.646	-0.63488	41.299
								0.099	222.373	-0.68545	41.683
								0.101	226.920	-0.7393	42.092
								0.101	226.920	-0.78591	42.446
								0.101	226.920	-0.82675	42.757

Table C.5: Shear box results for the fresh shale material from Locality 3.

75 kPa				150 kPa				300 kPa			
Shear load (mV)	**Shear stress (kPa)**	**Hori disp. (mV)**	**Hori disp. (mm)**	**Shear load (mV)**	**Shear stress (kPa)**	**Hori disp. (mV)**	**Hori disp. (mm)**	**Shear load (mV)**	**Shear stress (kPa)**	**Hori disp. (mV)**	**Hori disp. (mm)**
0.000	0.000	0.000	0.000	0.000	0.000	0.000	0.000	0.000	0.000	0.000	0.000
0.003	4.104	2.653	1.001	0.003	4.104	1.988	0.631	0.006	10.925	3.767	0.596
0.004	6.377	2.565	1.672	0.005	8.651	1.833	1.802	0.008	15.472	3.657	1.437
0.005	8.651	2.393	2.980	0.006	10.925	1.644	3.241	0.011	22.293	3.513	2.531
0.006	10.925	2.276	3.868	0.007	13.198	1.470	4.563	0.016	33.661	3.362	3.675
0.007	13.198	2.119	5.059	0.007	13.198	1.303	5.831	0.028	60.945	3.251	4.524
0.009	17.745	1.952	6.332	0.007	13.198	1.138	7.087	0.032	70.039	3.151	5.285
0.011	22.293	1.800	7.486	0.012	24.566	0.993	8.187	0.037	81.407	3.043	6.105
0.012	24.566	1.654	8.598	0.016	33.661	0.845	9.314	0.041	90.502	2.941	6.874
0.013	26.840	1.505	9.724	0.020	42.755	0.705	10.381	0.044	97.323	2.839	7.649
0.014	29.114	1.382	10.666	0.023	49.576	0.573	11.380	0.047	104.144	2.747	8.354
0.016	33.661	1.244	11.709	0.026	56.397	0.451	12.311	0.050	110.965	2.660	9.016
0.017	35.935	1.103	12.782	0.028	60.945	0.329	13.234	0.052	115.512	2.594	9.513
0.018	38.208	0.970	13.793	0.029	63.218	0.202	14.203	0.057	126.880	2.448	10.623
0.020	42.755	0.837	14.808	0.030	65.492	0.084	15.098	0.061	135.975	2.305	11.713
0.021	45.029	0.715	15.733	0.033	72.313	0.055	15.315	0.063	140.522	2.168	12.754
0.022	47.303	0.596	16.638	0.035	76.860	0.056	15.311	0.064	142.795	2.047	13.672
0.022	47.303	0.474	17.567	0.036	79.134	0.020	15.586	0.066	147.343	1.921	14.627
0.023	49.576	0.356	18.457	0.038	83.681	-0.081	16.349	0.069	154.164	1.805	15.507
0.023	49.576	0.238	19.358	0.039	85.955	-0.186	17.152	0.071	158.711	1.709	16.244
0.024	51.850	0.120	20.251	0.040	88.228	-0.287	17.914	0.071	158.711	1.611	16.987
0.025	54.124	0.002	21.152	0.041	90.502	-0.391	18.706	0.073	163.258	1.516	17.709
0.026	56.397	-0.116	22.044	0.043	95.049	-0.490	19.456	0.072	160.985	1.414	18.482
0.026	56.397	-0.229	22.903	0.042	92.775	-0.591	20.224	0.075	167.805	1.330	19.120
0.027	58.671	-0.341	23.755	0.043	95.049	-0.688	20.961	0.077	172.353	1.250	19.728
0.028	60.945	-0.455	24.620	0.043	95.049	-0.801	21.827	0.076	170.079	1.168	20.349

0.028	60.945	-0.569	25.486	0.044	97.323	-0.903	22.596	0.074	165.532	1.089	20.955
0.028	60.945	-0.682	26.349	0.046	101.870	-1.001	23.341	0.075	167.805	1.007	21.572
0.028	60.945	-0.795	27.204	0.048	106.417	-1.095	24.057	0.077	172.353	0.949	22.016
0.028	60.945	-0.909	28.072	0.049	108.691	-1.188	24.765	0.076	170.079	0.874	22.590
0.028	60.945	-1.026	28.967	0.049	108.691	-1.288	25.522	0.077	172.353	0.802	23.130
0.029	63.218	-1.136	29.802	0.050	110.965	-1.380	26.225	0.077	172.353	0.728	23.694
0.029	63.218	-1.256	30.709	0.051	113.238	-1.468	26.891	0.077	172.353	0.661	24.205
0.030	65.492	-1.369	31.569	0.050	110.965	-1.562	27.605	0.079	176.900	0.593	24.725
0.029	63.218	-1.485	32.449	0.053	117.785	-1.643	28.222	0.081	181.447	0.541	25.115
0.029	63.218	-1.609	33.398	0.055	122.333	-1.736	28.930	0.081	181.447	0.481	25.574
0.029	63.218	-1.724	34.266	0.055	122.333	-1.822	29.582	0.082	183.721	0.429	25.970
0.029	63.218	-1.847	35.202	0.056	124.606	-1.915	30.293	0.083	185.995	0.375	26.378
0.029	63.218	-1.962	36.079	0.058	129.154	-2.033	31.187	0.083	185.995	0.326	26.754
0.030	65.492	-2.081	36.985	0.059	131.427	-2.163	32.171	0.083	185.995	0.278	27.116
0.031	67.765	-2.199	37.876	0.061	135.975	-2.340	33.524	0.085	190.542	0.214	27.605
0.030	65.492	-2.310	38.719	0.063	140.522	-2.493	34.680	0.087	195.089	0.132	28.225
0.029	63.218	-2.439	39.705	0.063	140.522	-2.635	35.758	0.089	199.636	0.019	29.085
0.028	60.945	-2.556	40.593	0.065	145.069	-2.778	36.852	0.089	199.636	-0.085	29.876
0.028	60.945	-2.681	41.543	0.063	140.522	-2.966	38.278	0.090	201.910	-0.183	30.620
0.028	60.945	-2.798	42.427	0.065	145.069	-3.119	39.437	0.092	206.457	-0.271	31.287
0.028	60.945	-2.914	43.312	0.067	149.616	-3.287	40.718	0.092	206.457	-0.348	31.874
0.028	60.945	-3.030	44.190	0.065	145.069	-3.437	41.860	0.091	204.184	-0.430	32.493
0.028	60.945	-3.140	45.033	0.064	142.795	-3.588	43.003	0.092	206.457	-0.513	33.131
0.029	63.218	-3.252	45.885	0.065	145.069	-3.705	43.895	0.094	211.005	-0.581	33.641
0.028	60.945	-3.351	46.630	0.063	140.522	-3.834	44.872	0.095	213.278	-0.638	34.081
0.028	60.945	-3.460	47.465	0.065	145.069	-3.959	45.824	0.097	217.825	-0.685	34.431
0.027	58.671	-3.565	48.256	0.064	142.795	-4.060	46.588	0.098	220.099	-0.725	34.740
0.027	58.671	-3.617	48.652	0.063	140.522	-4.209	47.724	0.097	217.825	-0.755	34.964
0.027	58.671	-3.667	49.035	0.061	135.975	-4.304	48.448	0.098	220.099	-0.785	35.192
				0.062	138.248	-4.404	49.208	0.097	217.825	-0.819	35.450
				0.062	138.248	-4.459	49.625	0.097	217.825	-0.866	35.811
				0.060	133.701	-4.522	50.103	0.097	217.825	-0.905	36.106
								0.098	220.099	-0.940	36.373
								0.098	220.099	-0.976	36.646
								0.099	222.373	-1.001	36.838
								0.098	220.099	-1.020	36.982
								0.099	222.373	-1.043	37.155

								0.100	224.646	-1.070	37.360
								0.100	224.646	-1.088	37.499
								0.101	226.920	-1.096	37.561
								0.101	226.920	-1.112	37.678
								0.101	226.920	-1.116	37.710
								0.101	226.920	-1.124	37.772
								0.101	226.920	-1.126	37.786
								0.101	226.920	-1.146	37.935
								0.101	226.920	-1.159	38.038
								0.101	226.920	-1.171	38.131
								0.100	224.646	-1.189	38.268
								0.101	226.920	-1.204	38.381
								0.099	222.373	-1.220	38.497
								0.100	224.646	-1.239	38.643
								0.100	224.646	-1.257	38.783
								0.100	224.646	-1.268	38.868
								0.099	222.373	-1.284	38.985

Table C.6: Shear box results for the weathered shale material from Locality 3.

75 kPa				**150 kPa**				**300 kPa**			
Shear load (mV)	**Shear stress (kPa)**	**Hori disp. (mV)**	**Hori disp. (mm)**	**Shear load (mV)**	**Shear stress (kPa)**	**Hori disp. (mV)**	**Hori disp. (mm)**	**Shear load (mV)**	**Shear stress (kPa)**	**Hori disp. (mV)**	**Hori disp. (mm)**
0.000	0.000	0.000	0.000	0.000	0.000	0.000	0.000	0.000	0.000	0.000	0.000
0.026	56.397	1.806	-2.328	0.009	17.745	2.313	1.065	0.013	26.840	3.401	-0.846
0.027	58.671	1.763	-2.656	0.014	29.114	2.131	2.449	0.016	33.661	3.173	0.883
0.030	65.492	1.580	-4.048	0.017	35.935	1.978	3.612	0.019	40.482	3.029	1.983
0.034	74.586	1.400	-5.415	0.020	42.755	1.800	4.965	0.022	47.303	2.860	3.265
0.037	81.407	1.231	-6.699	0.026	56.397	1.650	6.108	0.026	56.397	2.696	4.513
0.039	85.955	1.063	-7.972	0.034	74.586	1.499	7.252	0.034	74.586	2.529	5.780
0.041	90.502	0.903	-9.188	0.041	90.502	1.360	8.306	0.041	90.502	2.402	6.743
0.044	97.323	0.744	-10.402	0.047	104.144	1.219	9.377	0.045	99.596	2.270	7.749
0.043	95.049	0.591	-11.563	0.052	115.512	1.081	10.427	0.050	110.965	2.137	8.758
0.046	101.870	0.437	-12.730	0.057	126.880	0.949	11.431	0.054	120.059	2.017	9.667
0.048	106.417	0.286	-13.879	0.060	133.701	0.821	12.404	0.057	126.880	1.899	10.571
0.051	113.238	0.139	-14.999	0.063	140.522	0.702	13.308	0.059	131.427	1.792	11.378
0.052	115.512	-0.004	-16.087	0.067	149.616	0.587	14.182	0.062	138.248	1.685	12.193
0.054	120.059	-0.146	-17.163	0.071	158.711	0.474	15.044	0.064	142.795	1.577	13.014

0.057	126.880	-0.287	-18.236	0.075	167.805	0.364	15.876	0.065	145.069	1.481	13.745
0.056	124.606	-0.427	-19.296	0.077	172.353	0.259	16.677	0.067	149.616	1.385	14.471
0.058	129.154	-0.562	-20.325	0.078	174.626	0.155	17.463	0.069	154.164	1.298	15.137
0.059	131.427	-0.703	-21.395	0.078	174.626	0.054	18.237	0.071	158.711	1.205	15.840
0.060	133.701	-0.836	-22.406	0.081	181.447	-0.046	18.993	0.074	165.532	1.130	16.410
0.061	135.975	-0.974	-23.453	0.082	183.721	-0.145	19.748	0.075	167.805	1.047	17.040
0.062	138.248	-1.107	-24.467	0.084	188.268	-0.241	20.474	0.077	172.353	0.978	17.565
0.063	140.522	-1.239	-25.471	0.086	192.815	-0.331	21.163	0.080	179.174	0.907	18.106
0.062	138.248	-1.392	-26.636	0.088	197.363	-0.426	21.878	0.081	181.447	0.840	18.619
0.063	140.522	-1.533	-27.705	0.090	201.910	-0.515	22.555	0.082	183.721	0.778	19.084
0.063	140.522	-1.663	-28.696	0.088	197.363	-0.604	23.233	0.084	188.268	0.719	19.536
0.063	140.522	-1.802	-29.752	0.090	201.910	-0.695	23.926	0.085	190.542	0.662	19.968
0.058	129.154	-1.939	-30.789	0.092	206.457	-0.785	24.607	0.086	192.815	0.614	20.336
0.059	131.427	-2.081	-31.866	0.093	208.731	-0.880	25.328	0.087	195.089	0.561	20.739
0.059	131.427	-2.227	-32.980	0.094	211.005	-0.962	25.955	0.088	197.363	0.506	21.153
0.060	133.701	-2.362	-34.004	0.095	213.278	-1.047	26.598	0.089	199.636	0.462	21.489
0.059	131.427	-2.508	-35.116	0.098	220.099	-1.129	27.226	0.090	201.910	0.415	21.843
0.060	133.701	-2.645	-36.154	0.100	224.646	-1.266	28.265	0.090	201.910	0.372	22.172
0.060	133.701	-2.787	-37.237	0.102	229.194	-1.391	29.218	0.091	204.184	0.328	22.504
0.060	133.701	-2.925	-38.281	0.103	231.467	-1.520	30.193	0.092	206.457	0.292	22.781
0.061	135.975	-3.058	-39.294	0.103	231.467	-1.650	31.183	0.093	208.731	0.253	23.075
0.062	138.248	-3.180	-40.225	0.106	238.288	-1.783	32.198	0.094	211.005	0.218	23.340
0.063	140.522	-3.311	-41.216	0.105	236.015	-1.907	33.136	0.094	211.005	0.185	23.596
0.063	140.522	-3.454	-42.304	0.105	236.015	-2.030	34.075	0.095	213.278	0.151	23.851
0.062	138.248	-3.537	-42.938	0.104	233.741	-2.148	34.967	0.095	213.278	0.120	24.088
0.061	135.975	-3.681	-44.032	0.101	226.920	-2.286	36.014	0.094	211.005	0.087	24.340
0.061	135.975	-3.772	-44.718	0.101	226.920	-2.430	37.108	0.095	213.278	0.054	24.591
0.061	135.975	-3.877	-45.519	0.102	229.194	-2.561	38.106	0.096	215.552	0.022	24.832
0.061	135.975	-3.971	-46.235	0.101	226.920	-2.674	38.969	0.097	217.825	-0.009	25.070
0.061	135.975	-4.056	-46.876	0.100	224.646	-2.816	40.043	0.098	220.099	-0.038	25.289
0.060	133.701	-4.163	-47.694	0.099	222.373	-2.951	41.068	0.097	217.825	-0.066	25.503
0.060	133.701	-4.245	-48.314	0.100	224.646	-3.086	42.097	0.098	220.099	-0.094	25.715
0.058	129.154	-4.336	-49.010	0.101	226.920	-3.223	43.141	0.098	220.099	-0.120	25.914
0.058	129.154	-4.328	-48.944	0.102	229.194	-3.324	43.907	0.099	222.373	-0.145	26.104
0.058	129.154	-4.342	-49.057	0.102	229.194	-3.438	44.775	0.099	222.373	-0.171	26.299
0.059	131.427	-4.473	-50.048	0.103	231.467	-3.547	45.605	0.100	224.646	-0.194	26.478
0.060	133.701	-4.526	-50.451					0.099	222.373	-0.217	26.649

								0.100	224.646	-0.241	26.834
								0.102	229.194	-0.265	27.011
								0.103	231.467	-0.290	27.205
								0.105	236.015	-0.360	27.736
								0.110	247.383	-0.484	28.675
								0.114	256.477	-0.658	30.001
								0.114	256.477	-0.843	31.408
								0.117	263.298	-0.993	32.546
								0.118	265.572	-1.131	33.599
								0.120	270.119	-1.243	34.445
								0.121	272.393	-1.335	35.147
								0.123	276.940	-1.413	35.735
								0.124	279.214	-1.470	36.173
								0.125	281.487	-1.508	36.459
								0.125	281.487	-1.538	36.692
								0.125	281.487	-1.572	36.950
								0.125	281.487	-1.598	37.146
								0.125	281.487	-1.630	37.388
								0.125	281.487	-1.644	37.497
								0.125	281.487	-1.665	37.652
								0.125	281.487	-1.705	37.960
								0.125	281.487	-1.749	38.290
								0.125	281.487	-1.774	38.483
								0.125	281.487	-1.833	38.932
								0.125	281.487	-1.876	39.258
								0.125	281.487	-1.908	39.503
								0.126	283.761	-1.921	39.596
								0.126	283.761	-1.952	39.831
								0.125	281.487	-1.960	39.895
								0.125	281.487	-1.975	40.013
								0.126	283.761	-1.992	40.139
								0.126	283.761	-2.014	40.304
								0.126	283.761	-2.018	40.337
								0.123	276.940	-2.033	40.452
								0.122	274.666	-2.044	40.532
								0.121	272.393	-2.037	40.479

Table C.7: Shear box results for the mixture of the fresh and weathered shale material from Locality 3.

75 kPa				150 kPa				300 kPa			
Shear load (mV)	**Shear stress (kPa)**	**Hori disp. (mV)**	**Hori disp. (mm)**	**Shear load (mV)**	**Shear stress (kPa)**	**Hori disp. (mV)**	**Hori disp. (mm)**	**Shear load (mV)**	**Shear stress (kPa)**	**Hori disp. (mV)**	**Hori disp. (mm)**
0.000	0.000	0.000	0.000	0.000	0.000	0.000	0.000	0.000	0.000	0.000	0.000
0.010	20.019	4.951	0.619	0.008	15.472	4.791	0.508	0.000	0.000	4.982	0.147
0.013	26.840	4.885	1.120	0.012	24.566	4.665	1.472	0.017	35.935	4.984	0.167
0.015	31.387	4.804	1.742	0.021	45.029	4.495	2.759	0.024	51.850	4.974	0.225
0.017	35.935	4.738	2.237	0.025	54.124	4.328	4.030	0.027	58.671	4.934	0.533
0.018	38.208	4.590	3.362	0.030	65.492	4.171	5.219	0.028	60.945	4.837	1.264
0.020	42.755	4.380	4.958	0.034	74.586	4.000	6.519	0.029	63.218	4.725	2.116
0.022	47.303	4.147	6.732	0.036	79.134	3.811	7.959	0.031	67.765	4.576	3.251
0.024	51.850	3.884	8.731	0.038	83.681	3.616	9.440	0.035	76.860	4.313	5.250
0.026	56.397	3.634	10.630	0.041	90.502	3.376	11.264	0.039	85.95	4.117	6.742
0.027	58.671	3.345	12.828	0.043	95.049	3.201	12.592	0.043	95.05	3.861	8.687
0.029	63.218	3.056	15.020	0.046	101.870	3.002	14.109	0.048	106.417	3.633	10.414
0.032	70.039	2.750	17.352	0.047	104.144	2.809	15.574	0.053	117.785	3.444	11.850
0.033	72.313	2.445	19.665	0.050	110.965	2.610	17.086	0.057	126.880	3.271	13.165
0.034	74.586	2.145	21.950	0.052	115.512	2.406	18.634	0.063	140.522	3.085	14.580
0.036	79.134	1.859	24.119	0.053	117.785	2.206	20.160	0.066	147.343	2.936	15.713
0.038	83.681	1.588	26.178	0.053	117.785	1.999	21.727	0.067	149.616	2.775	16.936
0.039	85.955	1.315	28.255	0.055	122.333	1.817	23.113	0.068	151.890	2.613	18.168
0.041	90.502	1.060	30.193	0.058	129.154	1.641	24.454	0.073	163.258	2.470	19.257
0.041	90.502	0.818	32.033	0.057	126.880	1.470	25.751	0.074	165.532	2.359	20.101
0.041	90.502	0.571	33.907	0.058	129.154	1.305	27.001	0.078	174.626	2.257	20.877
0.042	92.775	0.323	35.795	0.058	129.154	1.143	28.237	0.079	176.900	2.144	21.732
0.043	95.049	0.078	37.654	0.061	135.975	0.984	29.445	0.079	176.900	2.036	22.556
0.042	92.775	-0.163	39.487	0.063	140.522	0.841	30.532	0.082	183.721	1.933	23.335
0.041	90.502	-0.413	41.387	0.063	140.522	0.694	31.651	0.084	188.268	1.828	24.132
0.042	92.775	-0.661	43.271	0.064	142.795	0.549	32.748	0.085	190.542	1.745	24.765
0.041	90.502	-0.919	45.232	0.065	145.069	0.405	33.841	0.087	195.089	1.663	25.386
0.041	90.502	-1.178	47.201	0.066	147.343	0.266	34.900	0.088	197.363	1.598	25.880
0.040	88.228	-1.432	49.135	0.069	154.164	0.129	35.941	0.093	208.731	1.311	28.066
0.039	85.955	-1.697	51.143	0.069	154.164	-0.003	36.949	0.099	222.373	0.855	31.534
0.040	88.228	-1.968	53.208	0.070	156.437	-0.134	37.940	0.099	222.373	0.484	34.353
				0.066	147.343	-0.260	38.896	0.102	229.194	0.146	36.921
				0.067	149.616	-0.395	39.924	0.108	242.835	-0.086	38.680

				0.069	154.164	-0.529	40.942	0.110	247.383	-0.244	39.881
				0.071	158.711	-0.659	41.928	0.104	233.741	-0.439	41.363
				0.071	158.711	-0.783	42.876	0.104	233.741	-0.700	43.345
				0.070	156.437	-0.908	43.822	0.106	238.288	-0.950	45.245
				0.070	156.437	-1.040	44.828	0.103	231.467	-1.212	47.239
				0.072	160.985	-1.161	45.749	0.103	231.467	-1.480	49.276
				0.074	165.532	-1.284	46.682	0.106	238.288	-1.730	51.177
				0.073	163.258	-1.403	47.584				
				0.074	165.532	-1.527	48.524				
				0.074	165.532	-1.646	49.429				
				0.075	167.805	-1.767	50.349				
				0.074	165.532	-1.884	51.242				
				0.074	165.532	-2.007	52.176				
				0.075	167.805	-2.125	53.076				

Table C.8: Shear box results for the fresh shale material from Locality 4.

75 kPa				**150 kPa**				**300 kPa**			
Shear load (mV)	**Shear stress (kPa)**	**Hori disp. (mV)**	**Hori disp. (mm)**	**Shear load (mV)**	**Shear stress (kPa)**	**Hori disp. (mV)**	**Hori disp. (mm)**	**Shear load (mV)**	**Shear stress (kPa)**	**Hori disp. (mV)**	**Hori disp. (mm)**
0.000	0.000	0.000	0.000	0.000	0.000	0.000	0.000	0.000	0.000	0.000	0.000
0.004	6.377	3.582	0.967	0.006	10.925	3.580	1.272	0.016	33.661	2.208	1.835
0.006	10.925	3.467	1.841	0.008	15.472	3.444	2.306	0.022	47.303	2.007	3.360
0.007	13.198	3.334	2.853	0.010	20.019	3.286	3.508	0.033	72.313	1.832	4.689
0.008	15.472	3.199	3.874	0.013	26.840	3.119	4.775	0.041	90.502	1.683	5.823
0.009	17.745	3.075	4.818	0.017	35.935	2.984	5.807	0.047	104.144	1.540	6.913
0.010	20.019	2.995	5.428	0.020	42.755	2.841	6.889	0.051	113.238	1.371	8.193
0.010	20.019	2.852	6.511	0.022	47.303	2.693	8.017	0.055	122.333	1.221	9.337
0.012	24.566	2.717	7.537	0.025	54.124	2.559	9.033	0.058	129.154	1.077	10.430
0.012	24.566	2.594	8.478	0.027	58.671	2.427	10.034	0.060	133.701	0.945	11.432
0.013	26.840	2.452	9.550	0.029	63.218	2.287	11.100	0.062	138.248	0.819	12.389
0.014	29.114	2.324	10.529	0.031	67.765	2.143	12.199	0.065	145.069	0.702	13.282
0.013	26.840	2.177	11.640	0.032	70.039	2.029	13.062	0.067	149.616	0.593	14.108
0.013	26.840	2.037	12.708	0.032	70.039	1.909	13.978	0.070	156.437	0.493	14.872
0.013	26.840	1.893	13.805	0.033	72.313	1.781	14.949	0.072	160.985	0.401	15.571
0.015	31.387	1.761	14.806	0.034	74.586	1.656	15.901	0.074	165.532	0.291	16.400
0.016	33.661	1.631	15.795	0.036	79.134	1.534	16.825	0.077	172.353	0.177	17.270
0.017	35.935	1.476	16.968	0.038	83.681	1.420	17.692	0.078	174.626	0.068	18.101

0.018	38.208	1.353	17.902	0.039	85.955	1.310	18.526	0.077	172.353	-0.036	18.890
0.019	40.482	1.231	18.831	0.041	90.502	1.198	19.374	0.077	172.353	-0.138	19.663
0.019	40.482	1.110	19.756	0.040	88.228	1.084	20.243	0.077	172.353	-0.243	20.460
0.020	42.755	0.991	20.659	0.038	83.681	0.979	21.040	0.078	174.626	-0.345	21.238
0.020	42.755	0.875	21.537	0.039	85.955	0.873	21.847	0.079	176.900	-0.441	21.964
0.020	42.755	0.760	22.415	0.039	85.955	0.765	22.669	0.082	183.721	-0.529	22.637
0.020	42.755	0.642	23.308	0.040	88.228	0.661	23.457	0.082	183.721	-0.610	23.251
0.020	42.755	0.525	24.202	0.041	90.502	0.557	24.247	0.083	185.995	-0.712	24.024
0.021	45.029	0.411	25.066	0.041	90.502	0.456	25.016	0.085	190.542	-0.808	24.754
0.021	45.029	0.296	25.942	0.041	90.502	0.347	25.843	0.085	190.542	-0.895	25.416
0.022	47.303	0.182	26.803	0.040	88.228	0.237	26.683	0.087	195.089	-0.978	26.047
0.023	49.576	0.070	27.655	0.042	92.775	0.131	27.487	0.087	195.089	-1.058	26.655
0.023	49.576	-0.042	28.506	0.043	95.049	0.029	28.263	0.088	197.363	-1.132	27.222
0.023	49.576	-0.155	29.364	0.044	97.323	-0.115	29.358	0.088	197.363	-1.210	27.813
0.022	47.303	-0.271	30.246	0.044	97.323	-0.274	30.564	0.089	199.636	-1.268	28.253
0.021	45.029	-0.387	31.128	0.044	97.323	-0.428	31.738	0.090	201.910	-1.323	28.672
0.021	45.029	-0.502	32.008	0.045	99.596	-0.587	32.943	0.091	204.184	-1.380	29.103
0.021	45.029	-0.620	32.901	0.046	101.870	-0.745	34.147	0.091	204.184	-1.422	29.422
0.021	45.029	-0.737	33.792	0.046	101.870	-0.895	35.283	0.091	204.184	-1.482	29.877
0.022	47.303	-0.859	34.721	0.047	104.144	-1.100	36.844	0.091	204.184	-1.535	30.277
0.023	49.576	-0.978	35.623	0.049	108.691	-1.330	38.593	0.092	206.457	-1.586	30.671
0.025	54.124	-1.226	37.508	0.053	117.785	-1.539	40.178	0.092	206.457	-1.622	30.939
0.023	49.576	-1.543	39.914	0.054	120.059	-1.736	41.679	0.092	206.457	-1.665	31.266
0.024	51.850	-1.657	40.781	0.052	115.512	-1.957	43.355	0.090	201.910	-1.705	31.575
0.024	51.850	-1.822	42.034	0.052	115.512	-2.157	44.876	0.091	204.184	-1.749	31.907
0.024	51.850	-1.973	43.182	0.053	117.785	-2.363	46.441	0.091	204.184	-1.796	32.263
0.024	51.850	-2.163	44.630	0.052	115.512	-2.573	48.040	0.092	206.457	-1.835	32.561
0.023	49.576	-2.354	46.083	0.051	113.238	-2.787	49.666	0.091	204.184	-1.896	33.021
0.022	47.303	-2.526	47.388	0.052	115.512	-2.996	51.249	0.092	206.457	-1.975	33.621
0.022	47.303	-2.692	48.647	0.051	113.238	-3.183	52.674	0.093	208.731	-2.051	34.205
0.023	49.576	-2.870	49.999	0.052	115.512	-3.382	54.186	0.093	208.731	-2.128	34.788
0.023	49.576	-3.016	51.110	0.049	108.691	-3.565	55.580	0.094	211.005	-2.215	35.451
				0.048	106.417	-3.741	56.916	0.095	213.278	-2.279	35.933
								0.097	217.825	-2.358	36.533
								0.097	217.825	-2.440	37.157
								0.097	217.825	-2.519	37.762
								0.098	220.099	-2.626	38.575

								0.098	220.099	-2.759	39.584
								0.099	222.373	-2.891	40.585
								0.101	226.920	-2.979	41.252
								0.103	231.467	-3.156	42.601
								0.103	231.467	-3.318	43.833
								0.103	231.467	-3.479	45.054
								0.103	231.467	-3.635	46.244
								0.103	231.467	-3.792	47.434
								0.107	239.688	-3.922	48.423
								0.103	231.467	-3.996	48.985
								0.103	231.467	-4.079	49.615
								0.103	231.467	-4.143	50.102

Appendix D: Settlement monitoring at the Cornubia development and rainfall data (mm)

NB: The settlement readings were taken on the first of each month (after a period of 30 days).

Table D.1: Settlement monitoring at the Cornubia development at the Fountains site.

Months	April	May	June	July	August	September	October	November	December	January	February	March	April
Platform 10	2000	1986	1982										
Platform 10	2000	1971	1956										
Platform 11	2000	1987	1970										
Platform 11	2000	1962	1958										
Platform 13	2000	1991	1991	1987	1983	1972	1967	1959	1956	1954	1952	1952	1937
Platform 13	2000	1989	1985	1979	1962	1951	1949	1939	1931	1927	1921	1916	
Platform 14	2000	1990	1983	1975	1964	1964	1952	1948	1941	1930	1927	1922	1919
Platform 14	2000	1976	1973	1971	1971	1962	1960	1951	1944	1939	1934	1932	1931

Table D.2: Settlement monitoring at the Cornubia development at the Vumani site.

Peg no.	**September**	**October**	**November**	**December**
1	2000	1984	1982	
2	2000	1995	1988	
3	2000	1981	1972	
4	2000	1986	1985	1978
5	2000	1986	1981	1973

Table D.3: Settlement monitoring at the Cornubia development at the Gralio site.

Peg No.	September	October	November	December	January
1	2000	1987	1981	1972	
2	2000	1993	1987	1980	1975

Rainfall data

VUMANI CIVILS C.C.

CORNUBIA PHASE 1B3 CONSTRUCTION OF INFRASTRUCTURE SERVICES – 4V-10211
SITE MEETING NO.14
– 10/02/2015

LABOUR REPORT

CONTRACTS DIRECTOR	:	Y. GOVENDER
CONTRACTS MANAGER	:	N. BALWANTH
GENERAL FOREMAN	:	P. PATANDIN
WATER FOREMAN	:	A.MUDALY
EARTHWORKS FOREMAN	:	S. MOLEFE
TECHNICIAN	:	A. SINGH
TECHNICIAN	:	P. LOKCHUNDAR
SAFETY MANAGER	:	M. HEUER
SAFETY OFFICER	:	S. NDLOVU
SUB CONTRACTOR SURVEYOR	:	MAYABA SURVEYS
SUBCONTRACTOR SURVEYOR	:	STS SURVEYS
SURVEY ASSISTANT	:	4 NO.
CLERK	:	1 NO.
CLO	:	1 NO.
UNSKILLED LABOUR (LOCAL)	:	15 NO.
SKILLED LABOUR	:	2 NO.
PLANT OPERATORS	:	27 NO.

PLANT

LDV'S	:	4 NO.
ADT'S	:	9 NO.
DOZERS	:	1 NO.
EXCAVATOR (30T)	:	4 NO.
10 TON ROLLER (PADFOOT)	:	1 NO.
10 TON ROLLER (SMOOTH DRUM)	:	1 NO.
TLB	:	3 NO.
WATERCART	:	2 NO.
GRADER	:	2 NO.

SMALL PLANT

GENERATOR	:	2 NO.
BREAKER	:	1 NO.
VIBRATOR MOTOR + NEEDLE	:	1 NO.
RAMMER	:	4 NO.
PEDESTRIAN ROLLER	:	1 NO.

SUBCONTRACTOR – MAHLOHLA HOLDINGS

SITE AGENT	:	1 NO.
ARTISAN (LOCAL)	:	2 NO.
SKILLED LABOUR	:	2 NO.
UNSKILLED LABOUR (LOCAL)	:	5 NO.

SUBCONTRACTOR – NMS HOLDINGS

SITE AGENT	:	1 NO.
ARTISAN	:	1 NO.
SKILLED LABOUR (LOCAL)	:	3 NO.
UNSKILLED LABOUR (LOCAL)	:	5 NO.

SUBCONTRACTOR –MWELE CONSTRUCTION

SITE AGENT	:	1 NO.
ARTISAN	:	5 NO.
SKILLED LABOUR (LOCAL)	:	5 NO.
UNSKILLED LABOUR (LOCAL)	:	6 NO.

SUBCONTRACTOR – TS & J CIVILS

SITE AGENT	:	1 NO.
ARTISAN	:	3 NO.
SKILLED LABOUR (LOCAL)	:	1 NO.
UNSKILLED LABOUR (LOCAL)	:	7 NO.

RAIN DAYS

28/11/2013	20mm	RAIN DAY
29/11/2013	8mm	RAIN DAY
02/12/2013	10mm	RAIN DAY
03/12/2013	17mm	RAIN DAY
05/12/2013	8mm	RAIN DAY
06/12/2013	8mm	CONSEQUENTIAL
10/12/2013	15mm	RAIN DAY
11/12/2013	15mm	RAIN DAY
12/12/2013	10mm	RAIN DAY
13/12/2013	0mm	CONSEQUENTIAL
30/01/2014	22mm	RAIN DAY
31/01/2014	0mm	CONSEQUENTIAL
03/02/2014	5mm	RAIN DAY
10/02/2014	7mm	HALF RAIN DAY
21/02/2014	5mm	RAIN DAY
24/02/2014	15mm	HALF RAIN DAY
04/03/2014	7mm	RAIN DAY
05/03/2014	5mm	RAIN DAY
06/03/2014	4mm	RAIN DAY
07/03/2014	2mm	RAIN DAY
10/03/2014	25mm	RAIN DAY
11/03/2014	3mm	RAIN DAY
12/03/2014	5mm	RAIN DAY
13/03/2014	2mm	LATE START – HALF DAY
27/03/2014	20mm	RAIN DAY
28/03/2014	10mm	RAIN DAY
16/04/2014	12mm	RAIN DAY
23/04/2014	4mm	CONSEQUENTIAL
27/06/2014	5mm	RAIN DAY
07/07/2014	5mm	RAIN DAY

16/08/2014	2mm	RAIN DAY
29/09/2014	32mm	RAIN DAY
30/09/2014	15mm	½ RAIN DAY
02/10/2014	13mm	½ RAIN DAY
03/10/2014	6mm	½ RAIN DAY
16/10/2014	6mm	½ RAIN DAY
17/10/2014	30mm	RAIN DAY
27/10/2014	35mm	CONSEQUENTIAL
03/11/2014	15mm	
06/11/2014	1mm	
08/11/2014	3mm	
11/11/2014	25mm	RAIN DAY
12/11/2014	2mm	
13/11/2014	2mm	
21/11/2014	10mm	
24/11/2014	5mm	
26/11/2014	1mm	
27/11/2014	11mm	
28/11/2014	5mm	
01/12/2014	7mm	
05/12/2014	5mm	
15/12/2014	20mm	
17/12/2014	15mm	
14/01/2015	5mm	
17/01/2015	5mm	
19/01/2015	5mm	
20/01/2015	4mm	
26/01/2015	1mm	
28/01/2015	20mm	½ RAIN DAY
29/01/2015	10mm	RAIN DAY
30/01/2015	5mm	
02/02/2015	100mm	RAIN DAY
03/02/2015	15mm	
06/02/2015	15mm	
09/02/2015	50mm	